REFERENCE ONLY

UNIVERSITY OF LONDON THESIS

Degree PhD Year 2006 Name of Author HOWARD
Daniel Paul

Unravelling Ophiolite Emplacement History With Microfossils – The Baer-Bassit Ophiolite of NW Syria

Daniel Paul Howard

Thesis submitted for the degree of Doctor of Philosophy
Department of Earth Sciences
University College London
February 2006

ProQuest LLC
789 East Eisenhower Parkway
P.O. Box 1346
Ann Arbor, MI 48106-1346

ABSTRACT

The Baer-Bassit ophiolite of NW Syria is one of a number of ophiolites that form a chain from Cyprus in the West to Oman in the East. Micropalaeontological analyses of samples collected from the Baer-Bassit area reveal details of the various stages of evolution of the ophiolite as well as the Arabian continental margin. Interpillow sediments and cements proved to be barren of any microfauna or microflora, unlike comparable sediments from the Cyprus Troodos ophiolite, therefore no age of formation of the ophiolite can be inferred.

Campanian age sediments from the autochthonous carbonate platform structurally beneath the ophiolite are here reported for the first time, and are dated by the presence of zonal radioalaria including *Amphipyndax pseudoconulus* and *Foremanina schona.* Planktonic foraminifera including *Globotruncana calcarata* also indicate a Campanian age for the sediments immediately beneath the overlying ophiolite. The youngest autochthonous sediments are perhaps earliest Maastrichtian, but although no specific marker taxa were recovered the overall assemblages from these samples indicate a Campanian age is more likely. Immediately prior to ophiolite emplacement southwards onto the Arabian continental margin, an increase in water depth, reflected in the microfossil assemblages recovered, perhaps signalled flexural loading of the continental shelf by the approaching ophiolitic nappes.

After emplacement the ophiolite was emerged and eroded for a short time (c 2-3Ma) before being transgressed during the latest Campanian - earliest Maastrichtian. Shallow water sandstones and conglomerates, with common larger benthic foraminifera were then locally deposited for a short time before pelagic sedimentation was re-established. The dating of the sediments structurally beneath and overlying the ophiolite limits the age of emplacement of the Baer-Bassit ophiolite to the latest Campanian – earliest Maastrichtian. The deposition of pelagic carbonates continued until the latest Maastrichtian. The Cretaceous-Tertiary boundary is marked by a sedimentary hiatus spanning planktonic foraminiferal zones Pα, P0 and P1a. There is no visible change in lithology between the Cretaceous and early Tertiary sediments with both consisting of monotonous marls and marly limestones.

Reworked Cretaceous foraminifera occur commonly in the Danian sediments, sometimes dominating assemblages, particularly within sediments dated as belonging to the P1c *Globanomalina compressa/Praemurica inconstans-Praemurica uncinata* Interval Subzone. Pelagic carbonate sedimentation then continued until the Upper Eocene, when regional tectonics (suturing of the Eurasian and Arabian plates) caused syn-depositional deformation as well as regional uplift, reflected in the depositional of nummulitic limestones.

TABLE OF CONTENTS

LIST OF FIGURES AND TABLES IN THE TEXT

Figures

Text Tables

Plates

CHAPTER 1: INTRODUCTION

1.1 INTRODUCTION

The Baer-Bassit ophiolite of northwest Syria is part of the Peri-Arabic ophiolite crescent (Ricou, 1971) that extends to Cyprus in the west and Oman in the east and is part of a broader chain of ophiolites that stretches from the Alps to the Himalayas. During the late Mesozoic and early Tertiary closure of Neotethys these Peri-Arabic ophiolites were emplaced southward onto the Arabian continental margin. Of all the ophiolites in the Peri-Arabic crescent, Baer-Bassit remains one of the least well known. In particular, there is a lack of micropalaeontological studies constraining the age of Mesozoic passive margin sediments (the Baer-Bassit mélange), ophiolite formation and emplacement, and the subsequent sedimentary history of the area.

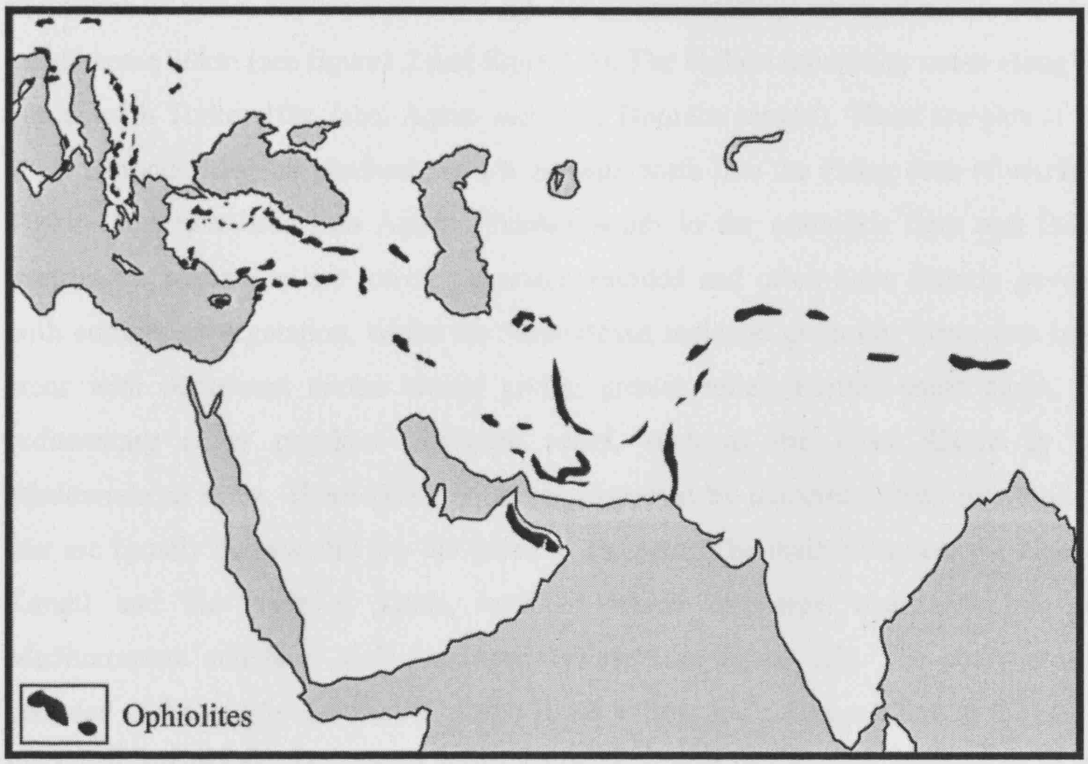

Figure 1.1. Sketch map showing the distribution of ophiolites through the eastern Mediterranean, the Middle East and western Asia. Modified from Lippard *et al.* (1986).

Ophiolites are preserved fragments of oceanic lithosphere and associated sediments that have been obducted onto continental crust, and were first recognised as such in the 1970's after the unifying theory of plate tectonics provided a model for their

occurrence. Previously these bodies of mafic to ultramafic rocks were thought to be either intrusive or extrusive in nature with a cumulate or magmatic origin. However, an inherent problem with these models was the lack of any contact metamorphic aureole in the sedimentary rocks within which they occurred (see Chapter 2). Once ophiolites were recognised as obducted slabs of oceanic crust a flurry of papers emerged proposing various massifs as ophiolites, including Troodos on Cyprus. Since then most of the ophiolites of the Peri-Arabic crescent have been extensively studied, particularly Troodos and the Semail ophiolite of Oman.

1.2 PHYSICAL GEOGRAPHY OF THE BAER-BASSIT AREA

The study area extends some 50km from the border with Turkey in the northwest of Syria, southwards down the Levantine coastline to the Latakia area and inland some 30km (see figure1.2 and figure1.3). The highest mountains occur along the border with Turkey (the Jebel Aqraa and Qara Dourâne ranges). These are part of the autochthonous Arabian platform, which extends north into the Hatay area of southern Turkey and eastwards into Arabia. Further south in the ophiolitic Baer and Bassit massifs the mountains are lower, generally rounded and often quite densely covered with coniferous vegetation, whilst the Baer-Bassit mélange generally forms low lying areas with occasional exotic blocks giving greater relief. Further south again, the sedimentary cover provides moderate relief, such as the Jebel Rhouz by the Mediterranean coast. These hills are deeply dissected by numerous steep river valleys that are usually narrow and dry for much of the year. The main rivers are the Nahr el Kandil and the Nahr el Kebir, both of which discharge westwards into the Mediterranean and have well-developed valleys (see figure 1.3). The study area is bounded to the east by the Nahr el Kebir River valley, and a further 30km to the east is the Ghab depression. This broad north-south orientated valley is an expression of the northwards extension of the Dead Sea Fault system.

Vegetation is largely dependent upon the underlying geology. The mountainous Jebel Aqraa and Qara Dourâne are sparsely vegetated with low-lying scrub whilst, as previously stated, the Baer and Bassit massifs are often densely wooded. The low-lying areas underlain by the mélange are mostly used for the cultivation of olive trees whilst citrus fruits are the dominant harvest on the alluvium of the valley floors and to a lesser

extent on the sedimentary cover. The climate is quite typical of Mediterranean countries with hot and dry, though often humid, summers, and cool wet winters.

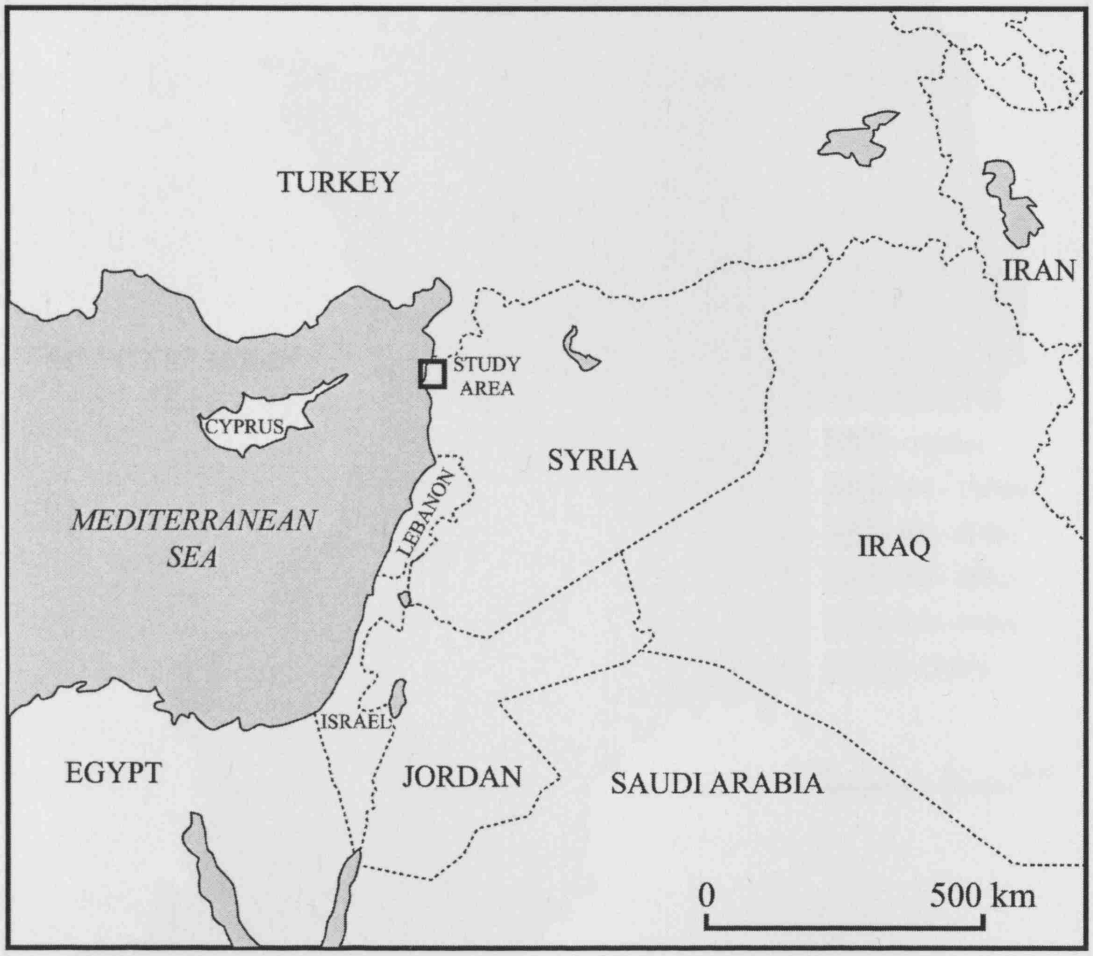

Figure 1.2 Map of the Eastern Mediterranean and the Arabian platform.

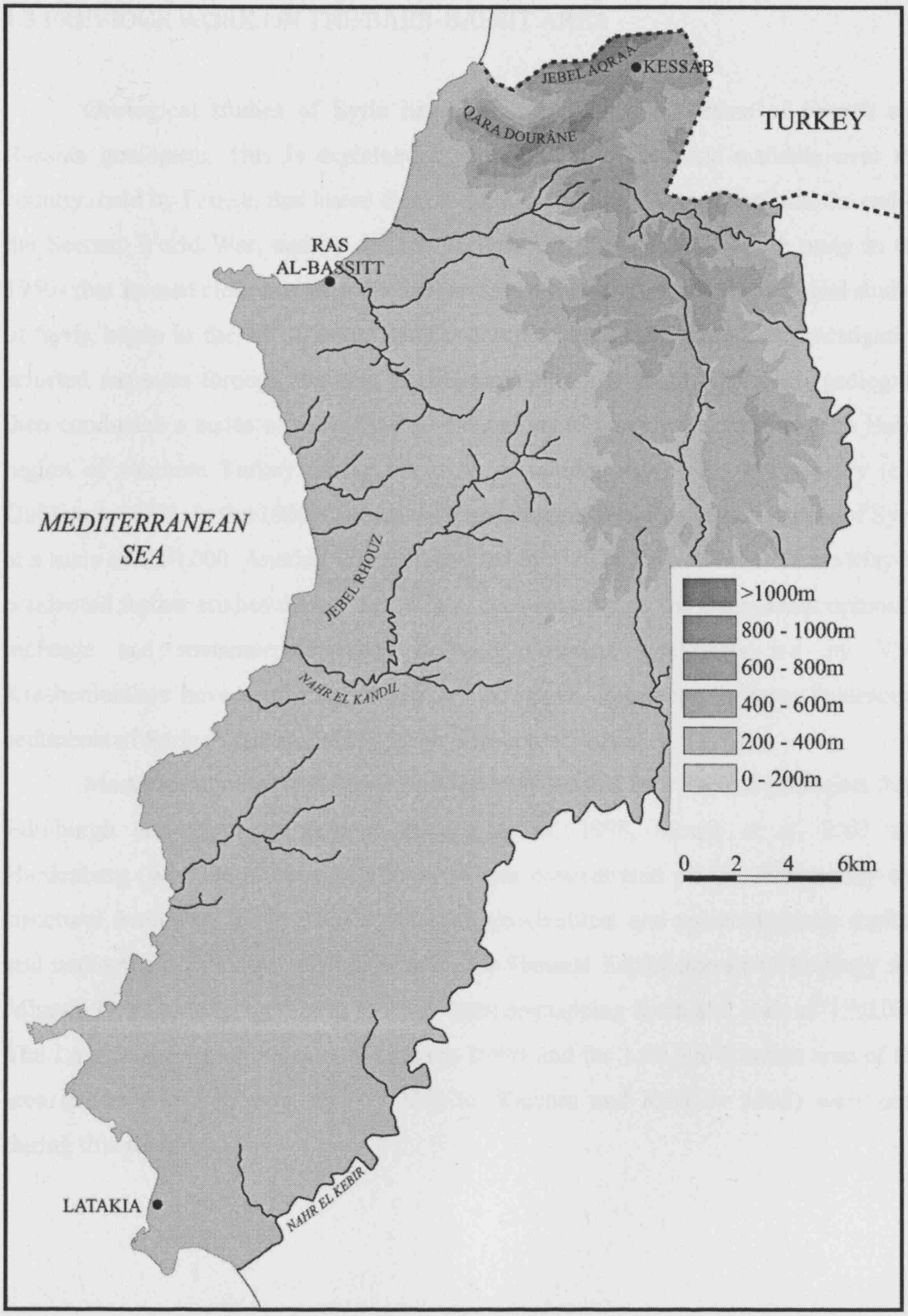

Figure 1.3 Topographic map of the study area showing the main rivers and the mountainous border area.

1.3 PREVIOUS WORK ON THE BAER-BASSIT AREA

Geological studies of Syria have been dominated by teams of French and Russian geologists. This is explained by the League of Nations mandate over the country, held by France, that lasted from the end of the First World War until the end of the Second World War, and by the rise to power of the socialist Ba'ath party in the 1950s that formed close ties with the former Soviet Union. The initial geological studies of Syria began in the 19th Century with a group of European geologists investigating selected transects through the area (Al-Riyami, 2000). A group of French geologists then conducted a series of geological investigations of north-west Syria and the Hatay region of southern Turkey during the early to middle part of the last century (e.g. Dubertret, 1953). In the 1960's, a team of Russian geologists mapped the whole of Syria at a scale of 1:50,000. Another French team, led by J. F. Parrot and M. Delaune-Mayère conducted further studies during the 1970's, concentrating on the Baer-Bassit ophiolite, mélange and metamorphic sole. Recently, Russian geologists led by V.A. Krasheninnikov have conducted studies on the upper Cretaceous to lower Palaeocene sediments of Syria (Krasheninnikov 1994, Krasheninnikov *et al.* 1996).

Most recently the Baer-Bassit area has been studied by a team of geologists from Edinburgh and Plymouth (e.g. Al-Riyami *et al.* 1998, Morris *et al.* 2001 and Hardenberg (work in progress)). This work has concentrated on the sedimentary and structural evolution of the Baer-Bassit area, geochemical and palaeomagnetic studies, and neotectonics. Finally, geologists from the General Establishment of Geology and Mineral Resources in Syria have recently been re-mapping Syria at a scale of 1:50,000. The Latakia sheet (Adjemian and Khatoun 1999) and the 1:50,000 Russian map of the area (Sheet I-36-XXIV-4b, d; I-37-XIX-3c, Kazmin and Kulakov 1968) were used during this study.

1.4 PROJECT AIMS

Recent work on the Baer-Bassit area (e.g. Al-Riyami, 2000) has primarily concentrated on structural investigations of the Baer-Bassit ophiolite and associated mélange, with less attention paid to the underlying and overlying sediments. A limited number of samples from the mélange were dated using radiolaria, but otherwise previously published dates for units were accepted. Ongoing work on the sedimentary cover has concentrated largely on the role of strike-slip faulting (M. Hardenberg, Edinburgh University).

The aims of this present project were to attempt to:

1. Constrain the age of ophiolite formation.
2. Constrain the age of ophiolite emplacement onto the Arabian platform margin.
3. Examine the post-emplacement sedimentary history with regard to the age and palaeoenvironment of the sediments.
4: Examine aspects of the Baer-Bassit mélange to give a greater understanding of the history of a Mesozoic passive margin.

The dating of ophiolite formation was attempted by the study of umberiferous sediments within and overlying the pillow lavas. Umbers from Oman and Cyprus have yielded radiolaria (e.g. Tippit and Pessagno 1981) and Cypriot umbers have also yielded palynomorphs (Urquhart, pers. com). The age of ophiolite emplacement was constrained by dating the underlying sediments of the Arabian platform and the overlying sedimentary cover. Further samples were taken from the Baer-Bassit mélange as well as from sedimentary cover units on a more regional scale for age confirmation and elucidation of depositional environments.

1.5 FIELD AND LABORATORY WORK.

Fieldwork was undertaken during three field seasons. During the first field season in the autumn of 2000, spot samples were taken from throughout the study area, including from the Baer-Bassit melange. The majority of sample collection was undertaken during the second field season, in the summer of 2001, when the sediments immediately above and below the ophiolite were extensively sampled. A final field season in the summer of 2003 was undertaken to collect samples from sediments within the pillow lavas of the

Baer-Bassit ophiolite, as well as to collect any other samples from areas that were proving problematic.

In total 94 samples were collected from 11 logged sections and a further 128 spot samples were collected from 32 different areas. Of these samples 135 smear slides were made for nannofossil studies, 178 samples were washed for planktonic foraminifera and general microfossils, 24 samples were specifically processed for radiolaria, 10 samples were processed for palynology and 35 samples were sectioned for larger benthic foraminifera or because the samples were too hard to process in the normal way.

Figure 1.4 is a simple geological map indicating all the localities of samples that are mentioned in the text, and more detailed location maps can be found in the relevant chapters. Figure 1.5 is a summary of the stratigraphy of the field area with the stratigraphic intervals that were studied highlighted.

1.6 THESIS LAYOUT

This thesis uses microfossils as time and environmental indices but is not a taxonomic project in nature. Therefore a full list of key literature used for their identification is given in Appendix 1.2.

Processing methods used to liberate microfossils from collected samples are listed and, when appropriate, described in Appendix 1.1

Appendix 1.3 lists sample localities and brief lithological descriptions whilst Appendix 1.4 lists all the fauna found in studied samples. All important fauna are mentioned in the relevant chapters.

The samples, residues and studied slides are deposited in the collections of the Department of Earth Sciences, University College London.

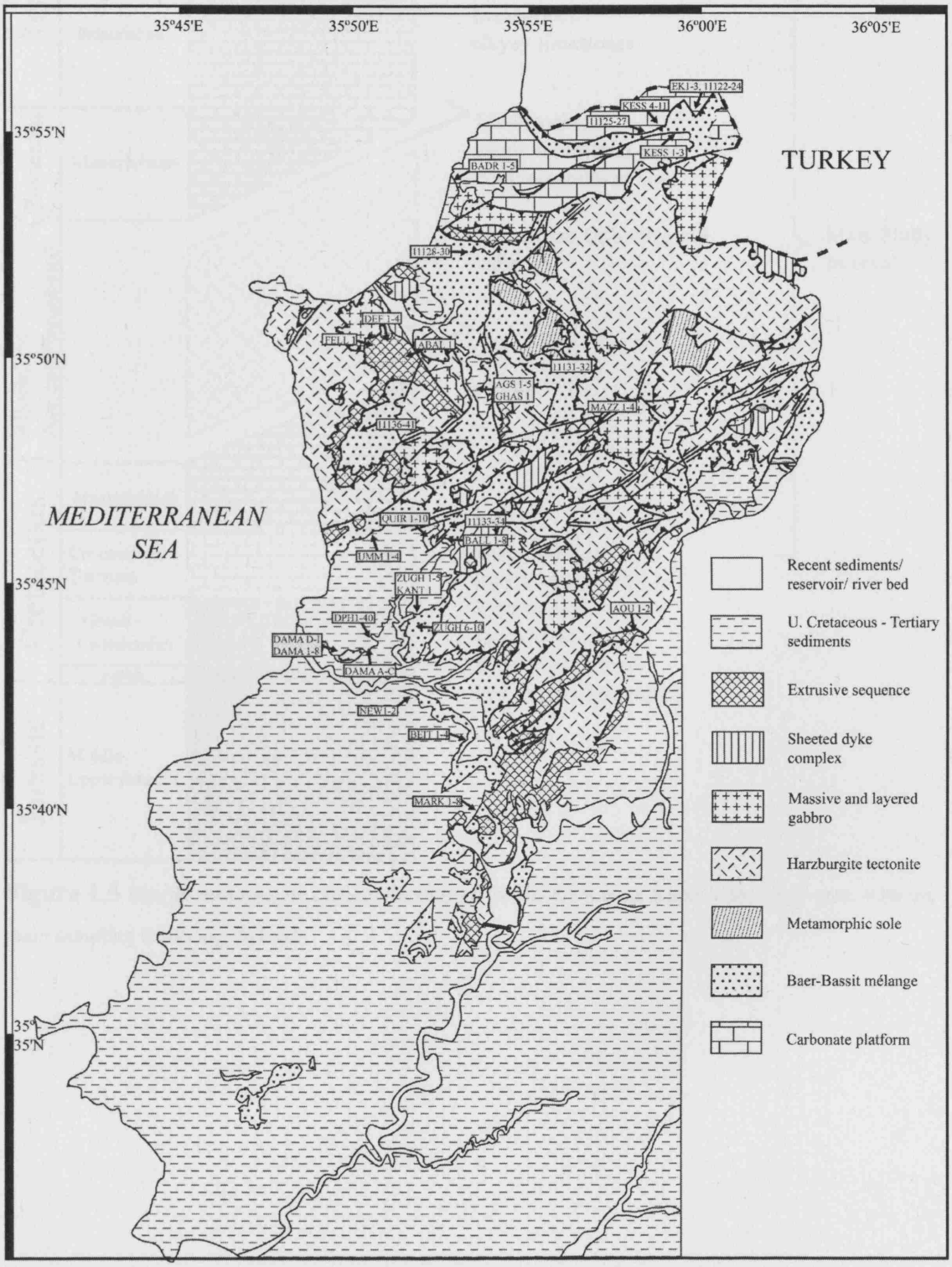

Figure 1.4 Geological map of the study area indicating sampling localities of samples mentioned in the text.

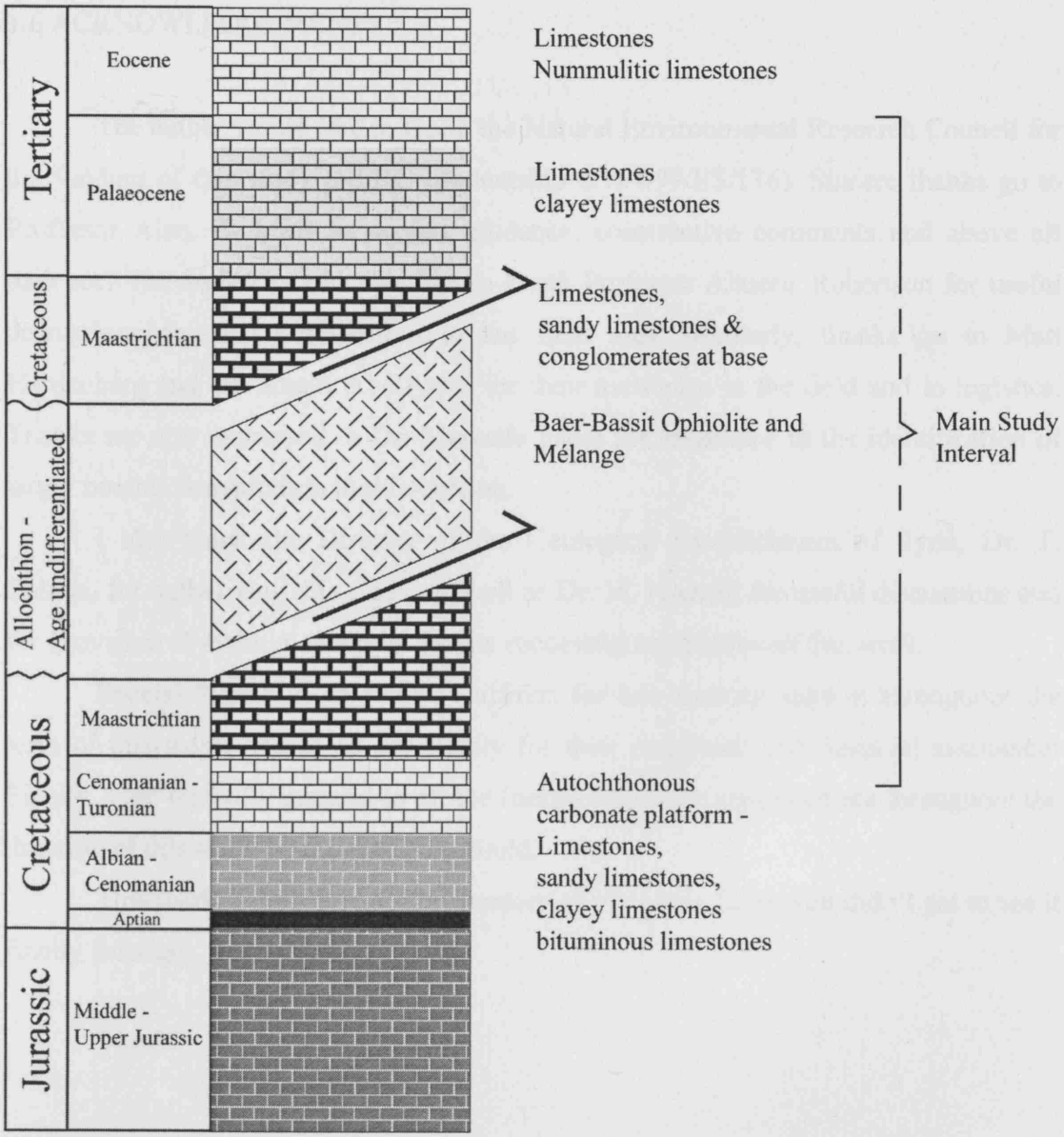

Figure 1.5 Simple stratigraphic column illustrating the different units found in the study area, with the main sampling levels highlighted

1.6 ACKNOWLEDGEMENTS

The author would like to thank the Natural Environmental Research Council for the funding of this study (NERC Studentship GT04/99/ES/176). Sincere thanks go to Professor Alan. R. Lord for expert guidance, constructive comments and above all patience! The author would also like to thank Professor Alastair Robertson for useful discussions and the introduction to the field area. Similarly, thanks go to Matt Hardenberg and Dr. Khalil Al-Riyami for their assistance in the field and in logistics. Thanks are also expressed to Dr. Marcelle Fadel for assistance in the identification of larger benthic foraminifera in thin-section.

I also thank the Director of the Geological Establishment of Syria, Dr. T. Ballani, for authorizing this study, as well as Dr. M. Humedi for useful discussions and the provision of material essential for the successful completion of this work.

Special thanks go to Freyja Coffman for her constant support throughout the term of this work, and to all my family for their emotional and financial assistance! Finally, I am eternally grateful to all the friends who have supported me throughout the duration of this study in any way they could.

This work is dedicated to the memory of my mum. Sorry you didn't get to see it finally finished.

CHAPTER 2: OPHIOLITES AND REGIONAL GEOLOGY OF THE EASTERN MEDITERRANEAN

2.1 INTRODUCTION

This chapter outlines the development of our understanding of how ophiolites are formed, and ties in current understanding of ophiolites with theories on the geological evolution of the Eastern Mediterranean. A review of the development of the ophiolite concept is undertaken and ophiolite genesis and models for obduction are discussed. The ophiolites of the Eastern Mediterranean, and their part in the Tethyan chain, are then briefly discussed along with their origins and role in the broader geological evolution of the Eastern Mediterranean.

This chapter therefore provides the reader with the necessary knowledge to understand the concepts discussed in more detail elsewhere, as well as the importance of ophiolitic study and the methods employed during this work.

2.2 DEVELOPMENT OF THE OPHIOLITE CONCEPT

The history of the development of the ophiolite concept has been nicely summarised by, among others, Coleman (1977), Moores (1982), McCall (1983) and Nicolas (1988).

As noted by Coleman (1977), Brongniart (1813) first used the term "ophiolite" to describe iron oxide, or various other disseminated minerals, enclosed in a serpentine matrix with a compact (unstratified) structure, and these serpentinites were seen to grade into talc schists and limestones with serpentine. Indeed the word "ophiolite" derives from the Greek root "ophi" which means snake or serpent, hence a snake-like rock, and in this respect it can be seen that Brongniart was initially using the term ophiolite synonymously with serpentinite. In later papers (Brongniart, 1821, 1827) he also included altered volcanics and gabbros, often associated with cherts, within his term ophiolite.

As noted by Coleman (1977) and Moores (1982) the first real attempt at the definition of an ophiolitic association was by Steinmann (1905, 1927). In these papers,

Steinmann, based mainly on observations he made in the Apennines, defined the term "ophiolite", which he applied to an association of peridotites, gabbros and diabase-spilites, as well as deep-water radiolarian cherts, clays and *Calpionella*-bearing limestones. In particular, the association of peridotites, diabase and deep-water radiolarites became known as the "Steinmann Trinity". In the later paper, Steinmann (1927) also argued for a magmatic origin for the igneous parts of the trinity, that is an assemblage of deep-water volcanics and associated sediments (McCall, 1983). However, as recalled by Nicolas (1988), despite the importance of the Steinmann's work, Amstutz (1980) argued that the ophiolitic association had been better defined by earlier workers, e.g. Lotti (1886) and Frianchi (1902).

From the 1930's until the unifying concept of plate tectonics was developed in the 1960's, two main schools of thought regarding the origin of ophiolites, and in particular the peridotite component, were established, and this history is dealt with in detail by Moores (1982) and Coleman (1977). In summary, either a magmatic or a cumulate origin was proposed for ophiolitic peridotites. The magmatic origin, proposed by Benson (1926), was based primarily on his work on Alpine peridotites, which he envisaged were the result of plutonic masses intruded into geosynclinal sediments (Coleman, 1977). The cumulate origin for peridotites was based largely on the experimental work of Bowen (1927) and work on stratiform complexes. Bowen (1927) suggested that peridotites were the result of gravitational settling of olivine crystals, that he showed were the first phase to form during fractional crystallisation of a basaltic magma (Moores, 1982).

For the next 30 years, as Moores (1982) summarises, the ophiolite concept was dominated by attempts at bringing these two opposite camps together. Vogt (1924) suggested that the addition of iron to the olivine system might allow the melting temperature of the system to be lowered significantly, thus accounting for the lack of metamorphic aureoles around peridotite complexes. However, Bowen and Schairer (1935) concluded that this was not the case. Hess (1938) then proposed a low temperature primary hydrous peridotite magma to account for the lack of significant metamorphic aureoles and the formation of serpentine. Again this was refuted by experimental evidence (Bowen and Tuttle, 1949), and thus the discrepancy between experimental models of peridotite formation and field observations remained.

As described by Moores (1982) and Coleman (1977), the work of Brunn (1940, 1959, 1960, 1961) primarily based on field studies at Vourinos in Greece was to provide

the next step in the development of the ophiolite concept. Brunn (1959) drew a comparison between the ophiolitic association and the characters of the mid-Atlantic ridge, and considered differentiation of a mafic magma extruded into rifts in the sea-floor to be responsible for the ophiolitic sequence of peridotites, gabbros and basalts, (Brunn 1960). This idea was further developed a few years later with respect to "geosynclines" by a co-worker of Brunn, Aubouin (1964). However, the differentiation of a basaltic magma could not produce the relative proportions of the mafic to ultramafic rocks seen in ophiolite suites, and as such an ultramafic parental magma was proposed (e.g. Maxwell and Azzaroli 1962, Vuagnat 1963).

The advent of the plate tectonic theory finally provided a mechanism by which high temperature ultramafic and mafic rocks could be emplaced within sediments without evidence of contact metamorphism. A number of papers then appeared proposing various ophiolites as fragments of oceanic crust obducted onto continental margins, including Moores (1970), Coleman (1971), Dewey and Bird, (1971), Davies, (1971), Moores and Vine (1971) and Church (1972). With the rapid progress in the field of ophiolite studies, a field-based symposium on ophiolites was convened, and out of this conference came the now widely accepted "Penrose" definition of an ophiolite:

"Ophiolite refers to a distinct assemblage of mafic to ultramafic rocks. It should not be used as a rock name or a petrologic unit in mapping. In a completely developed ophiolite, the rock types occur in the following sequence, starting from the bottom and working up:

Ultramafic complex, consisting of variable proportions of harzburgite, lherzolite and dunite, usually with a metamorphic tectonic fabric (more or less serpentinized);

Gabbroic complex, ordinarily with cumulus textures commonly containing cumulus peridotites and pyroxenites and usually less deformed than the ultramafic complex;

Mafic sheeted dike complex;

Mafic volcanic complex, commonly pillowed.

Associated rock types include (1) an overlying sedimentary section typically including ribbon cherts, thin shale interbeds, and minor limestones; (2) podiform bodies of chromite generally associated with dunite; and (3) sodic felsic intrusive and extrusive rocks.

Faulted contacts between mappable units are common. Whole sections may be missing. An ophiolite may be incomplete, dismembered, or metamorphosed. Although

ophiolite generally is interpreted to be oceanic crust and upper mantle, the use of the term should be independent of its supposed origin." Anon (1972).

However, a number of predominantly marine geologists and geophysicists were not convinced of these origins for various reasons. These included discrepancy between the thickness of average ophiolite complexes and of oceanic crust, and the tendency for ophiolitic rocks to display a calc-alkaline trend as opposed to the tholeiitic trend one would expect from mid-ocean ridge basalts, as well as other major and minor element differences (Moores 1982). In particular Miyashiro (1973, 1975a, b, c), using geochemical data, argued for an island arc origin for the Troodos complex, and further geochemical work led to many other ophiolites being assigned to different tectonic settings rather than the mid-ocean ridge origin widely proposed (Nicolas 1988). Another problem with the Penrose definition was that it also failed to mention the importance of associated mélanges (McCall 1983). Thus Moores (1982) was led to produce an expanded ophiolite association to help infer the origin and the emplacement, the main points of which are as follows:

1: A crystalline basement and a shallow water platform sedimentary sequence unconformably deposited over it.
2: A tectonic unit involving a series of thrust slices and/or a melange complex, superposed over the crystalline basement.
3: Metamorphic rocks.
4: Ultramafic tectonite zone.
5: Cumulate complexes.
6: Noncumulus units.
7: Dike complex.
8: Extrusive section.
9: Oceanic sediments.
10: Post-emplacement deposits.

The above definition is that which has been generally followed since 1982 and was used during this work, though as will be seen this is an idealised association and commonly several of the above units may be either poorly represented or entirely absent.

2.3 OPHIOLITE GENESIS AND THEIR ROLES IN THE STUDY OF OCEANIC CRUST.

The study of oceanic lithosphere is inherently made problematic by the difficulties in directly sampling the crust, and studies have largely relied on indirect observation methods. The initial recognition that ophiolites represented portions of oceanic crust and upper mantle that had been tectonically emplaced during orogenic episodes provided an opportunity to directly sample and study oceanic lithosphere. Consequently, a wealth of studies in the early seventies concentrated on ophiolites throughout the world, in an attempt to tell us about the genesis of oceanic crust, ocean-ridge processes and tectonic emplacement or obduction. Initial studies suggested that ophiolites represented typical oceanic crust formed at mid-oceanic ridges, however, subsequent geochemical studies (e.g. Miyashiro 1973, Pearce & Cann 1973) challenged this idea and suggested that most ophiolites in fact represent atypical oceanic crust formed in a variety of settings. It is now generally accepted that the considerable variation in ophiolite geochemistry is due to a number of factors including tectonic setting of formation and oceanic spreading rate. Tectonic settings proposed for ophiolite genesis include both fast and slow spreading mid-ocean ridges that may be close to, or far from continental margins, back-arc basins, narrow or incipient ocean basins, island arcs, mid-plate settings (hot spot related) and supra-subduction zones (Moores 1982). Early attempts to distinguish ophiolites and their possible modes and sites of formation concentrated on the major and trace element data of the extrusives and dykes (e.g. Miyashiro 1973), whilst recently increasing emphasis has been placed on the ultramafics as well as geologic and structural relationships. The complementary studies of ophiolites and oceanic lithosphere are vast subjects involving structural, geochemical and petrological data from both sources. The ideal situation would be to be able to delineate processes occurring today by the study of ophiolites, and conversely, understand the processes that led to the formation of ophiolites by studying present day oceanic lithosphere formation.

Despite the inherent problems in associating two relative unknowns, attempts have been made to assign various types of ophiolites to present day tectonic settings and vice-versa. Broadly speaking, it is thought that fast spreading and slow spreading ridges can be identified in ophiolites (e.g. Nicolas & Boudier 1975, Nicolas 1988, Alexander & Harper 1992, Smith 1993) by comparison with features identified at modern ridges

(e.g. Macdonald 1982). Fast spreading ridges are typically of the harzburgite type whilst slow spreading ridges are lherzolitic due to the degree of partial melting (higher at fast spreading and lower at slow spreading ridges). Structural features also differ depending on spreading rate, e.g. rift development, and these features are largely independent of the tectonic setting of the spreading ridge (Alexander & Harper 1992). Based on their geochemistry, many different ophiolites have been assigned to different tectonic settings. A large number of the eastern Tethyan ophiolites are thought to have formed above supra-subduction zones to explain the highly magnesian boninitic lavas, formed by the partial melting of hydrated oceanic lithosphere (e.g. Pearce *et al.* 1984) as well as their trace element signature and the development of chromite mineralization (Roberts 1992).

Intimately associated with many ophiolites are fine-grained mudstones, rich in iron and manganese oxides and oxy-hydroxides and enriched in trace elements relative to associated overlying sediments (Robertson and Hudson 1973, 1974; Fleet and Robertson 1980). These sediments are called umbers, and were first described in detail by Robertson and Hudson (1973) from the Troodos ophiolite of Cyprus, where they are associated with the upper pillow lava sequence of the ophiolite. Due to their porous nature they are usually of fairly low density, and the colour is variable from shades of orange through reds and browns to black. Umbers are often associated with ochres, from which they differ by being enriched in manganese, and radiolarian cherts. A typical succession would see umbers within and just above a pillow lava unit, passing up into radiolarites and radiolarian cherts and then pelagic carbonates.

Umbers were originally thought to have been secondary products formed by the weathering and alteration of volcanic sediments (see Robertson 1975 for a review). Gradually a primary source for the umbers was accepted, with theories ranging from sub-marine weathering of pillow lavas (Constantinou and Govett 1972) through to association with sulphide mineralization and ochre formation (e.g. Corliss *et al.* 1972) and biologically formed sediments (Zomensis 1972). It is now widely accepted that umbers are the result of slightly off-axis hydrothermal activity, with circulating waters discharging metal laden brines onto the sea floor and within the upper levels of the pillow lavas (e.g. Bostrom 1973; Robertson 1975; Fleet & Robertson 1980; Goulding *et al.* 1998). This theory has been reinforced by the large amount of data gathered during the DSDP, ODP and NOAA cruises, where such processes have been observed forming umbers and other metalliferous sediments at the present day, for example, on the TAG

hydrothermal mound at 26°N, Mid-Atlantic Ridge (Rona 1980, Goulding *et al.* 1998) and on the East Pacific Rise (Froelich *et al.* 1977, Heath & Dymond 1977).

2.4 OPHIOLITE EMPLACEMENT MODELS.

In considering emplacement models, as well as looking at the origins of the ophiolitic units, it is necessary to study where the vast majority of ophiolites occur today. Ophiolite distribution can largely be divided into three structural environments: passive margins, active margins and collision belts (e.g. Nicolas 1988). Ultimately, the fate of all ophiolites is in collision belts and the emplacement can be seen as an evolutionary sequence involving either passive or active margins. All these settings are discussed together below.

1) *Initial detachment of oceanic lithosphere.* Ophiolites were initially thought to be emplaced during continental collision, however, subsequent studies suggest that the majority of ophiolites were initially detached and emplaced whilst relatively young and still hot, as evidenced by the inverse high temperature-low pressure (HT) metamorphic aureoles or "metamorphic soles" located beneath many ophiolite complexes. These soles, though often incomplete or dismembered, ideally display pyroxene-hornfels to granulitic or amphibolite facies just below the basal thrust of the ophiolite, passing down to greenschist facies within just a few hundred metres (Nicolas 1988), thus displaying a steep inverse metamorphic gradient. The overlying ultramafics are usually highly tectonised. The high temperatures required to metamorphose the underlying protoliths (typically up to 1000°C) therefore support the model of initial detachment and emplacement of the ophiolite whilst still hot in an intraoceanic setting. The establishment of the age of formation of these metamorphic soles by K-Ar radiometric dating also supports this idea of initial detachment and emplacement of the lithosphere whilst still young, with obduction onto continental crust occurring significantly later (e.g. Thuizat *et al.* 1981, Whitechurch *et al.* 1984, Jones *et al.* 1991, Alexander & Harper 1992; Spray *et al.* 1984). Many models have been proposed to explain the initial detachment of a slab of oceanic lithosphere, with most requiring the transformation from an extensional to a compressional regime in the oceanic realm. Nicolas (1988) summarises the two main geodynamic models proposed

for the initiation of an oceanic thrust, a pre-requisite for detachment. The first is illustrated in figure 2.1a, and occurs at the spreading ridge at which the ophiolite is created. In this model, a rapid change from oceanic spreading to compression provides a decoupling surface between the lithosphere and the asthenosphere, which remains at shallow depths. Robertson & Dixon (1984) propose asymmetrical ridge collapse as a model for the detachment of lithosphere at the ridge (figure 2.1b), whilst other authors, including Casey & Dewey (1984), suggest that a change in the direction of spreading along a transform system could result in detachment of oceanic crust (figure 2.1c).

The second main geodynamic model suggests detachment away from the ridge of origin, and is illustrated in figure 2.1d. The model, proposed by Dewey in 1976, and later developed by Nicolas and Le Pichon (1980) suggests that stresses in a young, subducting slab, could result in the seaward propagation of a thrust along the plane of maximum resolved shear stress.

2) *Intraoceanic thrusting and obduction.* After the development of a detachment surface, the next stage is intraoceanic displacement of the slab. In the case of ridge detachment (figures 2.1a-c) the detached thin lithospheric slab is thrust over oceanic crust. It is at this point that the metamorphic sole is developed. Thrusting can then proceed until the lithospheric nappe meets and is emplaced upon a passive margin, or the slab may remain in the oceanic realm becoming a plateau (Nicolas 1988). During emplacement another episode of metamorphism may occur, this time with a high pressure-low temperature (HP) signature. The margin of the continent or island-arc begins to enter the subduction zone under the weight of the overlying oceanic nappe or nappes, but this ceases when subduction is blocked by the buoyant crust, and the margin then rebounds (Moores 1982; Nicolas 1988). This situation has been proposed to explain the HP metamorphics of the Oman margin as well as occurrences of HP metamorphics within the margin formations beneath many other ophiolite complexes. The isostatic rebound of the margin could also facilitate the final emplacement of the ophiolite by gravity sliding.

3) *Incorporation into a collision belt.* This is the ultimate fate of most *Tethyan* type ophiolites, and ophiolite belts around the world mark ancient collision zones (see Chapter 2.5 for discussion).

In the case of ophiolite belts and active margins (so-called *Cordilleran*-type ophiolites), the situation is different. Initial detachment and intraoceanic thrusting follow the same evolution as for the *Tethyan* type ophiolites, though here figure 2.1d is also a viable model. Additionally, these ophiolites typically occur as glaucophanitic or eclogitic blocks within an HP metamorphic mélange (Nicolas 1988), and this reflects the emplacement processes responsible. Whether derived from the downgoing plate or the overriding plate, the lithosphere is subjected to high pressures as it is quickly buried in the subduction zone and incorporated into an accretionary complex. The processes involved in the exhumation of this material are still poorly understood (Nicolas 1988).

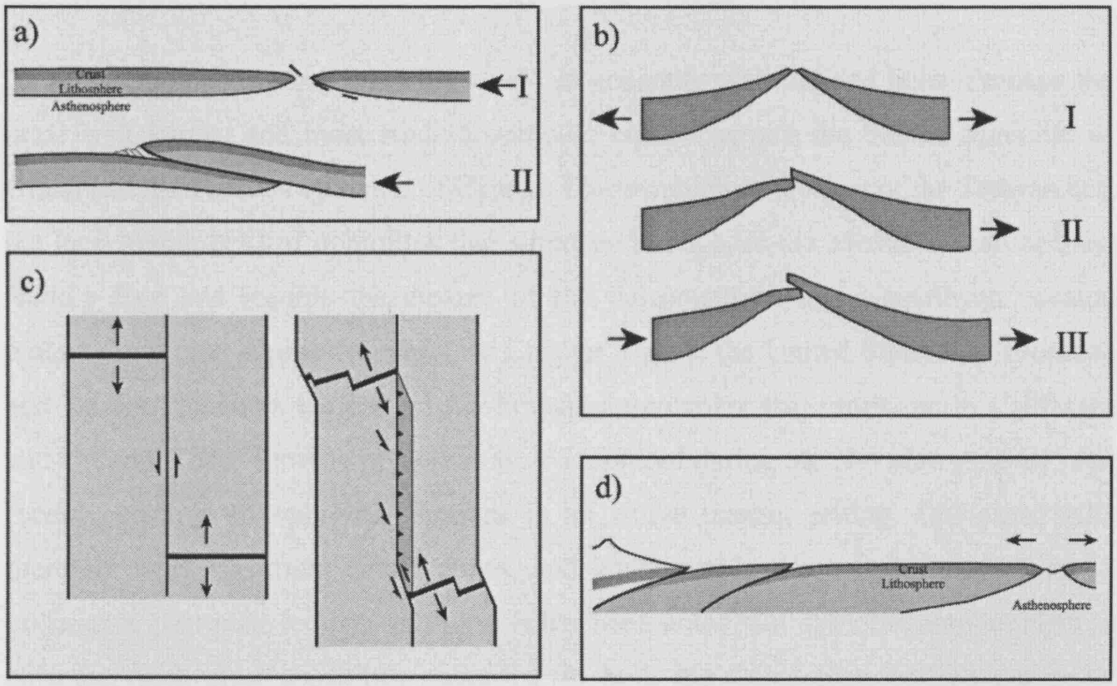

Figure 2.1. Different models for the initial detachment of oceanic crust. a) A rapid change from an extensional to compressional regime facilitates decoupling along the lithospheric/asthenospheric boundary (simplified from Boudier *et al.* 1982). b) Asymmetrical spreading causes the collapse of the left ridge (II) which then underthrusts the right ridge (III) (simplified from Robertson & Dixon 1984). c) A change in spreading orientation initiates a subduction zone within a transform system (simplified from Casey & Dewey 1984). d) Young oceanic crust entering a subduction zone fractures along the plane of maximum resolved shear stress (simplified after Boudier *et al.* 1982).

Ophiolitic mélanges are formed and incorporated into the ophiolitic complex during the emplacement process. They are generally a mixture of ophiolitic and exotic rocks within an often highly sheared matrix of either serpentinite and/or sedimentary rocks (Gansser 1974). It is clear that a variety of processes, both sedimentary and tectonic, lead to the formation of mélanges. Therefore, there is a variety of types of

mélange ranging from those with little or no matrix of either a sedimentary or igneous composition, to those almost entirely consisting of matrix with only scattered exotic blocks. Mélanges are preferentially produced during the emplacement of the *Tethyan* type ophiolites as demonstrated by their common occurrence throughout the Mediterranean but scarcity along the western coast of America (Gansser 1974). See Chapter 4 for further discussion.

2.5 OPHIOLITE DISTRIBUTION AND THEIR ROLE IN PLATE TECTONICS

Ophiolites occur around the world in generally well defined belts. Perhaps the most well known and most studied ophiolite complexes are the Semail ophiolite of Oman and the Troodos ophiolite of Cyprus. These ophiolites are part of the Tethyan belt (or Peri-Arabic belt) of ophiolites that stretches throughout the Mediterranean and the Middle East and records the closure of the Palaeotethyan and Neotethyan oceanic realms during the Alpine orogeny (see Chapter 2.6). In the United States the Josephine and Trinity ophiolites are part of the Fransiscan complex that crops out in California and Oregon. These Jurassic ophiolites were emplaced during the Nevadan orogeny, and record accretion of ophiolitic terranes in an active margin setting. Ophiolitic belts therefore mark important suture zones, and consequently are valuable in helping to understand past plate tectonic motions. It has been noted that ophiolite emplacement is episodic, with most ophiolites occurring in both the Caledonian or Tethyan belts, marking emplacement in two major pulses (Abbate et al. 1985, Sheridan 1987), and that in this way they are intimately linked to the Wilson Cycle (Dewey and Burke 1974).

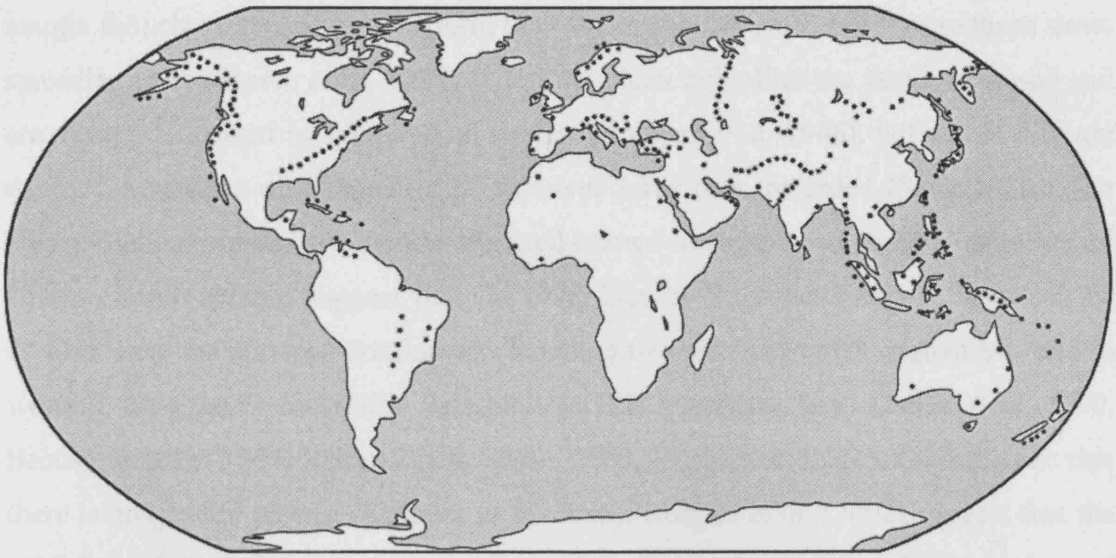

Figure 2.2. Distribution of the world's principal ophiolite belts (modified from Irwin & Coleman 1972)

2.6 OPHIOLITES OF THE EASTERN MEDITERRANEAN

The ophiolites of the eastern Mediterranean are part of the Tethyan chain of ophiolites that stretches from the Western Mediterranean to the Himalayas (see figure 1.1). These ophiolites were created in a variety of settings during the evolution of the Paleotethys and Neotethys oceans and many have been extensively studied to aid the understanding of the Tethyan region. It is now generally accepted that within the Mediterranean region of Tethys the ophiolitic belt can be roughly divided into older Jurassic complexes in the west and younger complexes to the east (Rocci *et al.* 1975, Abbate *et al.* 1983, 1985, Nicolas 1988). The Jurassic ophiolites of the western Mediterranean include the Ligurian ophiolites of the internal Alps and the Apennines, the Carpathians, and the N-S orientated Dinarides and Hellenides of the former Yugoslavia, Albania and Greece (Knipper *et al.* 1986, Koepke *et al.* 2002). The Ligurian ophiolites have dominant lherzolitic ultramafics and tholeiitic MORB-type extrusives (Beccaluva *et al.* 1979) and lack a well developed sheeted dyke complex (e.g. Koller & Höck 1990), with any dykes present post-dating initial emplacement. Ophicalcites are frequently developed at the base of the pillow lavas, or if these are absent, beneath overlying radiolarites and micritic limestones (Knipper *et al.* 1986). The proposed setting of formation therefore is a narrow ocean basin (as evidenced by silicic deposition during ophicalcite formation and infilling of the basin by a continental

margin fan) characterised by transform fault zones (Abbate *et al.* 1983) or perhaps slow-spreading rates (Pearce *et al.* 1984). The Carpathian ophiolites are poorly exposed and are mostly delineated by geophysical studies (Knipper *et al.* 1986), but where they are exposed extrusives of a tholeiitic MORB-type have been recorded (Savu 1980). The Dinaro-Hellenic ophiolites include the well-known Vourinos and Pindos ophiolites of Greece. Some authors suggest that the ophiolites in Yugoslavia and Albania can be divided into an eastern, dominantly harzburgitic belt with SSZ signatures, and a western, dominantly lherzolitic belt with MORB signatures (e.g. Shallo *et al.* 1990, Beccaluva *et al.* 1994, Robertson & Shallo 2000, Höck *et al.* 2001). Others argue that there is no general pattern (Knipper *et al.* 1986). Koepke *et al.* (2002) suggest that the ophiolites of Crete form the southern limit of the Dinaro-Hellenic ophiolites, and are of Jurassic age, whilst the ophiolites of Karpathos and Rhodes represent the western limit of the Cretaceous ophiolites of the Peri-Arabic crescent.

The Pontic and Lesser Caucasus ophiolites form a belt along the southern margin of the Pontides to the Caucasus. Within the Pontides the ophiolites range from Triassic to Late Cretaceous in age. These ophiolites are dominantly harzburgitic, with the Late Jurassic ophiolites having MORB-type and alkaline extrusives and the younger ophiolites having alkaline to calc-alkaline extrusives (Knipper *et al.* 1986). The ophiolites are largely dismembered, and in places show HP/LT metamorphism (Robertson 2002). The Jurassic ophiolites are presumed remnants of a Palaeotethyan ocean (e.g. Şengör *et al.* 1980, Ustaömer & Robertson 1997, Yilmaz *et al.* 1997). The Late Cretaceous ophiolites, including the Ankara mélange (Tankut 1984, Tankut & Gorton 1990), and the ophiolites of Central Anatolia, are remnants of a northern Neotethyan strand (Robertson 2002). The ophiolites of the Lesser Causacus have a long and complicated history but probably formed sometime before the Mid Jurassic (Knipper *et al.* 1986).

In southern Turkey the Tauric ophiolites crop out along both the northern and southern flalnks of the Tauride carbonate platform (the Calcareous Axis). Some authors consider the Tauric ophiolites as a western extension of the Cypriot and Arabian units further to the southeast (e.g. Knipper *et al.* 1986) whilst others consider them separate (e.g. Juteau 1980). There is also strong disagreement as to whether the Tauric ophiolites, and the more southerly Arabian units, originated from a single Neotethyan basin to the north (e.g. Ricou *et al.* 1984, Whitechurch *et al.* 1984) or if the different belts were derived from separate basins (e.g. Robertson & Dixon 1984). Regardless of

the origin, the Tauric, and more southerly ophiolites show remarkable similarities in structure, geochemistry and age. The Tauric ophiolites include the Lycian nappes, Antalya nappes, Beyşehir-Hoyran-Hadim nappes and the Pozanti-Karsanti, Mersin and Pinarbaşi ophiolites (Juteau 1980, Robertson 2002). These ophiolites are of harzburgitic type with SSZ signatures and were derived from a northern Neotethyan ocean (e.g. Juteau 1980, Sengör & Yilmaz 1981, Dilek & Moores 1990, Parlak *et al.* 1996a, b, 2002, Andrew & Robertson 2002, Robertson 2002) perhaps originally as a single thrust sheet (Robertson 2002).

The Peri-Arabic ophiolites include the ophiolites of Cyprus, the Hatay, Kocali and Amanos ophiolites of southern Turkey and Baer-Bassit. Further east are the Guleman and Cilo ophiolites of eastern Turkey, the Iranian ophiolites of the Bitlis-Zagros suture zone and the western Makran, and the Semail ophioite of Oman (Pişkin *et al.* 1986, Hassanipak & Ghazi 2000, Kananian *et al.* 2001). All these ophiolites are Late Cretaceous in age and interpreted as having formed in a SSZ setting (Al-Riyami 2000).

Umbers have been noted and described from many Tethyan ophiolites, most famously Troodos (e.g. Moores and Vine 1971, Moores 1982, Robertson 1975, Robertson and Hudson, 1973, 1974, Hall *et al.*, 1988, Pantazis, 1986, Prichard & Maliotis 1998, Ravizza *et al.* 2001, Richards and Boyle 1986, Swarbick and Naylor 1980 and Whitechurch *et al.* 1984) but also the Semail ophiolite of Oman (Fleet & Robertson 1980, Robertson & Woodcock 1983, Tippit & Pessagno 1981, Lippard *et al.* 1986), the Hatay ophiolite of Southern Turkey (Robertson 1986, Dilek and Thy 1998), the Khoy ophiolite of Iran (Hassasipak and Ghazi 2000) and the Baer-Bassit ophiolite (e.g. Parrot & Delaune-Mayere 1974).

Ophiolitic mélanges are also widely distributed throughout the Tethyan realm. They include the Hawasina mélange of Oman, the coloured mélange of the Kahnunj complex of Iran (Kananian *et al.* 2001), the Ankara mélange and Antalya complex of Turkey and the Moni mélange and Mamonia complex of Cyprus, as well as the Baer-Baasit mélange of NW Syria. Further west mélanges are also associated with the Dinaride and Hellenide ophiolites. See Chapter 4 for further discussion.

2.7 REGIONAL GEOLOGY OF THE EASTERN MEDITERRANEAN

Understanding of the present-day geology and plate configuration of the Mediterranean still has its controversies, and unsurprisingly these increase the further back in geologic time we go, with a wide number of plate tectonic configurations postulated. Recent years have seen a plethora of tectonic reconstructions suggested for the region, based on kinematics, geophysics, geology, palaeomagnetism and palaeontology. A brief resume of current theories regarding the tectonic development of the region will be assessed with regard to the study area of northwestern Syria, mostly following Robertson & Dixon (1984), Dercourt *et al.* (1986) and Robertson (1998). Whilst the tectonic history of units involved in the easternmost Mediterranean is considered, those units further west in the central and western Mediterranean are not discussed as this is outside the scope of this work. However, the tectonic evolution of the easternmost Mediterranean is related to the motion of the African and Eurasian plates where relevant.

The basic present day plate tectonic configuration of the study area is summarised in figure 2.3, whilst figure 2.4 shows a more detailed map of the Eastern Mediterranean including some of the terranes mentioned in this chapter.

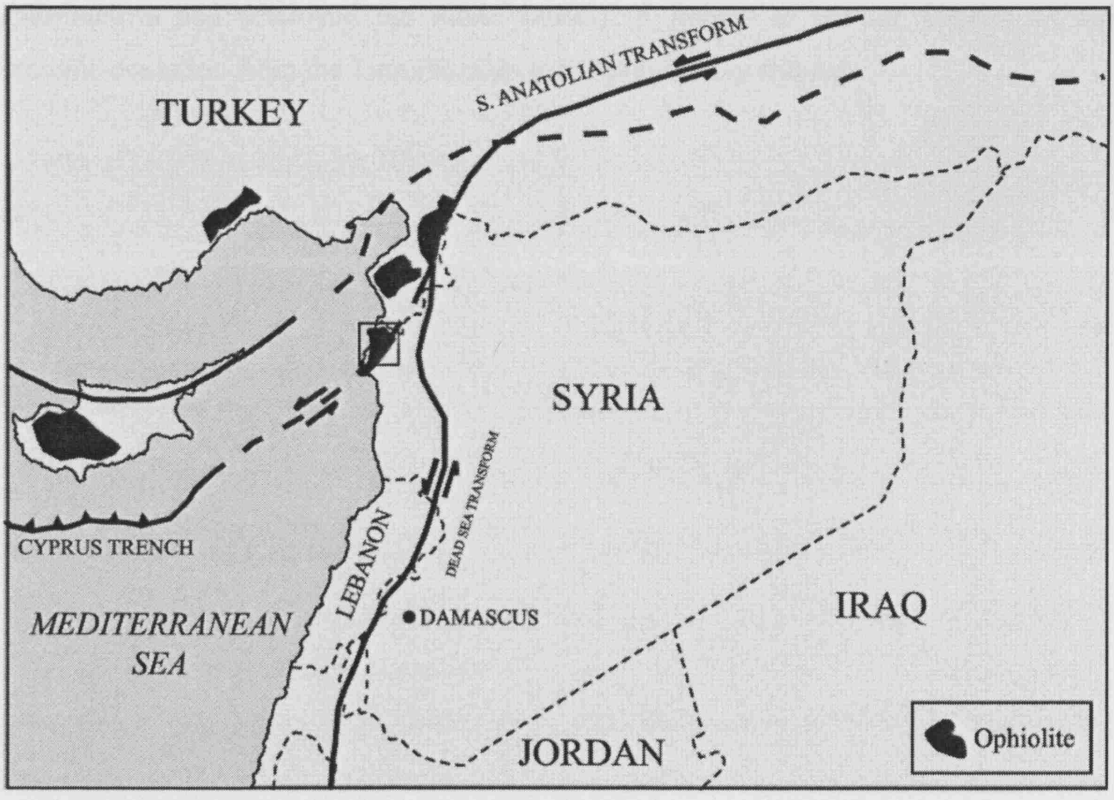

Figure 2.3 Simplified plate tectonic map of the study area.

Palaeotethys was formed during the Devonian to the Early Carboniferous when the European Hunic terranes rifted off Gondwana and moved north to collide with Laurussia, closing the Rheic ocean and opening up the Palaeotethys behind (Stampfli & Borel, 2002). Gondwana then moved north to collide with Laurussia and form the supercontinent of Pangea, with Palaeotethys existing as a wedge-shaped ocean to the east.

Whilst there are many conflicting theories on the continental configuration that formed Pangea (see Robertson and Dixon, 1984 for a discussion) there is general agreement that a wedge-shaped Palaeotethys ocean existed to the east, though its precise shape and extent are poorly constrained. The fate of this ocean is still the subject of major controversy with conflicting theories based on either a southerly subduction model (e.g. Şengör *et al.*, 1984) or a northerly subduction model (e.g. Adamia *et al.*, 1981). In most of the models for the closure of Palaeotethys (e.g. Robertson & Dixon, 1984, Dercourt *et al.*, 1986; 1990, Stampfli & Borel, 2002) the closure of the ocean is initiated by the rifting off of units from the northern margin of Gondwana, though the extent of these units varies considerably. As these units drifted northwards they closed Palaeotethys and opened up Neotethys behind (in much the same way as the opening of Palaeotethys had destroyed the Rheic Ocean). A review of current theories on the tectonic evolution from the Late Permian to the present day follows.

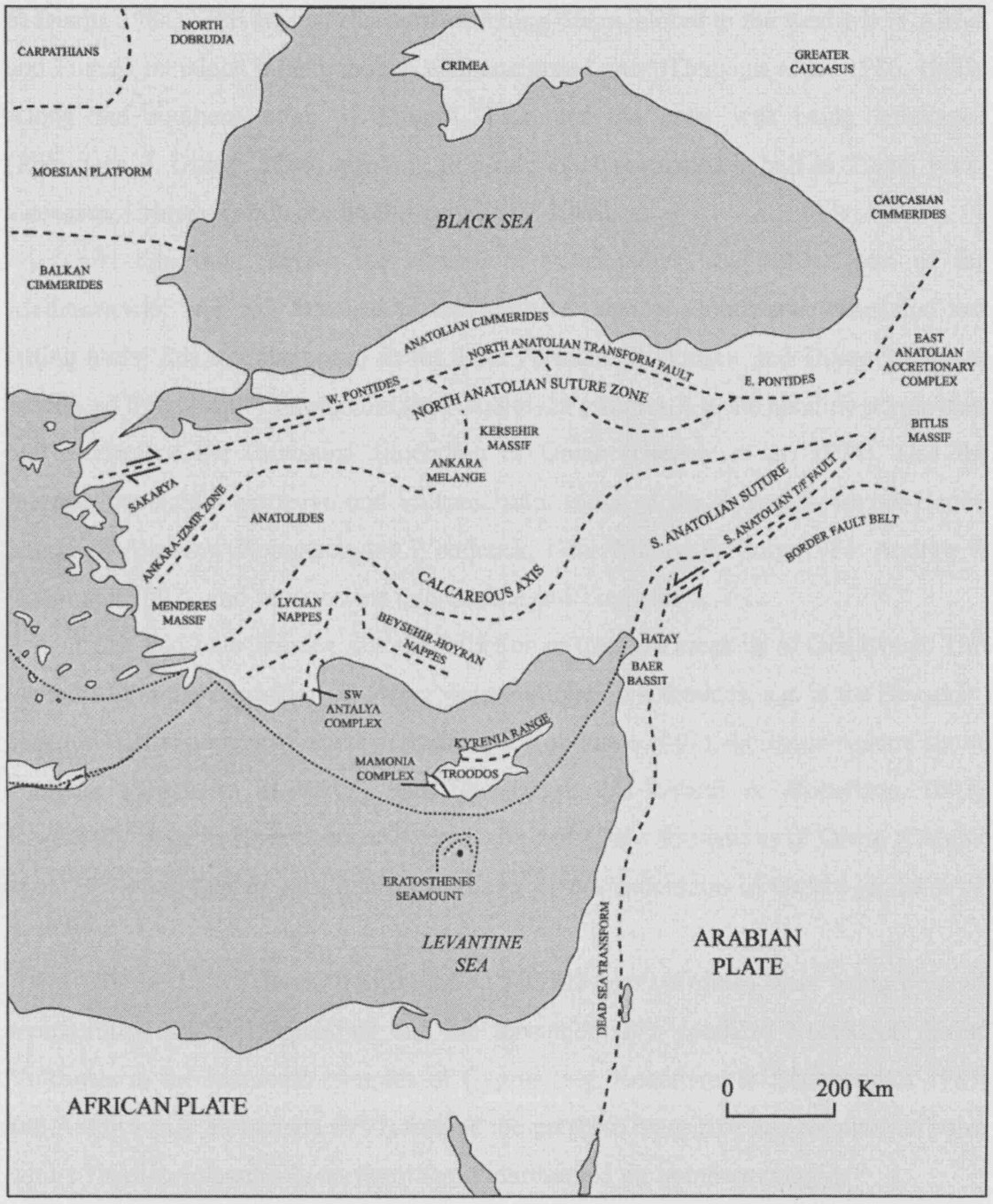

Figure 2.4. Outline sketch of the easternmost Mediterranean, illustrating the present day locality of some of the units mentioned in the text. Modified and simplified after Robertson and Dixon (1984).

2.7.1 LATE PERMIAN – TRIASSIC.

Conflicting palaeomagnetic and kinematic data prevent a confident reconstruction of the Tethyan region before the Jurassic (Savotsin *et al.*, 1986) but a number of conclusions can still be drawn. A major change in the shape of the supercontinent Pangea during the Permian to Triassic saw the creation of Palaeotethys by the dextral motion of Eurasia and North America with respect to Africa (Robertson

& Dixon, 1984). This was an eastward-widening ocean, closed to the west where Africa and Eurasia remained joined, though with attenuated crust (Dercourt *et al.*, 1986, 1990). Along the southern edge of Eurasia, Palaeotethyan crust was being subducted (Robertson & Dixon, 1984) resulting in a calc-alkaline magmatic belt in Turan, Fore-Caucasus, Crimea and Dobrudja (Kazmin *et al.*, 1986).

At this time, before the closure of Palaeotethys, the eastern part of the Mediterranean was still attached to the northern edge of Gondwana. Extension and rifting along this margin began in the Late Permian (Robertson and Dixon 1984), as evidenced by volcanics throughout the Neotethyan terranes, e.g. the alkaline porphryites and picrites of the Hawasina allochthon of Oman (Glennie *et al.* 1974), also the intermediate-acidic extrusive and volcaniclastic rocks of the Beyşehir-Hoyran-Hadim nappes of Anatalya (Robertson and Woodcock, 1984; Monod & Akay, 1984; Andrew & Robertson 2002), and further west into Greece and Yugoslavia.

The mid-Late Triassic saw the initiation of the final break up of Gondwana. This is recorded in the deposition of deeper water radiolarian sediments, e.g. in the Beyşehir–Hoyran–Hadim nappes of Turkey (Andrew & Robertson 2002), the Izmir-Ankara suture complex (Tekin *et al.* 2002) and Baer-Bassit (Al-Riyami & Robertson 2002). Regionally these sediments occur in the Halfa and Haliw formations of Oman (Glennie et al, 1974) and further west into the northern Pindos mountains of Greece (Jones et al. 1991).

By the Late Triassic transitional to MORB-type volcanics were being erupted, representing sea-floor spreading and the formation of a southern Neotethyan basin. Volcanics in the Mamonia complex of Cyprus (e.g. Robertson & Xenophontos 1983) and Antalya (e.g. Robertson 1990) formed the northern margin of this Neotethyan basin whilst Triassic volcanics in northern Syria represented the southern margin.

In conclusion, the Late Permian through to the Triassic saw the onset of closure of Palaeotethys by northward subduction along the south Eurasian margin and the creation of a southerly Neotethyan ocean as blocks rifted off the northern margin of Gondwana and migrated northwards (see figure 2.5).

2.7.2 JURASSIC

From the Early – Mid Jurassic to the early Late Jurassic, palaeomagnetic data suggest major strike-slip displacement between Africa and Eurasia, with Eurasia translating north-eastwards with respect to Africa and then back again along the same

track (Robertson & Dixon 1984). By the Late Jurassic the central Atlantic began to open, and Africa began to translate eastwards with respect to Eurasia, attaining a displacement of about 250km in 45My (Dercourt *et al.* 1986). Extension in the western Tethys and compression in the east followed (Robertson & Dixon 1984). This compression led to a narrowing of Neotethys to the east as well as a possible northward shift of the spreading centre (Dercourt *et al.* 1986). Robertson & Dixon (1984) suggest that a north-south Neotethyan ridge system in the Pindos Ocean collapsed under this compressive regime, leading to asymmetrical spreading and the formation of supra-subduction zone (SSZ) composition ophiolites.

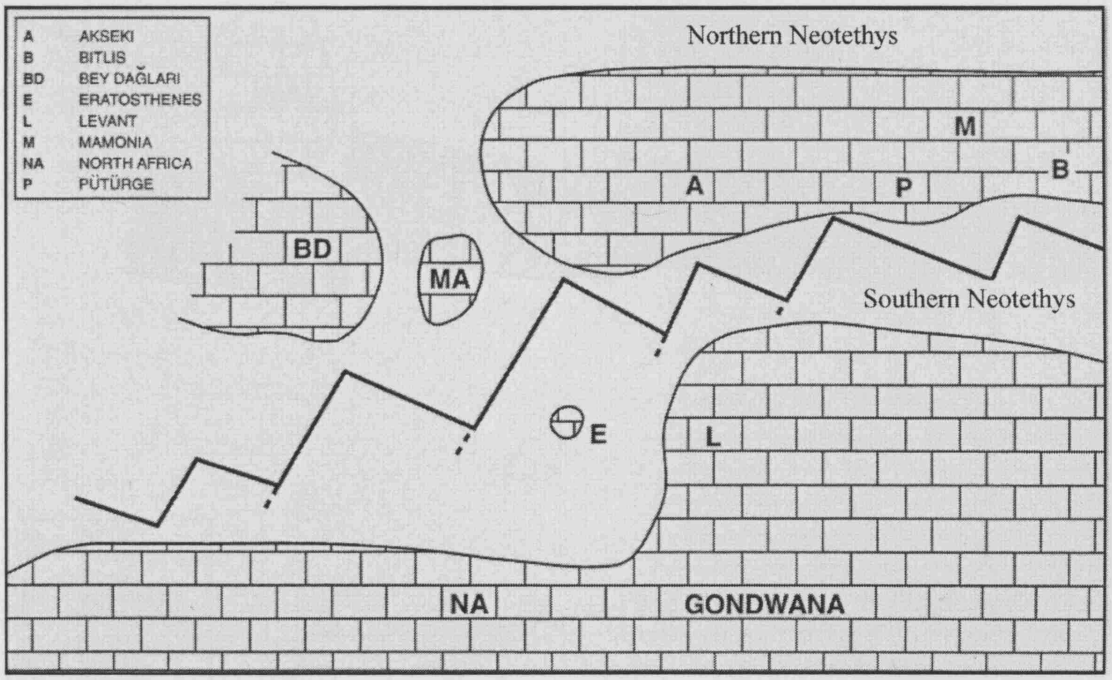

Figure 2.5. A plate tectonic reconstruction for the Late Triassic to Early Jurassic, modified after Robertson (1998).

Locally, during the Jurassic, passive margin subsidence and associated sedimentation was established on both the northern and southern margins of the southerly Neotethyan basin. Carbonate platforms and deep-water passive margin sediments developed and are preserved within the Taurides, the Levant, along the Levantine margin and in North Africa (Robertson 1998). Continental fragments along the northern edge of this southern Neotethyan basin experienced deep-water passive marine sedimentation around their fringes, later to be incorporated into allochthonous units such as the Mamonia and Antalya complexes (Robertson 1998).

2.7.3 EARLY – MID CRETACEOUS.

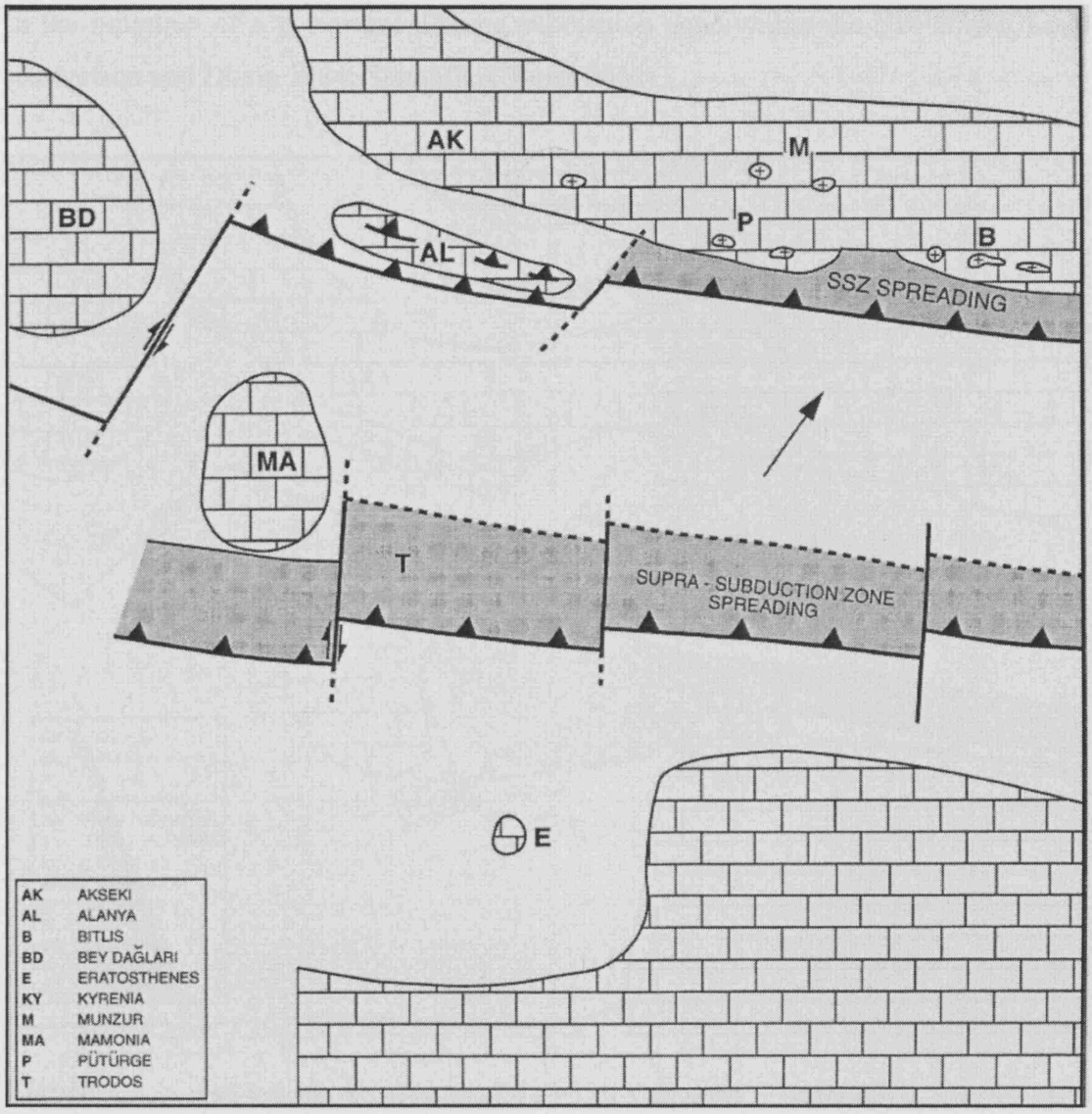

Figure 2.6. A plate tectonic reconstruction for the Cenomanian – Turonian, modified after Robertson (1998)

The translation of Africa eastwards relative to Eurasia continued until the mid-Cretaceous but declined in rate (Robertson 1998). The relative motion of the plates then changed to convergence due to the opening of the South Atlantic (e.g. Livermore & Smith 1984; Savotsin *et al.* 1986; Stampfli & Borel 2002; Rosenbaum *et al.* 2002). Passive margin subsidence continued on the margins of the southern Neotethyan basin (Ricou *et al.* 1984) and renewed oceanic spreading occurred as evidenced by MORB-type volcanics of early Cretaceous age in Antalya (Robertson 1998).

2.7.4 LATE CRETACEOUS

The convergence of Africa and Eurasia from the late Early Cretaceous resulted in the initiation of a northward dipping subduction zone within the Neotethyan basin (Robertson and Dixon 1984; Stampfli & Borel 2002).

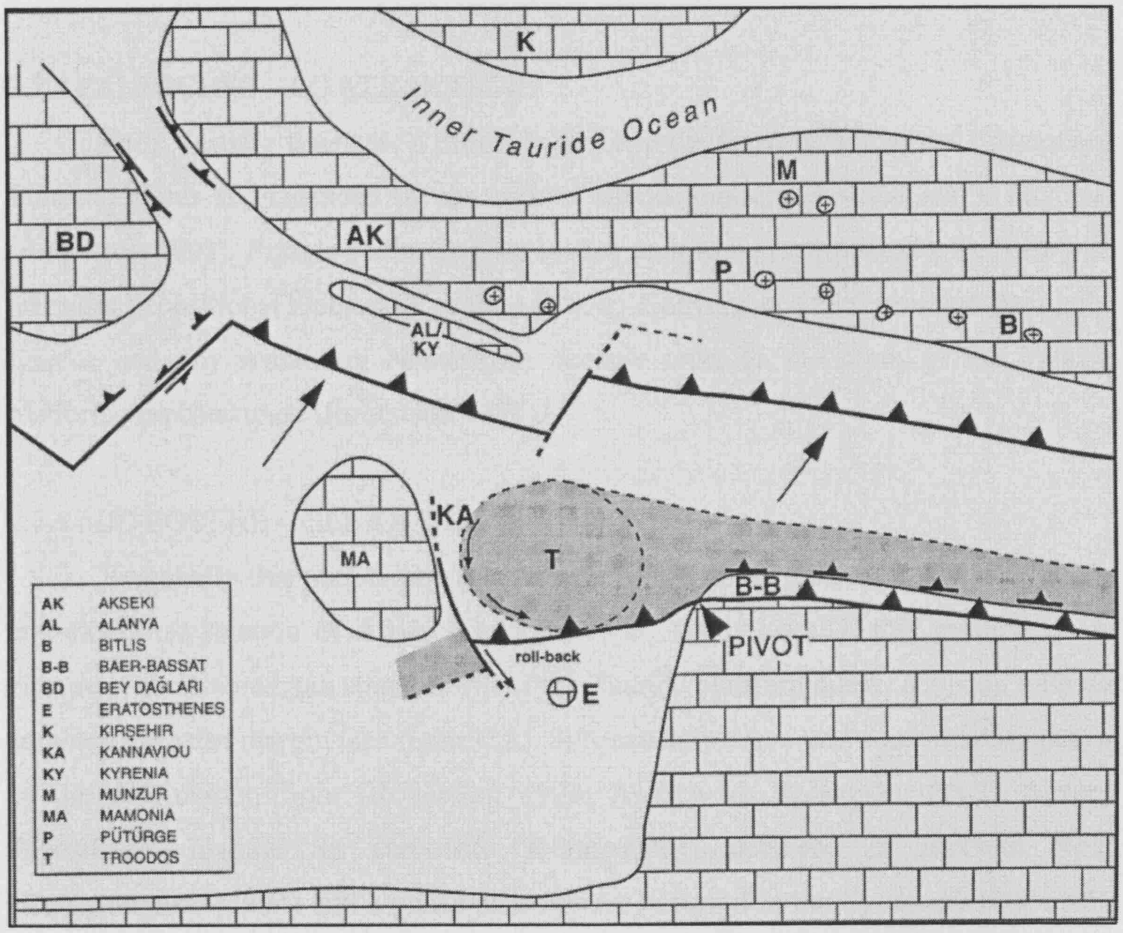

Figure 2.7. A plate tectonic reconstruction for the Late Campanian – Maastrichtian, after Robertson (1998).

Roll-back of the old Triassic oceanic crust allowed asthenospheric upwelling and the formation of supra-subduction zone ophiolites, e.g. Troodos, Baer-Bassit and Hatay (Robertson 1998) (see figure 2.6), and also led to the collapse of northern carbonate platforms and the onset of pelagic sedimentation (Robertson 1998).

Northward subduction continued during the Turonian – Late Campanian and subduction-accretionary complexes were formed as the Arabian passive margin approached the trench. A foredeep was formed as the Arabian passive margin collided

with the trench in the Late Campanian, and was followed by the southward translation of the ophiolites and associated mélanges of Baer-Bassit, Hatay and Kocali (Robertson 1998) and Oman (Knipper *et al.* 1986). A westward extension of the trench survived however, and began to pivot anti-clockwise as convergence between the African and Eurasian plates continued (see figure 2.7), resulting in rotation of the overriding Cyprus microplate that continued until the Early Eocene (Morris *et al.* 1990).

2.7.5 PALEOCENE – LOWER EOCENE

Early Tertiary time saw a probable pause in the convergence of the African and Eurasian plates as evidenced by the lack of subduction-related volcanics in this area (Robertson 1998). Pelagic sedimentation is also seen to be continuous in the area with no major depositional hiatuses (e.g. Baer-Bassit). Convergence then resumed during the Eocene and any remaining Neotethyan oceanic crust to the north of the Tauride platform was consumed (Robertson 1998).

2.7.6 MID EOCENE – OLIGOCENE

Regionally this period saw the plate convergence as greatest in the east, due to anti-clockwise rotation of Africa (Dercourt *et al.* 1986) Locally, this resulted in the closure of the Neotethyan strand north of the Tauride platform due to collision with the southern Eurasian margin (see figure 2.8). Subsequently, there was southward migration of the deformation front (Robertson 1998; Andrew & Robertson, 2002). Several depositional hiatuses in carbonate sedimentation occurred in northern Syria (Krasheninnikov 1994) and a phase of inversion occurred in the Syrian arc (Robertson 1998; Walley 1998). Troodos remained to the south of the deformation front however, as evidenced by the continuous deposition of pelagic carbonates of the Lefkara Formation (Robertson 1998).

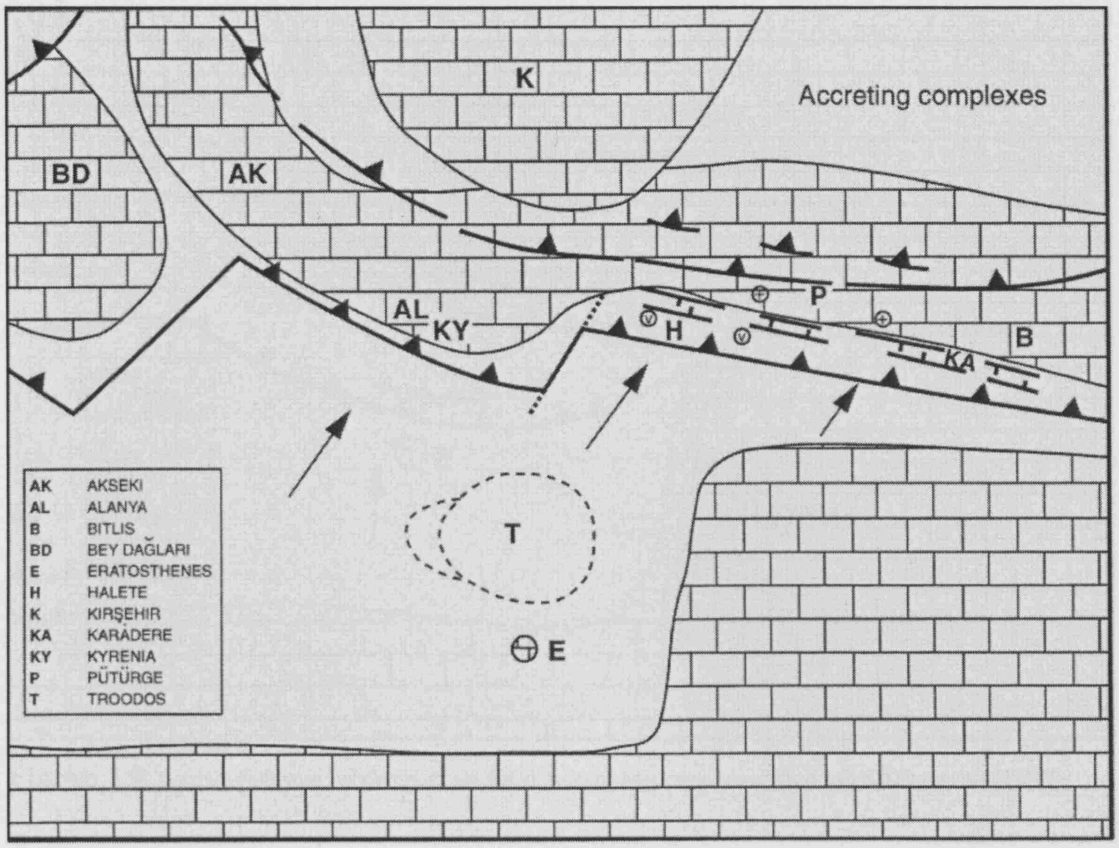

Figure 2.8. A plate tectonic reconstruction for the Mid to Late Eocene, after Robertson (1998).

2.7.7 MIOCENE

During Early Miocene time the subduction zone to the north of Cyprus migrated to the south of the island, possibly due to the arrival of less dense, supra-subduction type crust arriving at the trench, and the difficulty of subducting this. To the south of Cyprus cold dense early Mesozoic crust remained, and it is likely that subduction reactivated a Late Cretaceous subduction zone (see figure 2.9) (Robertson 1998). This subduction zone was part of the broader African – Eurasian plate boundary. Cyprus was situated on the overriding plate above the northward dipping subduction zone (see figure 2.9). An extensional regime then developed, forming the Polis Graben on Cyprus, the Antalya and Adana basins of S.Turkey and the Latakia basin of NW Syria (see figure2.10). This extensional regime was probably the result of southward rollback of early Mesozoic crust (Robertson 1998). The Messinian salinity crisis at this time saw the emergence and karstification of topographic highs, the precipitation of gypsum in previously shallow basins and halite precipitation in deeper waters (Robertson 1998). To the east final suturing of Arabia and SE Turkey occurred (Steininger & Rögel 1984).

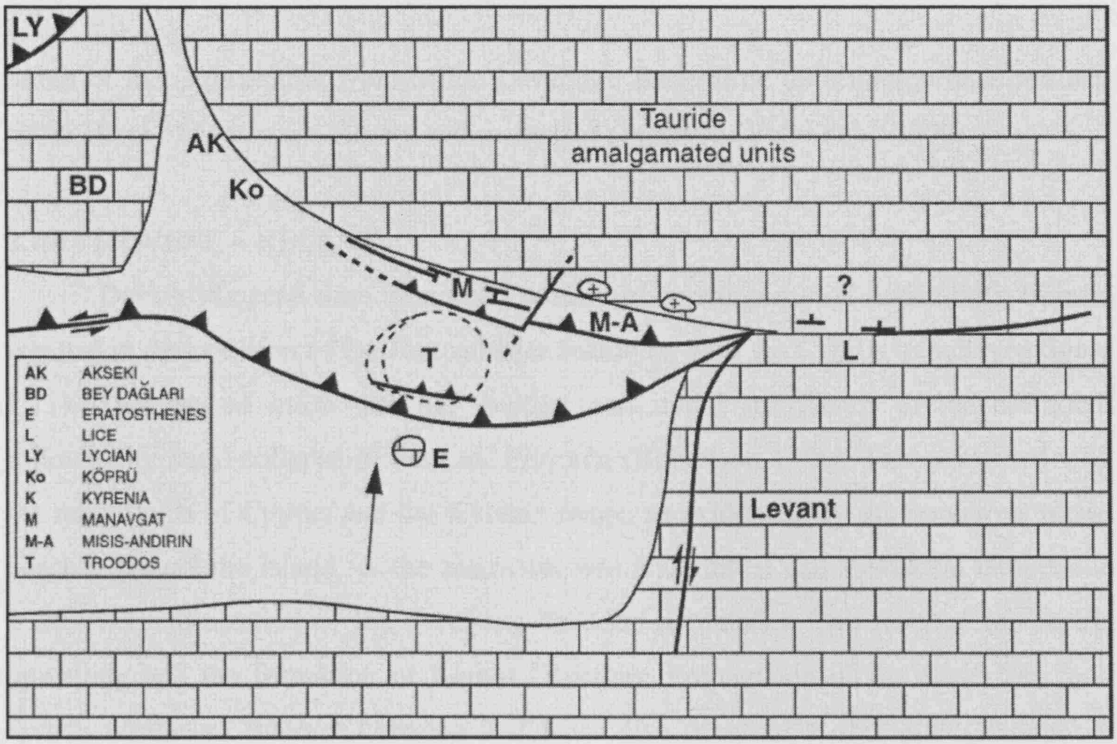

Figure 2.9. A plate tectonic reconstruction for the early Miocene, modified after Robertson (1998).

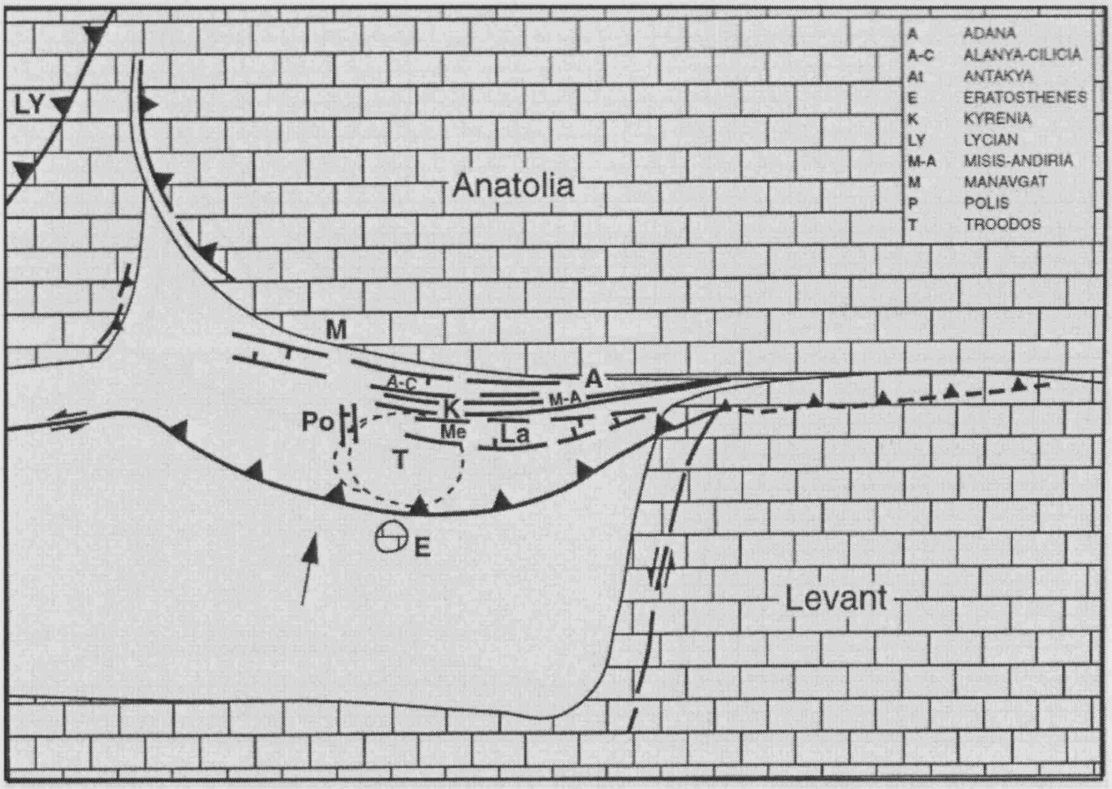

Figure 2.10. A plate tectonic reconstruction for the late Miocene, modified after Robertson (1998).

South of the deformation front in the Levantine Basin little deformation occurred and about 10km of Mesozoic–Recent sediments are preserved (Vidal *et al.* 2000)

2.7.8 PLIOCENE – RECENT

During Pliocene time continued northward convergence of Africa with Eurasia resulted in the collision of the Eratosthenes seamount with the Cyprus trench (see figure 2.11). This caused mass wasting, faulting and initial subsidence of the seamount followed by rapid collapse in the Late Pliocene (Robertson 1998). This coincided with the rapid uplift of Cyprus and the Kyrenia range, as evidenced by the numerous raised beaches around the island, as the seamount was underthrust and subducted (Robertson 1998). Serpentinization of the overlying Troodos ultramafics then resulted in diapiric upwelling and the formation of Mount Olympus. Propagation of the Dead Sea fault system northward through Lebanon and Syria also occurred at this time (Badawy & Horváth 1999) with associated volcanism (Adiyaman & Chorowicz 2002)

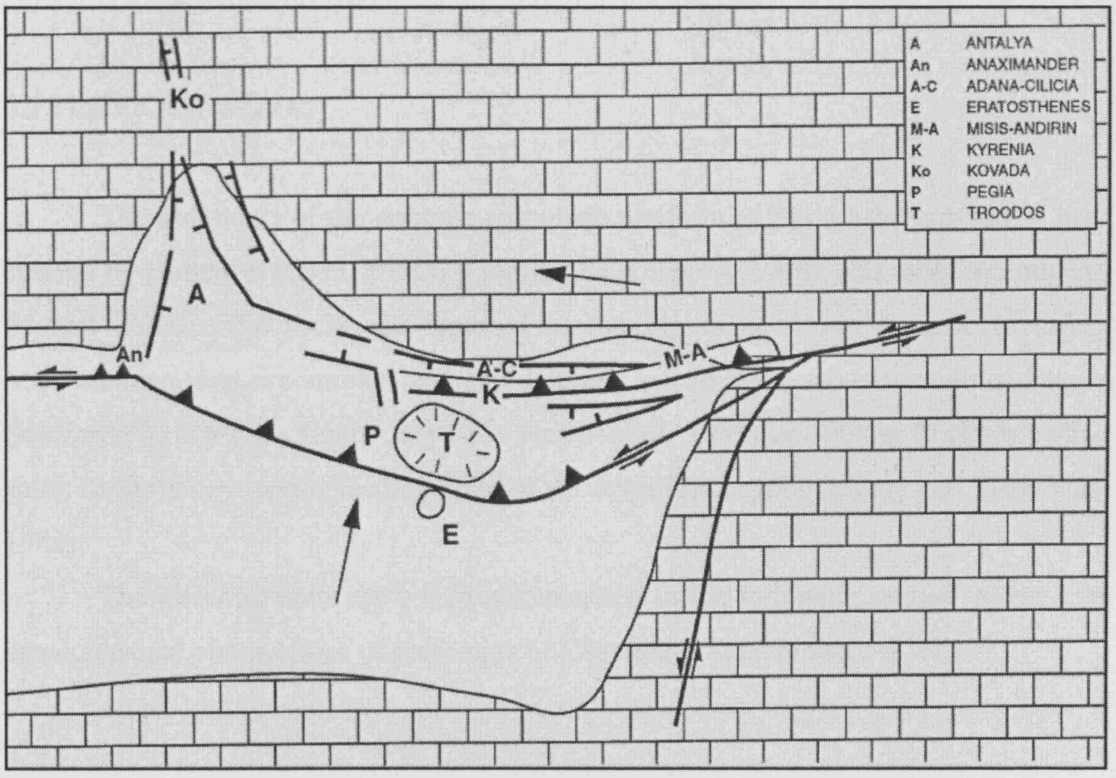

Figure 2.11. A plate tectonic reconstruction for the late Pliocene – Quaternary time, after Robertson (1998).

CHAPTER 3: PRE-EMPLACEMENT SEDIMENTATION HISTORY OF THE BAER-BASSIT AREA.

3.1 INTRODUCTION.

The autochthonous succession, the structural "basement" for the ophiolite, is a Mesozoic carbonate platform exposed in the north of the area near the border with Turkey, forming the Jebel Aqraa and Qara Dourane massifs (see figure 3.2). These Mesozoic carbonates continue into the Hatay area of southern Turkey as well as Kurd Dag and Amanos (see figure 3.1). The current mountainous topography is thought to be related to the final suturing of Neotethys in this part of the Mediterranean during the Oligocene consequent upon the collision of the Arabian and Eurasian plates. In this study sampling was concentrated near the boundary with the structurally overriding allochthonous units of the Baer-Bassit mélange and ophiolite, in order to obtain an age for the youngest autochthonous sediments structurally beneath the ophiolite. The oldest autochthonous sediments overlying the ophiolite are discussed in chapter 6.

3.2 PREVIOUS WORK.

The sediments of the Arabian carbonate platform in Syria have previously been studied by Dubertret (1933, 1955), Kazmin and Kulakov (1968), and most recently Al-Riyami (2000). The rocks are reported as ranging in age from Jurassic to Lower Maastrichtian, and are similar to those cropping out to the north-east in Kurd Dag in Southern Turkey (See figure 3.1) (Al- Maleh *et al.* 1992) as well as to those further south in Syria beyond the leading edge of the ophiolitic nappes (Mouty and Saint Marc 1982).

The different units are briefly summarised in the following section, along with some personal observations of sediments of Cenomanian age in section 3.4.3.

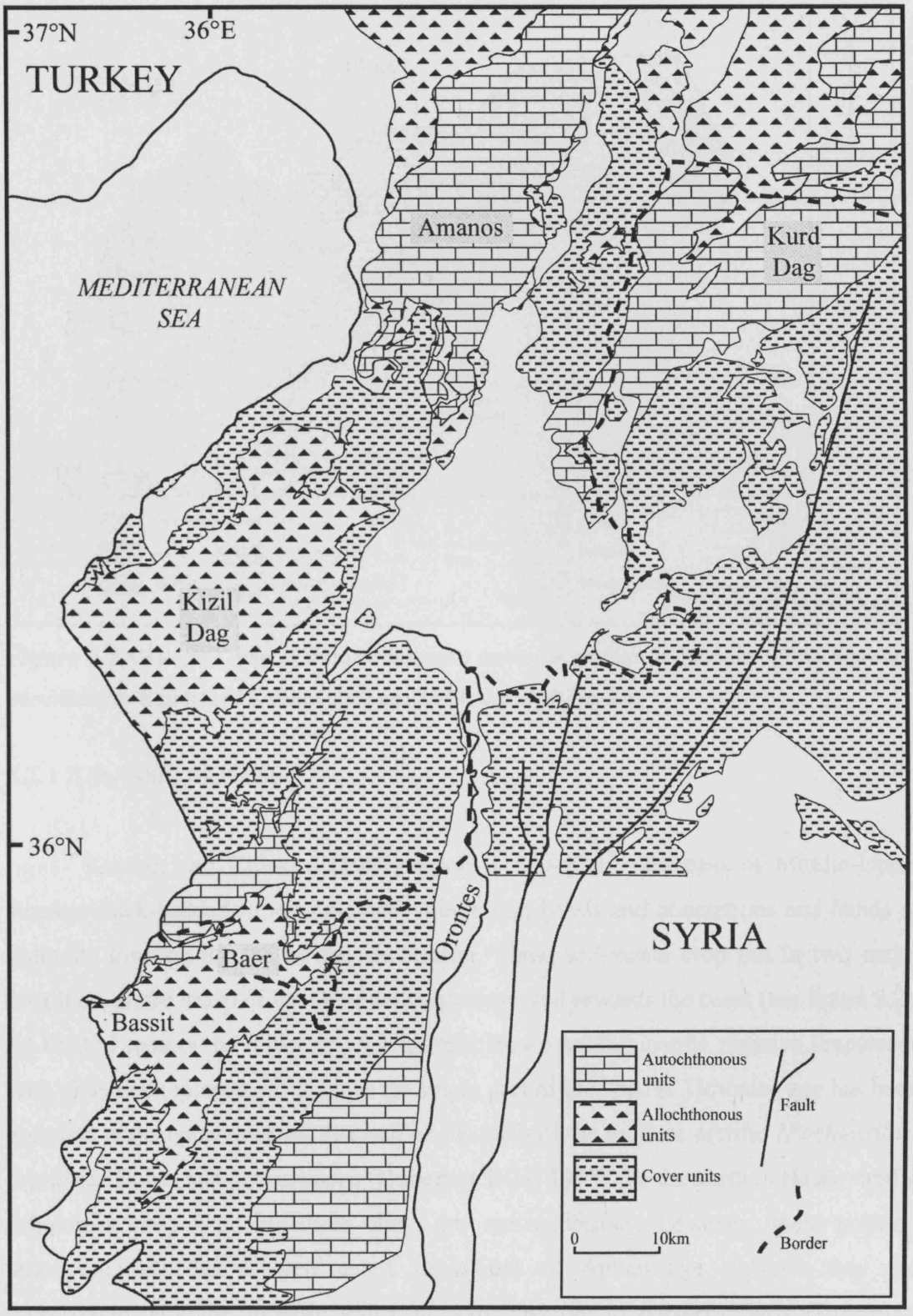

Figure 3.1 Geological map of the Arabian carbonate platform and ophiolites of the Eastern Mediterranean. Modified after Delaloye and Wagner 1984 and Piskin 1985.

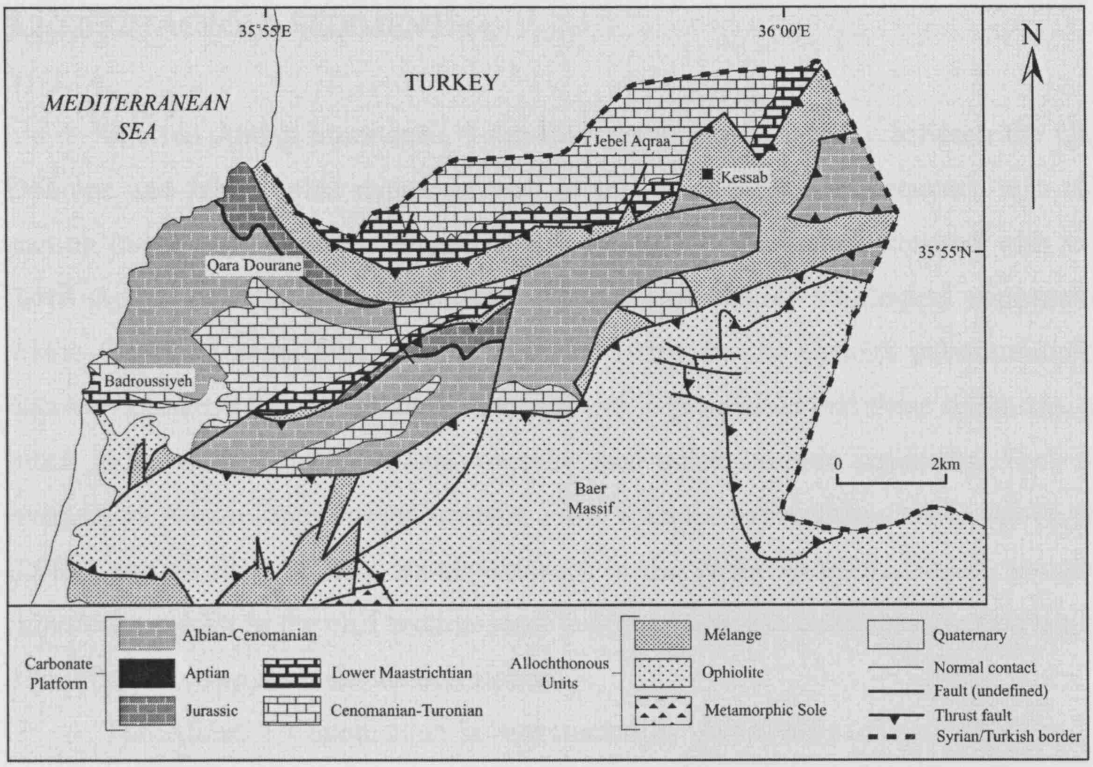

Figure 3.2 Geological map of the autochthonous carbonate platform in the north of the study area (modified after Kazmin and Kulakov 1968 and Al-Riyami 2000, Fig. 2.1)

3.2.1 JURASSIC SEDIMENTS.

Kazmin and Kulakov (1968) report a 400-500m thickness of Middle-Upper Jurassic thick-bedded limestones with minor flint bands and concretions and bands of dolomite towards the top of the succession. These sediments crop out in two major localities, on the scarp of the Qara Dourane range and towards the coast (see figure 3.2). Al-Riyami reports the rocks as grey to light brown predominantly massive limestones with abundant replacement chert in the upper part of the unit. A Tithonian age has been assigned to the upper parts of this unit on the basis of the mollusc *Mytilus (Pachmytilus) crassimus* Bohm and *Lovcenipora* (Dubertret 1933, 1955). To the north in Hatay similar lithologies crop out, but here they are unfossiliferous, however, their position stratigraphically below well dated sandstones of Aptian age suggests they are correlatable with the Jurassic sediments cropping out in northern Syria (Dubertret, 1955).

3.2.2 CRETACEOUS SEDIMENTS.

Inferred Aptian limestones, 3-4m thick, crop out in a valley between the Qara Dourane and Jebel Aqraa ranges as well as in a thicker 23-25m sequence in a cliff section in the Qara Dourane range (Al-Riyami, 2000). They are correlated with well dated Aptian sediments in Jebel Aqraa (Turkey) of similar lithological appearance, where they total some 30m thick (Dubertret, 1936), but no definite palaeontological data was obtained to support an Aptian age and it is possible that these sediments are much older as they unconformably overlie well dated Jurassic sediments. They are overlain by Albian limestones (Dubertret 1936, Kazmin and Kulakov 1968). Al-Riyami (2000), reports that the Baer-Bassit outcrops in the valley comprise brown, iron-rich limestones, whilst in the cliff section some 8-10m of massive dolomites are overlain by 15m of dark brown, bituminous limestones.

The Albian – Cenomanian is represented by about 900m of limestones and is dated on the presence of the molluscs *Amphidonta haliotidea* d'Orbigny and *Liostrea* cf. *delettrei* Coq (Kazmin & Kulakov, 1968). Outcrops are reported from north of Baddrousiyeh and on the northern scarp of the Qara Dourâne range, in the latter area the section is described as comprising alternations of hard grey, medium to thickly bedded limestones with minor replacement chert nodules and lenses, alternating with softer, brownish-grey bituminous limestones. Towards the top of the section detrital and foraminiferal limestones interbedded with dolomites and shelly beds become predominant (Kazmin & Kulakov, 1968). Al-Riyami (2000) reports the Albian-Cenomanian as dominated by lime mudstones which are occasionally rich in planktonic foraminifera, though no systematic identification was attempted. The limestones also contain radiolaria, shell and echinoid fragments. Preservation is generally poor.

The Cenomanian – Turonian is represented by 170-180m of thickly bedded, massive grey limestones (Kazmin & Kulakov, 1968). These crop out on the southern slopes of Qara Dourâne and Jebel Aqraa. Again, some of the limestones are bituminous with chert nodules. The succession was previously dated on the presence of the benthic foraminifera *Nerinea pseudonobilis* Choffat (Dubertret, 1936), though Al-Riyami (2000) also reports common planktonic foraminifera, including *Whiteinella* sp. and *Helvetoglobotruncana helvetica* (Bolli) within grain-supported packstones, suggesting the succession could be subdivided and biostratigraphical correlation refined.

Maastrichtian sediments are reported to unconformably overlie the Cenomanian-Turonian. Kazmin & Kulakov (1968) report a total thickness of 90m of hard limestones, marls and mudstones, cropping out on the southern slopes of the Jebel Aqraa and Qara Dourâne ranges as well as to the north of the coastal village of Baddrousiyeh. West of Kessab, Kazmin and Kulakov (1968) describe a section with brown, fine-grained calcareous sandstone unconformably overlying Cenomanian – Turonian limestones. Overlying the sandstone are a series of beds of hard, massive grey limestone that pass into nodular limestone and then into marly limestone. Towards the top of the section marls are dominant. Previous dating of a Lower Maastrichtian age was based on the presence of *Globotruncana arca* and *G. rosetta*, though both of these species are now know to extend well down towards the base of the Campanian. Towards the top of the section marls are dominant. Al-Riyami (2000) reports large colonies of Rudists from coastal exposures near the town of Badroussiyeh though these were not identified.

3.3 UPPER CRETACEOUS BIOSTRATIGRAPHY AND SAMPLING OVERVIEW.

Many biostratigraphic zonations have been proposed for Cretaceous planktonic foraminifera since the value of the Globotruncanidae as stratigraphic markers was first recognised in the first part of the last century. The first attempt to produce a globally applicable zonation was by Bolli (1966) and since then there have been numerous attempts at a standard global zonation, and even more at regionally applicable schemes. The marker species used have not fundamentally changed since the early scheme proposed by Bolli, but the accuracy of the individual zones has been greatly improved with correlation of foraminiferal zones to absolute dates now possible. The zonation scheme used in this chapter is that of Premoli Silva & Sliter (1999) which is essentially the same as that of Robazsynski & Caron (1995), apart from minor discrepancies in the placing of zonal boundaries, and the inclusion of an extra zone in the Maastrichtian in the scheme of Premoli Silva & Sliter (see figure 3.3). The characteristics of each zone will be discussed in the results section where applicable.

Much less work has been conducted on biostratigraphic zonations for radiolaria in the Tethyan region. Baumgartner *et al* (1995) have produced a detailed zonation for the Jurassic and Cretaceous of Tethys using unitary associations. Unfortunately this scheme only extends as far as the Aptian. In this study the zonal schemes of Sanfilippo and Riedel (1985) and Pessagno (1976, 1977) have been utilised, and their relationships

to each other and other zonal schemes are illustrated in figure 3.4. The former scheme is designed to be applicable to specimens identified under a normal light microscope, whilst the latter scheme, although ostensibly providing a greater biostratigraphical resolution, relies much more heavily on identification of minor features using scanning electron microscopy. Where possible, the more refined scheme of Pessagno (1976, 1977) has been utilised, but in many cases it was not applicable as will be discussed later.

Figure 3.5 combines the radiolaria and foraminifera zonal schemes, illustrating how they are correlated, and also illustrates the bio-events upon which the individual zones and subzones are based. A brief examination of the simple smear slides revealed that any nannofossils present were far too overgrown to allow identification so studies concentrated on planktonic foraminifera and radiolaria, and also on benthic foraminifera where this was deemed useful.

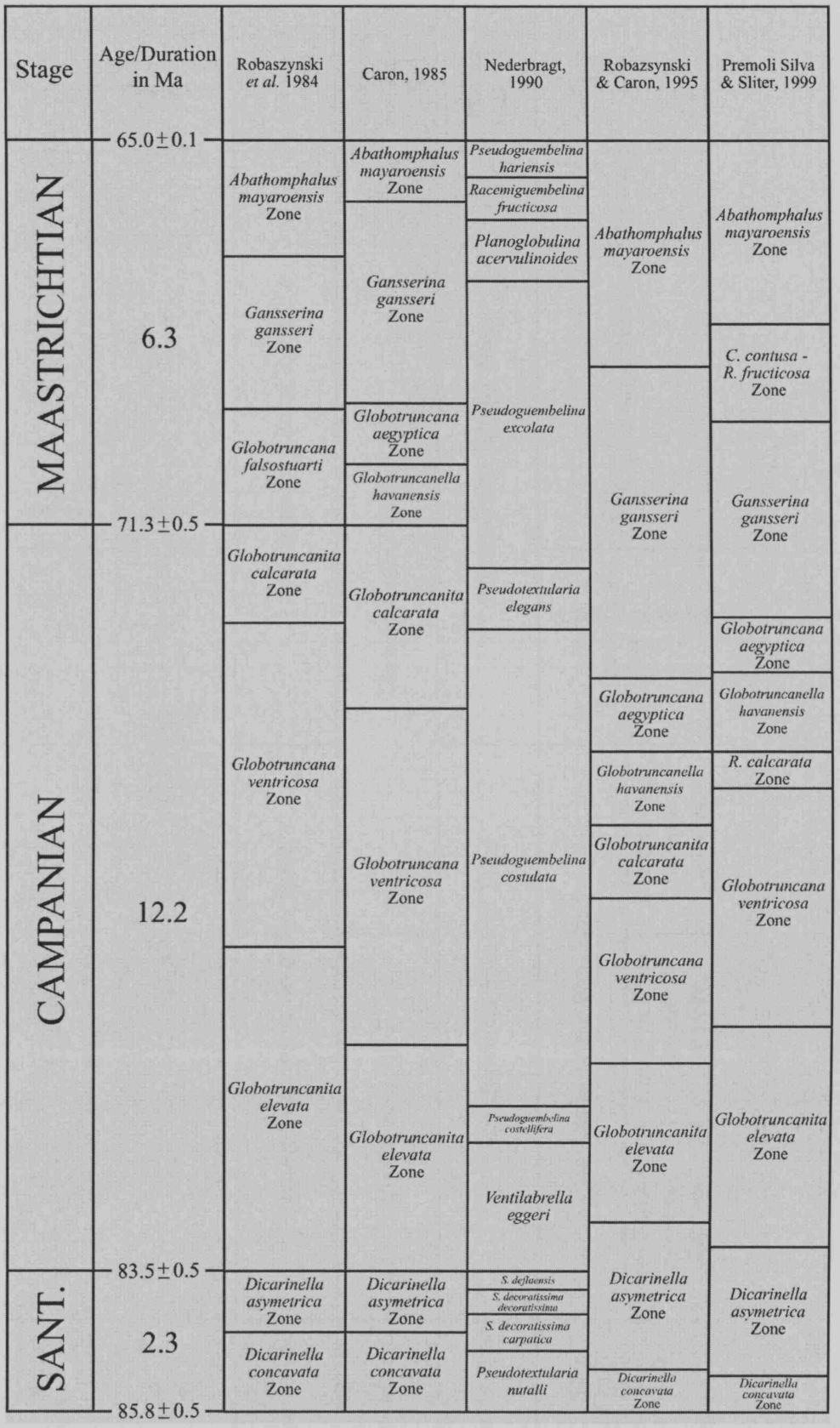

Figure 3.3 Comparison of various foraminiferal zonal schemes for the Late Cretaceous.

Figure 3.4 Comparison of various radiolaria zonal schemes for the Late Cretaceous.

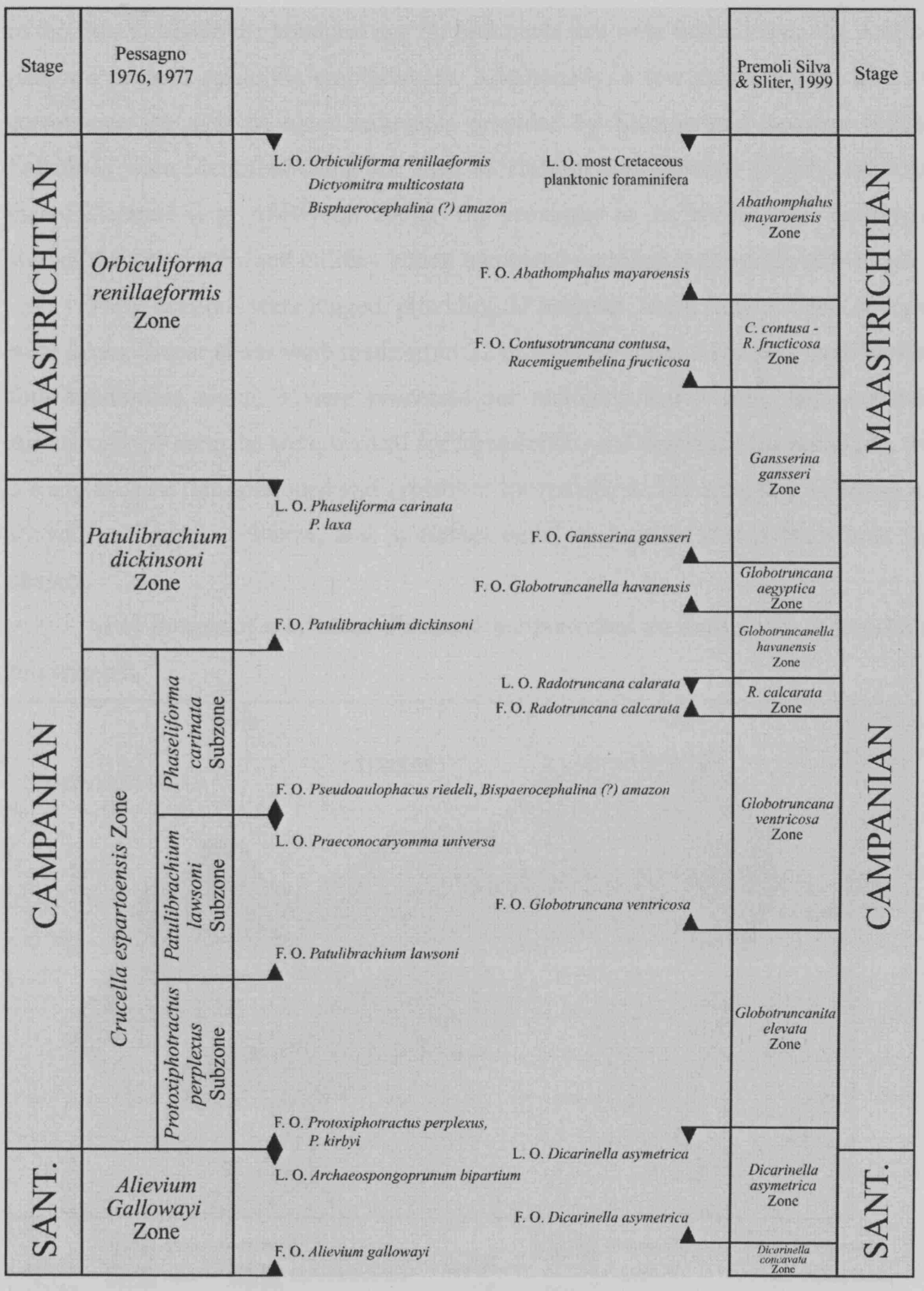

Figure 3.5 Comparison between the two main Late Cretaceous zonal schemes utilized in this chapter.

Sampling was concentrated on sediments, of previously reported Maastrichtian age, lying structurally just below thrust slices of the Baer-Bassit ophiolite. The purpose of this was to obtain the youngest age for sediments that were deposited on the Arabian platform prior to ophiolitic emplacement. Additionally, a few samples were taken to corroborate the ages of older sediments provided by Kazmin and Kulakov (1968). Localities were identified using the map of Kazmin and Kulakov (1968) and more recent literature (e.g. Al-Riyami 2000). The proximity to the border with Turkey, as well as the topography and military zones, hampered sampling in the north of the area.

Three sections were logged, providing 17 samples, and a further 9 spot samples were taken. Smear slides were made from 22 of these samples. 3 samples were washed for foraminifera alone, 3 were processed for radiolaria and 7 were thin-sectioned. Additionally, 9 samples were washed for foraminifera and processed for radiolaria, and 5 samples were thin-sectioned and processed for radiolaria. The sampling localities are shown on Figure 3.6 below, and in further detail on locality sketch maps later this chapter.

SEM images of specimens discussed are presented on three plates at the end of this chapter.

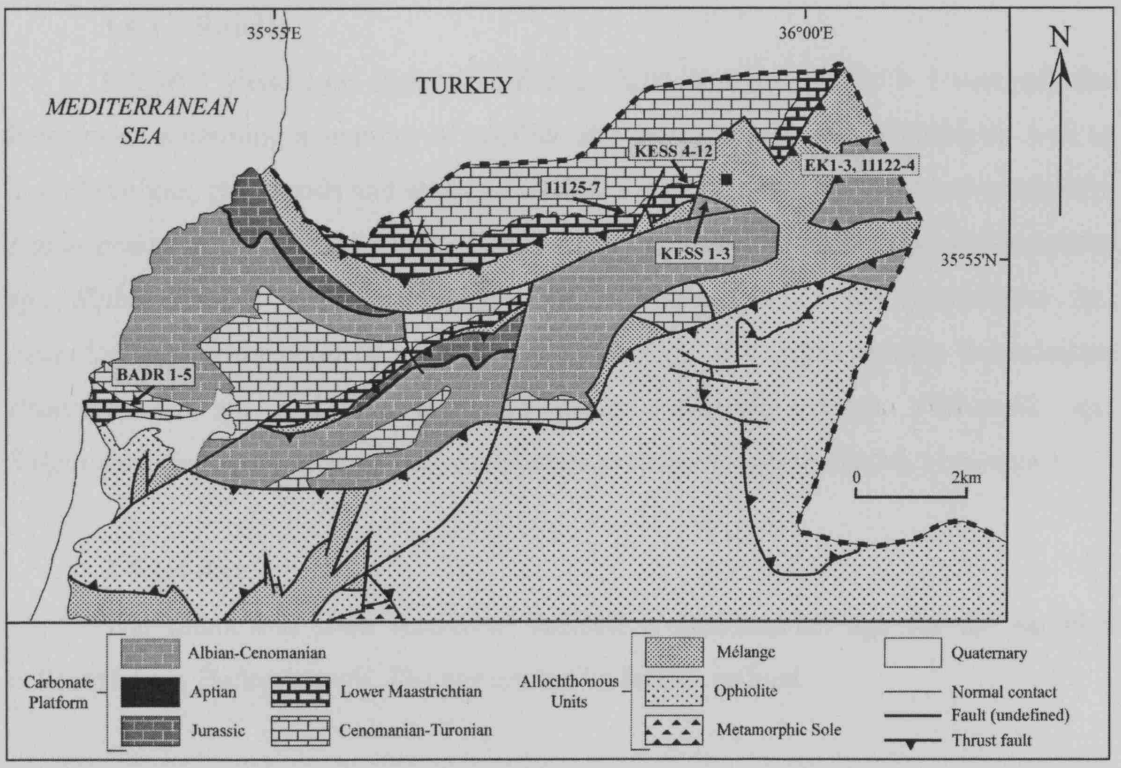

Figure 3.6 Sampling localities from the autochthonous carbonate platform that are mentioned in the text.

3.4 SAMPLING LOCALITIES AND RESULTS.

3.4.1 Badroussiyeh

3.4.1.1 Sampling

A section was logged and sampled near the coastal town of Badroussiyeh (see Figs. 3.2 and 3.6) where Maastrichtian age sediments have been recorded. Poor exposures in this area limited sampling opportunities. Vegetation was dense and scrubby and only two relatively extensive exposures were seen, one of which was inaccessible (military land). The samples collected were from a 15 m thick section of generally massive limestones dipping moderately to the SE, with individual samples taken from slightly softer beds sandwiched between very hard, massively bedded glauconitic limestones. The sampling levels are illustrated in figure 3.7.

3.4.1.2 Processing

Of the 5 samples collected at this locality only BADR 1 was soft enough for washing for foraminifera. Samples BADR 2 – 4 were all sectioned.

3.4.1.3 Results

BADR 1 yielded no discernible fauna whilst samples BADR 2- 5 were micritic limestones containing a number of smaller and larger benthic foraminifera as well as dasyclad algae, gastropods and small ostracods. Fauna included the benthic foraminifera *Daxia cenomana*, *Mangashtia* sp., *Chrysaldina* sp., *Ammobaculites* sp., *Buccicrenata* sp., *Siphovalvulina* sp., *Textulariopsis* sp., *Debarina* sp., *Everticycalmmina* sp., *Feurtilla* sp., *Gendrotella* sp. and *Monteschiana* sp., the larger benthic foraminifera *Praealveolina* sp. and the dasyclad algae *Palaeodasycladus*, *Pithonella* sp., *Salginoporella annulata* and *Thaumatoporella parvovesiculifera* (Fadel, pers. com.).

3.4.1.4 Age

The fauna and flora recovered indicate a Cenomanian age for the samples collected from Badroussiyeh. The age cannot be further refined.

3.4.1.5 Palaeoenvironment

The faunal and floral assemblage indicates a normal salinity, open marine inner shelf environment.

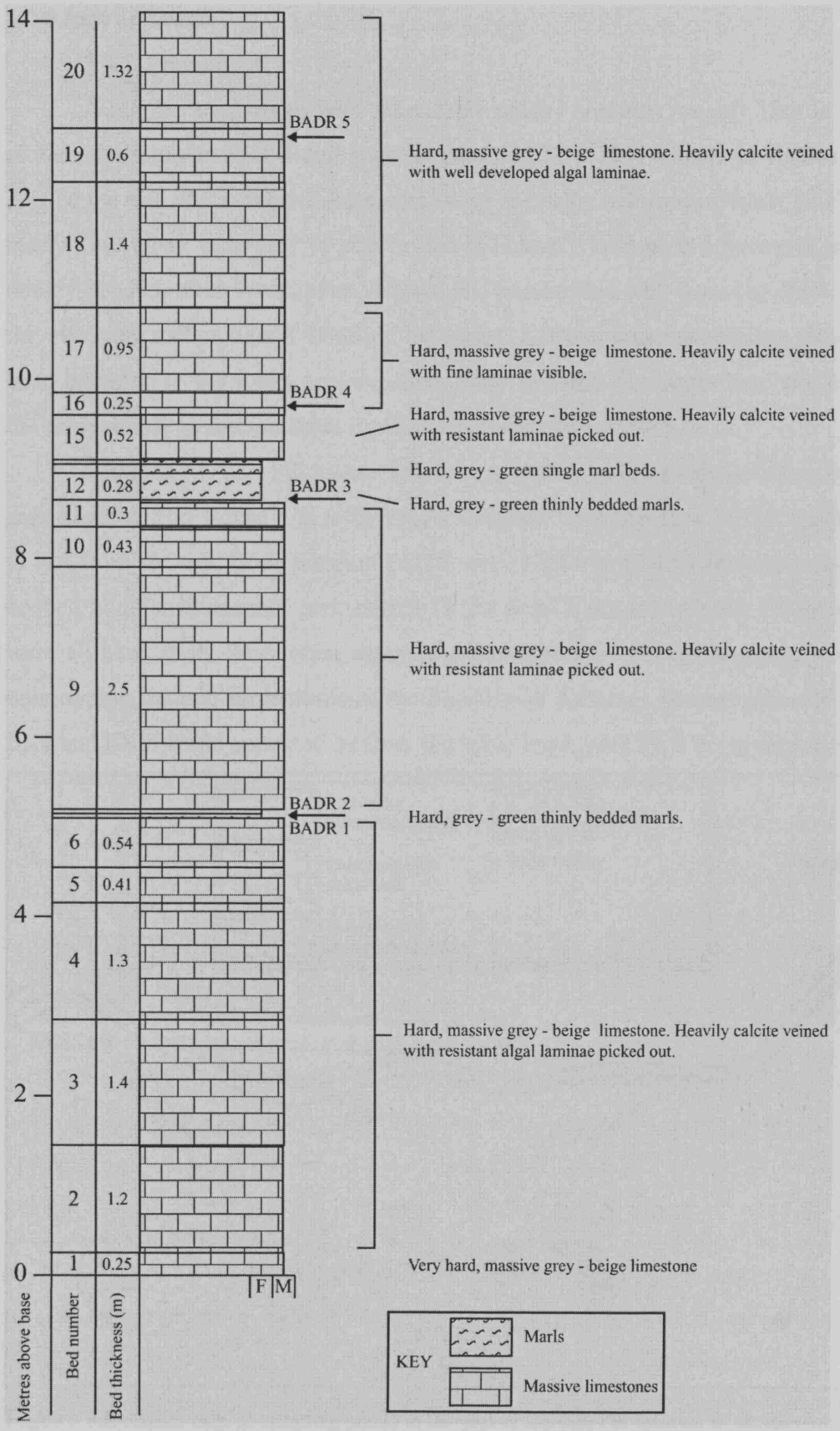

Figure 3.7 Lithological log of sampled section from the coastal town of Badroussiyeh.

3.4.2 East of Kessab

3.4.2.1 Sampling

A number of samples were taken from patchy outcrops roughly 1km to the ENE of Kessab (samples EK1-3 and spot samples 11122-11124) shown on figures 3.8 and 3.9. To the east of Kessab the sediments occur as patchy outcrops of thinly bedded, hard marly limestones, pale-grey to pale brown in colour. These pass downwards into more thickly bedded, often bituminous, limestones, interbedded with layers of chert. Close to the overlying mélange (and therefore the thrust) a strong pressure solution cleavage has been imparted to the rocks, making them platy in form. The rocks here are dipping to the fairly gently to the southeast (typically between 20 and 30°).

Samples 11122-11124 were taken from patchy outcrops about 500m NE of the area illustrated in figure 3.8, with 11122 sampled from the base of the sequence and 11124 from the top. Both samples 11122 and 11123 were taken from hard, massively bedded nodular limestones and sample 11124 from a platy limestone. Samples EK1-3 were all hard, platy limestones, sampled within about 5-40m of structurally overlying outcropping sheared serpentinite of the Baer-Bassit mélange. Stratigraphically, samples EK1 and EK2 would appear to be from the same level, with EK3 being slightly lower.

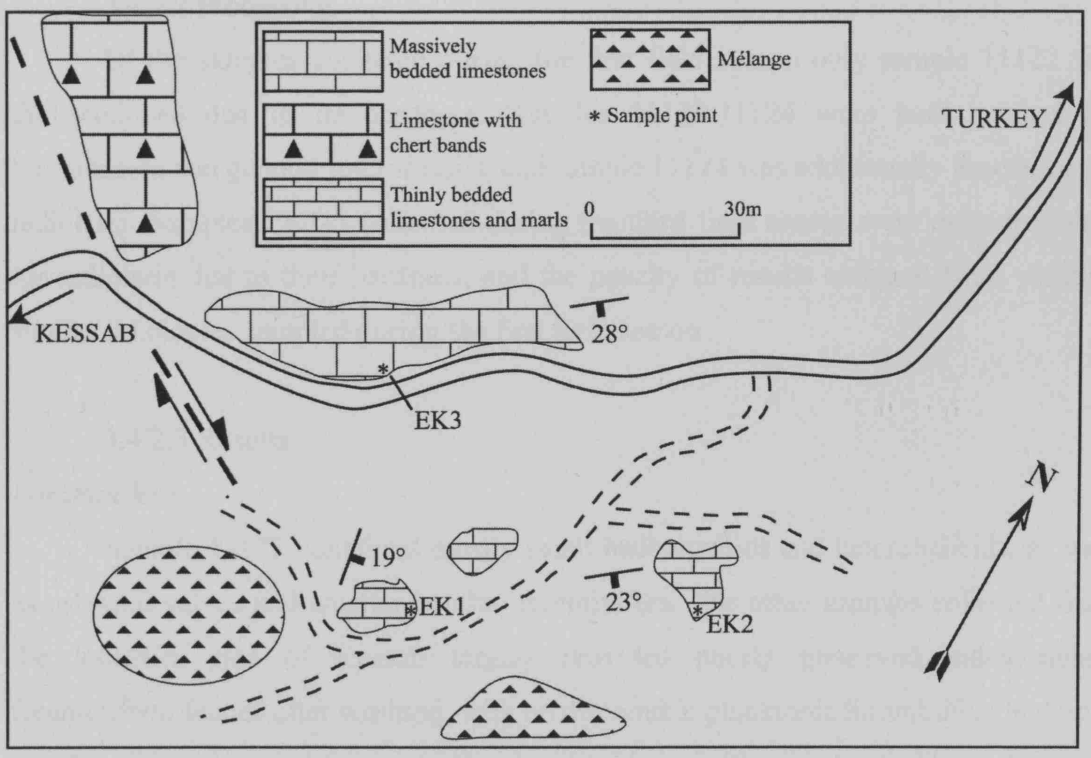

Figure 3.8 Sketch map of sampling points to the east of Kessab. For location of sketch map see figure 3.6.

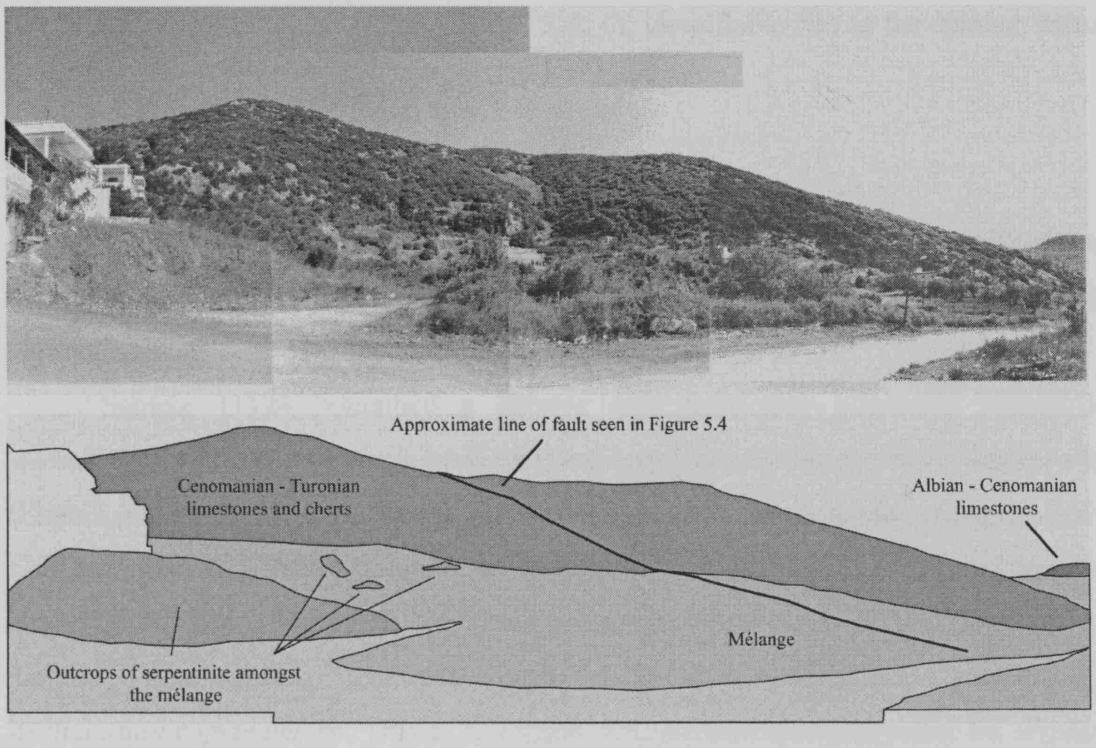

Figure 3.9 Photomontage and explanatory sketch of sampling area east of Kessab.

3.4.2.2 Processing

Of the samples collected during the first field season only sample 11122 was thin-sectioned due to its hardness. Samples 11123-11124 were both washed for foraminifera and general microfossils, and sample 11124 was additionally processed for radiolaria. Samples EK1-3 collected during the third field season were only processed for radiolaria due to their hardness, and the paucity of results obtained from washing similar lithologies sampled during the first field season.

3.4.2.3 Results

Foraminifera

Sample 11122 contained mostly small hedbergellids and heterohelicids, as well as ostracod valves and smaller benthic foraminifera. The other samples collected from the localities east of Kessab largely provided poorly preserved indeterminate foraminiferal faunas after washing, with no discernible planktonic foraminifera and only angular fragments and rare smaller benthic foraminifera present. However, after dissolution in HCl, the residues were seen to contain numerous partially dissolved benthic and planktonic foraminifera. Due to the dissolution identification was generally

impossible, however sample EK2 was seen to contain two specimens of *Globotruncanita calcarata* (Plate 1, Figs. 5 & 6), identifiable due to the spinose nature of the test.

Radiolaria

The exact faunal contents of the samples processed for radiolaria are illustrated in Text table 4.1. Below is a summary of the more important species recovered from the various residues.

Sample 11124 contained a diverse and moderately preserved radiolarian assemblage, dominated by *Archaeodictyomitra lamellicostata*, *Dictyomitra multicostata* (Plate 2, Figure 1), *Xitus spicularis*, *Foremanina schona*, *Amphipyndax pseudoconulus*, *Orbiculiforma* sp., *Pseudoaulophacus lenticulatus*, *P. floresensis*, *Rhopalosyringium magnificum* (Plate 2, Figure 10) and *Praeconocaryomma universa*. Other important taxa include *Phaseliforma carinata* and *Crucella espartoensis*. Additionally *Archaeospongoprunum* sp. (Plate 2, Figure 12), *Archaeospongoprunum* cf. *triplum*, (Plate 2, Figure 13), *A. andersoni* (Plate 2, Figure 14), *Crucella* sp. (Plate 2, Figure 18), *Patulibrachium* sp. (Plate 2, Figure 19) and *Alievium gallowayi* (Plate 3, Figure 8) were all identified.

Sample EK1 has a similar assemblage to sample 11124, with common *Archaeodictyomitra lamellicostata*, *Dictyomitra multicostata*, *Foremanina schona*, *Stichomitra asymbatos*, *Amphipyndax pseudoconulus*, *Patellula verteroensis* (Plate 3, Figs. 1 & 2), *Pseudoaulophacus lenticulatus*, *P. floresensis*, *P. parguerensis* (Plate 3, Figure 3), *Rhopalosyringium magnificum* and *Praeconocaryomma universa*. Other important taxa include *Pseudoaulophacus riedeli* (Plate 3, Figure 4), *Eastonerius acuminatus* and a single specimen of *Dictyomitra koslovae*

Sample EK2 contains the above taxa as well as common *Dictyomitra rhadina*, *Amphipyndax stocki* and *Patulibrachium marshensis*. Other notable taxa present include *Bisphaerocephalina amazon*, *Xitus spicularis*, *Halesium* ?sp. (Plate 2, Figure 16) and *Orbiculiforma* cf. *sacramentoensis*.

Finally, sample EK3 again contains a similar fauna, and also includes *Pseudoaulophacus vielseitigus*, *Crucella espartoensis*, *Amphipyndax* cf. *Tylotus* (Plate 2, Figure 6) and *Patulibrachium andersoni*.

3.4.2.4 Age

The microfossil assemblage identified in sample 11122 indicates only a broad Cretaceous age range from late Albian to Maastrichtian. Sample 11123 contained no discernible fauna and remains undated.

The radiolarian assemblage recovered from sample 11124 suggests a Campanian age, as *Amphipyndax pseudoconulus* and *Foremanina schona* are both restricted to the Campanian, whilst *Crucella espartoensis*, *Pseudoaulophacus lenticulatus*, *Praeconocaryomma universa* and *Phaseliforma carinata* all have last occurrences within the Campanian. The fauna recovered allows the sample to be dated as belonging to the *Crucella espartoensis* Zone, and perhaps even the *Phaseliforma carinata* Subzone of Pessagno. This suggests an age of early Late Campanian, however, *Praeconocaryomma universa* and the Praeconocaryommidae in general are reported as becoming extinct at the end of the Middle Campanian (*Patulibrachium lawsoni* Subzone of Pessagno) so the sample may be either slightly older or *Praeconocaryomma universa* may have a longer range than previously suggested. The latter seems likely, as *P. universa* is a common component of many of the samples collected, which have assemblages that would otherwise suggest a late Campanian age. Another interesting feature of the assemblage is a small number of specimens transitional between *Patulibrachium lawsoni* and *Patulibrachium dickinsoni* (Plate 2, Figure 17). Pessagno (1976) describes specimens of a transitional form and suggests that *P. dickinsoni* evolved from *P. lawsoni* during the late Campanian. Again, this agrees with a late Campanian age for sample 11124. Using the scheme of Sanfilippo and Riedel (1985) the sample is assigned to the lower part of the *Amphipyndax tylotus* Zone where the nominate taxon and *Amphipyndax pseudoconulus* co-occur.

The radiolaria liberated from sample EK1 also indicate a late Campanian age, falling within the *Crucella espartoensis* Zone and *Phaseliforma carinata* Subzone of Pessagno and the upper part of the *Amphipyndax enesseffi* Zone of Sanfilippo and Riedel (1985).

The two specimens of *Globotruncanita calcarata* recovered from sample EK2 indicate a late Campanian age. This species is a zone fossil for the late Campanian and dates the sample as belonging to the "*Radotruncana*" *calcarata* Zone which is based on the total range of that species. The radiolarian assemblage also indicates a late Campanian age for the sample, falling within the *Crucella espartoensis* Zone and *Phaseliforma carinata* Subzone of Pessagno and the upper part of the *Amphipyndax*

enesseffi Zone of Sanfilippo and Riedel. This is compatible with age based on the presence of *Globotruncanita calcarata*.

Within sample EK3, the co-occurrence of *Patulibrachium andersoni*, which has its last occurrence within the *Protoxiphotractus perplexus* Subzone (Pessagno), and *P. marshensis*, which first appears in the younger *Phaseliforma carinata* Subzone (Pessagno), is problematic. This sample is therefore simply assigned to the *Crucella espartoensis* Zone, and no finer assignment is attempted.

	Acanthocircus sp.	*Acientyle* sp.	*Alievium gallowayi*	*Alievium* sp.	*Amphipyndax pseudoconulus*	*Amphipyndax stocki*	*Amphipyndax tylotus*	*Amphipyndax* sp.	*Archaedictyomitra lamellicostata*	*Archaeospongoprunum andersoni*	*Archaeospongoprunum hueyi*	*Archaeospongoprunum* sp.	*Archicapsa* sp.	*Bisphaerocephalina amazon*	*Cavidiscus* sp.	*Crucella* cf. *espartoensis*	*Crucella* sp.	*Dictyomitra andersoni*	*Dictyomitra koslovae*	*Dictyomitra multicostata*	*Dictyomitra rhadina*	*Dictyomitra* sp.	*Eastoneritus acuminatus*	*Foremanina schona*	*Holocryptocanium barbui*	*Novixitus* sp.	*Orbiculiforma* sp.	*Orbiculiforma* cf. *sacramentoensis*	*Patellula euessceei*	*Patellula verteroensis*
11124	R		P		C	P	P	R	R	P	R	R	R				P			C	P	P			R	R				
EK1			P		P	P	P	R	C			R					P	R	R	A	P	P	R	P	P		P			P
EK2			P	R	C	P	P	P	C					R			R		R	A	P			P	P		P	P	P	C
EK3		P		P	P	P	P		C	R					C	R	R			A	P			P	P		P		P	

	Patulibrachium lawsoni - dickinsoni transitional form	*Patulibrachium marshensis*	*Patulibrachium teslaensis*	*Patulibrachium* sp.	*Phaseliforma carinata*	*Phaseliforma* sp.	*Praeconocaryomma universa*	*Praecrucella kabischa*	*Praestylosphaera* sp.	*Pseudoaulophacus floresensis*	*Pseudoaulophacus lenticulatis*	*Pseudoaulophacus pargueraensis*	*Pseudoaulophacus riedeli*	*Pseudoaulophacus vielseitigus*	*Rhopalosyringium kleinum*	*Rhopalosyringium magnificum*	*Saturnalis* sp.	*Sciadocapsa* sp.	*Spongosaturnalis* sp.	*Spongosaturninus* cf. *hueyi*	*Spongosaturninus* sp.	*Stichomitra asymbatos*	*Stichomitra communis*	*Stichomitra* sp.	*Theocampe apicata*	*Xitus spicularis*	*Xitus* sp.	Indeterminate spumellarians	Indeterminate nassellarians	
11124	P			P	R		P		P	A	C				P	P		C	P	R		P		R		C			P		*P. carinata* Subzone
EK1			R	P			A			A	P	R	R		R	C		R					P	R	R	P			P	R	*P. carinata* Subzone
EK2		P					P	P		C	C			P		P						P	P			P	P		P		*P. carinata* Subzone
EK3		R		P		P	C			A	P			P		C	R		R		R			P		C	P		P		*C. espartoensis* Zone

Text table 3.1 Radiolarian composition of the East Kessab samples. R (rare) = <1% of assemblage, P (present) = 1- 5%, C (common) = 6 – 10% and A (abundant) = >10%.

3.4.2.5 Palaeoenvironment

All the samples from this location were deposited in a sub-topical environment, in deep open marine conditions on a deeply submerged shelf.

3.4.3 West Of Kessab

3.4.3.1 Sampling

During the first field season a small number of spot samples (11125 – 11127) were collected from patchy outcrops about a mile west of Kessab. Sample 11126 was sampled in closest proximity to the overlying mélange whilst sample 11125 was furthest away and should therefore be stratigraphically oldest.

Immediately to the west of Kessab the sediments are better exposed in a steeply SSW dipping section on the north side of the main Kessab-Badroussiyeh road. The road has been built along the fault between the autochthon and the overlying allochthon, so that on the southern side of the road there are patchy outcrops of highly sheared serpentinite of the Baer-Bassit mélange (see figures 3.6 and 3.9). During the second field season two logged sections were sampled from this location on the western outskirts of Kessab, either side of an approximately north-south running fault. These localities are shown on Figure 3.6 and Figure 3.10.

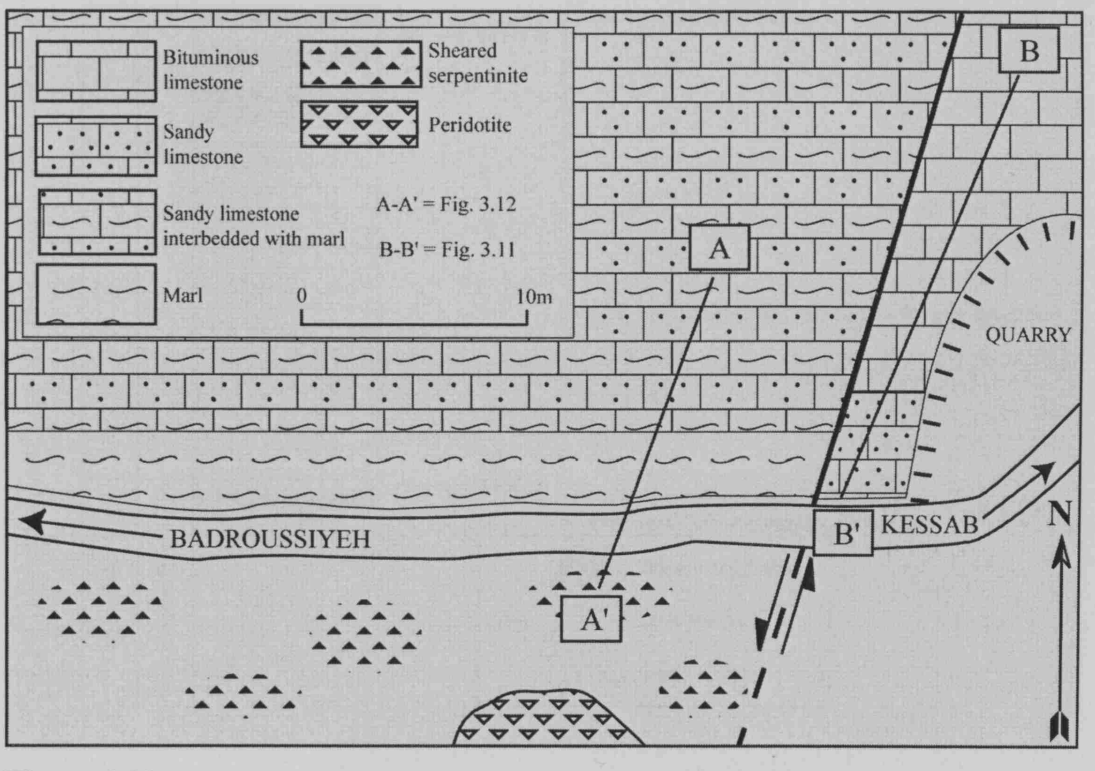

Figure 3.10 Sketch map of the section sampled to the west of Kessab. For location of sketch map see figure 3.6.

To the east of the fault marked on figure 3.10 a 30m quarry section exposes hard, massively bedded limestones dipping steeply to the south. These are occasionally

glauconitic and bituminous, and become sandy towards the top of the section (see figure 3.11). The rocks here are brecciated and pervasively penetrated by calcite veins. According to Kazmin and Kulakov (1968) these rocks should be Cenomanian – Turonian in age, and three samples were taken to check this was the case KESS1-3).

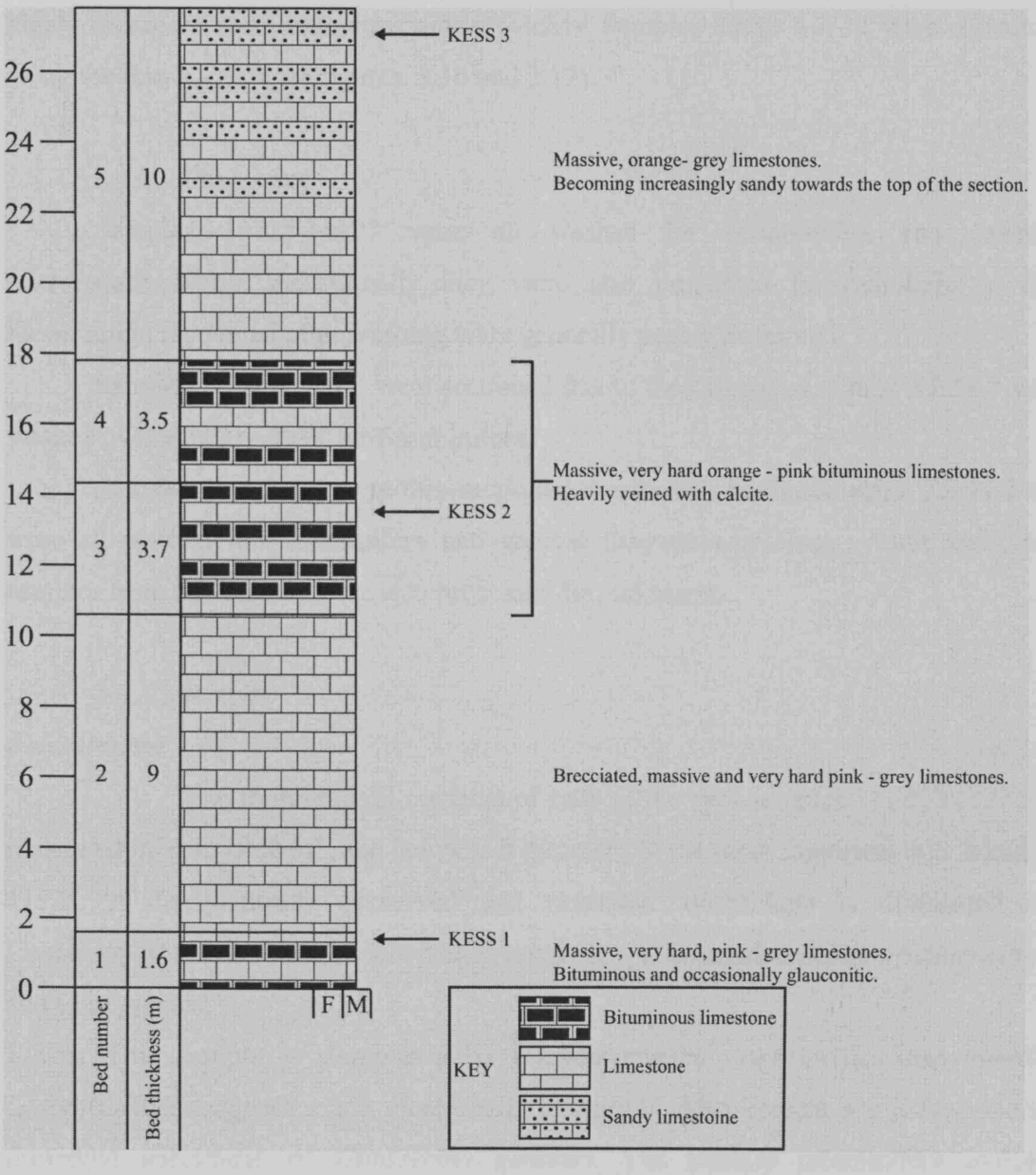

Figure 3.11 Lithological log of the section of Cenomanian sediments to the West of Kessab, with sampling levels indicated. For location of section see figure 3.10.

To the west of the fault on figure 3.10, thickly to medium bedded limestones and marls crop out. Again, these are steeply dipping to the SE. At the base of the succession, the limestones are massively bedded and quite sandy. There are minor, poorly exposed marl interbeds. Moving towards the top of the section medium bedded blue-grey marls become dominant. These are truncated by the road, and on the southern side of the road highly sheared serpentinite crops out in patches. Samples KESS 4 – 11 were collected along the line A – A' (see figures. 3.10 and 3.12).

3.4.3.2 Processing

Samples 11125-11127 were all washed for foraminifera and general micropalaeontology. Additionally they were also processed for radiolaria as the foraminifera recovered after washing were generally poorly preserved.

Samples KESS1 and 2 were sectioned due to their hardness, whilst KESS 3 was washed over a 63 μm sieve for foraminifera.

Samples KESS 4-6 were thin-sectioned due to their hardness whilst KESS 7-11 were all washed for foraminifera and general micropalaeontology. Additionally all samples from this section were also processed for radiolaria.

3.4.3.3 Results

Foraminifera

The foraminiferal contents of each of the spot samples 11125-11127 are illustrated in Text table 3.2, and below is a summary of the more important taxa found.

11125: A fairly poorly preserved and restricted assemblage is dominated by *Contusotruncana fornicata*, *Globotruncanita stuarti*, *Gta angulata*, *Globotruncana arca* and *G. aegyptica*.

11126: This sample is dominated by *Globotruncanita stuarti*, *Gta stuartiformis*, *Globotruncana aegyptica* and *Heterohelix globulosa*. Also present are a few poorly preserved specimens of *Gansserina gansseri*. The benthic foraminifera include *Spiroplectammina knebli* (Plate 1, Figure 11), *Gaudryina pyramidata*, *Neoflabelina suturalis*, *Neobulimina ?canadensis* (Plate 1, Figure 10), *Dorothia oxycona* (Plate 1, Figure 8), *Pullenia quaternaria* (Plate 1, Figs. 13 & 14), *Gyroidinoides globosus*, *Eponides mariei*, *Globorotalites* sp. (Plate 1, Figure 12) and *Bolivinoides* sp.

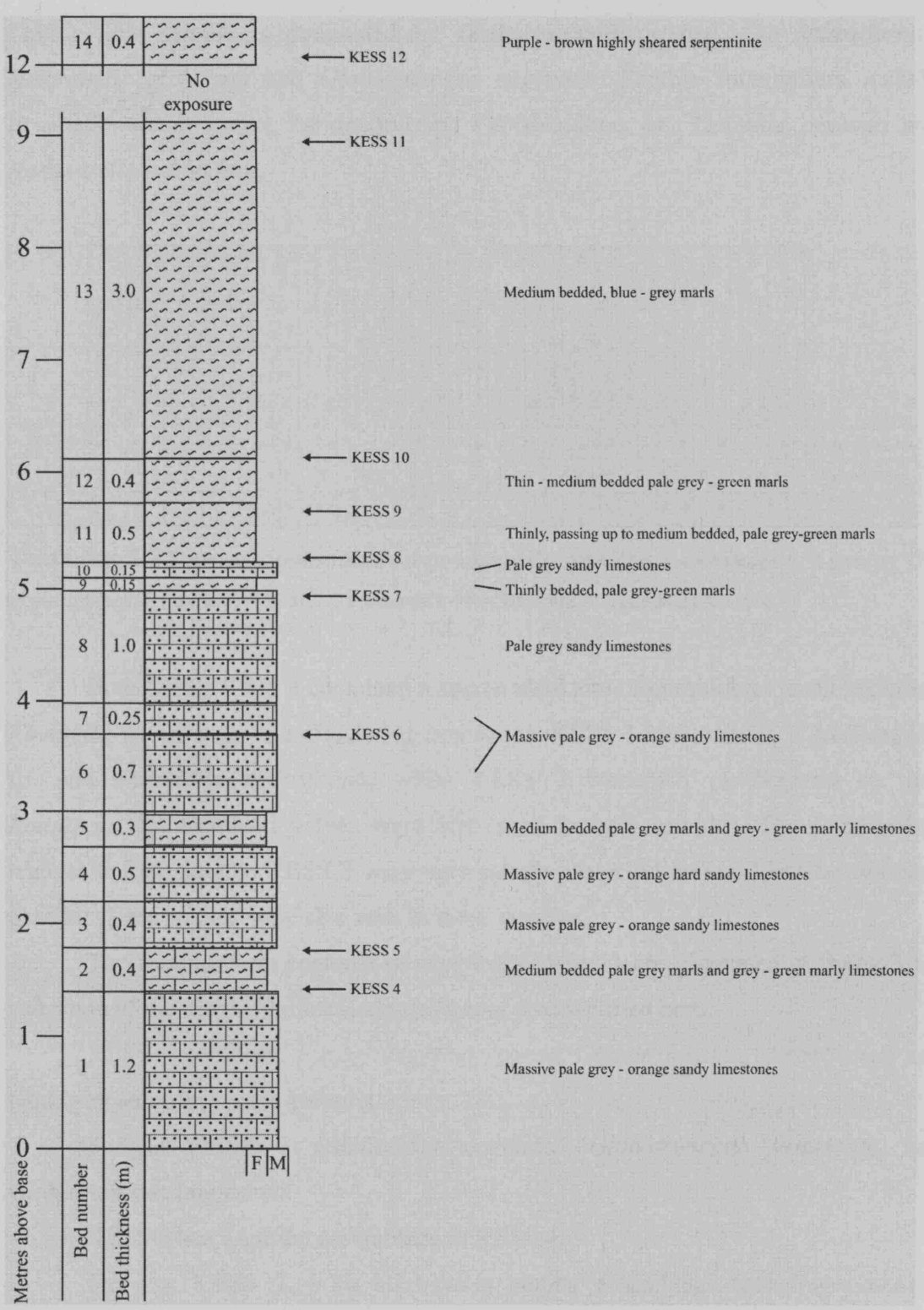

Figure 3.12 Lithological log of the sampled section to the west of Kessab. For location of section see figure 3.10.

11127: This sample is dominated by *Globotruncanita stuarti*, *Gta stuartiformis*, *Heterohelix globulosa* and *Globotruncana aegyptica*. Benthic foraminifera include *Praebulimina* cf. *reussi*, *Lenticulina* sp., *Globorotalites* sp., *Dorothia oxycona* and *Nodosarella subnodosa*.

	Archaeoglobigerina blowi	*Archaeoglobigerina cretacea*	*Contusotruncana fornicata*	*Globigerinelloides prairiehillensis*	*Globigerinelloides* sp.	*Gansserina gansseri*	*Globigerinelloides subcarinatus*	*Globigerinelloides* cf. *altamicra*	*Globigerinelloides volutus*	*Globotruncana aegyptica*	*Globotruncana arca*	*Globotruncana bulloides*	*Globotruncana falsostuarti*	*Globotruncana lapparenti*	*Globotruncana linneiana*	*Globotruncana ventricosa*	*Globotruncana rugosa*	*Globotruncana* sp.	*Globotruncanella* sp.	*Globotruncanita angulata*	*Globotruncanita conica*	*Globotruncanita* sp.	*Globotruncanita stuarti*	*Globotruncanita stuartiformis*	*Hedbergella holmdelensis*	*Hedbergella* sp.	*Heterohelix globulosa*	*Heterohelix navarroensis*	*Heterohelix punctulata*	*Heterohelix* sp.	*Laeviheterohelix* sp.	*Pseudoguembelina costulata*	*Pseudoguembelina* sp.	*Pseudotextularia elegans*	*Rugoglobigerina macrocephala*	*Rugoglobigerina rugosa*	*Rugoglobigerina* sp.	*Rugotruncana* sp.	
11125	P	R	A	P				P		A	C		A					R	P	P	R		C	P	P		C	R		R		P		R		C		P	*G. aegyptica* Zone
11126	R		P	P	P	P	R			A	P		C		R	R		P				R	A	C		P	A	P	P		P	P	P			P	P	R	*G. gansseri* Zone
11127			P						R	A	P	P	C	R			P	R		P			A	A			A	R			R	R		R		C			*G. aegyptica* Zone

Text table 3.2 Planktonic foraminiferal composition of the West Kessab spot samples. R (rare) = <1% of assemblage, P (present) = 1- 5%, C (common) = 6 – 10% and A (abundant) = >10%.

Both KESS 1 and 2 contained a sparse planktonic foraminiferal fauna including *Favusella washitensis* and *Shackoina cenomana*. KESS 1 also contained *Hedbergella* sp. and *Shackoina multispinata* while KESS 2 contained *Hedbergella* sp. and *Rotalipora* sp. Ostracod valves were also seen in both samples. The foraminifera recovered from sample KESS 3 were very poorly preserved and no identification was possible. Rare peloids were also seen in these samples.

The foraminiferal contents of samples KESS4-11 are illustrated in figure 3.13, and some of the more significant species found are identified here.

KESS 4 contained *Rugoglobigerina rugosa*, *Globotruncanita stuartiformis* and *Globigerinelloides prairiehillensis*.

Sample KESS 5 additionally contained *Globotruncana ventricosa* and *Globotruncana lapparenti*.

KESS 6 has a similar assemblage to KESS 4.

Samples KESS 7 – 10 all have a similar assemblage including common *Contusotruncana fornicata*, *Globotruncana aegyptica*, *Globotruncanita stuartiformis*, *Heterohelix globulosa* and *Pseudoguembelina costulata*.

KESS 11 contains few, poorly preserved foraminifera, including *Contusotruncana fornicata* (Plate1, Figs. 3 & 7), *Globigerinelloides prairiehillensis*, *Gl.*

subcarinata (Plate 1, Figs. 1 & 2), *Globotruncana aegyptica* and *Pseudoguembelina costulata* (Plate 1, Figure 4).

Radiolaria

The faunal composition of samples 11125 – 11127 are illustrated in Text table 4.3 and below is a summary of the more significant taxa.

Sample 11125 contains a moderately preserved assemblage dominated by dictyomitrids, particularly *Dictyomitra multicostata*, as well as *Archaeodictyomitra lamellicostata* (Plate 2, Figure 4), *Amphipyndax pseudoconulus, A. tylotus* and *A. stocki.* Other important taxa include *Theocapsomma comys*, *Alievium gallowayi*, *Pseudoaulophacus floresensis*, *Holocryptocanium barbui* (Plate 3, Figure 12) and *Phaseliforma* sp.

A restricted, moderately to poorly preserved assemblage was recovered from sample 11126, totally dominated by *Dictyomitra multicostata*, with rare *Praeconocaryomma* sp., *Holocryptocanium barbui*, *Amphipyndax* sp. and a small number of indeterminate nassellarians and spumellarians.

Sample 11127 contained a more diverse assemblage, including common *Dictyomitra multicostata*, *Amphipyndax pseudoconulus*, *Alievium gallowayi* and *Holocryptocanium barbui*. Other taxa present include *Dictyomitra rhadina* (Plate 2, Figure 2), *Amphipyndax tylotus*, *Foremanina schona* (Plate 2, Figure 5), *Pseudoaulophacus lenticulatus* and *Phaseliforma carinata.*

	Alievium gallowayi	*Aphipyndax* cf. *pseudoconulus*	*Amphipyndax* cf. *stocki*	*Amphipyndax* sp.	*Amphipyndax pseudoconulus*	*Amphipyndax stocki*	*Amphipyndax tylotus*	*Archaeodictyomitra lamellicostata*	*Archaeodictyomitra* sp.	*Archicapsa* sp.	*Cassiduscus* sp.	*Cryptamphorella* sp.	*Dictyomitra* cf. *koslovae*	*Dictyomitra multicostata*	*Dictyomitra rhadina*	*Dictyomitra* sp.	*Foremanina schona*	*Holocryptocanium barbui*	*Orbiculiforma* sp.	*Patellula euesseeei*	*Patellula verteroensis*	*Phaseliforma* sp.	*Phaseliforma carinata*	*Praeconocaryomma* sp.	*Pseudoaulophacus floresensis*	*Pseudoaulophacus lenticulatis*	*Pseudoaulophacus* sp.	*Novixitus* sp.	*Rhopalosyringium magnificum*	*Rhopalosyringium* sp.	*Stichomitra communis*	*Stichomitra* sp.	*Theocapsomma comys*	*Xitus spinularis*	*Xitus* sp.	Indeterminate nasellarians	Indeterminate spumellarians	
11125		P			C	P	P	P	R	R	R			A	P	P	R	P	R	P		P			P			R	P	P	R		R		P	R	R	*P. dickinsoni* Zone
11126				P										A				P						P												C	C	*P. dickinsoni* Zone ?
11127	C	C			A	P	P	P	P			R	R	A	P		R	P		R	R	R	R		P	P	P		P				C	C	P			*P. dickinsoni* Zone

Text table 3.3 Radiolarian composition of the west Kessab spot samples. R (rare) = <1% of assemblage, P (present) = 1- 5%, C (common) = 6 – 10% and A (abundant) = >10%.

Samples KESS4 -11 were all processed for radiolaria and the exact faunal content of these samples are illustrated in the figures 3.14 and 3.15. Figure 3.14

illustrates the nassellarians and figure 3.15 the spumellarians. Samples KESS 4-10 all contain common *Amphipyndax tylotus*. Other important taxa include members of the genera *Pseudoaulophacus*, *Praeconocaryomma*, *Phaseliforma* and *Protoxiphotractus*.
A specimen of *A.* cf. *bipartium* was recovered from sample KESS 4 and an additional three specimens were recovered from sample KESS 5. Other important species include *Archaeospongoprunum andersoni* and *A. hueyi*. Other taxa from these samples that are illustrated include *Praeconocaryomma universa* (Plate 3, Figure 13), *Pseudoaulophacus vielseitigus* (Plate 3, Figure 6), *Orbiculiforma* ?sp. (Plate 3, Figure 9), *Cavidiscus* sp. (Plate 3, Figure 11), *Protoxiphotractus* sp. (Plate 3, Figure 15) and *Praestylosphaera* sp. (Plate 3, Figure 16).

Samples KESS 6 – 9 contain fairly diverse and reasonably well preserved assemblages including *Pseudoaulophacus floresensis*, *Pseudoaulophacus lenticulatis*, *Theocampe apicata* (Plate 2, Figure 7), *Theocapsomma comys* (Plate 2, Figure 8) and members of the Praeconocaryommidae and the Phaseliformidae. The Praeconocaryommidae appear to become extinct by sample KESS 9 and the Phaseliformidae by sample KESS 10. Both then reappear in sample KESS 11, but this is taken as due to reworking as will be discussed later. Other taxa from these samples include *Amphipyndax pseudoconulus* (Plate 2, Figure 3), *Protunuma* sp. (Plate 2, Figure 15) and *Xitus* sp. (Plate 2, Figure 11)

KESS 10 overall contains a similar assemblage but *Theocapsomma comys*, *Orbiculiforma sacramentoensis* and several other taxa are absent. No significant new species appear however.

By sample KESS 11 a number of species and genera have disappeared and the sample is dominated by *Dictyomitra multicostata*.

3.4.3.4 Age

11125: The presence of the planktonic foraminifera *G. aegyptica* suggests the sample is no older than late Campanian in age, and this concurs with the age suggested by the radiolaria, where the co-occurrence of *Amphipyndax pseudoconulus* and *A. tylotus* are reported to co-occur towards the end of the formers range (Sanfilippo and Riedel, 1985) during the Late Campanian. The overall radiolarian assemblage indicates a late Campanian age for the sample; assignable to the *Patulibrachium dickinsoni* Zone (Pessagno) agreeing well with the date obtained using the foraminifera.

11126: The presence of specimens of *Gansserina gansseri* suggests a *Gansserina gansseri* Zone age. This zone ranges from the late Campanian to early Early Maastrichtian and the other planktonic foraminifera present do not allow the sample to be assigned with any confidence to one stage or the other. The benthic foraminifera however are indicative of a Campanian age. This sample is therefore tentatively placed within the lower part of the *Gansserina gansseri* Zone within the uppermost Campanian based on the foraminiferal content. All praeconocaryommid radiolaria are reported to become extinct by the end of the Campanian suggesting the sample is no younger than Campanian in age, though reworking is obviously a possibility. No other age diagnostic forms were determined, but the low diversity compared to other samples is an interesting feature, perhaps due to dissolution, though whether this was contemporaneous or occurred during diagenesis is unclear, and this could also be an indication of a more restricted environment. An uppermost Campanian age is therefore assigned to this sample based on the foraminiferal and radiolarian assemblages recovered.

11127: The presence of *Globotruncana aegyptica* dates the sample as no older than the Late Campanian *Globotruncana aegyptica* Zone. The absence of *Gansserina gansseri* suggests an age no younger than the *G. aegyptica* Zone. The Benthic foraminifera are also indicative of a Campanian age. The radiolarian assemblage also suggests a Late Campanian age for the sample, as *P. carinata* first appears during the late Campanian whilst *P. lenticulatus* is restricted to the Campanian. As with sample 11125, this sample is assignable to either the *Phaseliforma carinata* Subzone or *Patulibrachium dickinsoni* Zone of Pessagno. However, the foraminiferal data suggest the latter i.e. equivalent to the lower part of the *Amphipyndax tylotus* Zone of Sanfilippo and Riedel, 1985.

Samples KESS 1 and 2 were determined as Lower Cenomanian based on the presence of both *Favusella washitensis* and *Shackoina cenomana*, whilst no age determination was attempted for KESS 3 due to the paucity of the sample.

The section illustrated in Figure 3.12 can be divided into two, possibly three foraminiferal zones (see figure 3.13). The lower part of the section (Samples KESS 4 – 6) would appear to be older than the *Globotruncana aegyptica* Zone as this species is absent from all three samples, whilst the upper part of the section (Samples 7 -10)

belongs to the *Globotruncana aegyptica* Zone. Sample KESS 11 has a similar overall assemblage to spot sample 11126 and is therefore tentatively assigned to the *Gansserina gansseri* Zone. In general the radiolarian dating concurs with that achieved using foraminifera and the section can be tentatively divided into two radiolarian zones; the *Patulibrachium dickinsoni* Zone and the *Crucella espartoensis* Zone (which can be further divided into the *Protoxiphotractus perplexus* and *Patulibrachium lawsoni-Phaseliforma carinata* Subzones).

KESS 4 contains no age diagnostic species other than *Rugoglobigerina rugosa* that first appears during the *Globotruncanita elevata* Zone, giving an oldest age for this sample of early Campanian whilst the additional co-occurrence of *Globotruncana ventricosa* and *Globotruncana lapparenti* in KESS 5 indicates a mid-late Campanian age, i.e. *Globotruncana ventricosa* and *Globotruncanella havanensis* Zones. These two samples can also be confidently assigned to the *Amphipyndax tylotus* Zone (Sanfilippo and Riedel, 1985). The base of this zone is defined by the first evolutionary appearance of the nominate taxon, which is a common component of all the samples in this section apart from KESS 11. Other important taxa include members of the genera *Pseudoaulophacus*, *Praeconocaryomma*, *Phaseliforma* and *Protoxiphotractus*. The Pseudoaulophacidae, Praeconocaryommidae and a number of members of the Phaseliformidae all become extinct within or at the top of this zone.

Pessagno (1976) suggests it should be possible to further divide the *A. tylotus* Zone into the *Orbiculiforma renillaeformis* and *Patulibrachium dickinsoni* Zones, and the *Amphipyndax pseudoconulus* Zone (*Crucella espartoensis* Zone) into the *Protoxiphotractus perplexus*, *Patulibrachium lawsoni* and *Phaseliforma carinata* Subzones (see Figure 3.4), however, as discussed below the tentative identifications of many species due to only moderate preservation, and the co-occurrence of species that should be restricted to different zones and subzones makes this extremely difficult. Samples KESS 4 – 5 were initially tentatively assigned to the *Alievium gallowayi* Zone, which is essentially Santonian to early Campanian in age, and characterised by the first appearance of the nominate taxon at the base and the last appearance of *Archaeospongoprunum bipartium* at the top. Three specimens of *A.* cf. *bipartium* were recovered from sample KESS 5, additionally the nominate taxon is present in sample KESS 4. However, other species are present that are recorded as being younger in age, such as *Archaeospongoprunum andersoni* and *A. hueyi*. Therefore, it is probable that

the samples are younger in age than the *A. gallowayi* Zone and do in fact belong to the *Crucella espartoensis* Zone, and that the occurrences of specimens of *A.* cf. *bipartium* have either been mis-identified or reworked. The presence of *A. andersoni* does suggest an age for the samples older than those seen to the east of Kessab (although probably still part of the *Crucella espartoensis* Zone) and it is possible that samples KESS 4-5 are assignable to the *P. perplexus* Subzone during which *A. andersoni* becomes extinct. This agrees with the dating achieved using the foraminiferal content.

KESS 6 has a similar foraminiferal assemblage to KESS 4 but its position suggests that it is no older than the *Globotruncana ventricosa* Zone, whilst the radiolarian indicate a Campanian *Crucella espartoensis* Zone age for the sample

Samples KESS 7 – 9 appear to belong to the *Globotruncana aegyptica* Zone as the nominate taxon is present in all the samples and there are no occurrences of *Gansserina gansseri*, the first appearance of which marks the base of the *Gansserina gansseri* Zone. This does not entirely agree with the radiolarian evidence which suggests these samples should all be assigned to the *Crucella espartoensis* Zone due to a number of genera and species typical of that zone occurring in all samples including *Pseudoaulophacus floresensis*, *P. lenticulatis* and *Theocampe apicata*. The radiolaria therefore suggest a slightly older age for these samples than that suggested by the foraminifera. The samples can however be confidently dated as late Campanian in age.

KESS 10 has a similar foraminiferal assemblage to KESS 7 – 9 and is also assigned to the Late Campanian *Globotruncana aegyptica* Zone. This agrees well with the radiolarian evidence. The interval between the last occurrence of the Pseudoaulophacidae (apart from *Alievium gallowayi*) and the last occurrence of the Phaseliformidae is defined as the *Patulibrachium dickinsoni* Zone, and although the nominate taxon was not identified, sample KESS 10 is tentatively assigned to this zone due to the characteristics of the overall assemblage.

KESS 11 was taken from approximately the same stratigraphic level as spot sample 11126, has a similar overall assemblage and is therefore tentatively assigned to the lower part of the *Gansserina gansseri* Zone, though the nominate taxon is not present in this sample. The radiolaria suggest the sample is late Campanian to early Maastrichtian in age, based on the disappearance of a number of genera such as *Pseudoaulophacus* and *Phaseliforma* indicating it belongs to the *Patulibrachium dickinsoni* Zone. The reappearance of specimens of Praeconocaryommidae and Phaseliformidae is due to reworking as testified by their more worn appearance.

Figure 3.13 Foraminiferal content of sampled section west of Kessab. Dashed lines = recorded in thin section but no relative abundance estimated. Lines in increasing thickness represent rare = <1% of assemblage, present = 1- 5%, common = 6 – 10% and abundant = >10%.

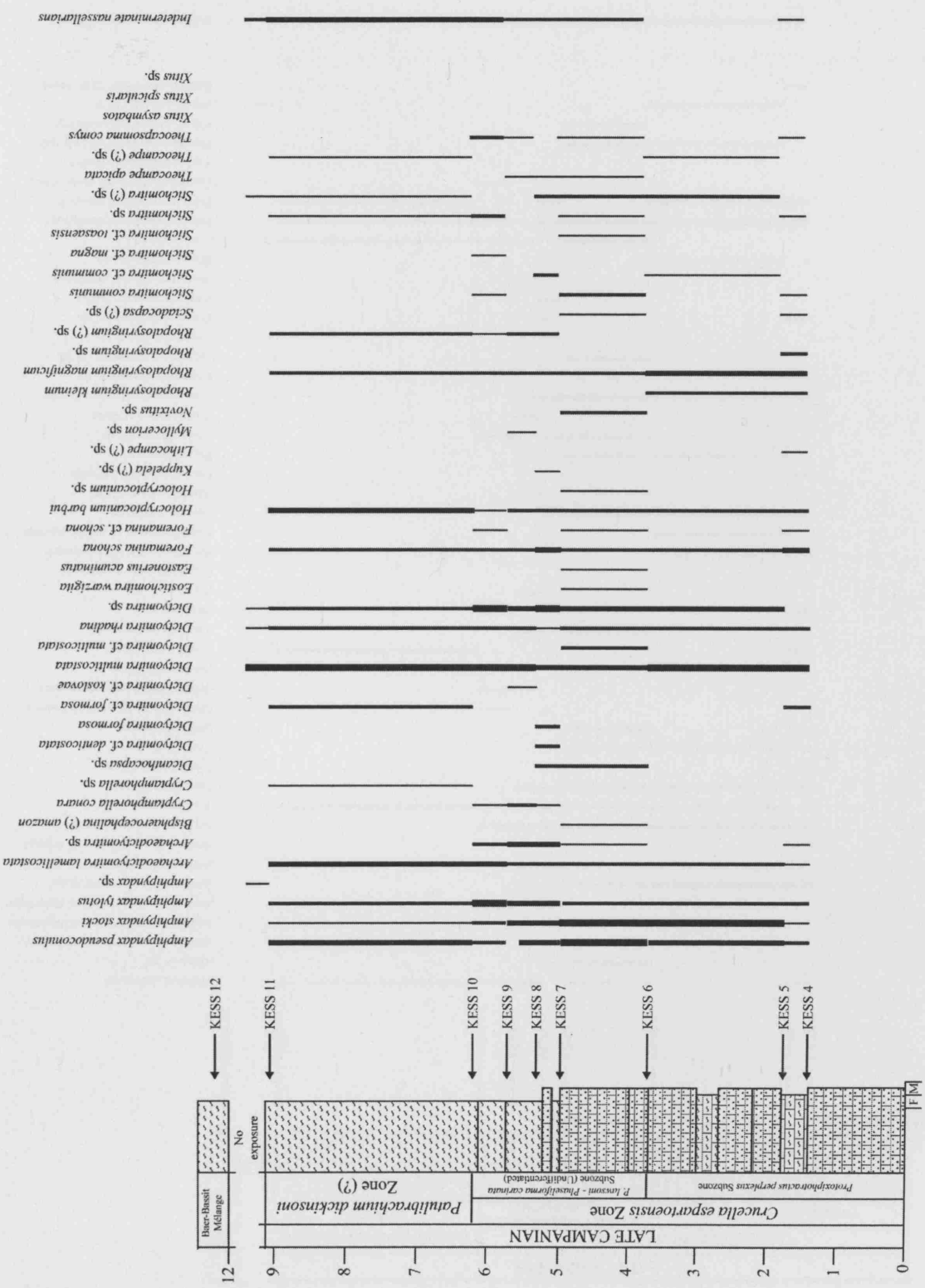

Figure 3.14 Nassellarian radiolaria content of sampled section west of Kessab. Lines in increasing thickness represent rare = <1% of assemblage, present = 1- 5%, common = 6 – 10% and abundant = >10%. Zones/subzones based on radiolaria recovered.

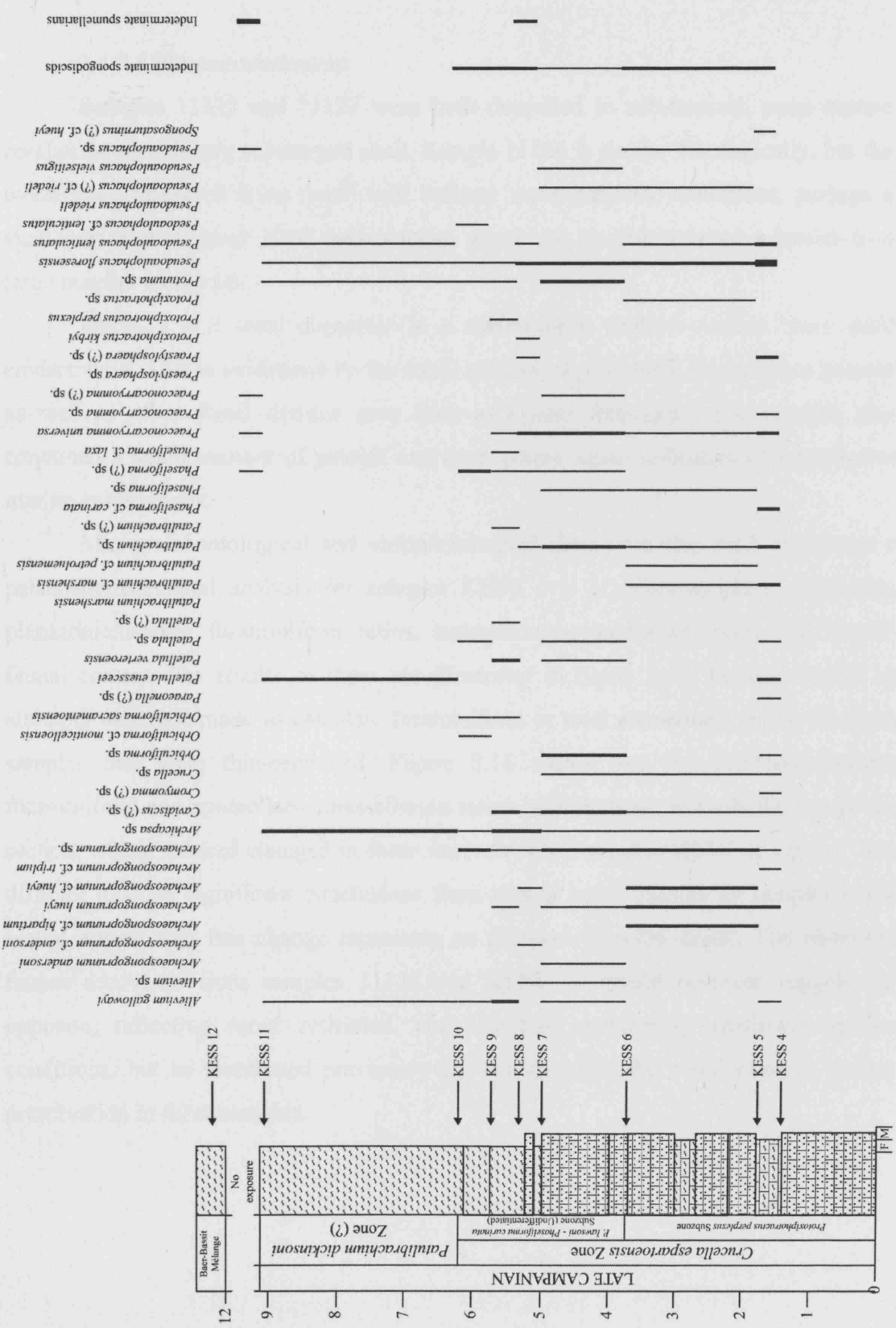

Figure 3.15 Spumellarian radiolaria content of sampled section west of Kessab. Lines in increasing thickness represent rare = <1% of assemblage, present = 1- 5%, common = 6 – 10% and abundant = >10%. Zones/subzones based on radiolaria recovered.

3.4.3.5 Palaeoenvironment

Samples 11125 and 11127 were both deposited in sub-tropical, open marine conditions on a deeply submerged shelf. Sample 11126 is similar lithologically, but the much more restricted fauna could well indicate more restricted conditions, perhaps a shallower marine, inner shelf environment, where the conditions were a barrier to a large number of species.

KESS 1 – 3 were deposited in a sub-tropical, shallow marine inner shelf environment. This is evidenced by the small number of planktonic foraminifera present as well as other fossil detritus seen such as Oyster fragments. The samples also contained a small number of peloids and sand grains, again indicative of a shallower marine environment.

Micropalaeontological and sedimentological data were also used to attempt a palaeoenvironmental analysis for samples KESS 4 – 11. This included calculating planktonic:benthic foraminiferal ratios, nassellarian:spumellarian ratios and overall faunal content The results of these are illustrated in figure 3.16, but are limited as attempts were not made to calculate foraminiferal or total assemblage ratios for those samples that were thin-sectioned. Figure 3.16 shows that the planktonic:benthic foraminiferal and spumellarian:nassellarian ratios both increase towards the top of the section, with a marked changed in these ratios between samples KESS 10 and 11. It is difficult to draw significant conclusions from such a small number of samples but it would appear that this change represents an increase in water depth. The restricted faunas recovered from samples 11126 and KESS 11 would however suggest the opposite, reflecting more restricted, and therefore presumably shallower marine conditions, but as mentioned previously this could simply be a reflection of poorer preservation in these samples.

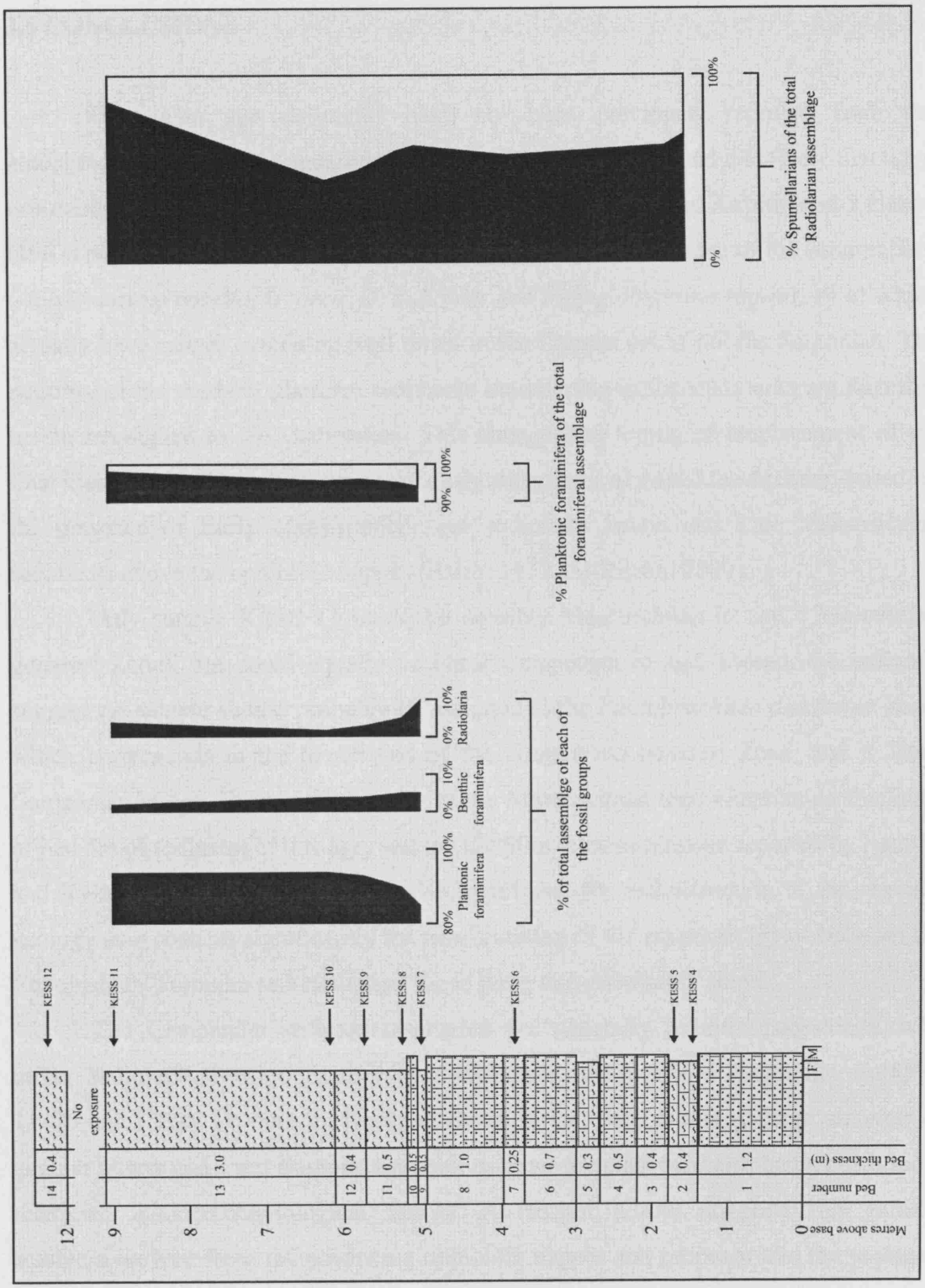

Figure 3.16 Plot of overall faunal composition, % planktonic foraminifera of the total foraminiferal assemblage and % spumellarians of total radiolarian assemblage against sampling levels west of Kessab.

3.5 CONCLUSIONS

Campanian age sediments have not been previously reported from the autochthonous carbonates underlying the Baer-Bassit ophiolite, and it is likely that these sediments were previously wrongly dated as Early Maastrichtian. Kazmin and Kulakov (1967) dated the "Lower Maastrichtian" limestones on the presence of the foraminifera *Globotruncana rosetta*, *G. arca*, *G. bulloides* and *Rugoglobigerina rugosa*, all of which actually have ranges extending well down in the Campanian, if not the Santonian. The majority of the Arabian platform sediments outcropping in the study area are therefore herein reassigned to the Campanian. This changes the timing of emplacement of the Baer-Bassit ophiolite, which was previously thought to be Mid-Maastrichtian based on the presence of Early Maastrichtian age sediments below and Late Maastrichtian sediments above the ophiolitic nappes (Parrot 1977, Al-Riyami 2000).

Only sample KESS 11 could be possibly Maastrichtian in age, (?*Gansserina gansseri* Zone), but could equally be latest Campanian in age. Indeed, the radioaria suggest the sample should probably be assigned to the *Patulibrachium dickinsoni* Zone, which corresponds to the lower part of the *Gansserina gansseri* Zone, and is latest Campanian in age. Even if these samples are Maastrichtian then a maximum thickness of just 5m of sediment of this age, and not the 90m thick succession reported by Kazmin and Kulakov (1968) crop out. It is also significant for reconstruction of the regional geology as it reduces significantly the time duration of the supposed hiatus between the Cenomanian-Turonian sediments and those lying unconformably above.

The Campanian sediments sampled are generally micritic packstones, with minor radiolaria, benthic foraminifera, ostracods and echinoid fragments. Samples 11126 and KESS 11 were markedly different in that they contained large amounts of angular quartz and chert fragments as well as other minerals (and also had a much more restricted micropalaeontological fauna). Al-Riyami (2000) suggests this reflects sediment derived from the advancing ophiolitic nappes and proposes that the youngest part of the carbonate platform was removed by thrusting, citing tectonically aligned and sheared sedimentary particles as evidence. This seems plausible, but the presence of ophiolitic derived detritus within the highest levels of the autochthon suggests these sediments were deposited just prior to the arrival of the ophiolitic nappes and that if any of the autochthonous sediments have been removed it is not of a significant thickness.

The possible relative increase in water depth reflected by the increase in planktonic:benthic ratios is also reflected in a change of planktonic assemblage. Parsons and Brasier (1986) suggest that a dominance of single keeled globotruncanids, such as *Globotruncanita stuarti* and *Gita stuartiformis*, along with double keeled forms with fewer than 5 chambers in the final whorl, such as *Contusotruncana fornicata*, are indicative of an open-marine, inner–outer shelf environment, whilst a dominance of double keeled forms with more than 5 final chambers in the final whorl, such as *Globotruncana arca* and *G. ventricosa* indicate a deeper, outer shelf environment. This pattern appears to be borne out in the section, though things are less clear in the results from the spot samples. In contrast the restricted fauna recovered from samples KESS 11 and 11126 would suggest a shallower and more restricted marine environment, but this could be an artefact of preservation. Another possibility is that water depth did increase, but the approaching ophiolitic nappes were creating a barrier to a number of planktonic species.

If there was an increase in water depth immediately prior to ophiolite emplacement it is likely this was caused by flexural loading of the shelf as the ophiolitic nappes approached. This apparent increase in water depth would therefore also indicate these sediments were deposited just prior to initial emplacement of the ophiolite upon the Arabian platform.

All the evidence suggests that ophiolite emplacement occurred shortly after the deposition of the youngest exposed autochthonous sediments. These are predominantly late Campanian in age, with a possible thin covering of earliest Maastrichtian marls.

The sediments of the Arabian platform in northern Syria have not been extensively studied since they were mapped by the team of Russian geologists in the late 1960's. It is likely therefore that a detailed micropalaeontological study could significantly refine the current stratigraphy and correct any possible discrepancies in the dating of the sediments. Text table 3.4 summarises the ages assigned to the samples collected from the autochthon

Sample No.	Foraminiferal zone	Radiolaria zone/subzone	Age assignment
Badroussiyeh			
BADR 1			Cenomanian
BADR 2			Cenomanian
BADR 3			Cenomanian
BADR 4			Cenomanian
BADR 5			Cenomanian
East Kessab			
11122			
11123			
11124		*Phaseliforma carinata* Subzone	late Campanian
EK 1		*Phaseliforma carinata* Subzone	late Campanian
EK2	*"Radotruncana" calcarata* Zone	*Phaseliforma carinata* Subzone	late Campanian
EK3		*Crucella espartoensis* Zone	Campanian
West Kessab			
11125	*Globotruncana aegyptica* Zone	*Patulibrachium dickinsoni* Zone	latest Campanian
11126	*Gansserina gansseri* Zone?	*Patulibrachium dickinsoni* Zone	latest Campanian
11127	*Globotruncana aegyptica* Zone	*Patulibrachium dickinsoni* Zone	latest Campanian
KESS 1			
KESS 2			Lower Cenomanian
KESS 3			Lower Cenomanian
KESS 4	*Gta elevata-G. ventricosa* Zones	*Protoxiphotractus perplexus* Subzone	early Campanian
KESS5	*G. ventricosa-Glla havanensis* Zones	*Protoxiphotractus perplexus* Subzone?	mid-late Campanian
KESS 6	*G. ventricosa-Glla havanensis* Zones	*P. lawsoni-Ph. carinata* Subzones	mid-late Campanian
KESS 7	*Globotruncana aegyptica* Zone	*P. lawsoni-Ph. carinata* Subzones	late Campanian
KESS 8	*Globotruncana aegyptica* Zone	*P. lawsoni-Ph. carinata* Subzones	late Campanian
KESS 9	*Globotruncana aegyptica* Zone	*P. lawsoni-Ph. carinata* Subzones	late Campanian
KESS 10	*Globotruncana aegyptica* Zone	*Patulibrachium dickinsoni* Zone?	latest Campanian
KESS 11	*Gansserina gansseri* Zone?	*Patulibrachium dickinsoni* Zone?	latest Campanian-Maastrichtian?

Text table 3.4 Summary of samples collected with their age assignments.

PLATE 1

Planktonic and benthic foraminifera from the autochthonous Arabian carbonate platform. Lengths given refer to maximum width.

1, 2. *Globigerinelloides subcarinata* (Brönnimann) 1952. Sample KESS11. 1, 2) lateral, x185, 198μm.

3, 7. *Contusotruncana fornicata* (Plummer) 1931. Sample KESS11. 3) ventral, x87.5, 381μm. 7) dorsal, x87.5, 381μm. Note poor preservation typical of specimens from autochthon samples.

4. *Pseudoguembelina costulata* (Cushman) 1938. Sample KESS11. Side view, x95, 223μm.

5, 6. *Globotruncanita calcarata* (Cushman) 1927. Sample EK2. 5) ventral, x92.5, 429μm. 6) dorsal, x92.5, 429μm. Note etching caused by processing method.

8. *Dorothia oxycona* (Reuss). Sample 11126. Side view, x46, 780μm.

9. Unidentified benthic foraminifera. Sample 11126. Side view, x85, 350μm.

10. *Neobulimina ?canadensis* (Cushman and Wickenden). Sample 11126. Side view, x45, 455μm.

11. *Spiroplectammina knebeli* Le Roy1953. Sample 11126. Side view, x67.5, 416μm.

12. *Globorotalites* sp. Sample 11126. ventral, x115, 329μm.

13, 14. *Pullenia quaternaria* (Reuss)1851. Sample 11126. 13) lateral, x90, 419μm. 14) umbilical view, x90, 377μm.

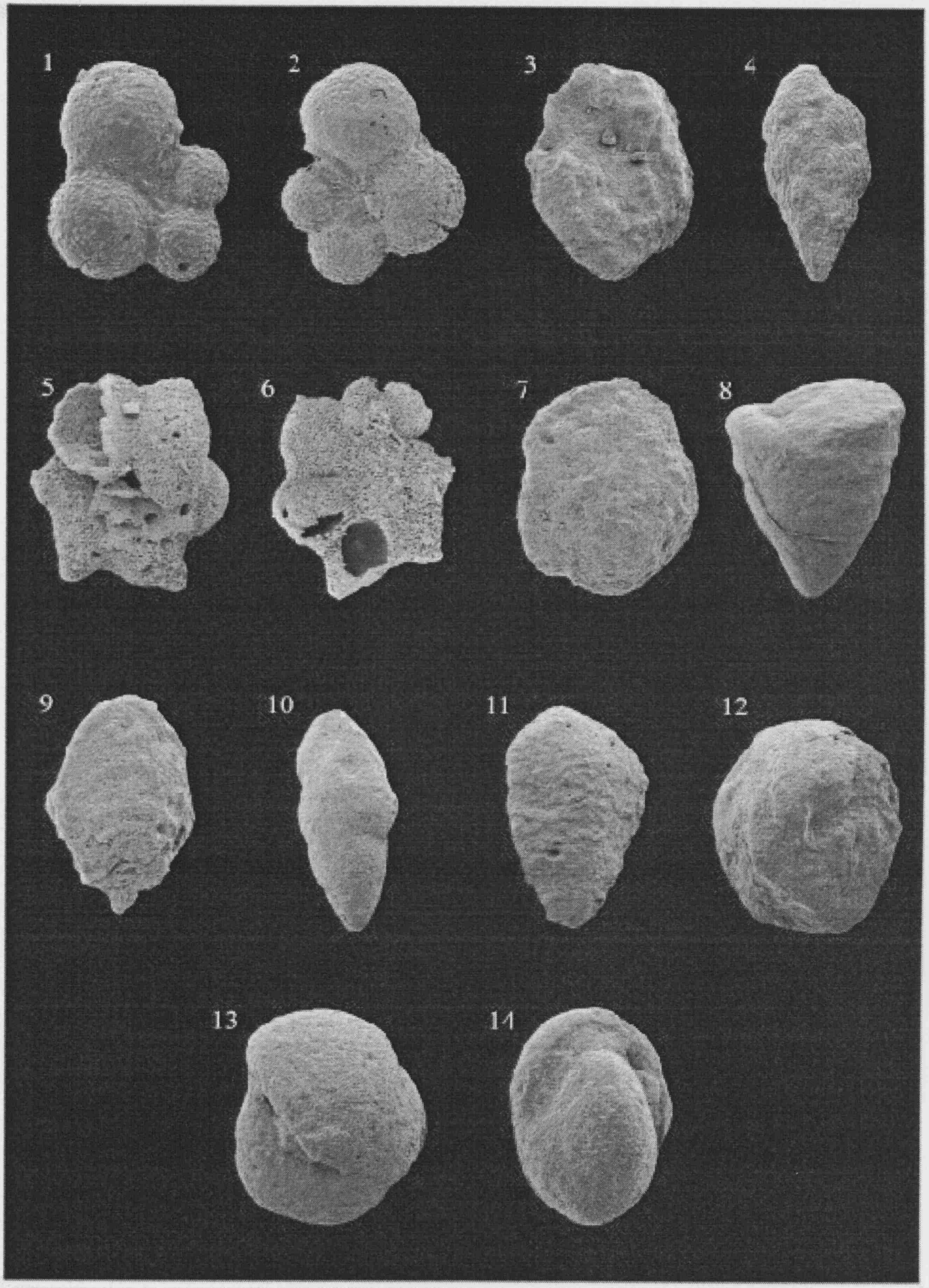

PLATE 1

PLATE 2

Radiolaria from the autochthonous Arabian carbonate platform. Lengths given refer to maximum width.

1. *Dictyomitra multicostata.* Sample 11124. x115, 152μm.
2. *Dictyomitra rhadina.* Sample 11127. x95, 110μm.
3. *Amphipyndax pseudoconulus.* Sample KESS8. x155, 123μm.
4. *Archaeodictyomitra lamellicostata.* Sample 11125. x175, 93μm.
5. *Foremanina schona.* Sample 11127. x135, 137μm.
6. *Amphipyndax* cf. *tylotus.* Sample EK3. x160, 112μm. Note more irregular distribution of surface nodes than on specimen 3.
7. *Theocampe apicata.* Sample KESS6. x 262.5, 100μm.
8. *Theocapsomma comys.* Sample KESS9. x225, 67μm.
9. *Stichomitra communis.* Sample KESS10. x190, 125μm.
10. *Rhopalosyringium magnificum.* Sample 11124. x155, 144μm.
11. *Xitus* sp. Sample KESS9. x312, 78 μm.
12. *Archaeospongoprunum* sp. Sample 11124. x100, 58μm.
13. *Archaeospongoprunum* cf. *triplum.* Sample 11124. x65, 89μm.
14. *Archaeospongoprunum andersoni.* Sample 11124. x97.5, 76μm.
15. *Protunuma* sp. Sample KESS9. x312.5, 90μm.
16. *Halesium* ?sp. Sample EK2. x130, 278μm.
17. *Patulibrachium lawsoni- P. dickinsoni* transitional form. Sample 11124. x105, 213μm.
18. *Crucella* sp. Sample 11124. x100, 421μm.
19. *Patulibrachium* sp. Sample 11124. x130, 272μm.

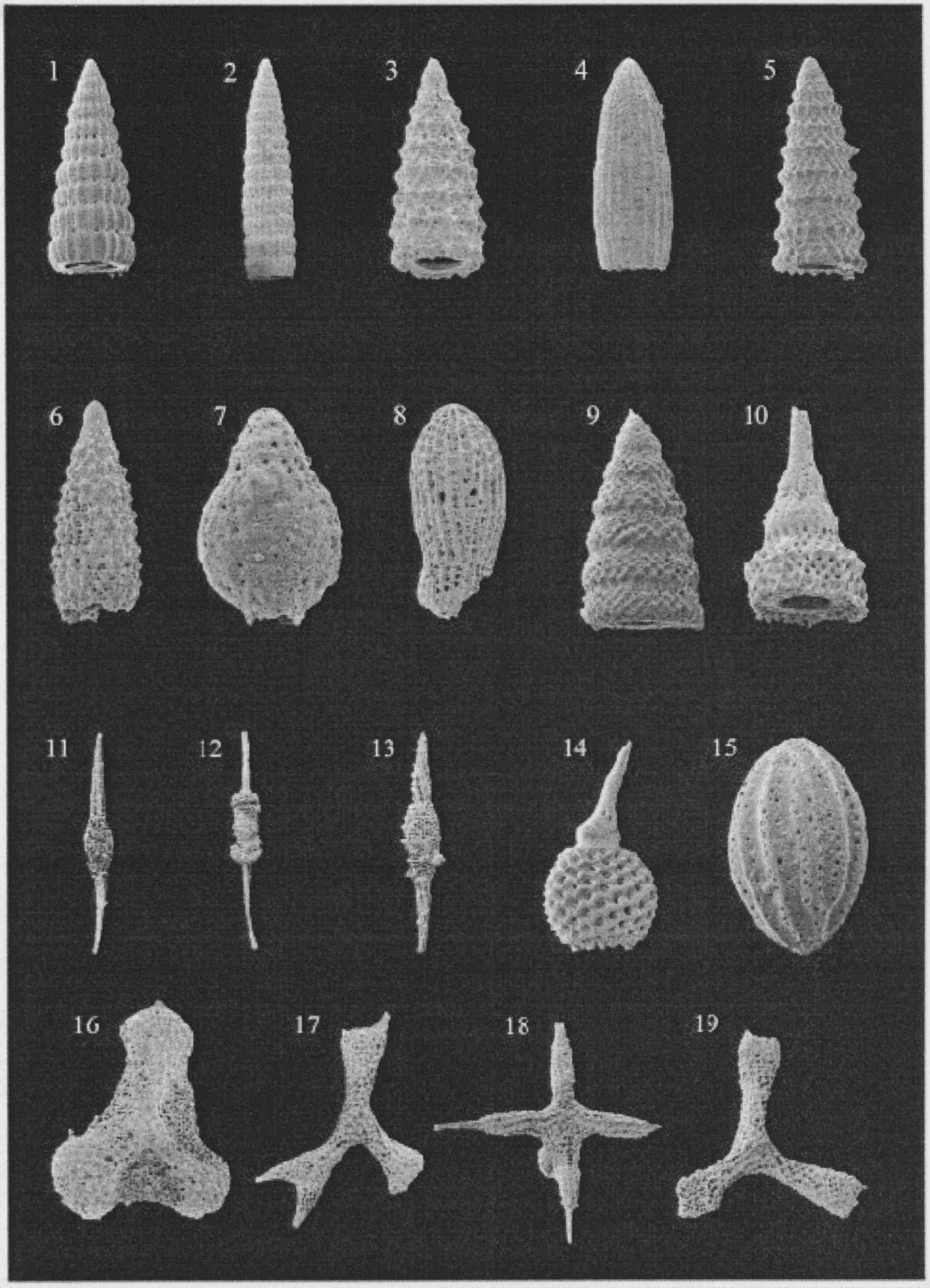

PLATE 2

PLATE 3

Radiolaria from the autochthonous Arabian carbonate platform. Lengths given refer to maximum width.

1, 2. *Patellula verteroensis* (Pessagno) 1963. 1) x145, 254μm. 2) edge view, x145, 166μm.

3. *Pseudoaulophacus parguerаensis* Pessagno 1963. Sample EK1. x150, 281μm.

4. *Pseudoaulophacus riedeli* Pessagno 1976. Sample EK1. x185, 200μm.

5. *Pseudoaulophacus lenticulatus* (White) 1928. Sample EK4. x65, 236μm.

6. *Pseudoaulophacus vielseitigus* Empson-Morin 1981. Sample KESS4. x190, 217μm.

7. *Pseudoaulophacus floresensis* Pessagno 1963. Sample EK4. x130, 334μm.

8. *Alievium gallowayi* (White) 1928. Sample 11124. x150. 223μm.

9. *Orbiculiforma* ?sp. Sample KESS4. x175, 244μm.

10. *Orbiculiforma* sp. Sample KESS11. x125, 314μm.

11. *Cavidiscus* sp. Sample KESS4. x170, 198μm.

12. *Holocryptocanium barbui* Sample 11125. x225, 174μm.

13. *Praeconocaryomma universa* Pessagno 1976. Sample KESS4. x200, 210μm.

14. *Phaseliforma laxa*. Sample KESS10. x195, 168μm.

15. *Protoxiphotractus* sp. (Spines broken off). Sample KESS4. x312, 91μm.

16. *Praestylosphaera* sp. Sample KESS4. x225, 113μm.

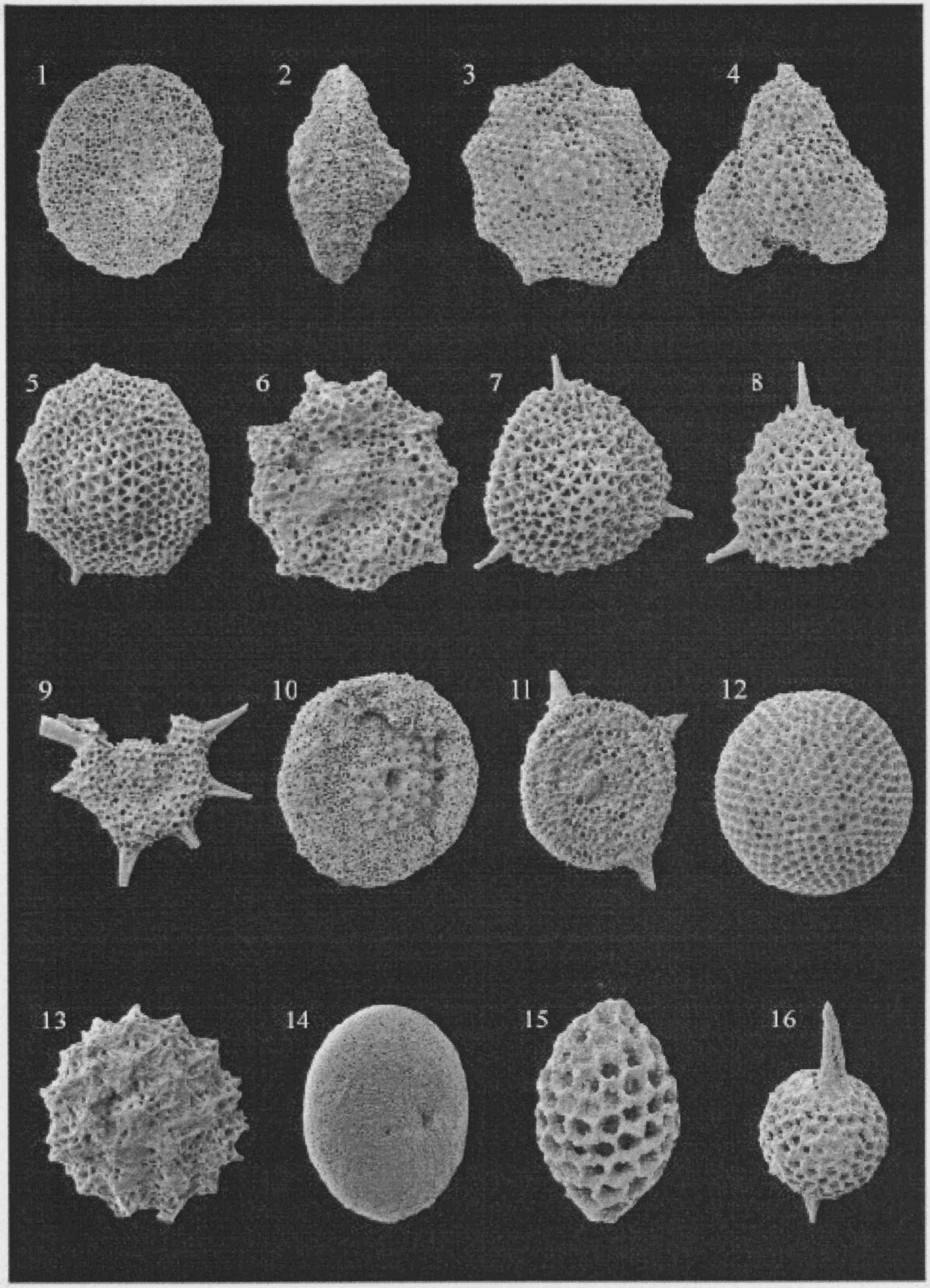

PLATE 3

CHAPTER 4: THE BAER-BASSIT MÉLANGE

4.1 INTRODUCTION

The Baer-Bassit mélange lies tectonically beneath the ophiolite, and is also intersliced with it in areas where out-of-sequence thrusting has occurred (Al-Riyami 2000). The mélange primarily comprises isolated blocks of sediments and volcanics of Late Triassic to Late Cretaceous age that are set within a poorly exposed "tectonic matrix" derived from the same lithologies. Ophiolitic and metamorphic blocks are also present and highly sheared serpentinite and shales are the usual lithologies of the "tectonic matrix". The mélange sediments and volcanics are interpreted as Arabian platform margin lithologies that have been emplaced onto the Arabian continental margin as disrupted thrust slices during the obduction of the Baer-Bassit ophiolite. Exposures of the mélange are generally limited to the more competent lithologies that form the isolated blocks, whilst the matrix tends to form areas of no exposure, only occasionally exposed in road cuttings, but typically producing a deep red soil.

The mélange is discussed as an integral part of the ophiolitic history. It was not studied in detail during this work however, as exposure was limited to isolated blocks and it was not thought that further micropalaeontological studies would yield much further relevant information. Additionally, an extensive micropalaeontological study of the mélange sediments has been recently undertaken by Al-Riyami (2000), particularly concentrating on the radiolarian cherts.

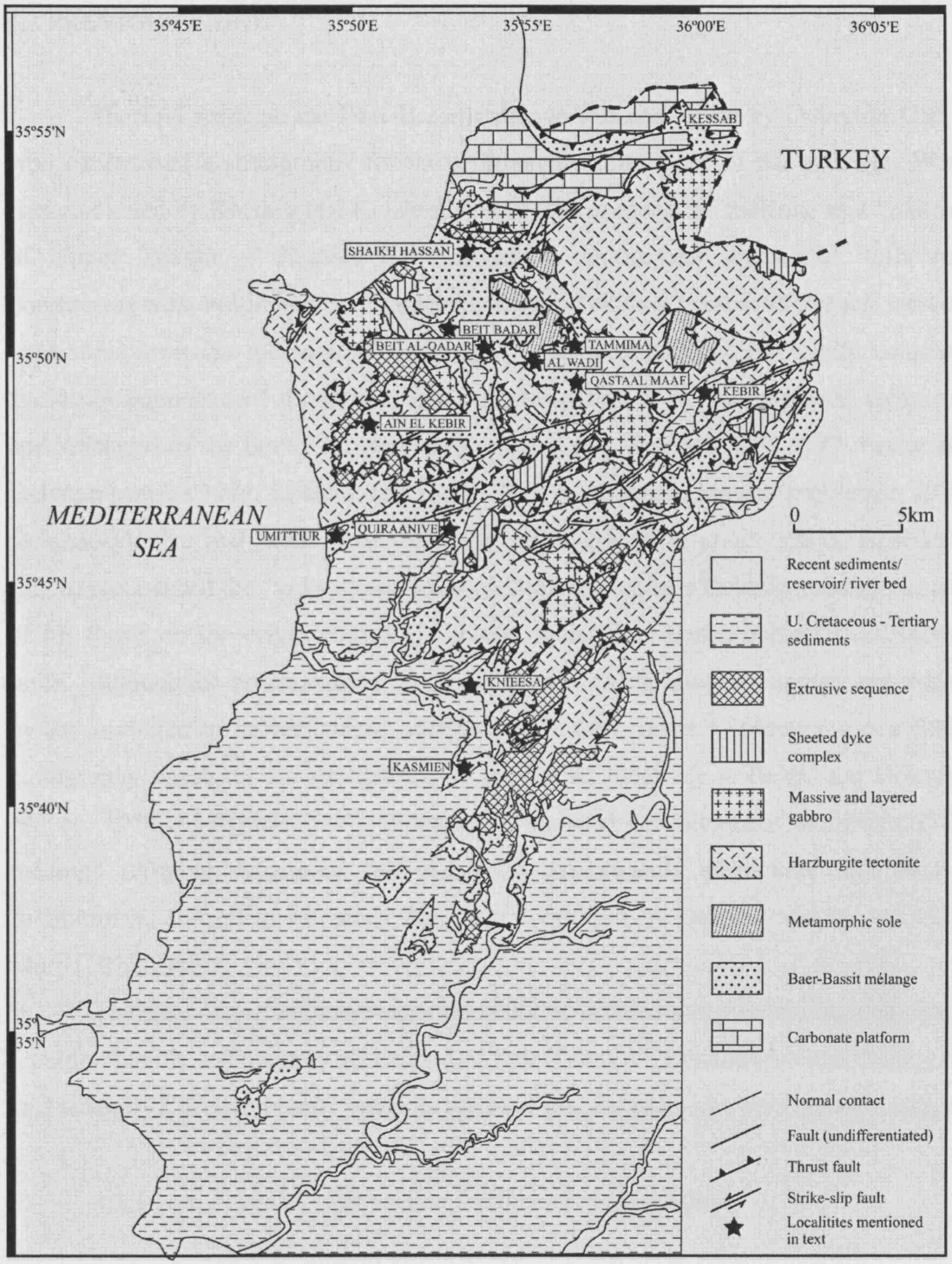

Figure 4.1 Geological sketch map of the Baer-Bassit area of NW Syria, indicating localities mentioned in the text. Modified after Kazmin and Kulakov (1968), Adjemian and Khatoun (1999) and Al-Riyami (2000).

4.2 PREVIOUS WORK

The first work on the Baer-Bassit mélange was conducted by Dubertret (1953) who constructed a stratigraphy for the sedimentary formations of the mélange. Work was continued by Kazmin and Kulakov (1968) who mapped the mélange as a "matrix" of Upper Triassic – Jurassic (?) radiolarites, mudstones, limestones, tuffs and porphyrites with exotic blocks. During the 1970's-1980's a number of French workers concentrated on the mélange, classifying it as a deformed but essentially complete "volcano-sedimentaire" formation, and first recognized it as the emplaced sediments and volcanics of the South Tethyan margin/ocean (e.g. Parrot 1974b, 1977; Parrot and Delaune-Mayère 1974; Delaune-Mayère 1978, 1983; Delaune-Mayère and Parrot, 1976; Delaune-Mayère and Saint-Marc 1979/80; Delaune-Mayère *et al.* 1983). Al-Riyami (2000) reclassified the "volcano-sedimentaire" succession as a tectonic mélange, as part of his thesis on the origin and emplacement of the Baer-Bassit ophiolite and related units. Although the broken nature of the mélange does not allow a complete succession in any one area to be recognised, attempts have been made to produce a composite stratigraphy based on the stratigraphy of individual blocks (e.g. Parrot and Delaune-Mayère 1974, Al-Riyami 2000). Biostratigraphic work on calcareous sediments of the mélange utilizing calcareous microfossils, predominantly planktonic and benthic foraminifera, as well as ostracods, has been conducted by Delaune-Mayère and Saint Marc (1979/1980).

The Baer-Bassit mélange can essentially be divided into two successions, firstly a predominantly sedimentary succession of Late Triassic – Cenomanian age lithologies, and secondly a predominantly volcanic series of mid Jurassic – Lower Cretaceous age.

4.2.1 Late Triassic – Cenomanian sedimentary succession.

This succession can be divided into three sequences of Late Triassic, Jurassic and Cretaceous age. The Upper Triassic is dominated by *Halobia* bivalve-bearing pelagic limestone blocks, limestone conglomerates, calcarenites and radiolarian cherts. The limestone conglomerates and calcirudites are interpreted as being the oldest sediments within the mélange, and are seen to contain a variety of bioclasts including corals, bivalves, gastropods, echinoids and benthic foraminifera (Al-Riyami and Robertson 2002). A number of blocks of limestone parabreccia-conglomerate were seen

in the Umit'tiur area, often containing large blocks of coral. These limestones stratigraphically underlie, and in some places are interbedded with, either blocks of pelagic *Halobia*-bearing limestone or calcarenite. The *Halobia* limestone blocks occur commonly within the mélange in the area of Umit'tiur (see figure 5.2). As well as containing the bivalve *Halobia*, Al-Riyami (2000) also reports that some samples collected contained up to 40% calcified radiolarians. *Ammonitico rosso* type limestones were also seen in the area of Umit'tiur, and Al-Riyami and Robertson (2002) report that the pelagic limestones show considerable local facies variation, both in colour and composition. The calcarenites often exhibit good sedimentary structures such as graded bedding and cross-lamination, allowing the way-up to be determined. Volcanic grains were seen in some samples, and many blocks were strongly folded. Al- Riyami (2000) dated a number of calcarenite samples as Norian (Late Triassic) based on dasyclad algae and benthic foraminifera, agreeing with the Late Triassic age obtained by Delaune-Mayère and Saint-Marc (1979/80) who recovered the foraminifera *Trocholina* sp., *Trochammina* aff. *jaunensis* Brönnimann and Page, *Semiinvoluta clari* Kristan and *Frondicularia* cf. *woodwardi* Howch.

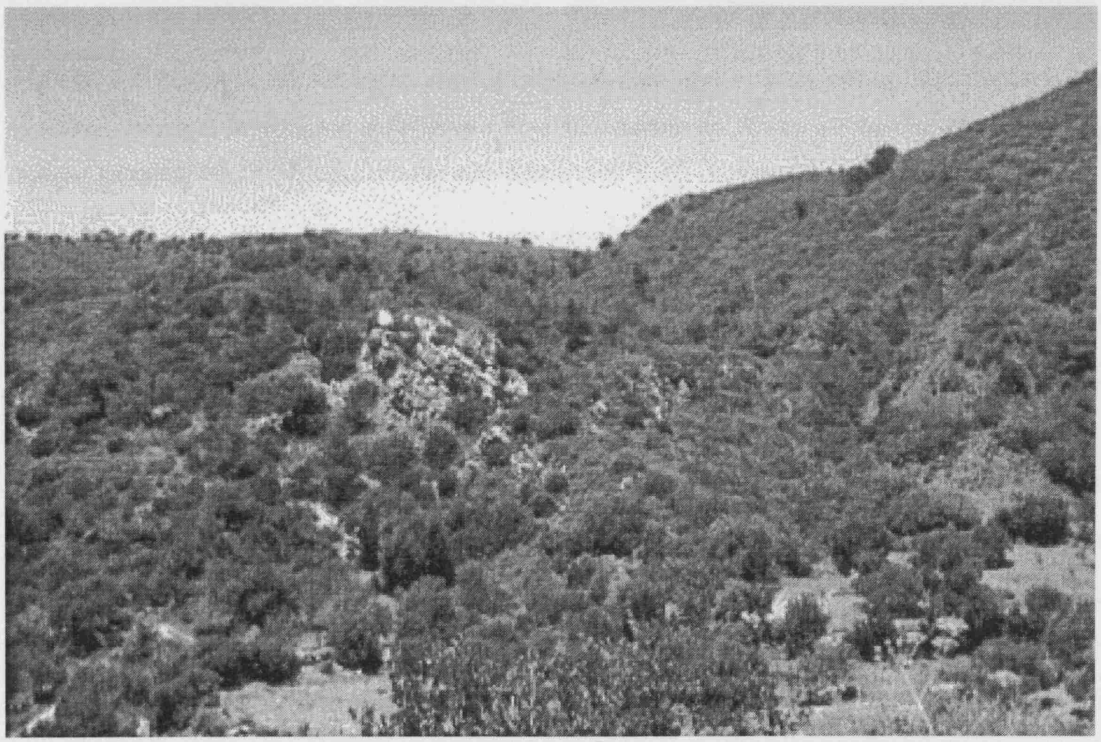

Figure 4.2 A large block of Triassic limestone (pale colour in centre of photograph) set in poorly exposed shales and radiolarian cherts, seen just north of Umit'tiur village. Outcrop is about 40m wide.

Radiolarian cherts can be seen throughout the Baer-Bassit area, and range from Triassic – Cretaceous in age. Al-Riyami and Robertson (2002) dated a sample of radiolarian chert, taken from a bed within the upper part of the *Halobia* limestone succession from the Umit'tiur area, as late Carnian based on the presence of *Spongostylus carnicus* Kozur and Mastler and *Capnodoce* De Wever. Large outcrops of radiolarian chert were seen at Umit'tiur, as well as south of Qastaal Maaf, though the age of the sediments exposed was not determined. Al-Riyami and Robertson (2002) report further outcrops of Late Triassic age radiolarian cherts from Shaikh Hassan and Toubaqli, near Kessab, and Upper Triassic limestones and radiolarites interbedded with flows and pillows of alkaline basalts near Al-Wadi.

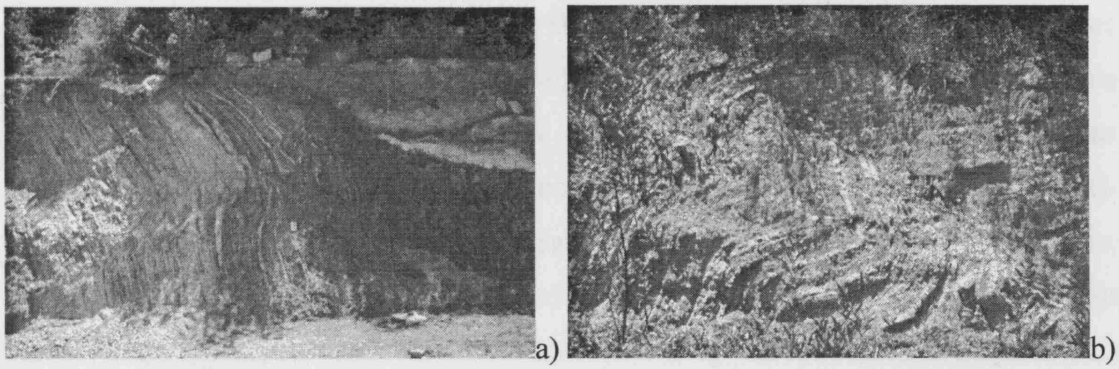
a) b)

Figure 4.3 Outcrops of radiolarian chert of undetermined age: a) large cutting in Umit'tiur village exposing disturbed, interbedded radiolarian cherts and mudstones. Width of outcrop ~20m. b) Folded radiolarian cherts from a roadside exposure in Ballourane. Width of outcrop 3m.

The Jurassic sediments are predominantly radiolarian cherts, shales, siliceous limestones, marls and calcarenites. The radiolarian cherts can also be seen interbedded with alkaline and peralkaline lavas at Tammima (Parrot 1977). Al-Riyami *et al.* (2002) dated a number of radiolarian cherts from the areas of Shaikh Hassan, Beit Badar, Kessab and Tammima as mid to late Jurassic in age (Bajocian – late Kimmeridgian/early Tithonian). A sample from Tammima proved Bajocian based on the presence of *Zartus jurassicus* Pessagno and Blome, limiting the age of the volcanics at that locality with which the radiolarites are interbedded. Previous dating of the volcanics by K/Ar whole rock method gave an age of 150Ma - Kimmeridgian/early Tithonian (Delaloye and Wagner 1984). Interbedded radiolarian cherts and volcanics are predominant in the north of the area whilst in the south the cherts are associated with thinly bedded silicified limestone, marls, shales and thin beds of sandstone (Al-Riyami

et al., 2000). The siliceous limestones have been dated as Bajocian, based on the presence of *Zartus jurassicus* Pessagno and Blome (Al-Riyami *et al.* 2002).

Cretaceous sediments include radiolarian cherts, conglomerates, calcarenites, limestones, sandy limestones, quartzose sandstones, claystones and marls (Delaune-Mayère and Saint Marc 1979/1980, Al-Riyami and Robertson 2002). Radiolarian cherts of Cretaceous age have been reported from Beit Al-Qadar (Upper Valangian-Hauterivian, Hauterivian-Barremian), Kasmien (Barremian) and Knieesa (Barremian) (Al-Riyami and Robertson 2002) and Tammima (Upper Valangian-Hauterivian) where they are again associated with alkaline-peralkaline volcanism (Delaune-Mayère and Saint Marc 1979/1980). Within the sediments a marked difference has been noted between the west and the east of the Baer-Bassit area (Delaune-Mayère and Saint Marc 1979/1980, Al-Riyami *et al.*, 2000). In the west of the area Aptian – Albian limestone conglomerates, calcarenites and marls pass up into lower-middle Cretaceous interbedded shales, radiolarites, calcarenites and locally thin bedded sandstones (Al-Riyami *et al.* 2000, Delaune-Mayère and Saint Marc 1979/1980). In the east of the area, e.g. at Kebir, thick bedded sandy limestones of late Aptian-mid Albian age dominate. At Kebir village quartzites, calcarenites and limestone conglomerates are also present. This difference in facies distribution reflects the more proximal location of the east of the area to the shoreline during the Mesozoic (Delaune-Mayère 1983).

4.2.2 Late Triassic – Cretaceous volcanic and volcaniclastic succession.

Exposures of Late Triassic basic pillows and minor lava breccias are fairly sparse within the field area. Where they do occur (e.g. near Al-Wadi) they are occasionally interbedded with radiolarites and *Halobia* limestone (see section 4.2.1) that are reliably dated as Late Triassic in age (Delaune-Mayère and Saint Marc 1979/80). Similar outcrops of Triassic pillow lavas were also seen at Qastaal Maaf and Quiraanive (Al-Riyami and Robertson 2002).

Middle Jurassic – Lower Cretaceous lavas, intrusives and volcaniclastics are much more widely distributed throughout the field area, with the largest exposure occurring in the vicinity of Tammima (Parrot 1974b, Al-Riyami 2000). Analyses of samples from both the Triassic and the younger extrusives revealed an alkaline –

peralkaline tendency suggesting within plate-type volcanism (Parrot 1974b, Al-Riyami *et al.* 2002).

4.3 SAMPLING OVERVIEW AND RESULTS

13 spot samples were deliberately taken from the mélange, and the sampling localities are given below, as well as indicated on figure 4.1. Exact grid references of sampling localities are given in the Appendix. Samples 11136 and 11141 were washed for foraminifera and general microfossils. All the other samples were thin-sectioned as they were too hard to process by washing.

4.3.1 SHAIKH HASSAN

Sample 11128 was taken from a block of pelagic limestone containing clasts of redeposited limestone and coral. The sample was taken from the matrix and is fossiliferous micrite, veined with sparite and containing numerous spumellarian Radiolaria as well as a few nassellarians, all of which have been altered to calcite. Also present were the long ranging benthic foraminifera *Reophax scorpius* and *Oolina*. These are not age diagnostic, but the sample could be as old as Triassic.

11129 was taken from a weathered-out block of peloidal, micritic limestone. Other allochems include dasyclad algae as well as the benthic foraminifera *Riyadhella* and *Siphovalvulina* suggesting a middle Jurassic to early Cretaceous age.

Sample 11130 was taken from a block of coarse calcarenite with visible volcanic grains. The sample is a micritic packstone and contains bryozoans, algae and rare foraminifera including miliolids and *Kilianina rahoensis* dating the sample as Bathonian. Lithic fragments of peloidal, micritic limestone and foraminiferal limestone are also present.

4.3.2 AL WADI

Sample 11131 was taken from an *Ammonitico rosso* type limestone. The heavily veined micritic limestone was barren of foraminifera but contained numerous simple spumellarian radiolarians, all of which had been altered to calcite. Age indeterminate.

11132 was taken from a block of massively bedded, dark grey and partially oolitic limestone. The ooid-bearing micritic limestone contained numerous ooids and

superficial ooids in a micritic matrix with sparry calcite veins. Other allochems included dasyclad algae and rare, non-age diagnostic benthic foraminifera.

4.3.3 QUIRAANIVE

Sample 11133, taken from a block of limestone, was a fossiliferous micrite containing lamelibranch valves and simple spumellarian Radiolaria. No age determination was possible.

Sample 11134 was essentially the same as 11133, though contained a greater number of Radiolaria, including a few nassellarians. Again no age determination was possible.

4.3.4 AIN EL KEBIR

Sample 11136 was taken from a green marl and washed for foraminifera. No foraminifera were recovered but a poorly preserved radiolarian assemblage included *Thanarla*, *Obesacapsula*, *Archaeodictyomitra apiara* and *Amphipyndax* sp. suggesting an early Cretaceous age.

11137, taken from a block of calcarenite, was a micritic/sparitic wackestone containing just a few indeterminate benthic foraminifera.

11138, taken from a block of calcarenite, was thin-sectioned and washed for foraminifera. The fossiliferous micrite contained featureless spumellarian radiolarians, ooids, peloids, dasyclad algae, *Heterohelix* sp. and *Hedbergella* sp. This assemblage suggests an early Cretaceous age.

Samples 11139-11141 were all taken from the same locality. 11139 was a calcarenite and contained *Valvulina lugeoni*, *Siphovalvulina* and *Quinqueloculina* suggesting a Callovian age. Samples 11140, a fine calcarenite, and 11141, a chalk, were both barren.

4.4 CONCLUSIONS

Limited micropalaeontological dating of mélange sediments during this study suggest that previous biostratigraphic work has been accurate, with no major discrepancies observed. By studying the volcanics and sediments of the mélange previous workers have attempted to reconstruct the Mesozoic sedimentary and igneous history of the of the area adjacent to the Arabian margin in a south Tethyan oceanic

basin (e.g. Delaune-Mayère 1983, Delaloye and Wagner 1984, Al-Riyami 2000, Al-Riyami *et al.* 2002). In summary the sedimentary succession represents deep water, base of slope accumulation of pelagic and hemipelagic sediments, as well as redeposited sediments from the carbonate platform including gravity deposits. Differences in sediment character are due to variations in the proximity of the source. The Late Triassic volcanics are presumed to be related to initial rifting of the African and Arabian plates and the formation of a south-Tethyan oceanic basin, whilst the Jurassic to Cretaceous volcanics and volcaniclastics are interpreted as plume related eruptions forming seamounts outboard of the continental margin. Their more distal origin is illustrated by the radiolarian cherts with which they are usually interbedded (Al-Riyami and Robertson, 2002).

CHAPTER 5: THE BAER-BASSIT OPHIOLITE

5.1 INTRODUCTION

During this study the ophiolite was not specifically examined apart from sediments associated with the extrusive units, and the mélange, which was discussed in the previous chapter. The following chapter is therefore largely a review of previous work with some personal observations. Overlying the mélange in the north of the area and interleaved with it in the south of the area is the Baer-Bassit ophiolite, *sensu stricto.* The area of the ophiolite complex comprises two main structural massifs: Baer in the northeast and Bassit in the northwest as well as smaller, more dismembered units that occur throughout the area (Al-Riyami *et al.*, 1998). Although now dismembered, a composite succession shows an originally complete ophiolite sequence with a basal metamorphic sole, harzburgitic tectonites, layered ultramafic cumulates, layered gabbroic cumulates, isotropic gabbros, a sheeted diabase dyke complex and pillow lavas with associated sediments (Delaloye and Wagner, 1984, Whitechurch *et al.,* 1984). Due to the highly dismembered nature of the ophiolite however, the total thickness of the different units cannot be satisfactorily estimated (Al-Riyami 2000). On the following pages are a composite section through the ophiolite (figure 5.1) and a geological sketch map of the Baer-Bassit area (figure 5.2).

The ophiolite is discussed as it is an integral part of the geological history of the area. All aspects of the ophiolite are briefly discussed but the emphasis is on the umbers and interpillow cements, and attempts to date ophiolite formation by processing these lithologies for micropalaeontology.

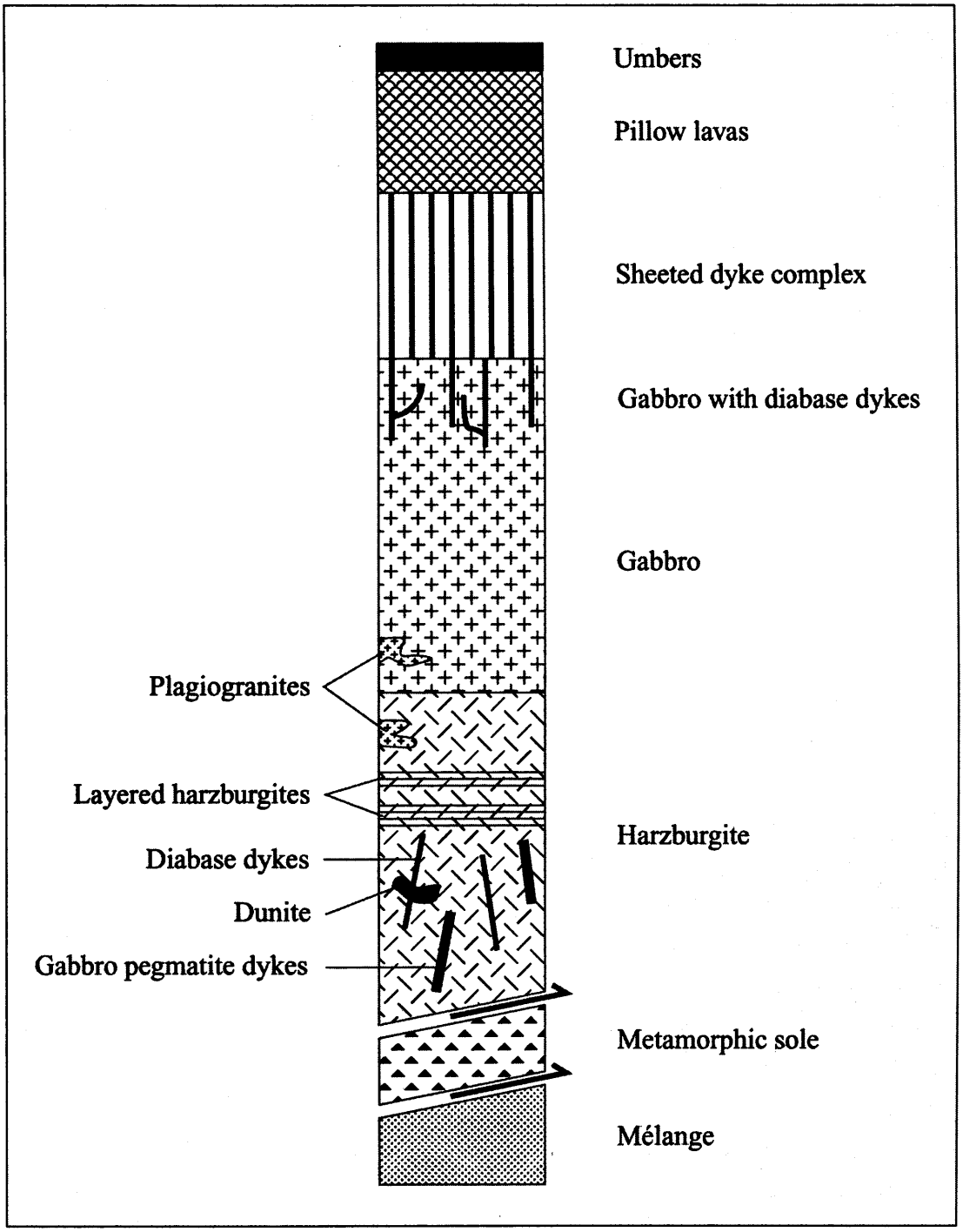

Figure 5.1 Composite section through the Baer-Bassit ophiolite and underlying mélange. After Al-Riyami (2000, fig. 5.3).

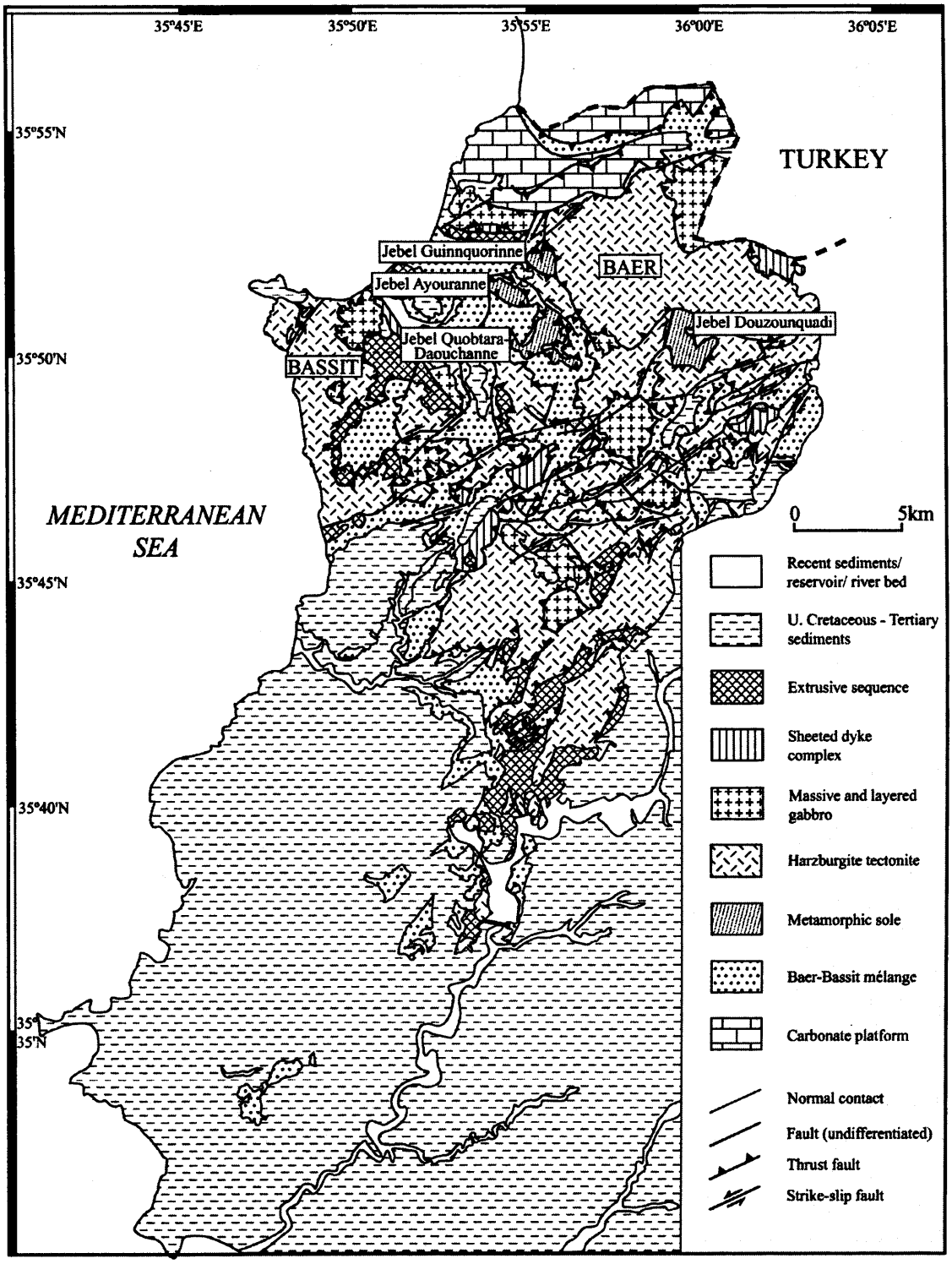

Figure 5.2 Geological sketch map of the Baer-Bassit area of NW Syria showing the main northern massifs of Baer and Bassit as well as minor scattered ophiolitic fragments further south. Modified after Kazmin and Kulakov (1968), Adjemian and Khatoun (1999) and Al-Riyami (2000).

5.2 METAMORPHIC SOLE.

As with other eastern Mediterranean ophiolites, Baer-Bassit exhibits a well developed metamorphic sole, typical of the structurally complex "Taurus-type ophiolites" of Whitechurch *et al.* (1984). Previous works on the metamorphic sole include Chenevoix (1953), Dubertret (1953), Lapierre & Parrot (1972), Whitechurch & Parrot (1974), Parrot (1977), Whitechurch (1977), Al-Riyami *et al.* (1998, 2002) and Al-Riyami (2000). The metamorphic sole is primarily developed beneath the major thrust slices of the Baer massif cumulates (Al-Riyami *et al.*, 1998). Four major and one minor outcrops occur in the north of the area with scattered minor outcrops occurring further south in the central area (see figure. 5.2). The thickness of the sole varies from 50 to 300m (Parrot, 1980), and comprises amphibolite grade rocks passing down into greenschist facies metasediments and metabasites, showing the typical inverted metamorphic facies gradient associated with ophiolites though in no one area is a complete succession from amphibolite to greenschist facies rocks preserved. A temperature of formation of up to 600+°C is estimated for the amphibolite grade rocks whilst the greenschist facies are estimated to have formed at temperature of <350°C (Al-Riyami *et al.*, 2002)

Detailed petrological and geochemical studies of sampled greenschists and amphibolites have been carried out by Whitechurch and Parrot (1974) and Al-Riyami (2000). Whitechurch *et al.* (1984) noted that each level within the metamorphic sole has a corresponding unmetamorphosed level within the underlying mélange. Detailed geochemical analysis on a number of metabasites revealed samples to be moderately to strongly alkaline in composition apart from one sample with a tholeiitic MORB signature similar to the Tammima volcanics in the underlying Baer-Bassit mélange (Al-Riyami *et al.*, 2002, Parrot, 1974b).

Most previous workers agree that polyphase deformation is recognisable in the sole rocks, passing from ductile to brittle deformation, Whitechurch and Parrot (1974) recognise 3 phases whilst Whitechurch (1977) and Al-Riyami *et* al. (1998) recognise four phases and suggest the deformation history is one of progressive ductile to brittle deformation, with foliations generally orientated NW-SE with parallel stretching lineations plunging NW, suggesting tectonic transportation from the NW to the SE.

As previously discussed the metamorphic sole is thought to be formed during initial detachment of the lithospheric slab within the oceanic realm. Continued

movement throughout the oceanic realm is reflected in the polyphase deformation structures. Dating of the Baer-Bassit metamorphic sole has been undertaken by Thuizat *et al.* (1981) and Delaloye and Wagner (1984), using the K-Ar method on separated amphiboles, with both calculating ages for the initial metamorphic event (F1) as 85-95Ma, corresponding to some time during the Cenomanian-Santonian interval.

5.3 ULTRAMAFIC UNIT.

In common with the other "Taurus-type ophiolites" the Baer-Bassit ophiolite contains a well developed ultramafic section, including both tectonites, and to a lesser extent cumulates. The main outcrops of ultramafics are in the Baer massif in the northeast of the area, which is underlain by a well developed metamorphic sole (see Chapter 5.2), and the Bassit massif in the west of the area, with well exposed coastal sections. Further south and southeast more scattered units continue to crop out until the Nahr el Kabir River, including the large southeastern massif forming the Jebel el Habes (see figure 5.3). A total thickness of the ultramafic sequence is probably in excess of 2km (Parrot, 1980).

The ultramafic units of the Baer-Bassit ophiolite are dominated by harzburgites with rare lherzolites. The Baer massif ultramafics overlie the well-developed metamorphic sole and comprise harzburgitic, and rare lherzolitic and feldspathic peridotites (Parrot 1980, Al-Riyami *et al.* 2002); exposure, however, is limited due to dense forest cover (see figure 5.3). Also present are small outcrops of cumulate ultramafics including dunites, wehrlites and pyroxenites, typical of SSZ type ophiolites (Al-Riyami *et al.* 2002. The Bassit massif largely includes the same lithologies as the Baer massif but with more widely developed dunite, chromite and plagiogranites, the latter cutting both the tectonites and cumulates (pers. obs., Parrot 1974a, 1980, Al-Riyami *et al.* 2002). The southern and southeastern units are more scattered and fragmentary in nature but display the same lithologies, and chromite pods are developed within dunites at several localities including Al-Malyea where lenses a few cm thick can be traced for up to 10m.

Figure 5.3 The view looking southeast, from near Balloûrâne, towards the southeastern massif and the hills of Jebel el Habes, illustrating the dense forest covering typical of the ultramafic unit. The reservoir in the foreground is relatively recent and has covered one of the umber localities reported by Parrot and Delaune-Mayère (1974) (see Chapter 5.7.1).

5.4 GABBROS

Massive, layered and pegmatitic gabbros crop out in both the Baer and Bassit massifs, as well as the southern and southeastern units, with a total thickness of ~1km (Parrot, 1980). Within the Baer massif the gabbros are typically strongly weathered and outcrops within the Bassit massif are limited to two localities (Al-Riyami *et al.* 2002). The base of the gabbroic succession comprises alternating layers of gabbros and harzburgites (Parrot 1980), whilst Al-Riyami *et al.* (2002) report thin gabbroic and pegmatitic gabbro intrusions within the harzburgite. Lithologies include troctolites, gabbros and noritic gabbros (Parrot 1980). Well-layered olivine gabbros, and olivine gabbro xenoliths within massive gabbro, are reported from the Baer-massif (Al-Riyami *et al.* 2002). As with the ultramafic unit, the gabbros are cut by isolated sub-parallel diabase dykes. These dykes cut both the massive and the layered gabbros.

Layering within the gabbros has been measured as 185/15°E in the Baer massif and 245/60° ESE within layered olivine gabbros at Umm Toyour on the Mediterranean coast (Al-Riyami *et al.* 2002). The cross-cutting doleritic dykes are reported to be subvertical by Parrot (1980), but only dipping at an average 24-34°, with an average strike of 130°in the Baer massif according to Al-Riyami *et al.* (1998).

5.5 SHEETED DYKE COMPLEX

The main outcrops of the dykes occur along the road to Raas Al-Bassit, in the northeast of the area around Ispanak, and around Beit Dakhne in the central area. Al-Riyami *et al.* (2002) also report a major outcrop NNE of Qastaal Maaf along the main Latakia-Kessab road. Swarms of diabase dykes are again a feature of "Taurus-type ophiolites" and are seen to intersect both the cumulate and ultramafic units, as well as the metamorphic sole in some ophiolites (Whitechurch *et al.* 1984). They are composed of plagioclase, clinopyroxene and lesser amounts of zeolite, olivine and opaques (Al-Riyami *et al.* 2002). Scattered dykes are also seen cross-cutting the main dyke swarm and some of these contain small amounts of quartz suggesting a distinct magma source (Parrot 1980). Similarly, the scattered dykes within the upper gabbroic levels also have a distinct composition with greater amounts of plagioclase and lesser amounts of clinopyroxene and opaques than the sheeted dykes (Parrot 1980).

The compositions of these dykes are assumed to have originally been tholeiitic before amphibolitization and albitization and were presumably feeder dykes for the overlying pillow lavas (Parrot 1980). Al-Riyami *et al.* (2002), however, suggest petrographic studies show that the dykes are less altered than the overlying extrusives. Consequently, a supra-subduction zone setting is inferred with a high degree of partial melting of a depleted source (Al-Riyami *et al.* 2002).

The dykes are sub-vertical to vertical and predominantly striking at 330° (NW-SE) (Al-Riyami *et al.* 1998 p. 9). Palaeomagnetic studies of dykes show that they, and thus the ophiolite, have experienced mild to extreme anticlockwise rotation about vertical axes, though timing of the rotations cannot be elucidated due to lack of progressive cross-cutting relationships, and consequently rotations may be due to any combination of intraoceanic detachment and deformation, emplacement and neotectonic deformation (Morris *et al.* 2001, Morris & Anderson 2002).

5.6 PILLOW LAVAS

The extrusive sequence comprises pillow lavas, lava breccias and occasional massive lava flows, together exceeding 500m in thickness, with rare dykes intruding the base of the pillow sequence (Al-Riyami *et al.* 2002). Pillow lavas were seen at several localities, including north of Mazzra and at Deflah village (see figure 5.4), whilst lava breccias dominate the outcrops in the villages of Al Baluta and Beit Aouâne (see figure 5.5). Associated with the pillow lavas at several localities are umbers and calcareous cements, and these will be dealt with in the next section.

At Deflah pillows range in size from 20cm up to 2m in diameter. Parrot (1980) divides the pillow-lavas into an upper and a lower unit, based on structural relationships, chemistry and morphology whilst Al-Riyami *et al.* (1998) suggest that a normal fault, probably of Tertiary age, is responsible for the spatial separation of the upper and lower lavas, and that initial geochemical and petrographic analysis suggests all the lavas are of a similar, high Mg composition. Pillow lavas at Deflah comprise clinopyroxene, plagioclase and variably altered olivine phenocrysts in a glassy matrix (pers. obs., Al-Riyami *et al.* 2002 p.228-229).

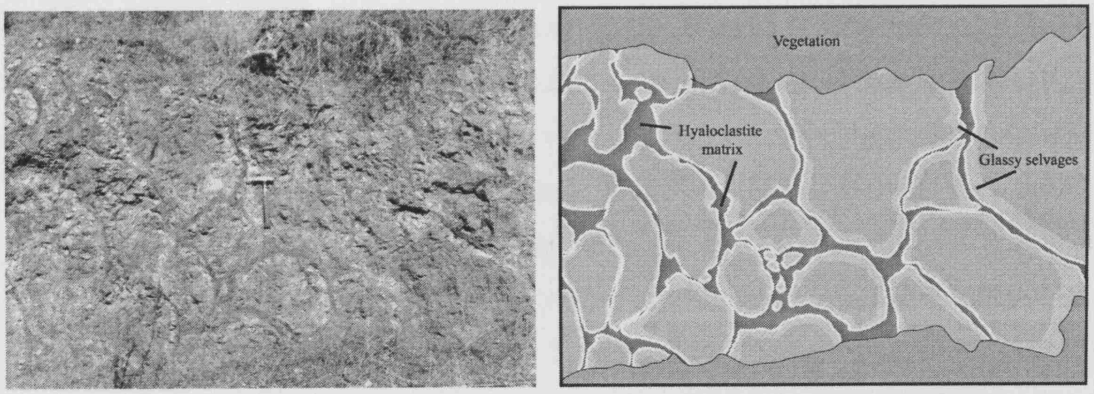

Figure 5.4 Photograph of an outcrop of pillow lavas at Deflah and a sketch of the same outcrop. Hammer is 30cm long.

5.7 UMBERS AND INTERPILLOW CEMENTS.

5.7.1. INTRODUCTION

Associated with the pillow lavas at several localities are ferromanganiferous umbers, occurring as either interpillow sediment, veins within the pillows or lava flows, or as a thin sedimentary covering, unlike in Cyprus where substantial deposits occur in fault-guided depressions. At other localities the pillows are set in a matrix of calcareous cement. Both of these lithologies were sampled for processing in order to constrain the age of pillow formation.

Current consensus sees umbers forming through the leaching of hot lavas by percolating sea-water and volatiles, and the precipitation of minerals out of solution on contact with cold sea-water. Manganese stays in solution longer than iron so umbers can form more distally from source than ochres. Umber formation is thought to take place off axis during the waning stages of volcanism, as testified by their occurrence in half grabens, often containing lava talus (Prichard & Maliotis 1998).

The Baer-Bassit umbers have previously been described by Parrot and Delaune-Mayère (1974) and Al-Riyami (2000). Outcrops have been described from Deflah, Qaba Mâzé (now called Al Baluta), Beit el Qassir, Ziaret Hamza, Balloûrâne and El Malyeh (see figure 5.5). At the majority of localities the umbers are developed as small pockets in pillow interstices, such as north of the village of Mazzra (see figure 5.6), elsewhere, lenses of sheared umber up to two metres thick have been reported, such as at El Malyeh (Al-Riyami *et al.* 2002), although this outcrop was not located during this study. At the village of Deflah umbers occur as veins within massive pillow flows similar to those described in Cyprus by Robertson (1975) (see figures 5.7 and 5.8). Elsewhere at this locality umbers are only seen as float among orchards. Locally the umbers are seen to pass upwards into pink to grey mudstone with sparse radiolaria (e.g. just north of Mazzra). As well as the umbers, a number of localities have pillow breccias set in a pink calcareous matrix, such as at Beit Aouâne and Fellah (see figure 5.9). Finally, ophicalcites have been reported from an unnamed locality in the south of the area, on the north bank of the Nahr el Kebir River (Knipper *et al.* 1990; See figure 5.5).

5.7.2 PETROLOGY, MINERALOGY AND GEOCHEMISTRY

The Baer-Bassit umbers vary in colour from light orange to reddish-brown, purple and nearly black. A composite succession has been suggested, with minor, orange interpillow sediments becoming more abundant upwards, overlain by lenticular bodies of red to brown umber that become increasingly dark and with an increasing argillaceous content upwards (Al-Riyami *et al.* 1998). Bedding and sedimentary structures are seldom present, though some umbers have been observed with small partings of tuffaceous material.

Mineralogically, the umbers are dominated by goethite, with generally lesser amounts of montmorillonite and no more than 4-5% accessory minerals of volcanic origin including analcime, pigeonite and albite (Parrot and Delaune-Mayère 1974) as well as quartz, haematite, kaolinite, chlorite and pyrolusite (Al-Riyami *et al.* 2002).

Geochemical analyses of major elements suggest that the Baer-Bassit umbers have relatively high concentrations of Fe_2O_3 and MnO (between 39-49% and 2-7% respectively) (Parrot and Delaune-Mayère, 1974), though lower than the respective percentages recorded for the Troodos umbers by Elderfield *et al.* (1972) with up to 56% and 17% respectively. Al-Riyami *et al.* (1998 p. 10-11), however, report a higher concentration of Fe_2O_3 in the Baer-Bassit umbers than the average concentration in the Troodos umbers as reported by Robertson and Hudson (1973). Higher concentrations of SiO_2, Al_2O_3 and MgO are also reported. The concentration of major elements varies between samples, with higher concentrations of SiO_2 and Al_2O_3 suggesting a greater terriginous and perhaps biogenic input, whilst higher concentrations of Fe_2O_3 and MnO are suggestive of a greater hydrothermal influence (Al-Riyami *et al.* 2002). Trace element analyses have also been conducted, showing general enrichment of those elements associated with hydrothermal sedimentation (e.g. Cu, Zn, Ni, Pb) whilst positive correlations are shown between Fe v Cu, Fe v V and Fe v Zn, again indicative of a hydrothermal influence (Al-Riyami *et al.* 2002).

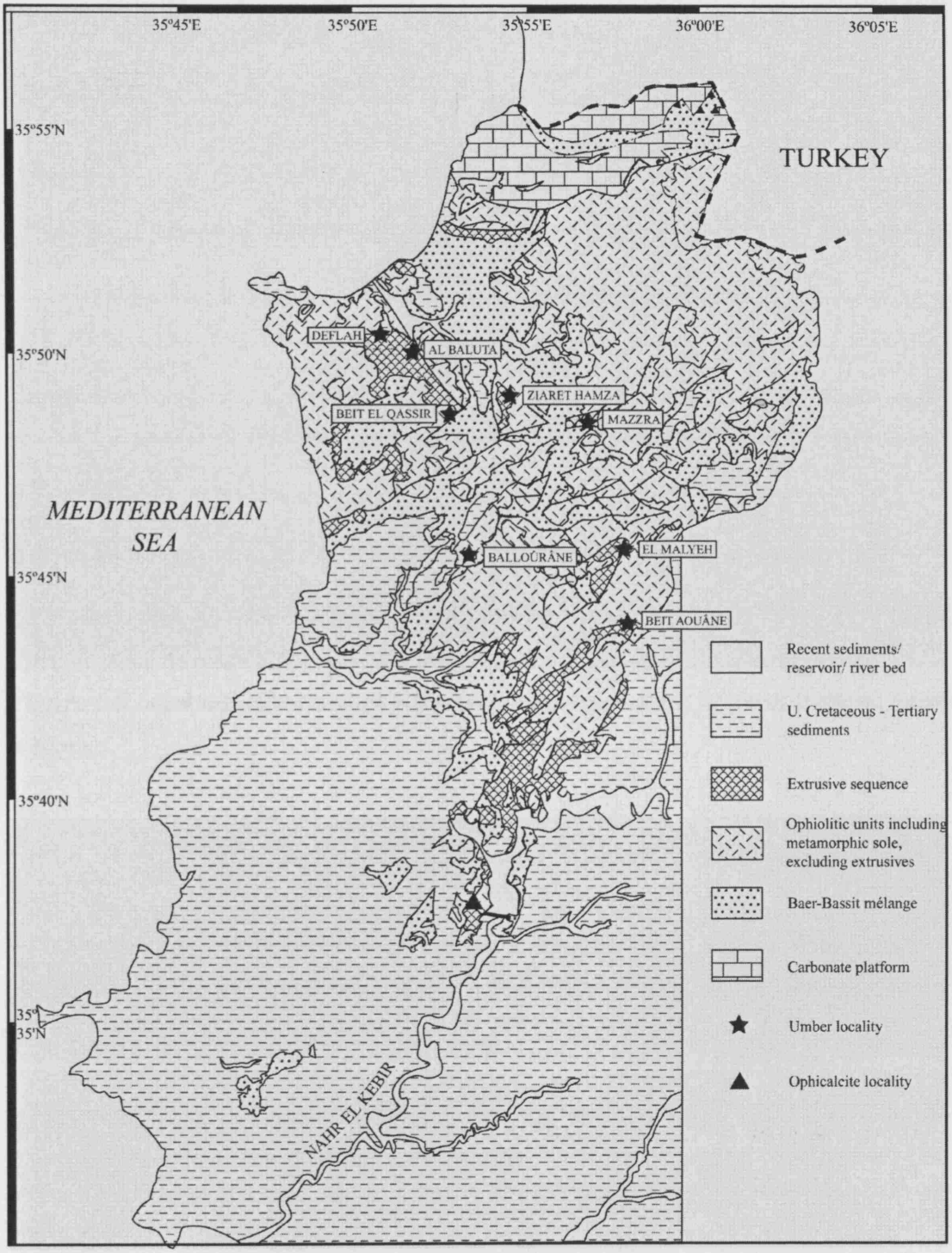

Figure 5.5 Simplified geological sketch map of the Baer-Bassit area. Localities of reported umber and ophicalcite outcrops illustrated.

Figure 5.6 Interstitial umbers amongst pillow lavas and pillow breccias just north of Mazzra (hammer is 30cm).

Figure 5.7 Veins of umber cutting up through massive basalts at Deflah. Hammer for scale, right-centre of photograph.

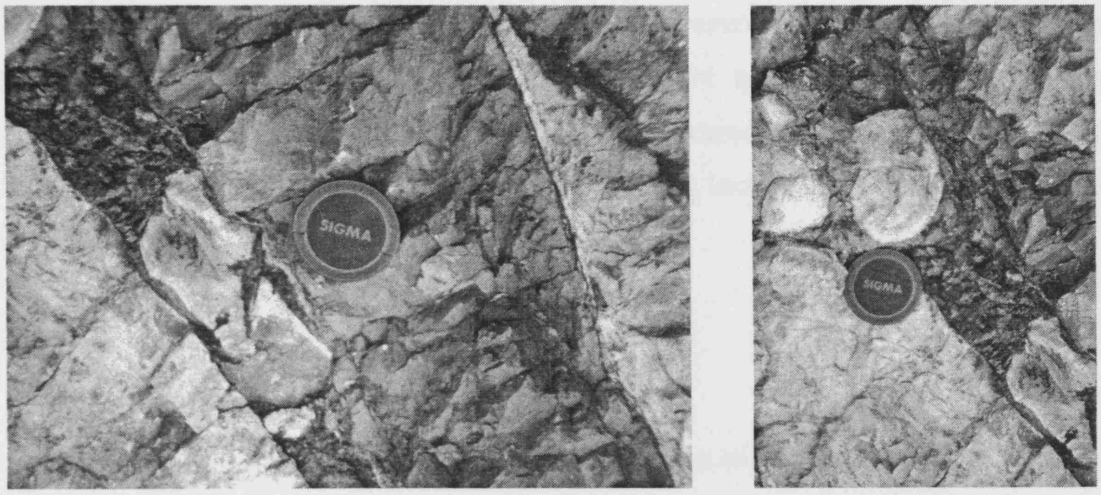

a) b)

Figure 5.8 a) Thick vein of umber cutting through basalt at Deflah; b) small pillow entrained in vein of umber at same locality. Lens cap 5cm in diameter.

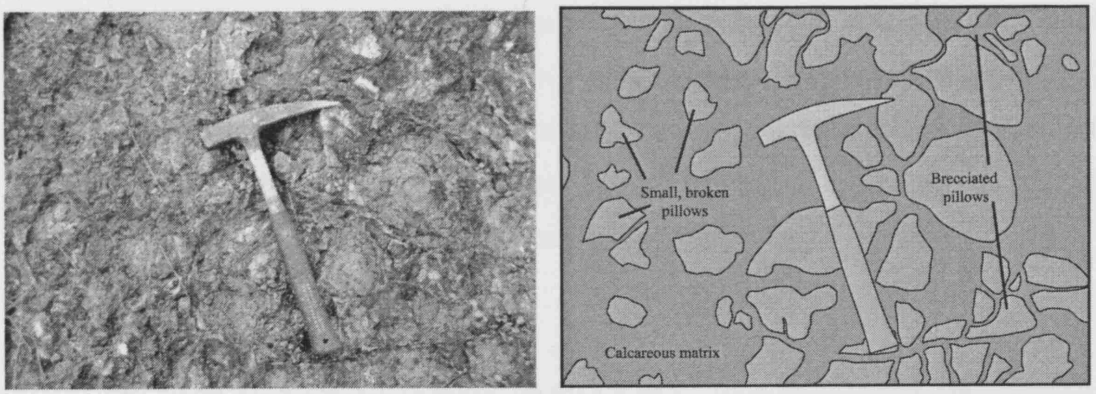

Figure 5.9 Small pillows and brecciated pillows set in a matrix of pink calcareous cement, accompanying sketch to emphasize the relationship. Outcrop in the village of Beit Aouâne.

5.7.3 SAMPLING OVERVIEW

A number of localities were visited to collect umbers. Previous workers have demonstrated that microfauna and flora are occasionally to be found in these manganiferous sediments. Radiolaria have been reported from the umbers of both the Troodos ophiolite of Cyprus and the Semail ophiolite of Oman (e.g. Tippit and Pessagno 1981, Blome and Irwin 1985, Urquhart and Banner 1991) whilst benthic foraminifera and organic matter have also been reported from the Cyprus umbers (Urquhart and Banner 1991, Urquhart pers. comm. 2000). Planktonic foraminifera have been reported from the ophicalcites in Syria (Knipper *et al.* 1990). These rocks are serpentine breccias with a calcareous matrix and were reported from the north bank of

the Nahr el Kebir river in the south of the area, but a reservoir now exists in the area and the location is no longer accessible. Samples were also therefore collected from localities where pillows and pillow breccias were encased in a calcite matrix as it was hoped these might yield some foraminifera. Sampling localities are illustrated on figure 5.5.

5.7.4 DEFLAH

5.7.4.1 Sampling

4 samples were collected from umbers amongst pillow lavas south of the village of Defla (see figure 5.5) and photographs of these umbers are illustrated in figures 5.7 to 5.8.

5.7.4.2 Processing

All samples were washed for foraminifera and general microfossils. The samples required repeated washing to break them down, in some cases over 30 washes. The >500μm fraction from each of the umbers was also processed for Radiolaria using the methods described in Appendix 1.1. A sub sample of each of these samples was also processed using standard palynological processing techniques (see Appendix 1.1)

5.7.4.3 Results

The umbers collected from Deflah all contained rare, badly preserved spumellarian radiolarians apart from DEF 4 which was barren; additionally, sample DEF 1 contained a single very badly preserved nassellarian Radiolaria. Due to the poor preservation the specimens are generally indeterminate as any surface structures are largely overgrown and obliterated. A solitary benthic foraminifera, possibly *Epithenella*?, and another very badly preserved foraminifera, possibly *Globigerinelloides*, were also found in sample DEF 1.

A palynology slide was only prepared for sample DEF 1, as during processing it became apparent that the other three samples were barren of any organic matter. The preparation was seen to be composed of nothing but densely packed octahedral crystallites with no palynomorphs visible however.

5.7.5 MAZZRA

5.7.5.1 Sampling

Just south of the village of Mazzra pillow lavas, with minor interpillow umbers developed (see figure 5.6), crop out in the western bank of the road. Sample MAZZ 1 and 3-4 were all sampled from the umbers. Pink-grey mudstones were seen in close proximity to the pillows and umbers, though the relationship between the two outcrops was unclear, and sample MAZZ 2 was collected from these mudstones.

5.7.5.2 Processing

The three umberiferous samples were all processed using the techniques in section 5.7.4.2, whilst MAZZ 2 was only washed for foraminifera and general microfossils.

5.7.5.3 Results

The samples from the village of Mazzra had a similarly impoverished assemblage to those recovered from the Defra samples. MAZZ 1 contained just a single badly preserved spumellarian radiolaria and 4 fish teeth. MAZZ 2, taken from mudstones overlying the pillow lavas proved barren of any microfauna. Sample MAZZ 3 contained rare fish teeth, indeterminate radiolaria and planktonic foraminifera. About 50 benthic foraminifera were also picked from the sample and although a single specimen of a juvenile ?globotruncanid was picked, the majority of the foraminifera were of predominantly Tertiary benthic genera such as *Elphidium* De Montfort, *Cibicides* De Montfort and *Hanzawaia* Assano. The sample was therefore obviously contaminated at source as the neo-autochthonous sediments prove the ophiolite was emplaced before the end of the Cretaceous (see chapter 6). No reliable age was therefore ascertained. Sample MAZZ 4 contained just a few very poorly preserved Radiolaria.

During processing it became apparent that MAZZ 4 was barren of organic matter so was not processed to the slide stage. MAZZ 1 was barren of palynomorphs, though some fine amorphous ?organic matter was present. MAZZ 3 contained just two palynomorphs, *?Botryococcus* and *?Xenascus* (Matthews, pers.comm. 2002). The latter is a Cretaceous genus but preservation was too poor to identify to species level. This, coupled with the apparent contamination of this sample as suggested by the benthic foraminiferal content, makes reliable dating impossible.

5.7.6 AL BALUTA

5.7.6.1 Sampling

Two samples were collected from a road section immediately south of the village of Al Baluta, on the main Latakia – Kessab road. Here about 30m of highly brecciated pillow lavas are exposed, as well some 60m of more massive lavas. Small amounts of orange coloured umber were developed between the brecciated pillows towards the southern limit of the section, and both samples were taken there.

5.7.6.2 Processing

Again both samples were processed using the techniques in section 5.7.4.2.

5.7.6.3 Results

Both samples were totally barren.

5.7.7 BEIT AOUÂNE

5.7.7.1 Sampling

Two samples, AOU1 – 2, were taken from an outcrop of brecciated pillow lavas at the NW limit if the village. Here the pillows were set in white-pink calcareous cement (see figure 5.9). Two samples of this cement were sampled.

5.7.7.2 Processing

Both samples were washed for foraminifera and processed for radiolaria.

5.7.7.3 Results

Both samples were barren of any microfauna.

5.7.8 CONCLUSIONS

Micropalaeontological and palynological studies of umbers and cements associated with the pillow lavas of the Baer-Bassit ophiolite have failed to provide any further age constraint on the formation of the ophiolite itself. It is possible that more extensive sampling may yield further samples with a richer faunal and floral content akin to those found in Cyprus and Oman, although the distribution and extent of umbers in Baer-Bassit is significantly less than in these areas. The age of ophiolite formation

can only be ascertained by age of emplacement. It has already been discussed that generally only very young oceanic crust can be emplaced, so formation therefore probably predated emplacement by a short time, sometime during the Campanian.

CHAPTER 6: SEDIMENTARY COVER SEQUENCE

6.1 INTRODUCTION.

Structurally overlying the Baer-Bassit ophiolite are sediments of Maastrichtian to Neogene age. The oldest sediments (Maastrichtian) are mainly exposed bordering the ophiolite complex to the south and south-west, in the southern banks of the Nahr el Kandil River, and on the southern slopes of the Jebel Rhouz hills (See figures 1.3 and 6.1). Younger sediments, of Paleogene to Neogene age, are extensively developed to the southeast and the southwest of the Baer-Bassit ophiolite, both north and south of the Nahr el Kebir and Nahr el Kandil rivers. Quaternary sediments predominantly occur in a broad coastal swathe from Latakia north to Borj Islam.

6.2 PREVIOUS WORK

Little work has been done on the Cretaceous – Tertiary cover sediments of the Baer-Bassit area since they were first mapped by Kazmin and Kulakov in 1968. Krasheninnikov (1994) did some work on the coastal sediments of the Baer-Bassit area, but this predominantly concentrated on the Paleogene sediments with only one section near Damate examined for Maastrichtian sediments. Krasheninnikov *et al.* (1996) also produced a paper on the Paleogene of Syria, including information on outcrops in the Baer-Bassit area. The area has recently been remapped at a scale of 1: 50,000 by a team of geologists from the Syrian Establishment of Geology (Adjemian and Khatoun, 1999). Other recent works include Al- Riyami (2000), who conducted a small amount of work on the Maastrichtian and Tertiary cover sediments as part of a broader work on the formation, emplacement, and structural history of the Baer-Bassit ophiolite and mélange. Concurrent with this work, Mr. M. Hardenberg (University of Edinburgh) has been studying the Tertiary cover with a primary aim of elucidating the neotectonic history of the area.

The Tertiary sediments of the Baer-Bassit area of Syria have been mapped by Kazmin and Kulakov (1968) and recently Adjemian and Khatoun (1999). Additionally, Krasheninnikov (1994) studied the stratigraphy of the Maastrichtian and Cenozoic

deposits of the coastal part of north-western Syria, as well as a larger work on the Paleogene of Syria as a whole (Krasheninnikov *et al.* 1996). A summary of the Tertiary sediments of the Baer-Bassit area was also produced by Al-Riyami (2000).

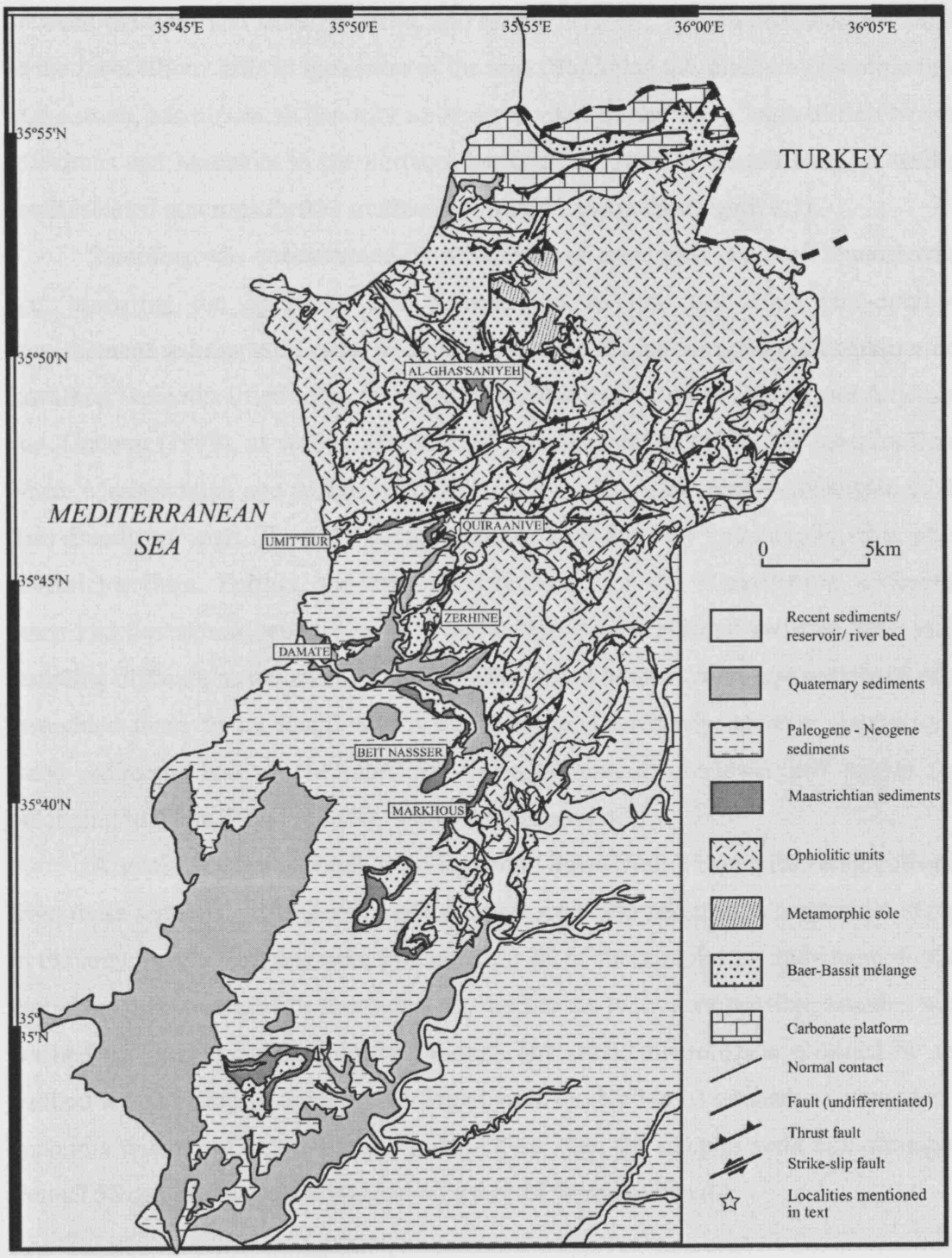

Figure 6.1 Geological sketch map of the Baer-Bassit area, showing main outcrops of Maastrichtian sediments and sampling localities mentioned in the text (modified after Kazmin and Kulakov 1968, Adjemian and Khatoun 1990, and al-Riyami, 2000)

6.3 SAMPLING OVERVIEW

6.3.1 CRETACEOUS SEDIMENTS

Cretaceous cover sediments were previously reported from a small inlier between the Baer and Bassit massifs, and on the northern, eastern and southern slopes of the Jebel Rhouz hills in the centre of the area. Bordering the southern ophiolitic units to the south, Maastrichtian deposits are also recorded around the villages of Beit Nasser, Markhous and Machkita in the northern banks of the Nahr el Kandil river, as well as small isolated outcrops further southwest towards Latakia (See figure 6.1).

Sampling was concentrated on sediments, of previously reported Maastrichtian age, bordering the ophiolite. The purpose was to find the oldest post-ophiolite emplacement sediments in order to further constrain the age of ophiolite emplacement. Localities were identified using the maps of Kazmin and Kulakov (1968), and Adjemian and Khatoun (1999), as well as literature by Krasheninnikov (1994). At most localities where Maastrichtian age sediments have been recorded, they overlie lithologies of the Baer-Bassit mélange. These lithologies tend to crop out only sporadically, if at all in several localities. Further, the lithologies recorded for the Maastrichtian sediments: marls and limestones, are also to be found within the Baer-Bassit mélange. This made sampling difficult, as the patchy outcrops of recorded Maastrichtian age sediments often resembled those to be found within the mélange. Conversely however, sampling of these sediments was all the more important in order to elucidate their origins (i.e. belonging to the mélange or to the Maastrichtian cover).

A total of seven sections were logged in detail with 24 samples being collected from these sections. A further 45 spot samples were also taken from scattered outcrops in the area. Smear samples were produced for 62 of the samples to study nannofossils, though calcitic overgrowth precluded any further study. Where possible samples were washed for planktonic foraminifera, though any useful microfossils obtained by this method were studied. Where the lithologies were too hard to be washed, or were seen to contain a number of larger benthic foraminifera, then the samples were thin-sectioned. In total 55 samples were washed and a further 14 were sectioned.

6.3.2 TERTIARY SEDIMENTS

The zonation scheme used in this section is that of Berggren and Norris (1997). Paleogene age sediments crop out mostly in the south and southwest of the study area. A complete section, from Upper Maastrichtian to Middle Eocene was mapped in the Jebel Rhouz hills north of the Nahr el Kandil valley in the vicinity of the villages of Damate and Qafar Fawkani, with the section continuing south of the valley around Slayeb, where rocks as young as uppermost Lutetian are exposed, and unconformably overlain by Neogene sediments (Kazmin and Kulakov, 1968). Krasheninnikov (1994) reports two hiatuses from the section, with both the Lower Eocene *Morozovella formosa* Zone (Zone P7) and the *Parvurugoglobigerina eugubina* Zone being absent. Sediments assigned to the Lower Paleocene *Turborotalia pseudobulloides* Zone rest directly on Maastrichtian age sediments, with no obvious lithological change or unconformity. He suggests that this is the case for most of Syria, although a section at Wadi El-Bardeh in the Palmyrides appears to be continuous across the Cretaceous-Tertiary boundary, and that a series of shallow water limestones some 2-3m thick may correspond to the *Parvurugoglobigerina eugubina* Zone, but contain only benthic and not planktonic foraminifera.

Further Paleogene sediments are reported in the north bank of the Nahr el Kebir River in the south of the area, and from the southeastern edge of the Baer massif where they unconformably overlie ophiolitic units (Kazmin and Kulakov 1968).

A number of spot samples were taken to ascertain the local stratigraphy and a long section through Palaeogene sediments was also sampled in the vicinity of Qafar Fawkani in order to study the sedimentation and consequently the geologic history following ophiolite emplacement. A number of spot samples were collected during the first field season to identify Palaeocene sections. These sections were then revisited during the second field season when a total of 48 samples were collected to study the sedimentology and biostratigraphy of the Palaeocene sediments. All of these samples were washed for foraminifera and general microfossils.

SEM images of specimens discussed are presented on three plates at the end of this chapter.

6.4 SAMPLING LOCALITIES AND RESULTS

6.4.1 AL-GHAS'SANIYEH.

6.4.1.1 Sampling

Within the Baer-Bassit ophiolitic complex itself Maastrichtian outcrops are limited to a small inlier exposed by the roadside between the villages of Al Ghas'saniyeh and Al-ieman (see figure 6.1). This section can be traced 100m along the road and then to the top of the hill some 60m above, by way of a winding forest track. The base of the section is about 3m above a large outcrop of tuffs, part of the Baer-Bassit mélange. The relationship between the two is unclear as the contact cannot be seen, but Kazmin and Kulakov (1968) suggest a normal, though unconformable contact. The lithologies found here proved unique to the area. The section starts at the NW of the locality, with thick beds of calcarenite, which contain ophiolitic clasts of greatly varying size that are angular to sub-angular in shape. The clasts comprise variably altered serpentinite, gabbro and basalt. There are also a number of clasts of chert and limestone. Larger benthic foraminifera are very common, in some beds constituting up to 80% of the volume of the rock, and there are also a number of large gastropods, up to 15cm in length, as well as other fossil detritus, indicating shallow water deposition within the photic zone. Moving SE up the section the number of clasts increase, though the average size diminishes, and the lithologies become matrix-supported conglomerates/gravels with interbedded and inter-fingering calcareous sandstone bodies, suggesting rapid lateral facies variation. These beds contain far less fossil detritus and larger foraminifera are absent. During the first field season two spot samples were taken from this section for analysis (samples 11143 from near the base of the section and 11144 from the gravelly beds further up) and further samples were taken from the lower part of the section (AGS 1-5, lower 20m) during the second field season. A final sample (GHAS1) was collected during the final field season from a lens of calcareous sandstone within the gravels (Figure 6.2). The beds here are dipping gently to the southeast.

The succession of lithologies seen at this locality were generally unique to the area, though poorly exposed calcarenites were seen around the coastal village of Umit'tiur and loose blocks of calcareous sandstone packed with larger foraminifera were seen amongst float near the village of Markhous. Conglomerates were also seen near the village of Ballourane but were barren of any larger foraminifera.

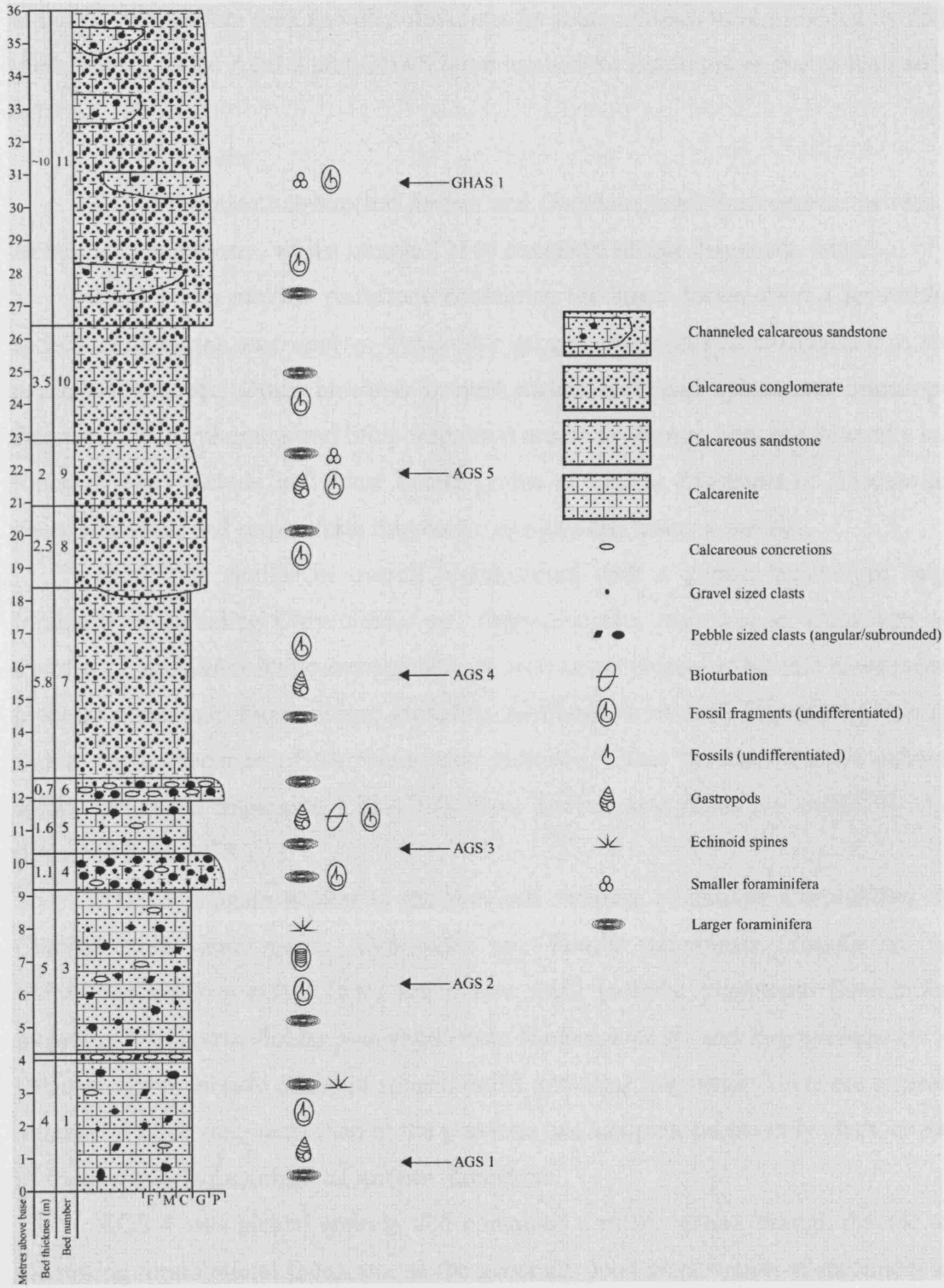

Figure 6.2 Lithological log of the roadside section between the villages of Al Ghas'saniyeh and Al ieman, illustrating sampling levels.

6.4.1.2 Processing

Samples 11143-4, AGS 1-3 and AGS 5 were thin-sectioned due to the number of larger foraminifera seen and identifications for these samples were provided by Fadel (pers. com.), whilst AGS 4 and GHAS were washed for foraminifera due to their softer nature.

6.4.1.3 Results

11143 contained *Orbitolites faufasi* and *Omphalocyclus macroporus*, as well as *Heterohelix globulosa* , whilst sample 11144 contained no age diagnostic fauna.

AGS 1 is a micritic packstone containing the larger foraminifera *Chrysalidina* sp., *Omphalocyclus macroporus*, *Orbitoides* sp. and *Siderolites calcitropoides*, as well as *Heterohelix* sp., Other bioclasts present include echinoid spines and brachiopod fragments. Mineral grains and lithic fragments are up to 3mm in size, and generally sub-rounded. They include individual quartz grains as well as fragments of siltstone and chert, limestone and serpentinite fragments, opaques and heavy minerals.

AGS 2 is similar in overall composition, with a greater number of larger foraminifera including *Chrysalidina* sp., *Omphalocyclus macroporus*, *Orbitoides* sp., *Rotalia* sp. and *Siderolites calcitropoides*, as well as a few smaller benthic foraminifera, globular planktonic foraminifera, including *Hedbergella* sp. and *Rugoglobigerina* sp., and a single specimen of *Globotruncana bulloides*. Other bioclasts include echinoid spines and rudist fragments. Lithic fragments and mineral grains are similar to those described from AGS 1.

AGS 3 is again similar to the previous samples, containing *Chrysalidina* sp., *Omphalocyclus macroporus*, *Orbitoides* sp., *Rotalia skourensis*, *Rotalia* sp. and *Siderolites calcitropoides*. There are a few small globular planktonic foraminifera, including *Globigerinelloides prairiehillensis*, *Hedbergella* sp. and *Rugoglobigerina* sp. Other bioclasts include echinoid spines, rudist and algal fragments. There are a greater number of lithic fragments than in the previous two samples, particularly chert, as well as fragments of a foraminiferal micritic limestone.

AGS 4 was picked entirely and contained a rather sparse, though diverse and interesting foraminiferal fauna, due to the generally good preservation of specimens not seen elsewhere. Among the planktonic foraminifera were *Pseudotextularia elegans, Planoglobulina* sp., *Globotruncana arca* (Plate 4, Figs. 3 & 4), *G. aegyptica* (Plate 4, Figs. 1 & 2), *G. ventricosa*, *Globotruncanita stuarti*, *Gta stuartiformis*,

Contusotruncana fornicata, *Rugoglobigerina rugosa* and ?*Rugotruncana* sp. Smaller benthic foraminifera include *Cibicides* sp., *Lagena* (?) sp., *Galvelinella* sp., *Epistomaroides* sp., *Lenticulina* sp., *Globorotalites* sp. and *Spiroplectammina* sp.

AGS 5 contains fewer larger foraminifera than AGS 1-3 but *Omphalocyclus macroporus, Orbitoides sp., Pseudedomia sp., Rotalia skourensis* and *Siderolites calcitropoides* are all still present. In addition there are a few smaller benthic foraminifera, and small globular planktonic foraminifera including *Globigerinelloides* sp., *Hedbergella* sp. and *Rugoglobigerina* sp. There are also two specimens of *Heterohelix* sp. and a single specimen of *Globotruncanita* sp. Lithic fragments and mineral grains are similar to those seen in sample AGS 3.

GHAS contains a sparse and poorly preserved fauna. Just two planktonic foraminifera are present; *Globotruncana aegyptica* and *G. linneiana*, along with the benthic foraminifera *Globorotalites* sp. and *Galvelinella* sp.

6.4.1.4 Age

From the first field season sample 11143 was dated as Maastrichtian, whilst 11144 could not be dated as it was barren.

Samples AGS 1-3 were also all dated as Maastrichtian in age though no further refinement was possible with the rather limited fauna. A more diverse assemblage was recovered from sample AGS 4 that indicated an age no older than the Campanian *G. aegyptica* Zone, whilst AGS 5, with a similar fauna to AGS 1-3, was dated as Maastrichtian. Finally, GHAS was dated as Late Campanian to Maastrichtian in age.

6.4.1.5 Palaeoenvironment

The section is interpreted as reflecting a shallow marine, channelised environment with rapid lateral facies variation. Moving up the section the reduction in clast size indicates a possible deepening, but the fauna present, including corals and larger benthic foraminifera, indicate the sediments here were all deposited well within the photic zone. This is reflected in the small number of planktonic foraminifera recovered, with those present interpreted as having drifted in from deeper waters.

6.4.2 UMIT'TIUR

6.4.2.1 Sampling

A thin ribbon outcrop of Maastrichtian sediments is also reported from near the village of Umit'tiur on the Mediterranean coast, overlying the Baer-Bassit mélange at the base of the northern slopes of the Jebel Rhouz hills (Kazmin and Kulakov, 1968) (See figures 6.1 and 6.3).

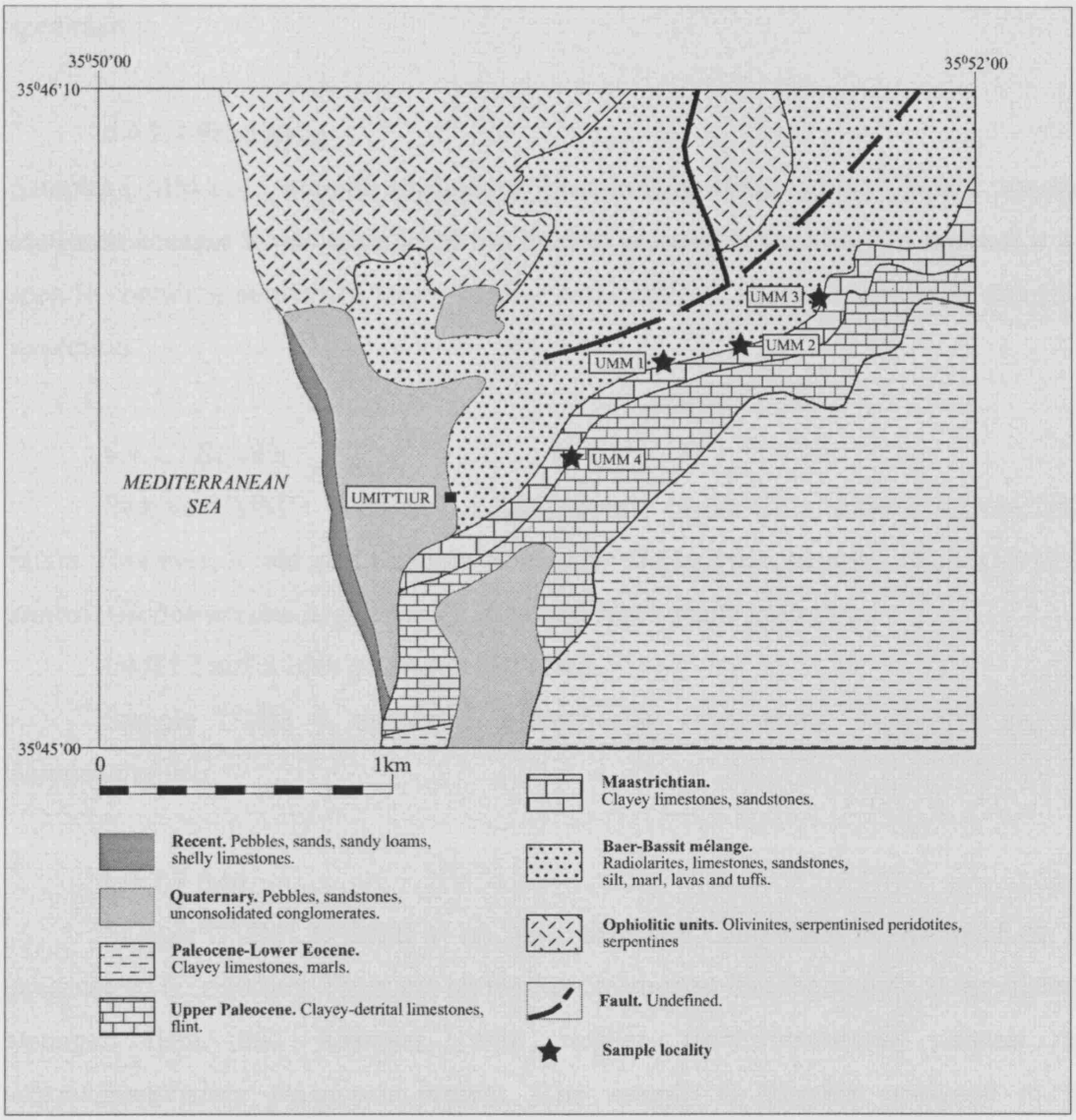

Figure 6.3. Geological sketch map of the sampling localities in the Umit'tiur area (modified after Kazmin and Kulakov, 1968).

Exposures here are poor and sampling was limited to a number of spot samples. Sample UMM 1 was taken from a small trackside exposure of chalky limestones with minor grey marls. UMM 2 was taken from a small exposure of rubbly conglomeratic

chalk, containing rounded clasts of chert and limestone. Amongst olive groves near the valley floor, are occasional outcrops of well-bedded calcarenites, generally dipping gently to the south. Sample UMM 3 was taken from an outcrop of this lithology that resembled the calcarenites seen at Al Ghas'saniyeh, containing visible larger benthic foraminifera. Sample UMM 4 was taken from a bed of hard sandy limestone overlying conglomerates and calcarenites about 1 km southwest of sampling point UMM3). Though essentially similar to the previous sample, no foraminifera were seen in hand specimen.

6.4.2.2 Processing

Samples UMM 1 – 3 were all washed for foraminifera, whilst sample UMM 4 was thin-sectioned because it was considered too hard to process by washing and because it was seen to contain a number of larger benthic foraminifera. These are generally identified in section.

6.4.2.3 Results

Sample UMM 1 contained a fairly poorly preserved planktonic foraminiferal fauna. However, it was still possible to identify *Gansserina gansseri*, *Globotruncanita stuarti*, *Globotruncana aegyptica*, *G. arca* and *Heterohelix globulosa*.

UMM 2 and 3 both proved to be barren.

Sample UMM 4 contained *Morozovella velascoensis*, Alveolina sp. and *Nummulites* sp.

6.4.2.4 Age

Sample UMM1 is dated as no older than late Campanian in age based on the presence of *G. gansseri*. There are no markers to suggest that the sample is significantly younger than this however, with neither *Contusotruncana contusa* nor *Racemiguembelina fructicosa* present. The sample is therefore assigned to the *Gansserina gansseri* Zone.

UMM 2 and 3 were both barren and therefore no dating was possible, whilst UMM 4 was dated late Paleocene to middle Eocene based on the occurrence of *Morozovella velascoensis*.

6.4.2.5 Palaeoenvironment

A shallow inner shelf environment is interpreted for the samples described. This is suggested by the sedimentology as well as the palaeontology. Although samples UMM 2 and 3 were barren, the paucity of planktonic foraminifera in UMM 1 as well as the larger benthic foraminifera agree with this.

6.4.3 DAMATE

6.4.3.1 Sampling

Krasheninnikov (1994) reports that the best exposures of Maastrichtian age cover sediments are to be found on the southern slopes of the Jebel Rhouz hills, near the villages of Qafar Fawkani and Damate (figure 6.1). Both of the maps used (Kazmin and Kulakov, 1968 and Adjemian and Khatoun. 1999) also suggest that Maastrichtian sediments are extensively developed in this area. A number of sections were sampled in this area and spot samples were also taken from minor outcrops. The lithologies were dominated by hard chalks and marls with no exposures seen of the calcarenites and conglomerates found at Al-Ghas'saniyeh and Umit'tiur. Kazmin and Kulakov report that the base of the succession here begins with brown calcareous sandstone before passing up into chalks and marls. This sequence was not seen during this study however, despite extensive sampling in the area, and chalks and marls appear to lie directly on the Baer-Bassit mélange and an exposure of serpentinite in the west of the area (see figure 6.5).

Sample DAMA 1 was taken from a bed of blue-grey marl in a small outcrop of interbedded marls and chalks west of Damate that has been mapped as both Maastrichtian (Adjemian and Khatoun, 1999) and Paleocene (Kazmin and Kulakov, 1968) in age.

Samples DAMA 2-3, were taken from the western limit of a 60 m thick section of reported Maastrichtian sediments. The steeply northward dipping sediments comprise interbedded marls, marly limestones and chalks. The section lies within the extent of the Maastrichtian sediments on both the Russian and Syrian maps. DAMA 2 was taken from a 30cm thick bed of blue-grey marl just under 9m above the base of the section. DAMA 3 was taken from the base of a 20cm thick bed of chalk 11m above the base of the section. The chalk contained rip-up marl clasts and a lot of fossil detritus visible in hand specimen.

Samples DAMA 4-8 were all taken from a 20m thick section of moderately northward dipping, interbedded marls and marly limestones. Both the Russian and Syrian maps clearly show this protrusion of strata southward into the valley, and identify it as Maastrichtian in age (see figure 6.5).

DAMA 4 was taken from a 15cm thick bed of soft, pale beige coloured marls near the base of the section (bed 2). DAMA 5 was sampled 5cm from the top of bed 13, a 1m thick sequence of thinly interbedded chalks and marls. Sample DAMA 6 was taken from a 15cm thick bed of fairly hard grey-brown marl 7m above the section base (bed 25. DAMA 7 was from a 30cm bed of blue-grey marls about 9m above the base of the section (bed 38). Sample DAMA 8 was taken from a 48cm thick bed of beige coloured chalky marls about 17.5m above the base of the section, and the first visible bed after nearly 3m of no exposure.

During the first field season samples 11145 and 11146 were taken from reported Maastrichtian chalks about 1km east of Daqmate and sample DAMA A was taken from the same area during the second season, from a small, heavily faulted outcrop in the bank of a field. The lithologies here are grey-green, strongly bioturbated, marly chalks. Sample DAMA B was taken about 100m further west, again from a highly disturbed outcrop, but here the beds are thicker and the lithology is chalkier. The Baer-Bassit mélange can be seen cropping out in a dry stream bed just 100m west of this locality. Sample DAMA C was taken further west from a small outcrop of chalks just 50m northeast from a large block of serpentinite (see figures 6.4 and 6.5). In this outcrop a single 6cm thick bed of chert is visible. Further west, just south of Damate, chalks and marls can be seen cropping out near large outcrops of serpentinite, and no more than 10m above (See figure 6.4). Sample DAMA D was taken from a 6m thickness of patchily exposed marls and hard marly limestones no more than 25m northwest of a number of outcrops of serpentinite.

Samples DAMA E-I were all taken from a roadside exposure of thickly bedded chalky limestones with minor marl interbeds, passing into more marl dominated lithologies. The base of the section is no more than 10m above an outcrop of serpentinite. DAMA E was taken from the base of the section, a 1.4m packet of medium bedded, hard chalky limestones. DAMA F was taken from the base of a 7m unit of massively bedded hard limestones 3m above the base of the section (bed 4). DAMA G was sampled 22m above the base of the section, after about 14m of no exposure, from the base of a 1m thick packet of medium bedded, blue-grey marls (bed 13). DAMA H

was taken from a 40cm thick unit of medium bedded grey-green marls, 26m above the base of the section (bed 16 DAMA I was taken from a bed of marls a further 60m along the road after an interval of non exposure.

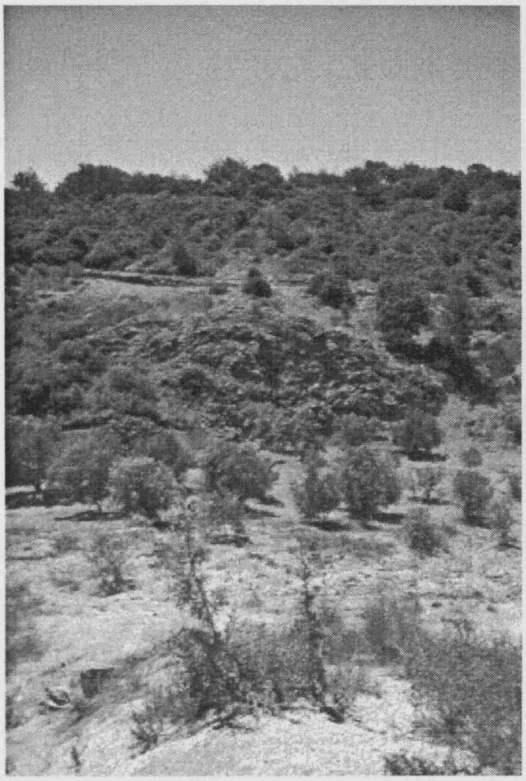

Figure 6.4. Pale marls and marly limestones (foreground) cropping out in close proximity to a large outcrop of serpentinite (middle ground) that itself is cropping out amongst generally poorly to non-exposed melange.

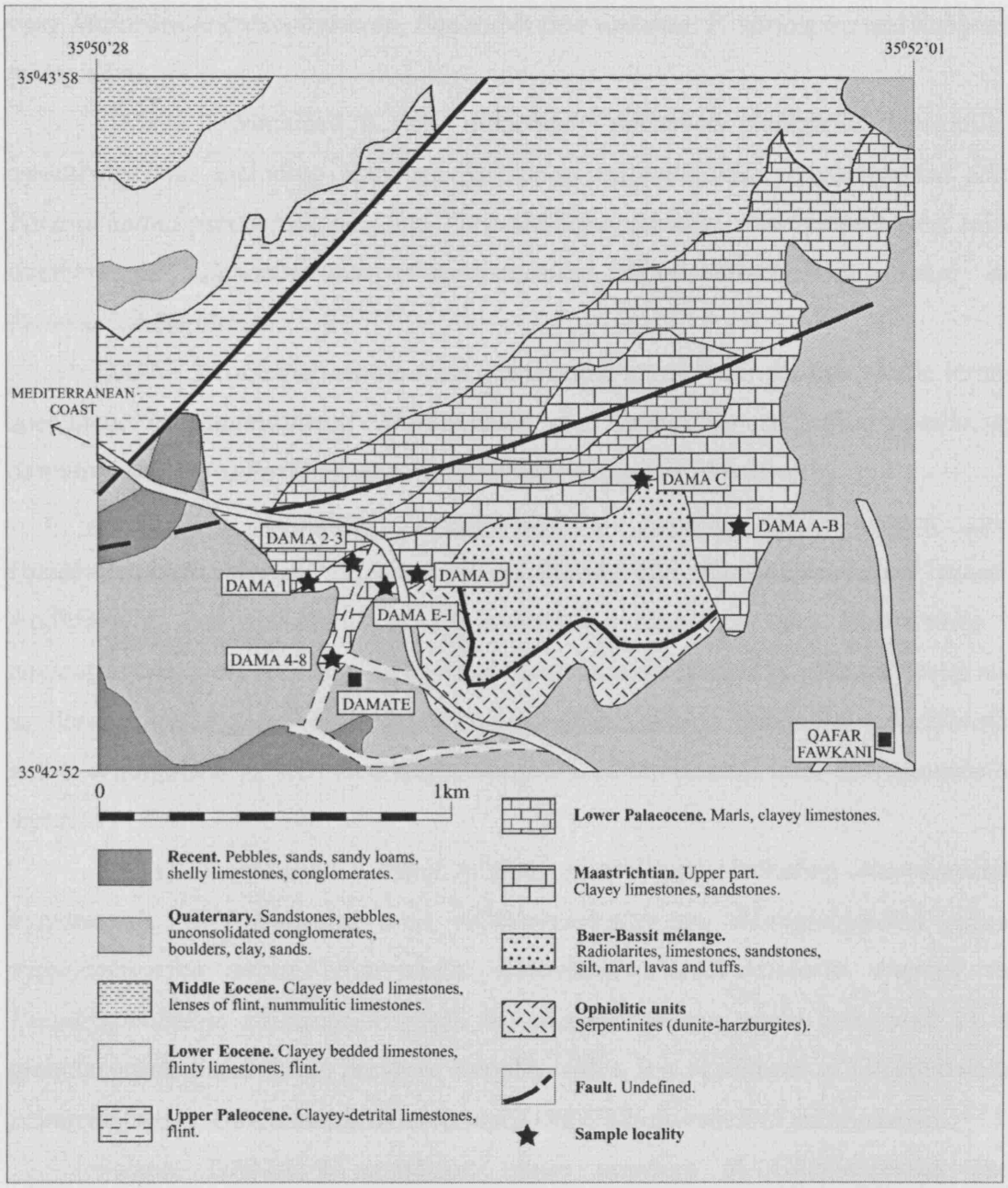

Figure 6.5. Geological sketch map of the sampling localities around the villages of Damate and Qafar Fawkani (modified after Adjemian and Khatoun, 1999).

6.4.3.2 Processing

All of the samples from this area were washed for foraminifera and general microfossils, apart from DAMA 3 which was thin-sectioned due to its hardness.

6.4.3.3 Results

Sample DAMA 1 was dominated by specimens of *Morozovella angulata*, *P. pseudobulloides* and *Subbotina triloculinoides*. Other species represented

were *Morozovella conicotruncata*, *Parasubbotina varianta*, *P. variospira* and *Subbotina triangularis*.

DAMA 2 contained a rich, moderately preserved planktonic foraminiferal assemblage was including abundant *Subbotina triloculinoides*, *Eoglobigerina edita*, *Parasubbotina pseudobulloides* and *Parasubbotina varianta*. Also present were minor numbers of *Globanomalina planocompressa*, *Globanomalina compressa* and *Praemurica inconstans*.

DAMA 3 contained rip-up marl clasts and a lot of fossil detritus visible in hand specimen. In thin-sectioned *Morozovella* sp., *Operculina* sp., *Ranikothalia* sp., *Smoutina* sp., *Rhiyadhella* sp. and *Siphovalvulina* sp. were identified.

DAMA 4 contained *Rugoglobigerina rugosa*, *Globotruncana arca*, *Pseudotextularia elegans*, *Heterohelix globulosa* and *Racemiguembelina powelli*. Additionally, rare specimens of *Globanomalina compressa* and *Morozovella* cf. *conicotruncata* were recovered. The assemblage was dominated by globular forms such as *Parasubbotina pseudobulloides*, *Parasubbotina varianta*, *Subbotina triloculinoides* and *S. triangularis* as well as a single specimen of the biserial form *Chiloguembelina morsei*.

DAMA 5 contained a small number of specimens including *Abathomphalus mayaroensis*, *Globotruncana arca*, *Globotruncanita* sp., *Rugoglobigerina rugosa*, *Rugoglobigerina scotti*, *Heterohelix globulosa*, *Pseudotextularia elegans* and *Pseudoguembelina costulata*. Overall, the assemblage was again dominated by the globular forms listed in the previous sample, with a few specimens of *Globanomalina planocompressa*, *Globanomalina compressa* and *Chiloguembelina midwayensis*.

Sample DAMA 6 contained minor numbers of *Globotruncana arca*, *Globotruncanita stuartiformis*, *Globotruncanella petaloidea*, *Pseudotextularia elegans*, *Heterohelix striata* and *Pseudoguembelina costulata*. Globular forms such as those listed under sample DAMA 4 again dominate the fauna, however there are a far greater number of globanomanilinids including *G. planocompressa*, *G. compressa* and *G. imitate* and several specimens of *Chiloguembelina* sp.

DAMA 7 again contained minor numbers of *Globotruncana arca*, *Globotruncanita stuartiformis*, *Rugoglobigerina rugosa*, *Globotruncanella petaloidea*, *Heterohelix* sp. and *Pseudoguembelina* sp. Other taxa included *Subbotina triloculinoides*, *S. triangularis*, *Parasubbotina varianta*, *Parasubbotina*

pseudobulloides, *Praemurica taurica*, *P. inconstans*, *Globanomalina planocompressa* and *G. compressa*.

Sample DAMA 8 included *Subbotina triloculinoides*, *S. trivialis*, *S. triangularis*, *Parasubbotina varianta*, *Parasubbotina pseudobulloides*, *Praemurica taurica*, *P. inconstans*, *P. uncinata* and *Globanomalina compressa*.

Less than 3% of the assemblage recovered from sample DAMA A comprised the following species; *Globotruncana arca*, *G. bulloides*, *Globotruncanita stuartiformis*, *Gansserina gansseri*, *Rugoglobigerina rugosa*, *R. rotundata*, *Contusotruncana walfischensis*, *Heterohelix globulosa* and *Pseudotextularia elegans*. The majority of the assemblage was dominated by moderately sized globular forms including *Eoglobigerina edita*, *Subbotina triloculinoides*, *S. trivialis*, *Parasubbotina pseudobulloides*, *P. varianta*, *Praemurica pseudoinconstans* and *P. inconstans*. *Globanomalina planocompressa* is rare in this sample.

DAMA B contains the marker species *Abathomphalus mayaroensis*. The dominant fauna are *Rugoglobigerina rugosa*, *Globotruncanita stuartiformis*, *Globotruncana aegyptica* and *Heterohelix globulosa*.

DAMA C contained specimens of *Globotruncana arca*, *G. aegyptica*, *Globotruncanita stuartiformis*, *G. stuarti*, *Rugoglobigerina rugosa*, *Contusotruncana* contusa, *C. walfischensis*, *Globigerinelloides ultramicra*, *Pseudotextularia elegans* and *Heterohelix globulosa*. Other, more poorly preserved fauna, included *Globanomalina planocompressa*, *Subbotina triloculinoides*, *S. trivialis*, *Parasubbotina pseudobulloides* and *Eoglobigerina edita*.

DAMA D was dominated by specimens of *Globotruncana*, *Globotruncanita*, *Rugoglobigerina*, *Heterohelix* and *Pseudotextularia*. Small numbers of poorly preserved specimens of *Subbotina* sp., *Parasubbotina pseudobulloides*, *Eoglobigerina* sp. and *Globanomalina planocompressa* were also recovered.

DAMA E contained a few specimens of *Globotruncana* sp., *Rugoglobigerina rugosa*, *Globigerinelloides subcarinatus* and *Heterohelix* sp. The assemblage was dominated by specimens of *Subbotina triloculinoides*, *Eoglobigerina eobulloides* and *Praemurica pseudoinconstans*.

DAMA F contained a moderately well preserved and diverse including a number of specimens of *Globotruncana* and *Globotruncanita*, *Rugoglobigerina rugosa*, *R. hexacamerata*, *R. scotti*, *Globotruncanella petaloidea*, *Pseudotextularia elegans*, *Heterohelix globulosa* and *Planoglobulina acervulinoides*. Other less well preserved

specimens, comprise only about 20% of the total assemblage, included *Globanomalina compressa*, *Globanomalina planocompressa*, *Parasubbotina pseudobulloides*, *Subbotina* sp. and *Chiloguembelina* (?) sp.

DAMA G essentially contained the same fauna as for DAMA F with the addition of a couple of specimens of *Contusotruncana contusa*. The preservation and species distribution is also the same as for the previous sample.

About 2% of the assemblage recovered from DAMA H comprised specimens of *Globotruncana arca*, *Rugotruncana* sp., *Heterohelix globulosa* and *Pseudotextularia elegans*. The remainder of the fauna was dominated by specimens of *Subbotina triloculinoides*, *Parasubbotina pseudobulloides*, *Eoglobigerina edita* and *Globanomalina planocompressa*.

About 20% of DAMA I comprised specimens of *Rugoglobigerina rugosa* ,Pseudotextularids and Heterohelicids. The other 80% contained poorly preserved specimens of *Subbotina triloculinoides*, *Parasubbotina pseudobulloides*, *Eoglobigerina edita* and *Globanomalina planocompressa* similar to the previous sample.

6.4.3.4 Age

Sample DAMA 1 should have been Maastrichtian according to the map of Adjemian and Khatoun (1999) and Paleocene according to Kazmin and Kulakov (1968). The presence of *Morozovella angulata* and *Morozovella conicotruncata*, together with the absence of *Igorina albeari*, allows the sample to be confidently assigned to the early Late Paleocene Subzone P3a (*Morozovella angulata-Igorina albeari* Interval Subzone).

Samples DAMA 2-3 were taken from a section that lies within the extent of the Maastrichtian sediments on both the Russian and Syrian maps.

DAMA 2 was dated as belonging to the early Paleocene P1c *Globanomalina compressa-Praemurica inconstans* Interval Subzone based on the presence of both *Globanomalina compressa* and *G. planocompressa*.

The fauna identified in sample DAMA 3 suggest a late Paleocene age but no zonal assignment is possible.

Samples DAMA 4-8 were all taken from a section clearly identified as Maastrichtian in age (see figure 6.5) according to both the Russian and Syrian maps

DAMA 4 contained a number of reworked Maastrichtian taxa but the Paleocene taxa, including *Globanomalina compressa* and *Morozovella* cf. *conicotruncata*, suggest

an earliest late Paleocene age for the sample assigning it to the P3a *Morozovella angulata-Igorina albeari* Interval Subzone. It seems likely however, that the single specimen of a keeled morozovellid present may be a contaminant, as the sample appears early Paleocene in age based on the overall assemblage. The sample is therefore assigned to the early Paleocene P1c *Globanomalina compressa/Praemurica inconstans-P. uncinata* Interval Subzone, with reworked mid-late Maastrichtian specimens.

DAMA 5 also contained a number of reworked Maastrichtian specimens but these comprise <5% of the total assemblage. The presence of the Paleocene planktonic foraminifera *Globanomalina planocompressa* and *Gl. compressa* therefore assign this sample to the early Paleocene P1c *Globanomalina compressa/Praemurica inconstans-P. uncinata* Interval Subzone.

DAMA 6 also contained a small percentage of reworked Maastrichtian fauna, but the Paleocene fauna, similar to DAMA 5, indicate an early Paleocene P1c *Globanomalina compressa/Praemurica inconstans-P. uncinata* Interval Subzone age for the sample.

DAMA 7 contained a small number of specimens of Maastrichtian age and these were better preserved than the younger, and dominant, Paleocene taxa. Once again specimens of *Globanomalina planocompressa* and *G. compressa* indicate that this sample is no older than the P1c *Globanomalina compressa/Praemurica inconstans-P. uncinata* Interval Subzone.

Unlike the other samples taken from this section, sample DAMA 8 contained no Maastrichtian taxa, and the average sizes of the Paleocene species were noticeably larger than in the previous samples. The presence of *P. uncinata* places this sample within the early Paleocene P2 *P. uncinata-Morozovella angulata* Interval Zone. In addition the angularity of the final chamber is not that well developed suggesting an early form, and from this, combined with the absence of any specimens of *M. angulata* it seems likely the sample belongs to the lower part of the zone.

Sample DAMA A also contained reworked Maastrichtian species comprise <3% of the total assemblage. The assemblage of Paleocene taxa dates this sample as belonging to the early Paleocene P1c *Globanomalina compressa/Praemurica inconstans-P. uncinata* Interval Subzone.

DAMA B was the only sample from this area to not contain any Paleocene specimens. The presence of the marker species *Abathomphalus mayaroensis* dates this sample as belonging to the Maastrichtian *A. mayaroensis* Zone. *Gansserina gansseri* is

absent from the assemblage suggesting the sample is from the upper part of this zone and is latest Maastrichtian in age.

DAMA C was dated as Paleocene in age with reworked Maastrichtian foraminifera. The presence of *Globanomalina planocompressa* and *Eoglobigerina edita* date this sample as belonging to the early Paleocene P1 *Parvularugoglobigerina eugubina-Praemurica uncinata* Interval Zone. This cannot be further refined.

DAMA D was dominated by reworked Maastrichtian fauna. The poorly preserved Paleocene fauna allow the sample to be dated as early Paleocene P1b-P1c, *Subbotina triloculinoides-Globanomalina compressa/Praemurica inconstans* Interval Subzone - *Globanomalina compressa/Praemurica inconstans-P. uncinata* Interval Subzone, based on the presence of both *Globanomalina compressa* and *Parasubbotina pseudobulloides*.

DAMA E again contained reworked Maastrichtian foraminifera but was dominated by poorly preserved Palaeocene specimens. The co-occurrence of *Subbotina triloculinoides* and *Eoglobigerina eobulloides* dates this sample P1b *Subbotina triloculinoides-Globanomalina compressa/Praemurica inconstans* Interval Subzone in age.

DAMA F is dominated by reworked Maastrichtian foraminifera that are both moderately well preserved and diverse. The Paleocene taxa are not as well preserved but *Globanomalina compressa* and *Globanomalina planocompressa* were both identified, dating the sample as belonging to the early Paleocene P1c *Globanomalina compressa/Praemurica inconstans-P. uncinata* Interval Subzone.

DAMA G is also assigned to the early Paleocene P1c *Globanomalina compressa/Praemurica inconstans-P. uncinata* Interval Subzone, based on the presence of the same species as for the previous sample.

DAMA H was dominated by Paleocene taxa. *Subbotina triloculinoides*, *Parasubbotina pseudobulloides* and *Globanomalina planocompressa* date the sample as belonging to the early Paleocene P1b-c *Subbotina triloculinoides-Globanomalina compressa/Praemurica inconstans* to *Globanomalina compressa/ Praemurica inconstans-Praemurica uncinata* Interval Subzones.

DAMA I contains the same species as sample DAMA H and therefore is assigned to the same P1b-c Interval Subzones.

6.4.3.5 Palaeoenvironment

The limestones and marls reflect pelagic and hemipelagic sedimentation on a deeply submerged shelf. The dominance of planktonic foraminifera in all of the samples from this area also reflects these deep, open marine conditions.

6.4.4 ZERHINE.

6.4.4.1 Sampling

Northeast of Damate, Cretaceous sediments are reported to crop out near the villages of Zerhine and Kantil Jouk, east of the Nahr el Kerjalia River (see figure 6.1). The main outcrops are mapped as a thin ribbon of sediments, duplicated by faulting, bordering the Baer-Bassit mélange to the southeast. Two small inliers of Maastrichtian age sediments are also indicated (Adjemian and Khatoun 1999) (See figure 6.7). Samples ZUGH 1-3 were taken from an outcrop of disturbed chalks and marls directly overlying the Baer-Bassit mélange. Sample ZUGH 1 was a clean hard chalk with no ophiolitic detritus visible in hand specimen. Samples ZUGH 2 and 3 were soft marls, white and pink in colour respectively.

ZUGH 4 was taken further west from a small outcrop of hard, grey-green marly limestones. To the northeast well-bedded marly limestones and chalks can be seen cropping out in a cliff face, but the precipitous nature of this section made logging and detailed sampling impossible. A spot sample (ZUGH 5) was however taken.

Samples ZUGH 6-10 were taken from a 3m thick section exposed in the bank of a tobacco field. This fairly coherent outcrop comprised thinly interbedded marls and chalks, with two thicker individual chalk beds. The lithologies and sampling points for ZUGH 6-10 are illustrated on figure 6.6 and the sampling localities are illustrated on figure 6.7. Sample KANT 1 was taken from a small patch of blocky limestones cropping out in a field about ½ km northeast of Kantil Jouk.

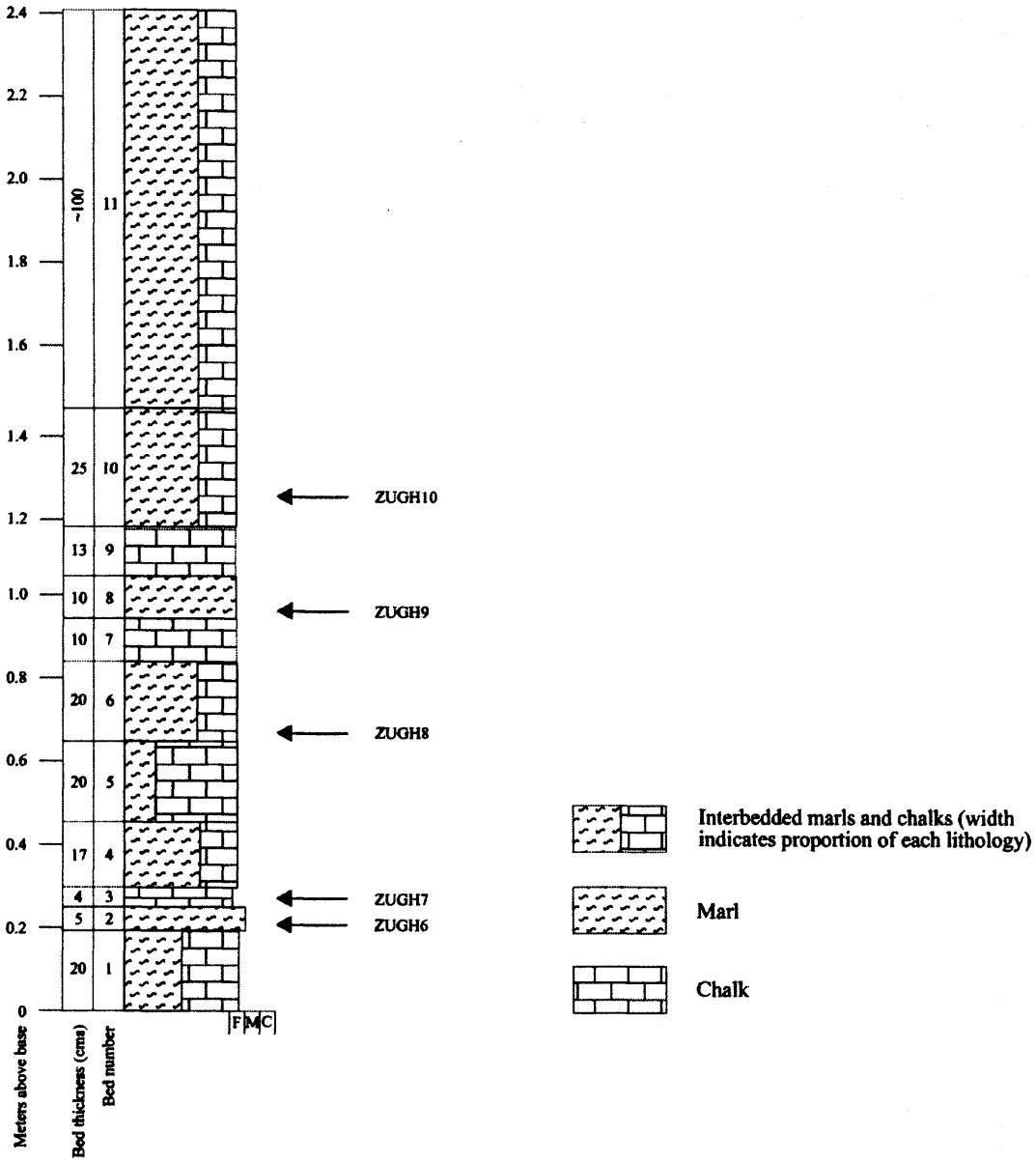

Figure 6.6. Lithological log of the main Zerhine section with sampling levels indicated

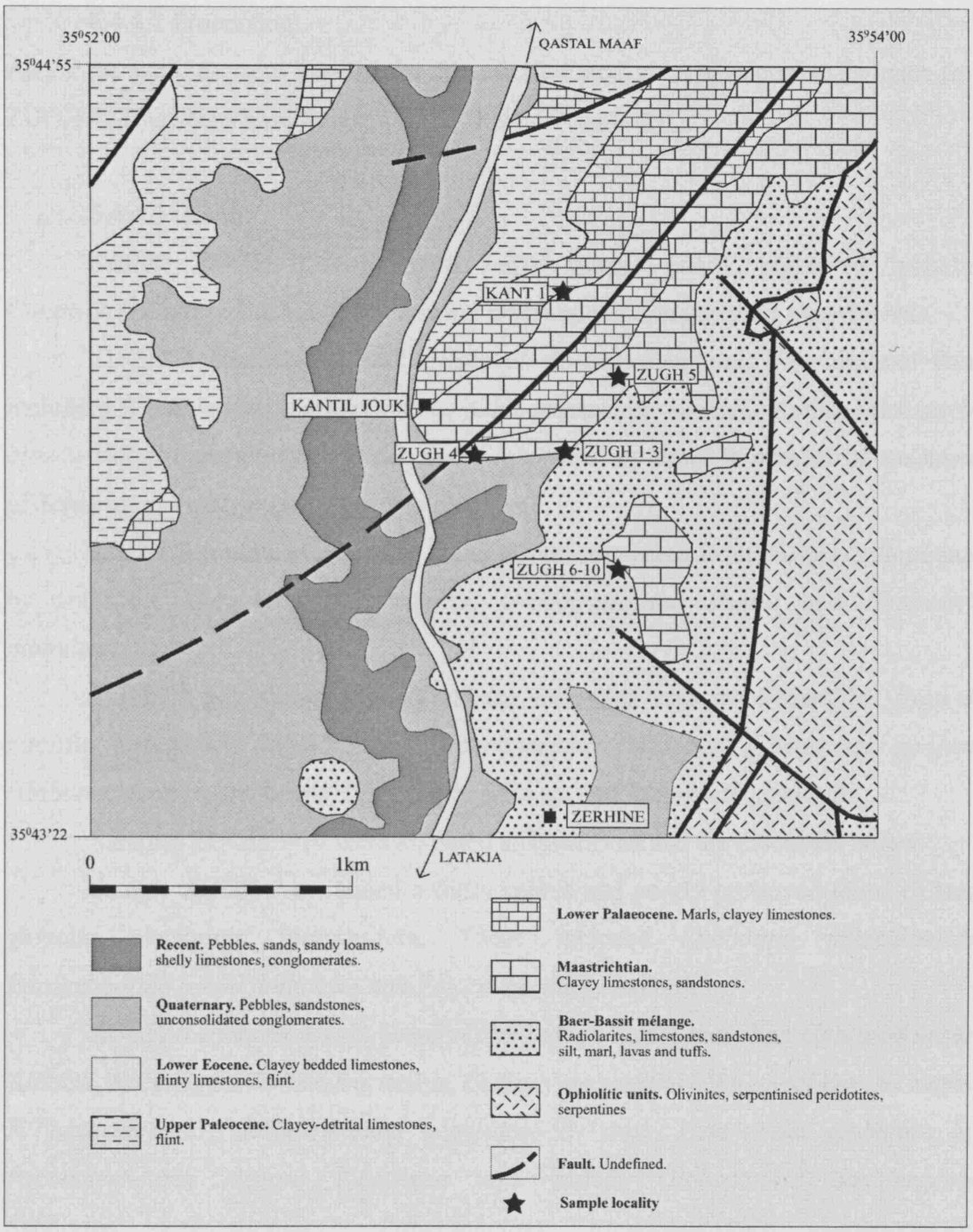

Figure 6.7. Geological sketch map of the localities around the villages of Zerhine and Kantil Jouk (modified after Adjemian and Khatoun, 1999).

6.4.4.2 Processing

All of the samples were washed for foraminifera and general microfossils apart from ZUGH 4. This was a hard limestone and was thin-sectioned.

6.4.4.3 Results

Sample ZUGH 1 contains a fairly sparse, poorly preserved including *Contusotruncana contusa*, *Globotruncana arca* and *Globotruncanita stuartiformis*.

ZUGH 2 contained a well preserved diverse planktonic foraminiferal fauna including *Contusotruncana fornicata*, *Globotruncanita stuarti*, *Archaeoglobigerina blowi*, *Globotruncanella petaloidea* and *Globotruncana arca*. A number of specimens of *Schackoina multispinata* were also recovered.

ZUGH 3 contained a similar fauna to that recovered from ZUGH 2, dominated by abundant *Rugoglobigerina rugosa*, *Globotruncanita stuarti* and *Heterohelix globulosa*.

ZUGH 4 was thin-sectioned and the following taxa were identified from the micritic packstone: *Bulimina* sp. *Globotruncana fornicata*, *Gansserina gansseri*, *Globotruncana stuartiformis*, *Planohedbegella* sp. and *Rugoglobigerina* sp.

Samples ZUGH 5-10 were all dated as Paleocene and are discussed below.

Sample ZUGH 5 contained a fairly sparse and poorly preserved fauna of small globular planktonic foraminifera. These included *Subbotina triloculinoides*, *Parasubbotina pseudobulloides* and *Eoglobigerina eobulloides*.

ZUGH 6 contains a well-preserved reworked fauna, including *Contusotruncana contusa*, *Racemiguembelina fructicosa*, *Gansserina gansseri*, *Rugoglobigerina rugosa*, *R. hexacamerata*, *Globotruncana aegyptica*, *G. arca*, *Heterohelix globulosa* and *Pseudotextularia elegans* Paleocene taxa include *Globoconusa daubjergensis*, *Subbotina triloculinoides*, *Parasubbotina pseudobulloides*, *Globanomalina planocompressa*, *Parasubbotina varianta*, *Praemurica pseudoinconstans* and *Chiloguembelina* sp.

ZUGH 7 contains reworked Maastrichtian globotruncanids and rugoglobigerinids. A number of fairly small globular Paleocene forms were recovered including *Parasubbotina pseudobulloides*, *P. varianta*, *Subbotina trivialis* and *S. triloculinoides*.

ZUGH 8 includes specimens of *Abathomphalus mayaroensis*, *Gansserina gansseri*, *Contusotruncana contusa* and *Racemiguembelina fructicosa*. Also present

were *Rugoglobigerina rugosa*, *Globotruncanita stuarti*, *Gta stuarti*, *Globotruncana arca* and *Pseudotextularia elegans*. Paleocene taxa include a similar, though more diverse, assemblage to that recovered from sample ZUGH 7, including *Subbotina triloculinoides*, *S. trivialis*, *Parasubbotina pseudobulloides*, *Globanomalina planocompressa*, *G. archaeocompressa*, *Parasubbotina varianta*, *Praemurica pseudoinconstans* and *Chiloguembelina* sp.

ZUGH 9 again contains a fairly well preserved Cretaceous fauna, dominated by rugoglobigerinids and also including *Globotruncanita stuarti*, *Gta stuartiformis*, *Globotruncana arca*, *Pseudotextularia elegans* and *Pta intermedius*. Paleocene fauna are similar to the assemblages seen in the previous samples including *Globanomalina planocompressa* and *Subbotina triloculinoides*.

ZUGH 10 contains a similar reworked assemblage to the previous sample with the addition of *Racemiguembelina fructicosa*. Palaeocene foraminifera recovered are essentially the same as for the previous three samples.

KANT 1 yielded a fairly poorly preserved fauna dominated by *Rugoglobigerina rugosa*, *Contusotruncana fornicata* and *Heterohelix globulosa*. Also recovered were *Globotruncanella havanensis* and *Globotruncana aegyptica*.

6.4.4.4 Age

Despite the paucity of the assemblage recovered from sample ZUGH 1 the presence of *Contusotruncana contusa* means it is no older than mid-Maastrichtian in age and assignable to the *C. contusa-R. fructicosa* Zone of Premoli-Silva and Sliter (1999) or the upper part of the *Gansserina gansseri* Zone of Robazsynski and Caron (1995). No other age diagnostic fauna are present.

The overall assemblage recovered from ZUGH 2 would appear to be late Campanian in age, as there are no Maastrichtian markers such as *Gansserina gansseri* and *Contusotruncana contusa*. No zonal markers were recovered. The presence of a several specimens of *Schackoina multispinata* may just be an artefact of the good preservation of this assemblage.

ZUGH 3 cannot be more accurately dated than being assigned to the Late Campanian *Globotruncana aegyptica* Zone or perhaps slightly younger. The lack of any specimens of *G. gansseri* does not necessarily mean the sample cannot belong to this zone, as this species is seldom a common component of latest Campanian-Early Maastrichtian assemblages.

The presence of *Gansserina gansseri* in sample ZUGH 4 allows the sample to be assigned to the latest Campanian – early Maastrichtian *G. gansseri* Zone.

ZUGH 5 was dated as belonging to the early Paleocene P1b *Subbotina triloculinoides-Globanomalina compressa/Praemurica inconstans* Interval Subzone, based on the co-occurrence of *Parasubbotina pseudobulloides* and *Eoglobigerina eobulloides*.

Samples ZUGH 6–10 were all taken from the same section, mapped as a small inlier of Maastrichtian sediments surrounded by facies of the Baer-Bassit melange by both Kazmin and Kulakov (1968) and Adjemian and Khatoun (1999). All of these samples proved to be Paleocene in age however, though with common to abundant reworked Maastrichtian fauna. An interesting feature of this section is that the percentage of reworked Cretaceous fauna increases up the section, corresponding with an increase in the number of benthic foraminifera as a percentage of the total Paleocene fauna. These data could possibly indicate a relative sea-level fall during this period, exposing previously deposited sediments to reworking as well as allowing a greater number of benthic fauna.

The reworked Cretaceous fauna recovered from sample ZUGH 6 are assigned to the lower Maastrichtian *C. contusotruncana-R. fructicosa* Zone of Premoli-Silva and Sliter (1999) or the upper part of the *Gansserina gansseri* Zone of Robazsynski and Caron (1995), based on the presence of *Contusotruncana contusa*, *Racemiguembelina fructicosa* and *Gansserina gansseri*. The sample itself is assigned to within the early Paleocene Zone P1b of Berggren and Norris (1995) based on presence of *Subbotina triloculinoides*, *Parasubbotina pseudobulloides* and *Globanomalina planocompressa*.

ZUGH 7 again contains reworked Cretaceous foraminifera but these are fairly poorly preserved. The Palaeocene fauna cannot date the sample more accurately than early Palaeocene P1c to P3, however, the sample is assigned to Zone P1b as the adjacent samples are of this age.

The reworked specimens recovered from ZUGH 8 are dated as belonging to the lower part of the late Maastrichtian age *A. mayaroensis* Zone based on the occurrence of the markers *Abathomphalus mayaroensis*, *Gansserina gansseri*, *Contusotruncana contusa* and *Racemiguembelina fructicosa*. The co-occurrence of the Paleocene taxa *Subbotina triloculinoides*, *Parasubbotina pseudobulloides*, *Globanomalina planocompressa* and *G. archaeocompressa* assign the sample to the early Paleocene P1b Zone.

ZUGH 9 contains specimens of *Gansserina gansseri* suggesting derivation from sediments of late Campanian-Maastrichtian age, though it seems unlikely that the reworked sediments were significantly older than those found in the sample below. The Paleocene fauna are similar to the assemblages seen in the previous samples with no younger taxa identified, and the sample is therefore also assigned to Zone P1b

ZUGH 10 An early Maastrichtian age is assigned to the reworked sediment provenance in ZUGH 10, and the sample itself is assigned to the lower Paleocene Zone P1b based on the fauna that are similar to those seen in the previous samples, including *Globanomalina planocompressa* and *Subbotina triloculinoides.*

KANT 1 was dated as late Campanian to Maastrichtian in age by the zonal markers *Globotruncanella havanensis* and *Globotruncana aegyptica.* No younger markers were recovered suggesting a Campanian age is more likely.

6.4.4.5 Palaeoenvironment

As with the samples collected from the Damate area the sediments reflect pelagic and hemipelagic sedimentation on a deeply submerged shelf. Planktonic foraminifera again dominate all of the reflecting deep, open marine conditions

6.4.5 QUIRAANIVE AND BALLOURANE

6.4.5.1 Sampling

Between the villages of Quiraanive and Ballourane, steep, deeply incised sections of well-bedded marls and chalks can be seen. These are mapped as Paleocene-Eocene in age but, as at Umit'tiur and Damate, Maastrichtian sediments are recorded as cropping out at the base of this succession. Samples were taken along the line of the boundary between the mélange and these overlying sediments and the localities are illustrated on figure 6.8.

Sample QUIR 1 was taken from a small outcrop in the middle of an olive grove. The float in the olive grove was dominantly chalk, whilst 15m to the SE the soil was deep red in colour, indicative of underlying mélange. The sample was a very light, pink weathering finely laminated marly chalk, with clasts of chert and harder rounded chalk, similar to sample UMM 2 from Umit'tiur. A number of samples were then taken just to the southwest of this locality. An outcrop of ribbon cherts appeared to be cut by a channel of rubbly, conglomeratic chalks and both these lithologies were sampled (QUIR 4-5). Also at this location a disturbed, 10m thick section of interbedded chalks and

marls was seen to overlie ribbon cherts, and samples QUIR 6-8 were taken here. Samples QUIR 2-3 were taken from more extensive outcrops of chalks and marls about 1km to the southwest whilst samples QUIR 9 and 10 were spot samples taken from patchy outcrops of chalks to the north of Quiraanive.

Samples BALL 1 and BALL 2-8 were all taken from close proximity to each other. BALL 1 was sampled from a bed of grey-green marls near the base of a thick section of chalks. About 50m to the west of this point a thick section of steeply dipping to vertical rocks were seen cropping out in the bank of an orchard (BALL 2-6, Figure 6.9). The lithologies in this outcrop were not similar to any other purported Maastrichtian sediments and its position suggested it may be part of the mélange. However, it was equally possible this was a section displaying progressive transgression of the ophiolite. The base of the succession, at the southeastern limit of the outcrop, begins with a thin bed of red-brown, graded conglomerate, with sub-angular to rounded clasts of chert and ophiolitic rocks. Three cycles of fining-upwards conglomerates constitute the next 5m, with foraminiferal rich clasts of chalk seen. There is then a 14m thickness of interbedded chalks and marls, though the true thickness is not ascertainable as it is highly disturbed by faulting. A 1m thick bed of calcareous sandstone overlies the marls and chalks, with ophiolitic and chert clasts up to 3mm in size, and this in turn is overlain a 5m thick massive bed of matrix-supported conglomerate. Clasts are up to 20cm in size, are sub-angular to rounded, and include chert, limestone and serpentinite. The matrix is mud-sand sized and the deposit is chaotic in nature with no sedimentary structures visible. Above this are two beds of calcarenite, conglomeratic at the base, containing clasts similar to those seen in the previous beds. A third bed of calcarenite lacks a basal conglomerate. The section is capped by about 9m of disturbed chalky marls. The section and the sampling points are illustrated figure 6.9.

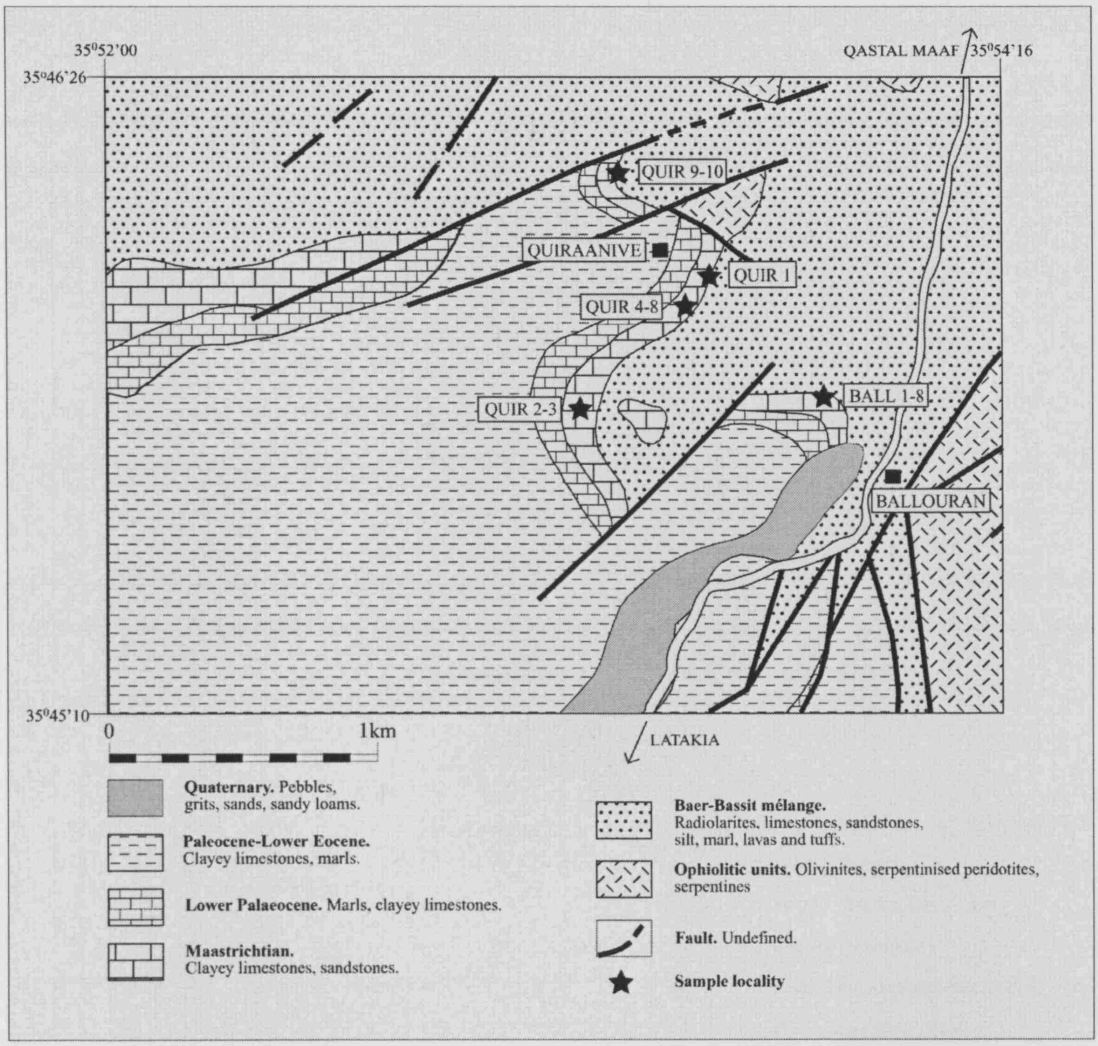

Figure 6.8. Geological sketch map of the sampling localities around the villages of Quiraanive and Ballourane (modified after Kazmin and Kulakov, 1968).

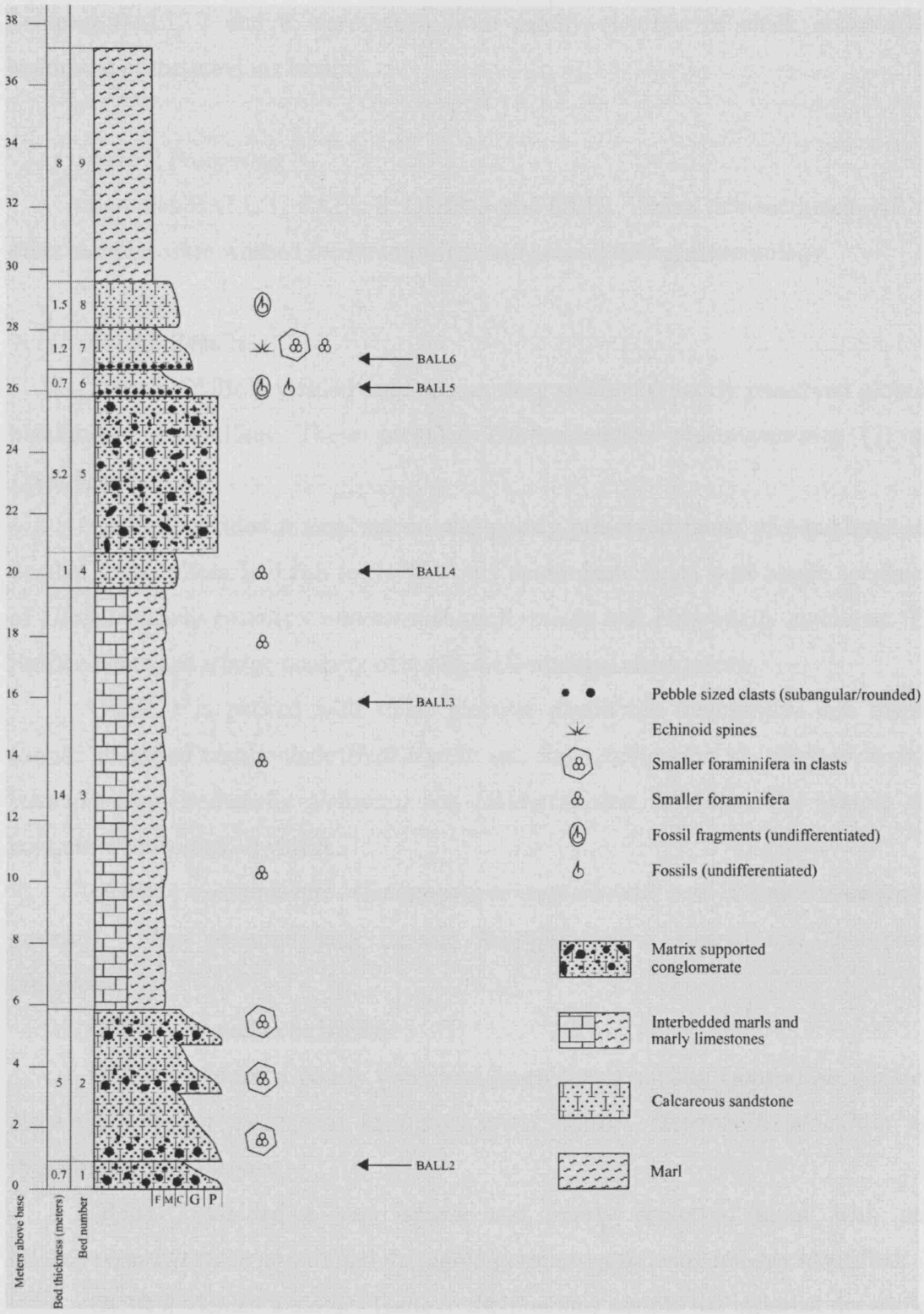

Figure 6.9. Lithological log of the sampled section near the village of Ballourane, sampling levels indicated.

Samples BALL 7 and 8 were taken from patchy outcrops of chalk about 100m southwest of the previous locality.

6.4.5.2 Processing

Samples BALL 1, BALL 8, QUIR 3 and QUIR 5 were thin-sectioned. All the other samples were washed for foraminifera and general micropalaeontology.

6.4.5.3 Results

Sample QUIR 1 yielded only sparse, very small and poorly preserved globular planktonic foraminifera. These included *Globanomalina planocompressa* (?) and *Eoglobigerina* sp.

QUIR 2 yielded a very sparse and poorly preserved fauna of planktonic and benthic foraminifera, and fish teeth. The only determinate fauna were single specimens of *Globotruncana rosetta*, *Contusotruncana fornicata* and *Heterohelix globulosa*. The residue contained a large quantity of small, well-rounded chert pieces.

QUIR 3 is packed with small globular planktonic foraminifera and biserial forms. Identified taxa include *Hedbergella* sp., *Rugoglobigerina* sp., *Globotruncanita stuartiformis*, *Heterohelix globulosa* and *Globotruncana bulloides*. The sample also contains a few ostracod valves.

QUIR 4 contains rare *Abathomphalus mayaroensis* and common *Gansserina gansseri*. Other common taxa include *Rugoglobigerina rugosa* and *Heterohelix globulosa*.

QUIR 5 proved to be barren.

QUIR 6 yielded a poorly preserved fauna that including *Gansserina gansseri*, *Racemiguembelina fructicosa*. *Rugoglobigerina rugosa*, *Heterohelix globulosa* and *Pseudotextularia elegans*.

QUIR 7 yielded a very sparse and poorly preserved fauna with only *Globotruncanita stuartiformis* and *Rugoglobigerina rugosa* being reliably identified.

QUIR 8 yielded a similar fauna to the previous sample but included the marker *Racemiguembelina fructicosa*.

BALL 1 was sectioned, revealing a micritic packstone rich in planktonic foraminifera, these included *Globotruncana arca*, *Contusotruncana fornicata*, *Globotruncana linneiana*, *Globotruncanita stuartiformis*, *Hedbergella* sp. and *Rugoglobigerina* sp.

BALL 2 only yielded the planktonic foraminifera *Contusotruncana fornicata* and *Heterohelix globulosa.* However, a number of Radiolaria were picked. These were mostly simple spumellarians, but also included *Mirfusis* sp.

BALL 3 yielded abundant *Rugoglobigerina rugosa, Contusotruncana fornicata, Globotruncanita stuartiformis* and *Globotruncana arca.* Other notable taxa included *Gansserina gansseri, Rugotruncana subcircumnodifer* and *Pseudotextularia elegans.*

Sample BALL 4 was barren of any microfossils, whilst BALL 5 was dominated by planoconvex benthic foraminifera as well as *Glomospira* and ostracods. Planktonic foraminifera included *Rugoglobigerina rugosa, Globotruncana ventricosa, Globotruncana arca* and *Contusotruncana fornicata.*

BALL 6 was thin-sectioned and contained rare benthic foraminifera and indeterminate small globular planktonic foraminifera as well as some sea urchin spines. *Rotalia* and *Siderolites* sp. were also noted.

BALL 7 and 8 both contained abundant *Contusotruncana fornicata, Rugoglobigerina rugosa* and *Globotruncana arca.*

6.4.5.4 Age

The presence of *Globanomalina planocompressa* (?) and *Eoglobigerina* sp. In QUIR 1 date the sample as early Paleocene in age. A more refined date is not possible.

QUIR 2 was dated as Campanian-Maastrichtian in age based on the few planktonic foraminifera retrieved. Again a more refined date is not possible.

QUIR 3 contained a typical Campanian - Maastrichtian assemblage, though no marker species were recovered.

The co-occurrence of rare *Abathomphalus mayaroensis* and common *Gansserina gansseri* in QUIR 4 assign it to the lower part of the late Maastrichtian *A. mayaroensis* Zone.

QUIR 5 could not be dated is it was barren.

QUIR is assigned to the Maastrichtian *C. contusa-R. fructicosa* Zone of Premoli-Silva and Sliter (1999) or the upper part of the *Gansserina gansseri* Zone of Robazsynski and Caron (1995), based on the marker species *Gansserina gansseri* and *Racemiguembelina fructicosa.*

No age determination is possible from the species recovered from QUIR 7, but the level of the sample suggests it is no younger than Campanian-Maastrichtian in age.

QUIR 8 is assigned to the Maastrichtian *C. contusa-R. fructicosa* Zone of Premoli-Silva and Sliter (1999) or the upper part of the *Gansserina gansseri* Zone of Robazsynski and Caron (1995) based on the presence of the marker *Racemiguembelina fructicosa.*

BALL 1 was dated as late Campanian – Maastrichtian age, based on the Globotruncanids identified.

BALL 2 can be dated no more closely than Campanian – Maastrichtian in age based on the planktonic foraminifera recovered. The radiolaria *Mirfusis* is a Jurassic genus, and it is concluded that the radiolaria are all reworked from chert clasts within the conglomerate.

BALL 3 is assigned to the *Gansserina gansseri* Zone based on the presence of the nominate taxon.

Sample BALL 4 was barren and could therefore not be dated, whilst BALL 5 can be dated no more precisely than Campanian-Maastrichtian in age, based on the presence of *Globotruncana ventricosa* and *Globotruncana arca.*

The presence of the foraminifera *Rotalia* sp. and *Siderolites* sp. dates BALL 6 as Campanian-Maastrichtian in age.

BALL 7 and 8 are dated as late Campanian in age, or early Maastrichtian at the youngest, as no Maastrichtian markers were present (*G. gansseri, C. contusa, A. mayaroensis*).

6.4.5.5 Palaeoenvironment

Samples QUIR 1, 3-9 are interpreted as pelagic/hemipelagic carbonates deposited on a deeply submerged shelf. QUIR 2 however, is interpreted as a hemipelagic sediment, with some terrigenous (small chert pebbles, probably derived from eroded melange sediments).The sparse planktonic foraminiferal fauna also suggests a significantly shallower environment. A shallow marine inner shelf environment is inferred.

BALL 1 was deposited in a deep marine, outer shelf or deeply submerged shelf environment. The other samples suggest more variable palaeoenvironments however. BALL 2 was deposited in a shallow marine, inner shelf high energy environment. Radiolaria were derived from eroded clasts of chert presumably derived from the ophiolitic melange, and the small numbers of planktonic foraminifera drifted in

from deeper waters. BALL 3 sees a return to hemipelagic sedimentation reflected in both the sedimentology and the large numbers of planktonic foraminifera.

Sample BALL 4-6 were all deposited in a shallow marine, inner shelf environment, with a lot of terrigenous input, and only small numbers of planktonic foraminifera. Unfortunately, as previously stated, the faulted nature of the outcrop makes the relationship between some of the beds difficult to determine, and it may well be that the carbonates from which sample BALL 3 was taken are actually out of sequence.

BALL 7 and 8 are both interpreted as being deposited in a deep outer shelf environment.

6.4.6 BEIT NASSER

6.4.6.1 Sampling

The most southerly sections sampled were between the Nahr el Kandil and Nahr el Kebir rivers. This area marks the leading southern edge of the ophiolitic nappes. The area around the village of Beit Nasser provided several good, though not extensive, exposures of chalks and marls in close proximity to the underlying Baer-Bassit mélange. The location of each of the samples is illustrated on figure 6.10. The first sample (BEIT 1) was taken from a small outcrop of westerly dipping, well bedded marls and chalky limestones, 100m to the northeast of the village of Beit Nasser, in the southwest bank of the main road. Planktonic foraminifera were visible in hand specimen. Just to the southeast of the village another roadside cutting exposes a 4m thickness of interbedded marls and chalky limestones in close proximity to the underlying Baer-Bassit mélange. Sample BEIT 2 was taken from a bed of medium hard marls, with planktonic foraminifera visible, at the base of this section. The boundary between the mélange and the overlying sediments was then traced northwards. Sample BEIT 3 was taken a further 100m northwards from an excellent exposure in the bank where the road doubles back on itself. Well-bedded chalks and marls are exposed in the bank but the sample (BEIT 3) was taken from a dry stream bed where the water had cut down into some blue marls that were no more than 10m above the mélange. A small track to the east of the road provided further exposures of marls no more than a few metres structurally above outcropping mélange (sample BEIT 4). The boundary was then followed north westwards with few exposures encountered. About 2km to the

northwest, sample NEW 2 was taken from a small E-W orientated outcrop of well-bedded chalky-limestones in a garden to the south of the road to As Saraskiyeh.

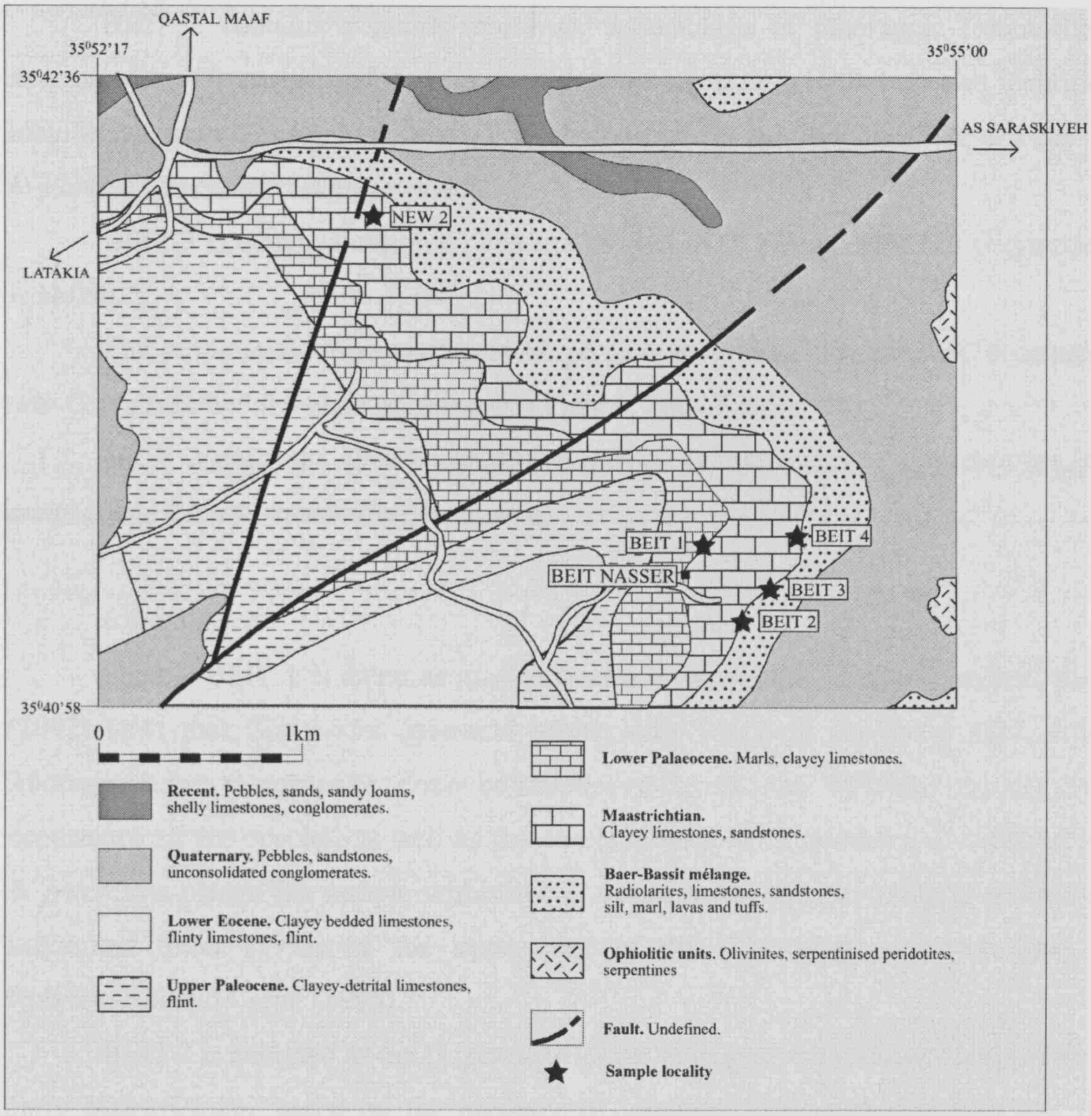

Figure 6.10. Geological sketch map of the sampling localities in the vicinity of Beit Nasser (modified after Adjemian and Khatoun, 1999).

6.4.6.2 Processing

All of the samples were washed for foraminifera and general microfossils.

6.4.6.3 Results

Sample BEIT 1 contained abundant, poorly to moderately preserved planktonic foraminifera. The assemblage was dominated by *Globotruncanita stuarti*, *Rugoglobigerina rugosa* and *Pseudotextularia elegans*. Important taxa present are

Gansserina gansseri, *Contusotruncana contusa* and *Racemiguembelina fructicosa*. *G. gansseri* is a common component of this assemblage.

BEIT 2 contains a poorly preserved assemblage of planktonic foraminifera dominated by *Heterohelix globulosa* and *Globotruncana arca*. Other species identified include common *Gansserina gansseri*, *Globotruncanella havanensis* (Plate 4, Figs. 11 & 12) and *Contusotruncana fornicata*.

BEIT 3 contains common *C. contusa* as well as *C. plicata* although *G. gansseri* is absent.

The moderately preserved assemblage recovered from sample BEIT 4 contains rare *C. contusa* but abundant *G. gansseri* (Plate 4, Figs. 7 & 8).

NEW 2 contains *Abathomphalus mayaroensis* and common *Contusotruncana contusa* and *Racemiguembelina fructicosa*.

6.4.6.4 Age

Sample BEIT 1 is dated as mid-early late Maastrichtian in age. Silva and Sliter (2002) state that *Gansserina gansseri* occurs only rarely in the lower half of the *Abathomphalus mayaroensis* Zone before becoming extinct, therefore the common occurrence of this species, as well as the co-occurrence of *G. gansseri*, *C. contusa* and *R. fructicosa* places this sample within the *C. contusa – R. fructicosa* Zone of Premoli Silva and Sliter (1999) or the upper part of the *Gansserina gansseri* Zone of Robazsynski and Caron (1995).

BEIT 2 is assigned to the *G. gansseri* Zone, giving an age of latest Campanian to early Maastrichtian, based on the presence of common *Gansserina gansseri* and the absence of *Contusotruncana contusa*.

BEIT 3 is assigned the upper part of the *C. contusa-R. fructicosa* of Zone of Premoli Silva and Sliter (1999) or the lower part of the *Abathomphalus mayaroensis* Zone of Robazsynski and Caron (1995), based on the presence of a number of specimens of *Contusotruncana contusa* and *C. plicata*, as well as the absence of *Gansserina gansseri*.

BEIT 4 is assigned to the *C. contusa – R. fructicosa* Zone of Premoli Silva and Sliter (1999) or the *Gansserina gansseri* Zone of Robazsynski and Caron (1995), suggesting a mid Maastrichtian age for the sample. This is based on the co-occurrence of *Contusotruncana contusa* and *Gansserina gansseri*, as well as the absence of *A. mayaroensis*.

NEW 2 is assigned to the *Abathomphalus mayaroensis* Zone based on the presence of the nominate taxon.

6.4.6.5 Palaeoenvironment

All of the samples are interpreted as having been deposited in a deep marine, outer shelf environment.

6.4.7 MARKHOUS AND MACHKITA

6.4.7.1 Sampling

The villages of Markhous and Machkita are located in the south of the area, just north of the Nahr el Kebir River (see figure 6.1). The maps of Kazmin and Kulakov (1968) and Adjemian and Khatoun (1999), differ quite considerably with regard to the location and the extent of Maastrichtian sediments in this area. Further, a large part of the area has been submerged by a reservoir since it was first mapped in 1968.

Sample MARK 1 was taken from a small outcrop exposed in a bank, and was a pale grey chalk with minor opaques and visible smaller foraminifera. Within the float at the base of the bank were numerous blocks of calcarenite packed with larger foraminifera similar to the lithologies seen at Al Ghas'saniyeh. It was not possible to find this lithology *in situ* but it is inferred that it occurs as bed rock beneath the field and a sample of a loose block was therefore collected (MARK 2). Another sample (MARK 3) was taken from a small outcrop of chalks about 20m to the west of the first location. These chalks contained dentritic burrows infilled with grey marl. Samples MARK 4 and 5 were taken from outcrops of chalk and marl respectively, that lie within the melange according to the Syrian map, but within the Maastrichtian cover sediments according to the Russian map. The latter appeared more likely in the field. Sample MARK 6 was taken from an outcrop of chalks about 150m further southwest.

The next sample taken (MARK 7) was from an outcrop of chalks with chert bands exposed in the northern bank of a road T-junction. Both maps indicated this outcrop should have been Paleocene in age and the sample was taken to confirm this, from just beneath the lowest chert band. The final sample (MARK 8) was taken from a patchy outcrop of chalks and marls about 500m due south of Markhous.

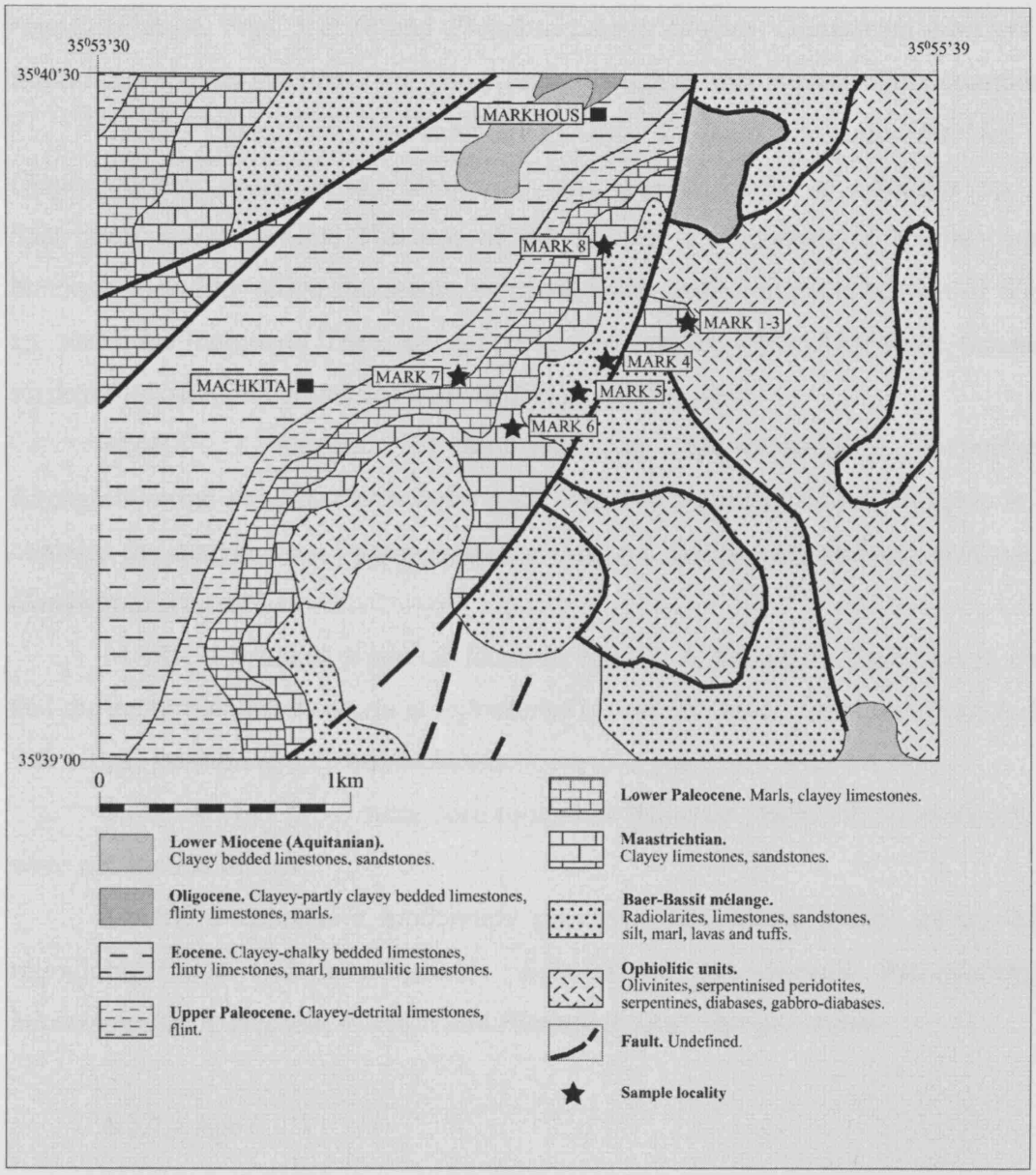

Figure 6.11. Geological sketch map of the sampling localities around the villages of Markhous and Machkita (modified after Adjemian and Khatoun, 1999)

6.4.7.2 Processing

Samples MARK 1 and MARK 3-8 were all washed for foraminfera whilst MARK 2 was thin-sectioned due to the large number of larger foraminifera visible in hand specimen. These constitute up to 80% of the volume of the sample.

6.4.7.3 Results

MARK 1 contains a moderately well preserved assemblage dominated by *Globotruncana aegyptica*, *G. arca*, *Globotruncanita stuartiformis*, *Rugoglobigerina*

rugosa (Plate 4, Figs. 5 & 6) and *Pseudotextularia elegans*. *Gansserina gansseri* and *Racemiguembelina fructicosa* are also present, though neither is particularly common.

Species identified in sample MARK 2 included *Lepiorbitoides* sp., *Omphalocyclus macroporus*, *Orbitoides* sp., *Pseudedomia* sp. *Rotalia* sp. and *Siderolites calcitropoides*. The rest of the sample is composed of sparite cement; bioclasts including rudist fragments, echinoid spines and a single specimen of *Sigalia* sp., and lithic fragments. These are generally well rounded and include chert, limestone, serpentinite, siltstone, immature fine sandstone and opaques.

MARK 3 sample is dominated by *Globotruncanita stuartiformis*, *Rugoglobigerina rugosa*, *Heterohelix globulosa* and *Pseudotextularia elegans*. It also contains the marker taxa *Contusotruncana contusa*, *Racemiguembelina fructicosa* and *Gansserina gansseri*.

MARK 4 contains a similar fauna to MARK 3, though *R. fructicosa* is absent and the genus *Contusotruncana* is represented by the species *C. fornicata* (Plate 4, Figs. 9 & 10), *C. contusa* and *C. walfischensis*.

Samples MARK 5-7 were seen to contain Miocene planktonic foraminifera and were not studied further.

MARK 8 contains a moderately preserved assemblage totally dominated by rugoglobigerinids and heterohelicids. Species of note include *Rugoglobigerina hexacamerata*, *R. reicheli*, *R. scotti* and *Planoglobulina acervulinoides*.

6.4.7.4 Age

MARK 1 is dated as no older than the upper part of the *G. gansseri* Zone of Robazsynski and Caron (1995), or the *C. contusa-R. fructicosa* Zone of Premoli-Silva and Sliter (1999) based on the co-occurrence of the nominate taxa. This sample is therefore mid Maastrichtian in age.

The larger benthic foraminiferal assemblage identified in sample MARK 2 indicate a Maastrichtian age.

MARK 3 is dated as belonging to the *C. contusa-R. fructicosa* Zone of Premoli-Silva and Sliter (1999) or the upper part of the *G. gansseri* Zone of Robazsynski and Caron (1995). This is because it contains all three of the nominate taxa.

Racemiguembelina fructicosa is absent from MARK 4 but overall the assemblage is very similar and is also dated as belonging to the *C. contusa-R. fructicosa* Zone of Premoli-Silva and Sliter (1999).

No marker species were recovered from MARK 8 but the overall assemblage, including a number of different species of *Rugoglobigerina*, suggests this sample is no older than late Campanian in age.

6.4.7.5 Palaeoenvironment

MARK 1, MARK 3-4 and MARK 8 are all interpreted as having been deposited in a deep open marine, outer shelf environment. MARK 2 was deposited in an open marine, shallow inner shelf environment, as evidenced by the larger benthic foramininfera.

6.4.8 QAFAR FAWKANI

6.4.8.1 Sampling

As well as the Palaeocene samples collected that were identified on the maps as Maastrichtian, a section starting from near the village of Qafar Fawkani and tracking north to the top of Jebel Rhouz hills was also sampled. This was to ascertain the thickness of Palaeogene sediments in the study area and which foraminiferal zones were present. A 400m thick section was studied with sampling points at every 10m (samples DPH1-40), the fauna recovered from these samples are illustrated on figures 6.12 and 6.13, plotted against a standard Paleocene foraminiferal zonal scheme (after Berrgren *et al.* 1995). The lithologies were rather monotonous marls and chalky limestones, with only minor variations in colour. For the lithology of the samples the reader is referred to the appendix. The top of the section was taken at the appearance of the first chert band, which Krasheninnikov (1994) describes as corresponding to the Paleocene/Eocene boundary.

6.4.8.2 Processing

All 40 samples were washed, primarily for their planktonic foraminiferal content.

6.4.8.3 Results

The contents of the individual samples are illustrated in the two Biostratigraphic logs; Figures 6.12 and 6.13. The more important taxa are discussed in section 6.4.8.4.

6.4.8.4 Age

The base of the 400m section sampled from near Qafar Fawkani began with assemblages typical of the early Paleocene *Globanomalina compressa/Praemurica inconstans-Praemurica uncinata* Interval Subzone (P1c) (Figure 6.14). This subzone is defined as the biostratigraphic interval between the FAD of *G. compressa* and/or *P. inconstans* and the FAD of *P. uncinata* (Berggren *et al.* 1995). Common constituents of this subzone include *Praemurica taurica*, *P. pseudoinconstans*, *P. inconstans*, *Globanomalina planocompressa*, *G. compressa*, *Parasubbotina varianta* and *P. pseudobulloides*. This subzone was only 20m thick in the measured sectioned, but many of the samples described from the Damate/Qafar Fawkani area that were previously mapped as Maastrichtian in age are actually assignable to this subzone. It seems safe to assume therefore, considering the distance between the base of this section and some of the aforementioned samples, that the sediments of this subzone attain an actual thickness in excess of 100m.

Moving up section a 50m thickness of thinly bedded marls and limestones can be assigned to the *Praemurica uncinata-Morozovella angulata* Interval Zone (P2), of the Danian. This is defined as the biostratigraphic interval between the FAD of *P. uncinata* and *M. angulata* (Berrgren *et al.*1995). Typical fauna of this section include *P. uncinata*, *P. pseudoinconstans*, *P. inconstans*, *M. praeangulata*, *Parasubbotina pseudobulloides*, *Subbotina triloculinoides* and *Chiloguembelina subtriangularis*. Sediments of this zone attain a thickness of about 40m.

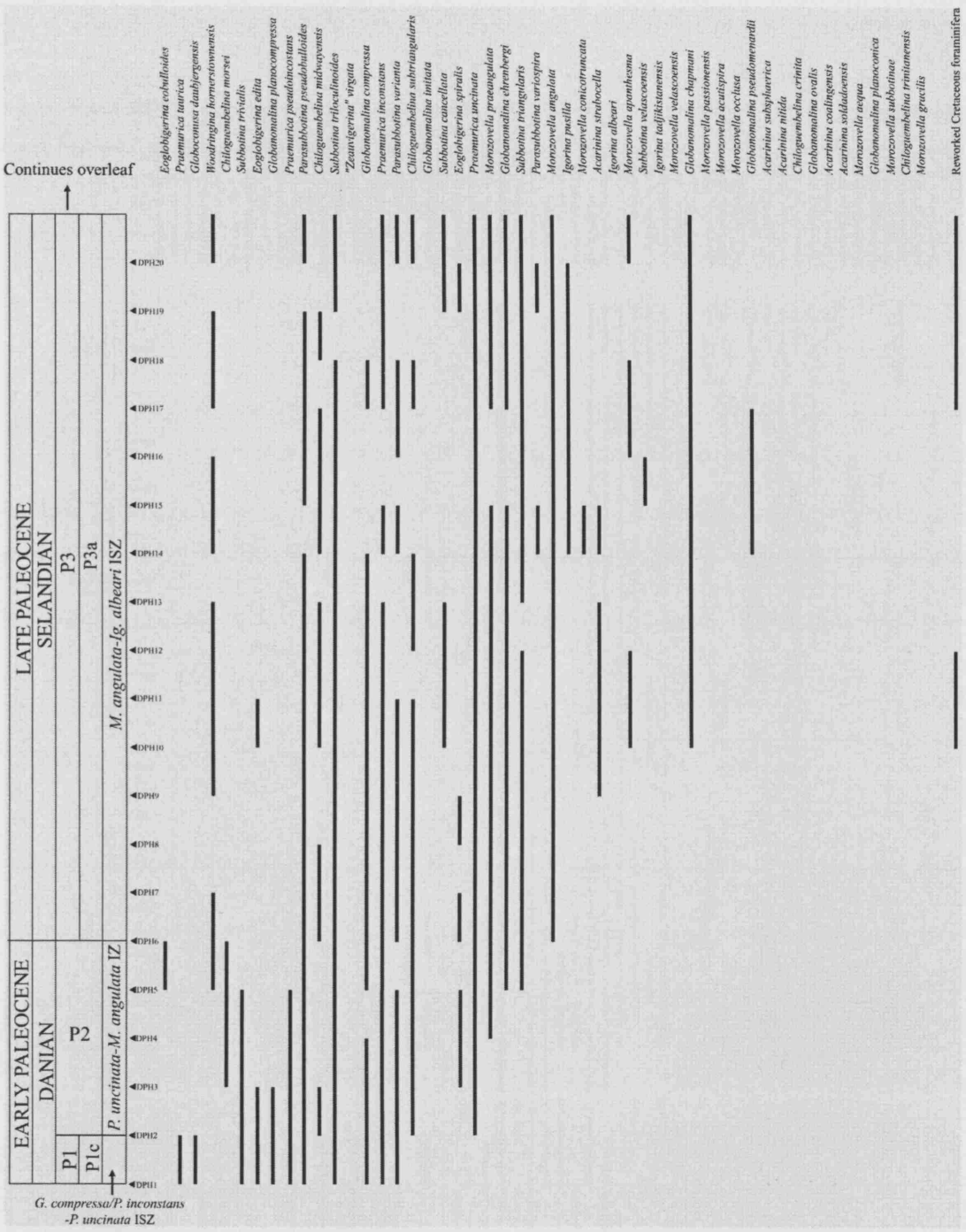

Figure 6.12 Biostratigraphic log of the lower 200m of the Qafar Fawkani section with sampling levels and foraminiferal occurrences plotted against the standard Paleocene planktonic foraminiferal zonal scheme of Berggren *et al.* 1995. Species listed are Paleocene planktonic foraminifera in order of first appearance (after Berggren and Norris, 1999). Lithologies are monotonous marls and limestones and the reader is referred to the Appendix for the lithology of individual samples.

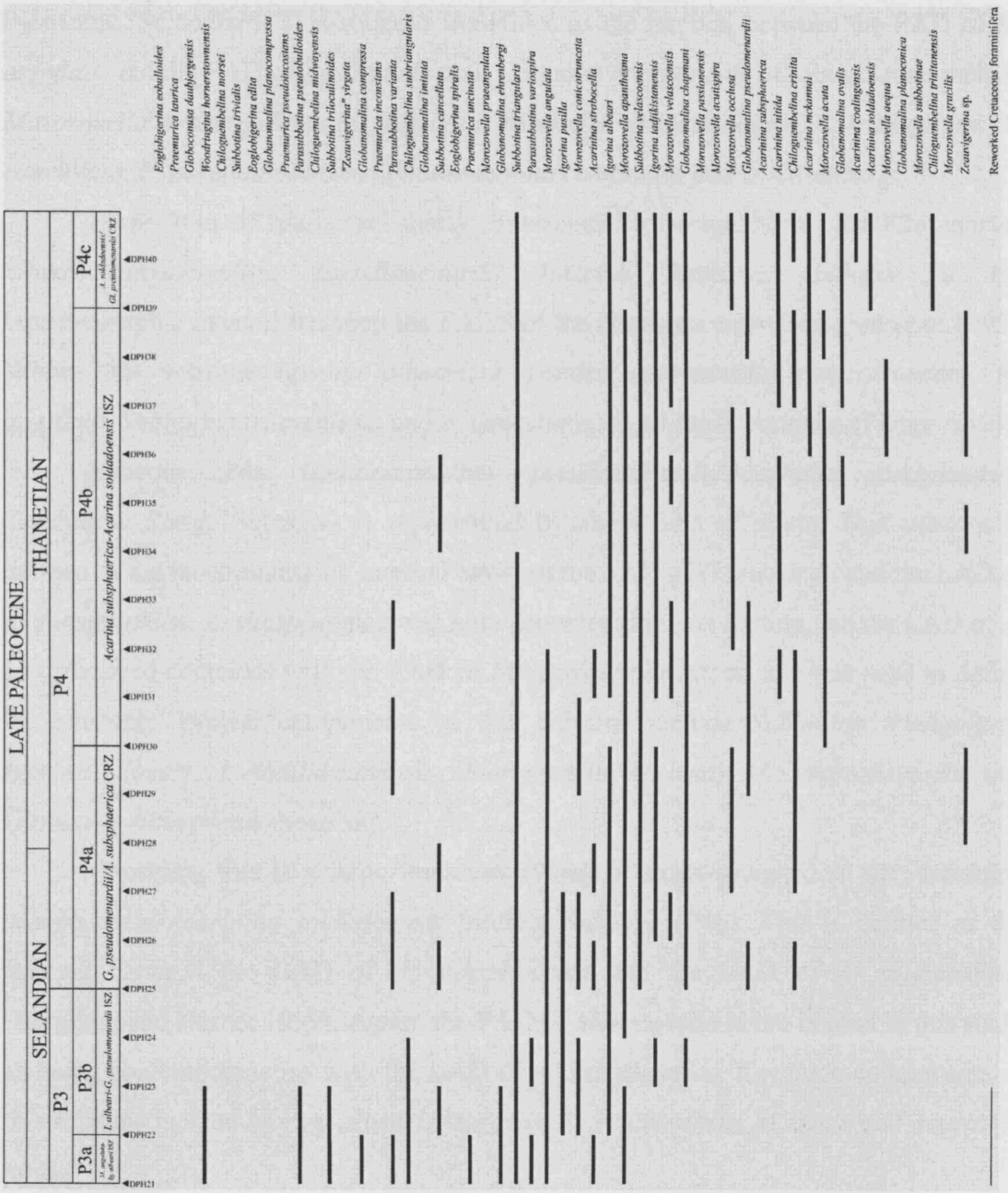

Figure 6.13 Biostratigraphic log of the upper 200m of the Qafar Fawkani section with sampling levels and foraminiferal occurrences plotted against the standard Paleocene planktonic foraminiferal zonal scheme of Berggren *et al.* 1995. Species listed are Paleocene planktonic foraminifera in order of first appearance (after Olsson *et al.* 1999). Lithologies are monotonous marls and limestones and the reader is referred to the Appendix for the lithology of individual samples.

Overlying this zone is a large thickness of sediments (about 170m) that belong to the *Morozovella angulata-Igorina albeari* Interval Subzone (P3a) of the late Paleocene (Selandian). This subzone is defined as the interval between the FAD of *M. angulata* and the FAD of *Igorina albeari*. Common components of this subzone include *Morozovella praeangulata, M. angulata, Subbotina triloculinoides, S. triangularis, S. cancellata, P. pseudobulloides, Globanomalina compressa* and *G. ehrenbergi.*

Some 30m of marls and marly limestones are assignable to the P3b *Igorina albeari-Globanomalina pseudomenardii* Interval Subzone, defined as the biostratigraphic interval between the FADS of the nominate taxa (Berggren *et al.*1995). Within this subzone *Igorina albeari, I. pusilla, Morozovella conicotruncata, M. angulata, Subbotina triangularis* and *S. cancellata* are all fairly common (Figure 6.15).

Subzone P4a (*Globanomalina pseudomenardii/Acarinina subsphaerica* Concurrent Range Subzone) is represented by about 50m of strata. This subzone is defined as the biostratigraphic interval between the FAD of *G. menardii* and the LAD of *A. subsphaerica. A. subsphaerica* was not encountered in this section, but the LAD of *A. subsphaerica* coincides with the FAD of *Morozovella acuta*, so this was used to define the subzone. Typical components of this subzone include *Subbotina triangularis, Igorina albeari, I. tadjikistanensis, Morozovella occlusa, M. conicotruncata* and *Globanomalina pseudomenardii.*

Overlying this is a large thickness (90m) of strata assigned to the *Acarinina subsphaerica-Acarinina soldadoensis* Interval Subzone (P4b). This is defined as the interval between the LAD of *A. subsphaerica* and the FAD of *A. soldadoensis* (Berggren and Norris, 1999). Again, the FAD of *Morozovella acuta* is used in this study as being contemporaneous with the LAD of *A. subsphaerica.* Common components of this subzone include *Igorina albeari, Morozovella velascoensis, M. acuta* and *Acarinina nitida.*

The final subzone represented is the *Acarinina soldadoensis/Globanomalina pseudomenardii* Concurrent Range Subzone (P4c), defined as the interval between the FAD of *A. soldadoensis* and the LAD of *G. pseudomenardii* (Berggren *et al.* 1995). *G. pseudomenardii* occurs in all the samples from the base of this subzone until the top of the sampled section (about 20m), thus the top of this subzone is not recognised. Common components include the nominate taxa, representatives of *Morozovella* decrease in abundance whilst those of *Acarinina* increase.

During this work no further detailed study was made on the late Paleocene and younger deposits of the supraophiolitic cover. Several spot samples were taken at different localities to check the accuracy of the Russian and Syrian maps and the results of these are listed in the Appendix.

Krasheninnikov reports that the total thickness of the *Morozovella velascoensis* Zone (equivalent to P4c) is about 125m. It is overlain by about 400m of Eocene deposits, predominantly interbedded limestones and marls, but also bedded cherts, which range from the *Morozovella subbotinae* Zone to the *Acarinina bulbrooki* Zone (Lower-Middle Eocene). South of the Nahr el Kandil valley, deposits of the *Morozovella lehneri* Zone–*Orbiculinoides beckmanni* Zone (Middle – Upper Middle Eocene) can be seen cropping out (Krasheninnikov, 1984). Upper Eocene and Oligocene deposits are not known from within the field area (Krasheninnikov, 1994) though Adjemian and Khatoun (1999) report Oligocene deposits in the area of Markhous, as well as further east in the Ghab depression. Spot samples were taken at the latter locality but proved barren.

6.4.8.5 Palaeoenvironment

The interbedded marls, marly limestones and chalks sampled from this section were all deposited in an open marine environment, on a deeply submerged shelf. The sediments are all pelagic or hemipelagic carbonated dominated by planktonic foraminifera.

6.5 CONCLUSIONS

Figure 6.14 below summarises the age assignment of samples from the sedimentary cover sequence that proved to be Cretaceous in age, and Figure 6.15 again illustrates the Cretaceous foraminiferal zones utilised.

Exact faunal contents for each of the samples studied are listed in the appendix

Sample No.	Foraminiferal zone/zones		Age Assignment
	Premoli Silva and Sliter (1999)	Robazsynski and Caron (1995)	
11143			(late Campanian?) - Maastrichtian
AGS 1			(late Campanian?) - Maastrichtian
AGS 2			(late Campanian?) - Maastrichtian
AGS 3			(late Campanian?) - Maastrichtian
AGS 4	*G. aegyptica - G. gansseri*	*G. aegyptica - G. gansseri*	late Campanian - early Maastrichtian
AGS 5			(late Campanian?) - Maastrichtian
GHAS 1	*G. aegyptica - G. gansseri*	*G. aegyptica - G. gansseri*	late Campanian - early Maastrichtian
UMM 1	*Gansserina gansseri*	*Gansserina gansseri*	late Campanian - early Maastrichtian
DAMA B	*Abathomphalus mayaroensis*	*Abathomphalus mayaroensis*	late Maastrichtian
ZUGH 1	*C. contusa - R. fructicosa*	*Gansserina gansseri*	mid Maastrichtian
ZUGH 2	*G. havanensis - G. gansseri*	*G. havanensis - G. gansseri*	late Campanian - early Maastrichtian
ZUGH 3	*G. aegyptica - G. gansseri*	*G. aegyptica - G. gansseri*	late Campanian - early Maastrichtian
ZUGH 4	*Gansserina gansseri*	*Gansserina gansseri*	late Campanian - early Maastrichtian
KANT 1	*G. aegyptica - G. gansseri*	*G. aegyptica - G. gansseri*	late Campanian - early Maastrichtian
QUIR 2			Campanian -Maastrichtain
QUIR 3			Campanian -Maastrichtain
QUIR 4	*Abathomphalus mayaroensis*	*Abathomphalus mayaroensis*	late Maastrichtian
QUIR 6	*C. contusa-R.fructiucosa*	*Gansserina gansseri*	mid Maastrichtian
QUIR 7			Campanian -Maastrichtain
QUIR 8	*C. contusa-R.fructiucosa*	*Gansserina gansseri*	mid Maastrichtian
BALL 1	*G. elevata -*	*G. elevata -*	late Campanian - early Maastrichtian
BALL 2			Campanian -Maastrichtain
BALL 3	*Gansserina gansseri*	*Gansserina gansseri*	late Campanian - early Maastrichtian
BALL 5			Campanian -Maastrichtain
BALL 6			Campanian -Maastrichtain
BALL 7			Campanian -Maastrichtain
BALL 8			Campanian -Maastrichtain
BEIT 1	*C.contusa - R.fructicosa*	*G. gansseri*	mid Maastrichtian
BEIT 2	*G. gansseri*	*G. gansseri*	late Campanian - early Maastrichtian
BEIT 3	*C.contusa - R.fructicosa*	*Abathomphalus mayaroensis*	mid Maastrichtian
BEIT 4	*C.contusa - R.fructicosa*	*G. gansseri*	mid Maastrichtian
NEW 2	*Abathomphalus mayaroensis*	*Abathomphalus mayaroensis*	late Maastrichtian
MARK 1	*C.contusa - R.fructicosa*	*G. gansseri*	mid Maastrichtian
MARK 2			Maastrichtian
MARK 3	*C.contusa - R.fructicosa*	*G. gansseri*	mid Maastrichtian
MARK 4	*C.contusa - R.fructicosa*	*G. gansseri*	mid Maastrichtian
MARK 8	*G. gansseri - A. mayaroensis*	*G. gansseri - A. mayaroensis*	late Campanian - Maastrichtian

Figure 6.14 Summary of samples collected with their age assignments.

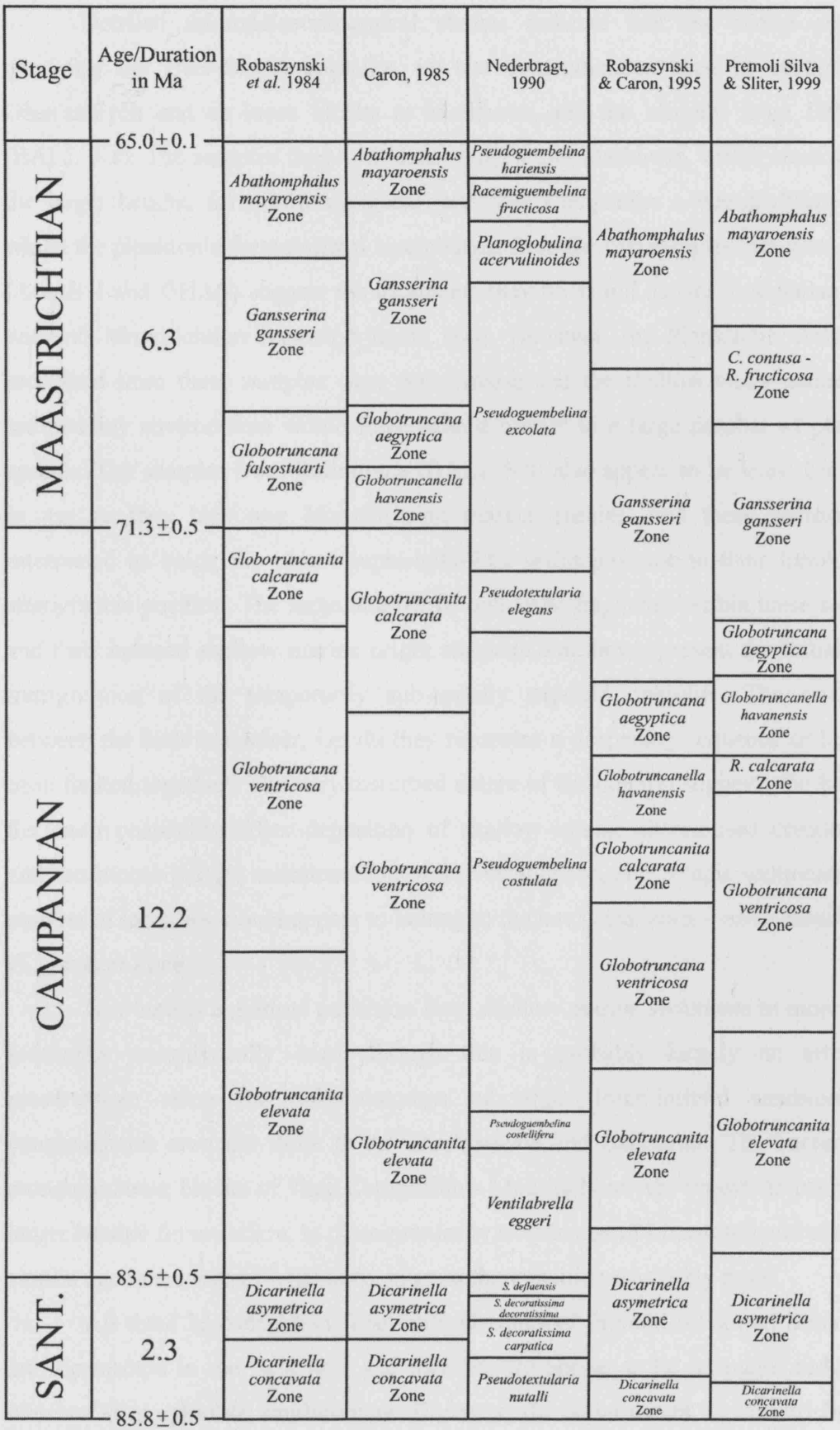

Figure 6.15. Comparison of various foraminiferal zonal schemes for the Late Cretaceous.

Detailed micropalaeontological studies indicate that the oldest sediments overlying the Baer-Bassit ophiolite are the conglomerates seen in section at Al Ghas'saniyeh and as loose blocks at Markhous, and the samples from Ballourane (BALL 5-8). The samples from Al Ghas'saniyeh and Markhous, which were dated by the larger benthic foraminifera present, are ?late Campanian - Maastrichtian in age, whilst the planktonic foraminiferal assemblages from the two samples that were washed (AGAS 4 and GHAS) suggest the sediments may be as old as late Campanian in age, with no Maastrichtian restricted fauna seen. However, the Planktonic assemblages recovered from these samples were quite sparse and the shallow water nature of the sedimentary environment would have been a barrier to a large number of planktonic species. The samples from Ballourane (BALL 5-8) also appear to be latest Campanian in age as they lack any Maastrichtian marker species, and these sediments are interpreted as being the oldest supra-ophiolitic sediments due to their lithology and stratigraphic position. The large number of ophiolitic fragments within these sediments and their inferred shallow marine origin suggests that they represent the initial marine transgression of the temporarily sub-aerially exposed ophiolite. The relationship between the beds is unclear, i.e. do they represent a deepening sequence or have they been faulted together? The very disturbed nature of the outcrop suggests the latter is at the least a possibility. After deposition of shallow marine channelised conglomerates and sandstones pelagic sedimentation was re-established, and pelagic sediments from a number of localities would appear to belong to the late Cretaceous – early Maastrichtian *G. gansseri* Zone.

Nowhere is a gradual transition from shallow marine sediments to more pelagic sediments unequivocally seen, though this is probably largely an artefact of preservation, since the only outcrops of larger foraminiferal sandstones and conglomerates seen are those at Al Ghas'saniyeh and Ballourane The occurrence of numerous loose blocks of ?late Campanian - Maastrichtian age limestone packed with larger benthic foraminifera, in close proximity to outcrops of limestones and chalks of a similar age in the area of Markhous, suggest the transition was fairly rapid.

All three Maastrichtian foraminiferal zones of Premoli-Silva and Sliter (1999) are represented in the field area and there would appear to be no major sedimentary hiatuses after ophiolite emplacement. However, the aerial extent of Maastrichtian age sediments overlying the ophiolite is considerably less than suggested by Kazmin and Kulakov (1968) and Adjemian and Khatoun (1999). A total of 27 samples taken from

localities previously mapped as Maastrichtian in age proved to be Palaeocene, and three discreet, substantial outcrops, from Zerhine, Damate and Quiraanive are all herein reassigned to the Palaeocene.

Although no lithological boundary or unconformity is evident between the Maastrichtian and Paleocene, there is a marked hiatus, with zones Pα, P0 and P1a not seen anywhere within the field area. It seems likely that the topmost Maastrichtian is also absent. Within lower Paleocene sediments reworking of Maastrichtian sediments is common, and in some samples reworked Maastrichtian faunas dominate the assemblage. It seems likely that the lithological similarities between the upper Maastrichtian and lower Paleocene sediments are the cause of the erroneous mapping, and that more extensive Maastrichtian sediments were reworked during the early Palaeocene. The 400m section sampled near Qafar Fawkani suggests fairly quiescent conditions during the Paleocene, with fairly high pelagic sedimentation rates and no significant hiatuses evident. Substantial reworking of Maastrichtian fauna within lower Paleocene sediments is indicative of possible changes in oceanic circulation including stronger bottom currents, but this appears to cease by the late Paleocene. The entire Baer-Bassit area has been strongly affected by neotectonic faulting associated with the final suturing of the Eurasian and Arabian plates. It is possible therefore that in the measured section duplication of sequence may have occurred, and equally possible that thicknesses of certain zones have been faulted out. It is difficult therefore to confidently estimate the true thickness of the Paleocene succession and of the individual foraminiferal zones/subzones. Benthic foraminifera were extremely rare in all Paleocene samples (frequently <<2% of the total assemblage).

The transition to the Lower Eocene sees a continuation of pelagic sedimentation, represented by alternating marls and limestones lithologically similar to the deposits of the upper Paleocene, although there is a gradual increase in the number of chert bands. Krasheninnikov (1984) reports a typical fauna of the *Morozovella aragonensis* and *Acarinina pentacamerata* Zones, including the nominate taxa as well as *Morozovella lensiformis*, *Acarinina soldadoensis* and *Subbotina pseudoeoceana*. Middle Eocene deposits are initially interbedded limestones and clayey marls but nummulitic limestones become prevalent higher in the sequence. These were seen on the coast west of Damate (See figure 6.1), where slumping was observed in the cliffside exposure. Slumping and faulting within lower-middle Eocene sediments are the result of syn-

depositional deformation due to the final collision of the Eurasian and Arabian plates, as are the absence of Upper Eocene, and apparently Oligocene deposits (Al-Riyami 2000).

Monotonous marls and chalky limestones dominate until the Eocene, when chert bands, and eventually nummulitic limestones break the monotony.

Neogene sediments were not studied during this work, although as with the Eocene sediments a number of spot samples were taken, mostly from the Latakia depression, and these are listed in the Appendix. Within the Baer-Bassit area Neogene deposits are sparse, with only one large exposure near Borj Islam, southwest of Damate near the Mediterranean coast. Deposits of this age are mostly developed within the Latakia depression and the Nahr El Kebir valley, to the south and southeast of the study area, where they attain thicknesses of several hundred metres. Again, marls and limestones dominate, but beds of sandstone are also present and local basal conglomerates where Miocene sediments unconformably overlie Paleogene sediments.

Pliocene and Quaternary sediments are mostly shallow marine siltstones and non-marine sandstones and conglomerates respectively, reflecting the onset of uplift and erosion in the area (Al-Riyami 2000).

PLATE 4

Foraminifera from the neo-autochthonous sedimentary cover sequence. Lengths given refer to maximum width.

1, 2. *Globotruncana aegyptica* Nakkady 1950. Sample AGAS4. 1) ventral, x170, 435μm. 2) dorsal, x170, 435μm.

3, 4. *Globotruncana arca* (Cushman) 1926. Sample AGAS4. 3) ventral, x62.5, 648μm. 4) dorsal, x62.5, 648μm.

5, 6. *Rugoglobigerina rugosa* (Plummer) 1927. Sample MARK1. 5) ventral, x97.5, 325μm. 6) dorsal, x97.5, 325μm.

7, 8. *Gansserina gansseri* (Bolli) 1951. Sample BEIT4. 7) ventral, x82.5, 512μm. 8) dorsal, x82.5, 512μm.

9,10. *Contusotruncana fornicata* (Plummer) 1931. Sample MARK4. 9) ventral, x75, 466μm. 10) dorsal, x 75, 466μm.

11, 12. *Globotruncanella havanensis* (Voorwijk) 1937. Sample MARK2. 11) ventral, x135, 307μm. 12) dorsal, x135, 307μm. Note broken final chamber.

13, 14. *Abathomphalus mayaroensis* (Bolli) 1951. Sample MARK1. 13) ventral, x65, 589μm. 14) dorsal, x65, 589μm.

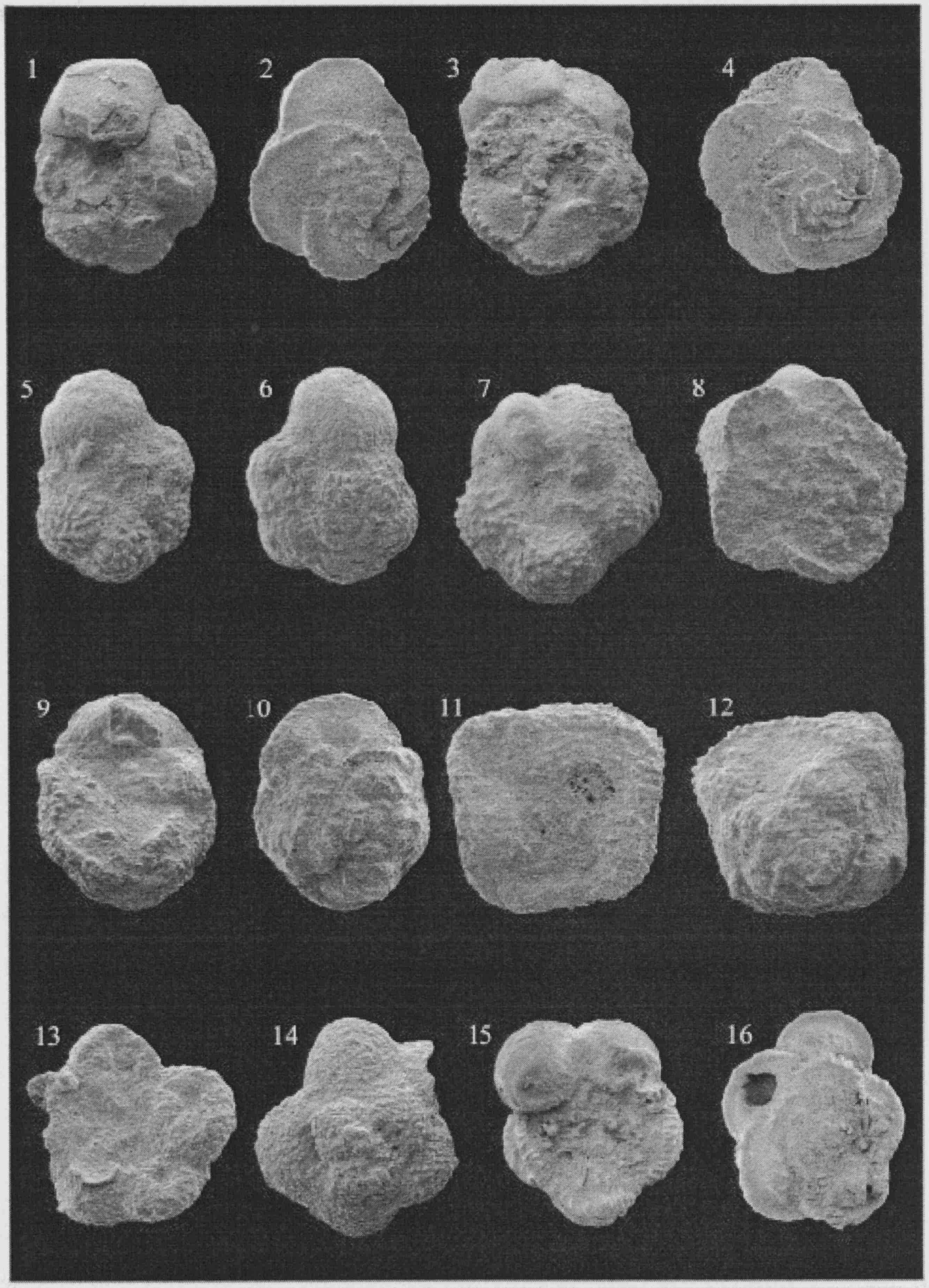

PLATE 4

PLATE 5

Paleocene planktonic foraminifera from Qafar Fawkani section. Lengths given are maximum width of specimen.

1, 2. *Globanomalina ehrenbergi* (Bolli) 1957. Sample DPH18, Subzone P3a. 1) ventral, x210, 158μm. 2) dorsal, x210, 158μm.

3, 4. *Globanomalina planocompressa* (Shutskaya) 1965. Sample DPH2, Subzone P1c. 3) ventral, x150, 226μm. 4) dorsal, x150, 226μm.

5, 6. *Globanomalina pseudomenardii* (Bolli) 1957. Sample DPH36, Subzone P4b. 5) ventral, x95, 317μm. 6) dorsal, x95, 317μm. Note rapidly enlarging chambers, and compressed test with "pinched" angular keel.

7,8. *Subbotina triloculinoides* (Plummer) 1926. Sample DPH3, Zone P2. 7) ventral, x130, 261μm. 8) ventral, x130, 261μm.

9, 10. *Praemurica inconstans* (Subbotina) 1953. Sample DPH5, Zone P2. 9) ventral, x105, 175μm. 10) dorsal, x105, 175μm.

11, 12. *Parasubbotina pseudobulloides* (Plummer) 1926. Sample DPH9, Subzone P3a. 11) ventral, x110, 272μm. 12) dorsal, x110, 272μm.

13. *Praemurica uncinata* (Bolli) 1957. Sample DPH20, Subzone P3a. Ventral, x105, 347μm.

14. *Subbotina cancellata* Blow 1979. Sample DPH35, SubzoneP4b. Ventral, x160, 208μm.

15, 16. *Morozovella praeangulata* (Blow) 1979. Sample DPH16, Subzone P3a. 15) ventral, x195, 170μm.

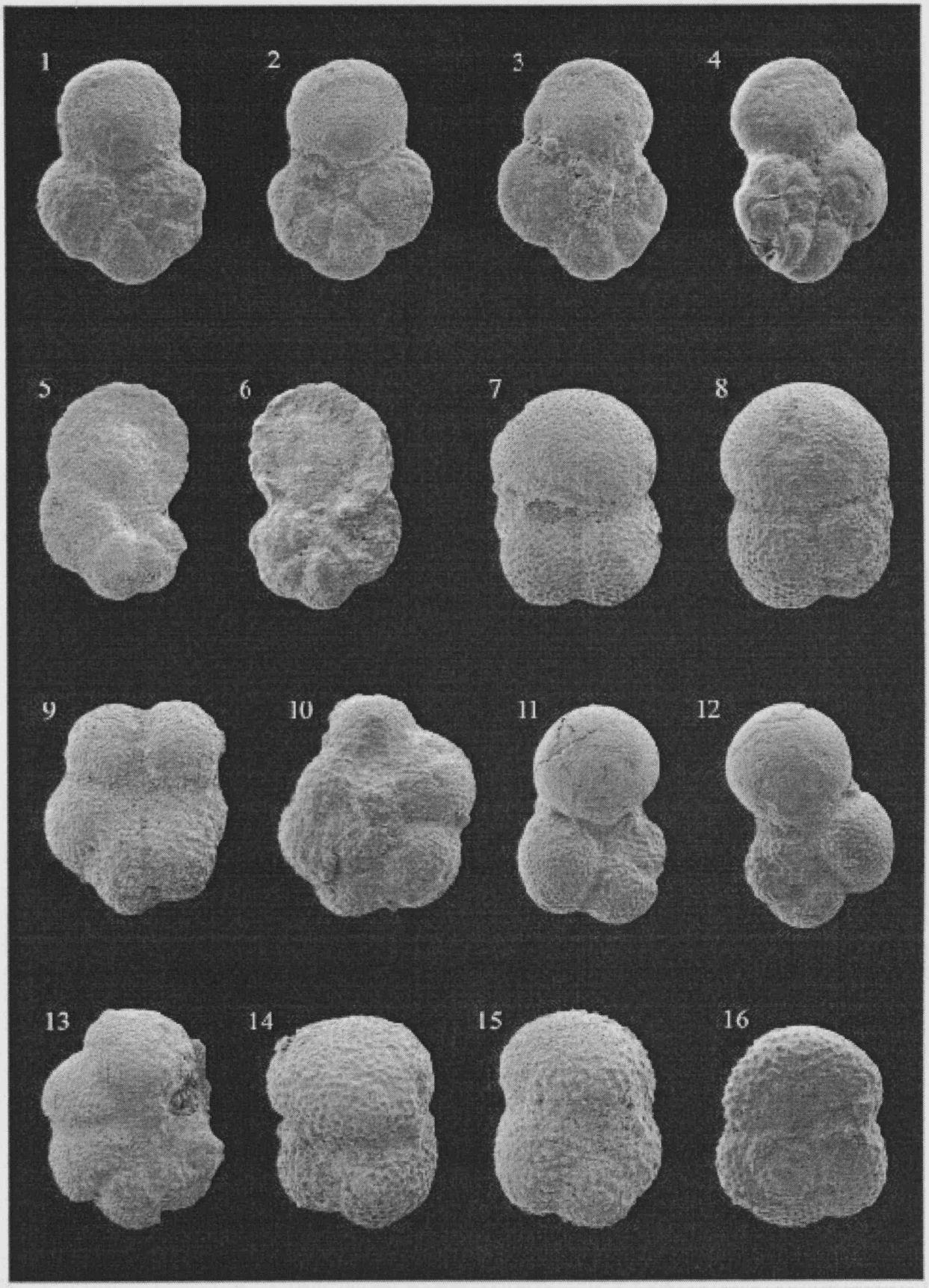

PLATE 5

PLATE 6

Paleocene planktonic foraminifera from Qafar Fawkani section. Lengths given are maximum width of specimen.

1, 2. *Igorina albeari* (Cushman and Bermudez) 1949. Sample DPH28, Subzone P4a. 1) ventral, x 205, 180μm. 2) dorsal, x205, 180μm.

3, 4. *Igorina tadjikistanensis* (Bykova) 1953. Sample DPH31, Subzone P4b. 3) ventral, x170, 187μm. 4) dorsal, x170, 187μm.

5, 6. *Morozovella velascoensis* (Cushman) 1925. Sample DPH36, Subzone P4b. 5) ventral, x57.5, 653μm. 6) dorsal, x57.5, 653μm. Note well developed umbilical shoulders and strongly lobate outline.

7, 8. *Morozovella acuta* (Toulmin) 1941. Sample DPH40, Subzone P4c. 7) ventral, x100, 330μm. 8) dorsal, x100, 330μm. Note concavity of final chamber.

9, 10. *Morozovella occlusa* (Loeblich and Tappan) 1957. Sample DPH40, Subzone P4c. 9) ventral, x95, 402μm. 10) dorsal, x95, 402μm.

11. *Morozovella conicotruncata* (Subbotina) 1953. Sample DPH23, SubzoneP3b. Ventral, x100, 356μm.

12. *Acarinina nitida* (Martin) 1943. Sample DPH40, Subzone P4c. Ventral, x120, 316μm.

13, 14. *Acarinina nitida* (Martin) 1943. Sample DPH40, Subzone P4c. 13) ventral x125, 303μm. 14) dorsal, x125, 303μm.

15, 16. *Acarinina mckannai* (White) 1928. Sample DPH40, Subzone P4c. 15) ventral x115, 203μm, 16) dorsal (specimen inverted), x 115, 203μm.

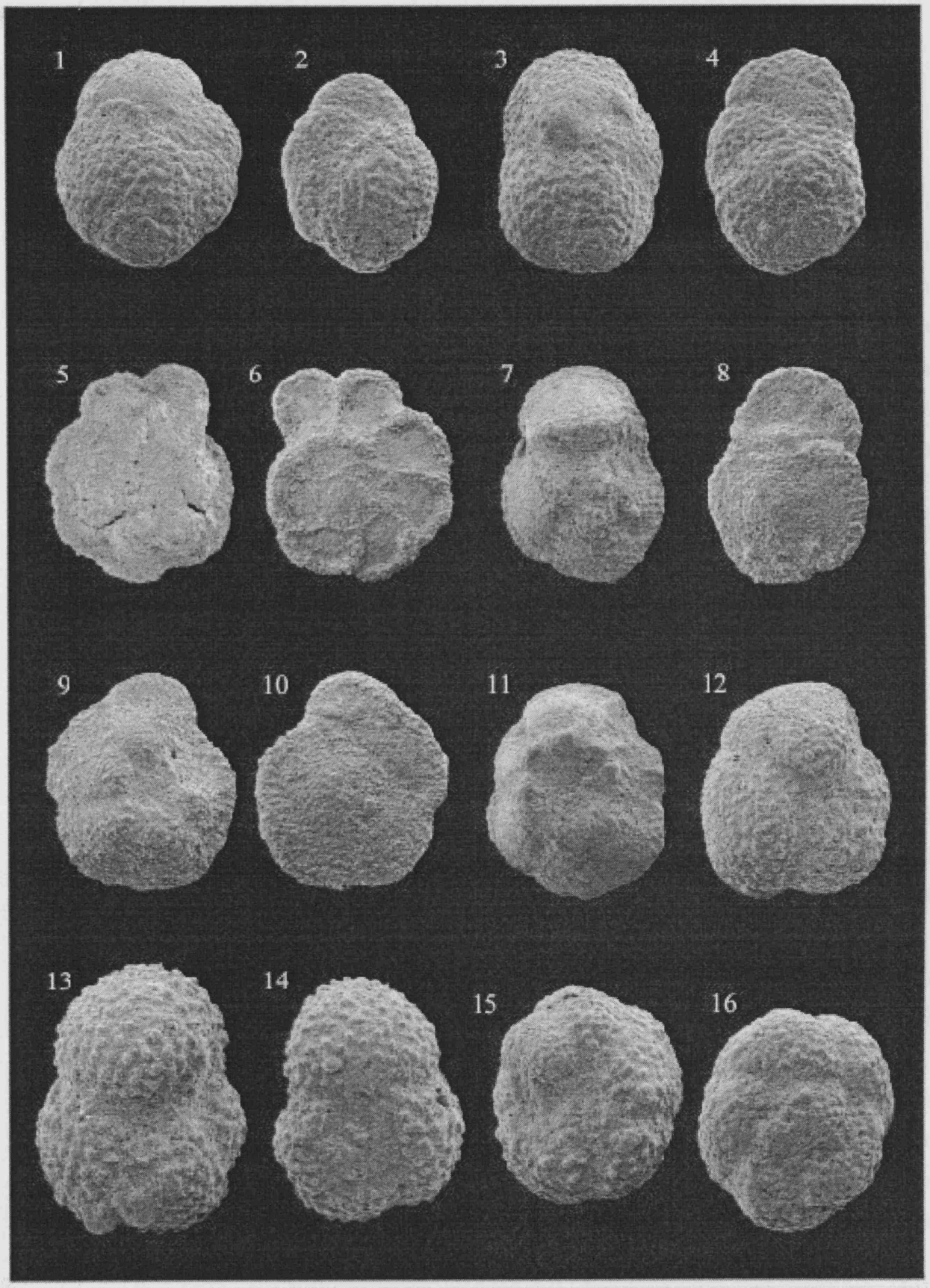

PLATE 6

CHAPTER 7: CONCLUSIONS

7.1 INTRODUCTION

The aims of this study were to use different microfossil groups within sediments in order to elucidate the various stages of evolution of the Baer-Bassit ophiolite, and to compare the results obtained with published data for other Eastern Mediterranean and Tethyan ophiolites. Specifically, to attempt to constrain the age of ophiolite formation and emplacement onto the Arabian platform margin, to examine the post emplacement sedimentary history with regard to the age and palaeoenvironment of the sediments and to investigate aspects of the Baer-Bassit mélange to give a greater understanding of the history of a Mesozoic passive margin.

Sediments are associated with every stage of evolution of the Baer-Bassit ophiolite. During oceanic crust formation, fine grained metalliferous mudstones called umbers are often deposited within pillow lava interstices and fault-bound depressions. Umbers from other ophiolites have been shown to contain microfossils that enable a youngest age of oceanic crust (ophiolite) formation to be biostratigraphically constrained.

Sediments are also associated with the period of ophiolitic cooling, occurring as ophiolitic cover, and with ophiolite transportation through the oceanic realm. These sediments are often incorporated into ophiolitic mélanges and record the oceanic environment and basement character through which the ophiolite has passed over between initial detachment and final emplacement.

Autochthonous sediments, lying structurally beneath the emplaced ophiolite, record the local depositional environment prior to, and in some cases during, ophiolitic emplacement as well as providing a time frame for final emplacement.

Supra-ophiolitic cover sediments record the depositional environment during and immediately after ophiolite emplacement, as well as the subsequent sedimentary history of the area. Additionally they provide a further time constraint on ophiolitic obduction onto the continental margin, with the oldest supra-ophiolitic cover sediments often recording a period of sub-aerial exposure reflecting the completion of obduction.

7.2 OPHIOLITE FORMATION

The Baer-Bassit ophiolite is interpreted to have formed in a supra-sudbuction zone setting in a southern neotethyan oceanic basin, and have been emplaced southward to its current position. It is highly dismembered as a result of deformation during initial emplacement in the oceanic realm, transportation and obduction onto the Arabian continental margin, and neotectonic strike slip faulting associated with the movement on the Dead Sea fault system and associated lineaments. Despite this, an essentially complete ophiolitic association can be recognised.

Previous attempts to constrain the age of formation of the Baer-Bassit ophiolite have concentrated on dating aspects of the metamorphic sole as well as gabbros, dykes and lavas of the ophiolite itself. Palaeomagnetic studies have also recently been conducted on various units of the ophiolite. The ages obtained from dating of the metamorphic sole range from 90-85Ma based on using the K-Ar method on separated amphiboles (Thuizat *et al.* 1981, Delaloye and Wagner 1984) to $88.4^{+}/_{-}0.4$Ma based on laser probe $^{40}Ar/^{39}Ar$ on separated amphiboles (Chan, pers. com.). These ages relate to the age of maximum metamorphism, which is itself thought to represent initial detachment and emplacement of the ophiolitic slab within the oceanic realm. This obviously provides some age constraint on oceanic crust formation, especially as initial emplacement is thought to occur whilst the oceanic lithosphere is still hot and relatively buoyant. The dates obtained by analysis of amphiboles correspond to the Turonian to Santonian interval, with the latter date ($84.4^{+}/_{-}0.4$Ma) approximately corresponding to the Santonian/Campanian boundary. Data obtained from K/Ar studies of dykes gave an age range of 73-99Ma (latest Albian – Campanian) (Delaloye and Wagner, 1984). The results obtained from pillow lavas were discounted due to intense weathering. Additionally, the authors state that results obtained from amphibolites from the gabbros gave older ages, perhaps suggesting the ophiolite is as old as Late Jurassic. Results from palaeomagnetic studies of the ophiolitic gabbros, dykes and lavas of the ophiolite suggest that ophiolite formation occurred during both normal and reversed polarities, with reversed polarities dominant (Morris *et* al. 1999, Morris & Anderson 2002). This contradicts the age of formation suggested by the dates obtained from amphiboles from the metamorphic sole. These data are incompatible, and it was hoped micropalaeontological studies of interpillow sediments would clarify the situation.

Within this study umbers were analysed for microfauna and microflora in an attempt to further constrain the age of ophiolite formation in that umbers are essentially contemporaneous as ophiolite formation. Despite the number of techniques used to extract any microfossils present no useful fossils were obtained, and therefore it is not currently possible to constrain the age of formation of the Baer-Bassit ophiolite. However, considering the above data it is most likely that it was formed during the late Cretaceous quiet interval and the Campanian C33R chron. Ophiolite emplacement during the late Campanian supports formation sometime prior to this during the Campanian. This generally agrees with dates of formation obtained by K-Ar method on separated amphiboles, even though this dating method is generally agreed to give unreliable data. Further work is needed to firmly establish the age of ophiolite formation, and it is possible that more extensive sampling of umberiferous sediments for micropalaeontological analyses could shed light on this problem. Umbers collected during this study are presumed to be barren because of the harsh, acidic conditions associated with their formation. These conditions are often likely to preclude preservation of delicate calcite or silica tests, though it was hoped that organic walled microfossils might have been preserved.

7.3 OPHIOLITE TRANSPORTATION THROUGH THE MARINE REALM.

The marine realm through which the Baer-Bassit ophiolite passed during transportation and eventual obduction is recorded within the sediments and volcanics of the Baer-Bassit mélange. Although the melange was not specifically studied during this work a number of conclusions can be drawn about the neotethyan basin through which the ophiolite was transported.

During the late Triassic carbonate material from the Arabian carbonate platform was being redeposited at the base of the slope as gravity deposits, and hemipelagic limestones were also being deposited. Further basinward pelagic siliceous sedimentation dominated, suggesting that this area was below the CCD. Interbedded with these siliceous sediments are minor alkaline volcanics that are possibly related to rifting within the southern neotethyan oceanic basin. Jurassic sedimentation is dominated by radiolarites suggesting a decrease in the depth of the CCD or relative sea-level rise. Carbonate deposition resumed during the Cretaceous, again with redeposition of carbonate platform material at base of slope, as well as hemipelagic and pelagic

carbonate sedimentation and localised proximal deposition of sandstones and conglomerates. Further basinward pelagic siliceous sedimentation continued, whilst alkaline volcanic seamounts were formed, perhaps related to plume activity. These were capped by pelagic carbonates indicating their elevation above the CCD.

7.4 FINAL OPHIOLITE EMPLACEMENT

The age of ophiolite emplacement onto the Arabian continental margin can be well constrained by dating the youngest autochthonous rocks structurally beneath the ophiolite and the oldest supra ophiolitic cover sediments.

The Mesozoic carbonate platform exposed in the north of the Baer-Bassit area, records Jurassic to Cretaceous sedimentation. Mid – Late Jurassic shallow marine carbonates are unconformably overlain by shallow marine carbonates of inferred Aptian to Cenomanian age. Cenomanian to Turonian pelagic carbonates are in turn overlain by Campanian to pelagic limestones and marls. The stratigraphic break between the Turonian and Campanian probably reflects erosion of the carbonate platform as opposed to a period of non-deposition (Al-Riyami, 2000). Campanian sediments from the autochthonous platform are recorded here for the first time. This is in part due to recent advances in Cretaceous planktonic foraminiferal biostratigraphy, which have reassigned Maastrichtian foraminiferal zones to the Campanian (i.e. the *Globotruncanella havanensis* and *Globotruncana aegyptica* Zones) whilst extending the *Gansserina gansseri* Zone down into the Campanian (previously assigned to the Upper Maastrichtian). Additionally, the planktonic foraminifera previously used to date the youngest autochthonous sediments, whilst typical of Maastrichtian assemblages, do in fact range down into the Campanian and in some cases Santonian. The new age assignment of these zones corresponds well with the data obtained by studying Radiolaria, which also suggest that the majority of the autochthonous sediments sampled in close proximity to the overlying ophiolite are Campanian in age. The youngest autochthonous sediments, sampled from immediately beneath the ophiolite, differ markedly from those lower in the sequence. Chert, quartz and other mineral fragments within these sediments are interpreted as being derived from the advancing ophiolitic nappes (including sediments and volcanics of the Baer-Bassit mélange), and the increase in water depth suggested by sedimentological and micropalaeontological data possibly reflects flexural loading caused by this. Restricted micropalaeontological

faunas recovered from these samples are inferred as being due to a restricted marine environment caused by the approaching ophiolitic nappes. These youngest sediments are assigned to the planktonic foraminiferal *Gansserina gansseri* Zone and radiolarian *Patulibrachium dickinsoni* Zone, are assumed to be latest Campanian in age. Extensive thicknesses of Lower Maastrichtian sediments were previously reported from the carbonate platform but this is clearly not the case. No unequivocally Maastrichtian age sediments were found. The presence of ophiolitic derived detritus within these sediments suggests that final emplacement of the Baer-Bassit ophiolite and associated mélange occurred shortly after their deposition.

The youngest *in situ* supra-ophiolitic sediments were seen between the villages of al Ghas'saniyeh and Al ieman, and at Ballourane. The sediments from the first locality were dated as ?late Campanian - Maastrichtian based on the larger benthic foraminifera present (Fadel, pers. com.), but assemblages recovered from washed samples suggested they were no older than late Campanian *Globotruncana aegyptica* Zone, though obviously these sediments could not this old as they would predate sediments lying beneath the ophiolite. The oldest samples from Ballourane are confidently assigned to the late Campanian- early Maastrichtian *Gansserina gansseri* Zone. This combined with the results obtained from the autochthon restricts emplacement of the Baer-Bassit ophiolite onto the Arabian margin as occurring between the latest Campanian and the early Maastrichtian, during a period of ~3My (73-70Ma), and maybe even entirely within the latest Campanian.

7.5 UPPER CRETACEOUS AND LOWER TERTIARY SEDIMENTATION OF THE BAER-BASSIT AREA.

After initial deposition of shallow water conglomerates, such as those seen at Al Ghas'saniyeh, there was a rapid return to pelagic sedimentation, with pelagic carbonates belonging to the latest Campanian-Lower Maastrichtian *Gansserina gansseri* sampled at a number of localities. Late Maastrichtian pelagic sediments are also seen at a number of localities within the field area, but these deposits are not as extensive as previously mapped. The K/T transition is not seen anywhere in the field area and the lowest Paleocene foraminiferal Zones (Pα, P0 and P1a) are also not represented, suggesting a hiatus of at least 0.5Ma. Pelagic carbonate sedimentation was re-established by the early Paleocene, with large thicknesses being deposited as at Qafar-Fawkani. Many lower

Palaeocene samples contained reworked Maastrichtian foraminifera, in some cases comprising over 80% of the assemblage. This suggests Maastrichtian (lower and upper) sediments were much more widely deposited than is reflected by present outcrops, but were systematically reworked during the lower Palaeocene either as a result of increased oceanic circulation or significant shallowing of marine conditions. Pelagic sedimentation continued until the mid Eocene when a gradual shallowing led to deposition of Nummulitic limestones, and the initial stages of the final suturing of the Arabian and Eurasian plates led to syn-depositional deformation, and eventually a late Eocene – early Miocene hiatus.

7.6 COMPARISONS WITH OTHER ADJACENT EASTERN MEDITERRANEAN OPHIOLITES.

7.6.1 Troodos, Cyprus.

The age of formation of the Troodos ophiolite, Cyprus, is constrained as 92-90Ma based on U-Pb dating of plagiogranites (Mukass and Ludden, 1987), corresponding to the Cenomanian – Turonian. Additionally, the pillow lavas have been dated as $75^{+}/_{-}5$Ma, corresponding to a late Campanian age (Delaloye and Desmet, 1979), whilst the dykes have been dated as $83^{+}/_{-}5$Ma corresponding to the Santonian-Campanian (Delaloye *et al.*, 1980). Biostratigraphical work on interpillow and supraophiolitic sediments has yielded maximum ages from Turonian (Blome and Irwin, 1985) to Santonian (Bragin and Bragina, 1991). Urquhart and Banner (1991) record Campanian age assemblages for radiolaria and foraminifera, and despite extensive sampling were unable to reproduce the biostratigraphical older ages of Blome and Irwin (1985).

Whilst the age of formation of the Baer-Bassit ophiolite remains quite poorly constrained it still seems likely that it was formed sometime during the late Santonian-early Campanian. This is therefore similar to ages suggested for the formation of Troodos, though different workers have suggested markedly different ages for this (Turonian-Campanian).

Unlike the Baer-Bassit ophiolite, the Troodos ophiolite has not been emplaced onto the continental margin, and therefore lacks the emplacement related deformational features seen in Syria, as well as the emplaced marginal sediments and volcanics seen in the Baer-Bassit melange. However, melanges are known from Cyprus, including the

Mammonia melange. This is interpreted as a passive margin sequence derived from the northern margin of a southern neotethyan ocean (Robertson 1998). There is considerable uncertainty as to how the Troodos ophiolite and Mammonia complexes became juxtaposed however.

Unlike in Baer-Bassit, deep marine sediments rest directly on the Troodos ophiolite. These include umbers, cherts, clays and mudstones of the Upper Cretaceous Perapedhi Formation. These pass into pelagic carbonates of the Lefkara Formation that range from upper Cretaceous to Oligocene in age. In comparison therefore, the Troodos ophiolite was not sub-aerially exposed after emplacement, as emplacement has occurred and remained within the oceanic realm. The umbers of the Baer-Bassit ophiolite contain more terrigenous derived material than the corresponding umbers of Cyprus, testifying to a less distal origin of the Baer-Bassit ophiolite during formation, radiolaria were found to be rare or absent from umbers sampled from Baer-Bassit, whereas numerous samples of umbers from Cyprus have yielded Radiolaria. Oligocene deposits are absent in NW Syria, but large thicknesses of Oligocene marls and chalks are developed on the Troodos ophiolite, again testifying to a deeper oceanic environment.

7.6.2 Hatay, Turkey.

The Hatay (Kizildağ) ophiolite of southern Turkey lies approximately 30km north of the Baer-Bassit area, on the northern side of the Jebel Aqraa carbonate platform. It is also thought to have formed above a subduction zone, indeed it is proposed that the Hatay, Koçali and Amanos ophiolites of southern Turkey, and the Baer-Bassit ophiolite of Syria were initially emplaced as a single thrust sheet that became dismembered by faulting and erosion (e.g. Robertson 2002). As with Baer-Bassit a typical ophiolitic association is present, though it lacks a metamorphic sole and is far less tectonically disrupted.

Delaloye and Wagner (1984) report a similar age for the origin of the Hatay and Baer-Bassit ophiolites, with sheeted dykes dated as between 99-73Ma (Albian/Cenomanian-Campanian), and separated green amphiboles from the gabbros giving a Late Jurassic age.

In the southern part of the Hatay area a tectonic mélange similar to that seen beneath the Baer-Bassit ophiolite is present, with blocks of ?Triassic, Jurassic and

Cretaceous bituminous calcarenites set in a matrix of sheared serpentinite (Robertson, 1986). In general though, the mélange is less well developed, presumably because the continental margin units were entrained within the leading edge of the ophiolitic nappe (i.e. the Baer-Bassit ophiolite).

The age of emplacement of the Hatay ophiolite onto the Arabian continental margin is constrained by the ages of the autochthonous platform sediments beneath the ophiolite and sedimentary cover sequence above. The youngest autochthonous sediments are Cenomanian-Santonian bituminous limestones and marls, significantly older than those beneath the Baer-Bassit ophiolite, whilst the oldest transgressive cover sediments are reportedly Upper Campanian - Maastrichtian (Piskin *et al.*, 1986).

After initial deposition of conglomerates and coarse sandstones, similar to those seen in the Al Ghas'saniyeh area in Baer-Bassit, there is a transformation to deeper water hemipelagic and pelagic marls and limestones (Piskin *et al.*, 1986). As in the Baer-Bassit area, Maastrichtian sediments are unconformably overlain by Paleocene to Eocene marls, limestones and pink chalks, similar to those of the Lefkara formation of Cyprus. Additionally, Eocene sediments contain redeposited calciturbidites, often nummulitic, reflecting tectonic instability as seen further south in the Baer-Bassit area (Robertson, 1986b). Finally, Miocene sediments are transgressive over all the previous units as in the Baer-Bassit area.

7.7 SUMMARY

Three field seasons were undertaken to collect samples from the Baer-Bassit area of northwestern Syria. During fieldwork a total of 222 samples were collected for micropalaeontological analysis. 135 smear slides were made for nannofossil studies, 178 samples were washed for planktonic foraminifera and general microfossils, 24 samples were specifically processed for Radiolaria, 10 samples were processed for palynology and 35 samples were sectioned for larger benthic foraminifera or because the samples were too hard to process in the normal way.

Identification of all fauna or flora recovered or revealed was attempted, including nannofossils, planktonic and benthic foraminifera, larger benthic foraminifera, radiolaria, ostracods, palynomorphs, algae and general fossil detritus. Nannofossil preservation in most samples was seen to be very poor, with considerable overgrowth in the samples studied. Studies therefore concentrated on foraminifera and radiolaria, with

other fauna and floras studied in more detail where no biostratigraphical or palaeoenvironmental data was achieved using these two main fossil groups. A simple, summary stratigraphic column shown in figure 7.1 illustrates the main differences in dating established during this work to previously reported ages. Maps showing the new distribution limits of Campanian and Maastrichtian strata were not attempted as the thicknesses involved would be too small.

The following main points have been established:

- An attempt to date the age of formation of the age of oceanic crust (and therefore the ophiolite) was attempted by sampling and processing of umbers and interpillow cements, which are accepted to be formed contemporaneously with the pillow lavas.

A total of 12 samples were collected from 4 different areas. These samples were processed by a variety of methods to ensure that any microfauna or flora present in the samples could be retrieved. The majority of the sediments however proved barren, apart from very rare fish teeth and a very small number of indeterminate foraminifera and radiolaria. One sample contained a number of well preserved Tertiary benthic foraminifera but this was discounted as contamination. The lack of any significant microfossil assemblages prevents dating of ophiolitic formation by this method but does however suggest a different environmental setting for the formation of the Baer-Bassit umbers to those of Troodos, which have been seen to contain radiolaria and foraminifera. Additionally, ophiolites are considered to be emplaced as young, and still hot, oceanic crust. Accurate dating of emplacement of the Baer-Bassit ophiolite onto the Arabian carbonate platform suggests that the ophiolite itself was probably formed during the Campanian.

- In order to obtain a maximum age for emplacement of the Baer-Bassit ophiolite onto the Arabian platform, 26 samples were taken from 5 different localities to date the youngest autochthonous sediments structurally beneath the ophiolite. Smear slides were produced from 22 of these samples, but as mentioned previously were not extensively studied due to extreme overgrowth of the nannoflora. 7 of the samples were thin-sectioned alone, 3 samples were washed for foraminifera, 3 were processed for radiolaria and 9 samples were washed for foraminifera and also processed for radiolaria.

5 samples were thin-sectioned due to their hardness but were also processed for radiolaria.

Three of the samples were Cenomanian in age and added little to previously published data. The majority of the samples however, were taken from sections previously mapped as lower Maastrichtian in age. Using radiolarian and foraminiferal biostratigraphy it is apparent that the majority of these samples are unequivocally Campanian in age and not Maastrichtian. Indeed, only two samples, taken from immediately beneath the overlying ophiolitic nappes, may possibly be Maastrichtian, and the micropalaeontological evidence suggests that they are more likely to belong to the lower part of the foraminiferal *Gansserina gannseri* Zone, which equates to the latest Campanian. Previous works suggest lower Maastrichtian sediments reach a thickness of about 90m in the study area. It is here stated that Maastrichtian sediments can total no more than 5m thickness, but micropalaeontological evidence suggests they are not developed beneath the ophiolite at all.

- Microfossil assemblages recovered from two samples taken from immediately beneath the ophiolite suggest a significant deepening prior to ophiolitic emplacement on the carbonate platform. This is indicated by an increase in the planktonic:benthic foraminiferal ratios as well as the spumellarians:nasselarian radiolarian ratios. Additionally, double keeled forms with more than 5 final chambers in the final whorl which it is suggested are more indicative of deeper marine conditions, are more common in these samples. The above samples also contained small amounts of chert and quartz grains, and these are interpreted as having been derived from the advancing ophiolitic nappes as opposed to having a terrigenous derivation. Further, the limited fauna recovered from these two samples are interpreted as reflecting restricted marine conditions caused by the approaching ophiolitic nappes acting as a barrier to a number of species. This would suggest these sediments were indeed deposited immediately prior to ophiolitic emplacement, and that no significant thickness of sediments was lost during emplacement.
- 67 samples were collected from sediments previously reported as upper Maastrichtian in age in order to ascertain the age of the oldest supra-ophiolitic sediments, and therefore constrain the time frame for ophiolitic emplacement. As with the samples from the autochthon, smear slides were produced from all the samples but were not extensively studied. 55 samples were washed for foraminifera and general

micropalaeontology and a further 14 sectioned, either because they were too hard to process by washing, or because they were seen to contain a number of larger benthic foraminifera which are generally identified in section. Samples were not specifically processed for radiolaria because, unlike a number of samples from the autochthon, the foraminiferal preservation was deemed sufficient for accurate identification.

The oldest sediments overlying the Baer-Bassit ophiolite were conglomerates seen at Al Ghas'saniyeh and Ballourane. The samples dated by larger benthic foraminifera were assigned a ?late Campanian - Maastrichtian age, whilst the planktonic foraminifera obtained from two of the samples suggested they may be as old as late Campanian in age. These samples contained a large volume of ophiolitic fragments and are interpreted as reflecting initial marine transgression of the Baer-Bassit ophiolite.

The age of ophiolite emplacement is therefore constrained to occurring between the latest Campanian and the early Maastrichtian, or maybe entirely within the latest Campanian.

- After deposition of shallow marine channelised conglomerates and sandstones pelagic sedimentation was re-established, and pelagic sediments from a number of localities would appear to belong to the late Campanian – early Maastrichtian *G. gansseri* Zone. A gradual transition from these shallow marine sediments to pelagic sedimentation is not seen and it is inferred that this was in fact fairly rapid.
- There appear to be no major hiatuses within the Maastrichtian sediments, with all three Maastrichtian foraminiferal zones of Premoli-Silva and Sliter (1999) represented, however, not all of the Maastrichtian is represented in any one area, and this is taken as due to extensive reworking of Maastrichtian and lower Palaeocene sediments.
- Maastrichtian age sediments overlying the ophiolite crop out considerably less than previous mapping suggests. In fact outcrops of Maastrichtian age are in fact extremely limited in extent, and conversely, Palaeocene sediments are developed much more widely. Significant numbers of reworked Maastrichtian fossils within lower Palaeocene sediments indicate that Maastrichtian sediments were once widespread but were reworked during the early Palaeocene.
- 64 samples collected from the Palaeocene strata show that the latest Maastrichtian-early Danian (Zone P1a) is represented by a hiatus in the entire Baer-

Bassit area, and, as aforementioned, in a number of localities the hiatus stretches further down into the Maastrichtian.

The oldest Tertiary sediments belong to the early Palaeocene P1b *Subbotina triloculinoides – Globanomalina compressa/Praemurica inconstans* Subzone. Sediments of this age are pelagic limestones and marls, and this sedimentation continued through the Palaeocene. Large thicknesses of Palaeocene strata are developed throughout the study area and no major hiatus' were noted using micropalaeontological techniques. These sediments pass up into siliceous marls, with common chert bands, of Eocene age, which in turn pass up into nummulitic limestones. There then followed a period of uplift and emergence.

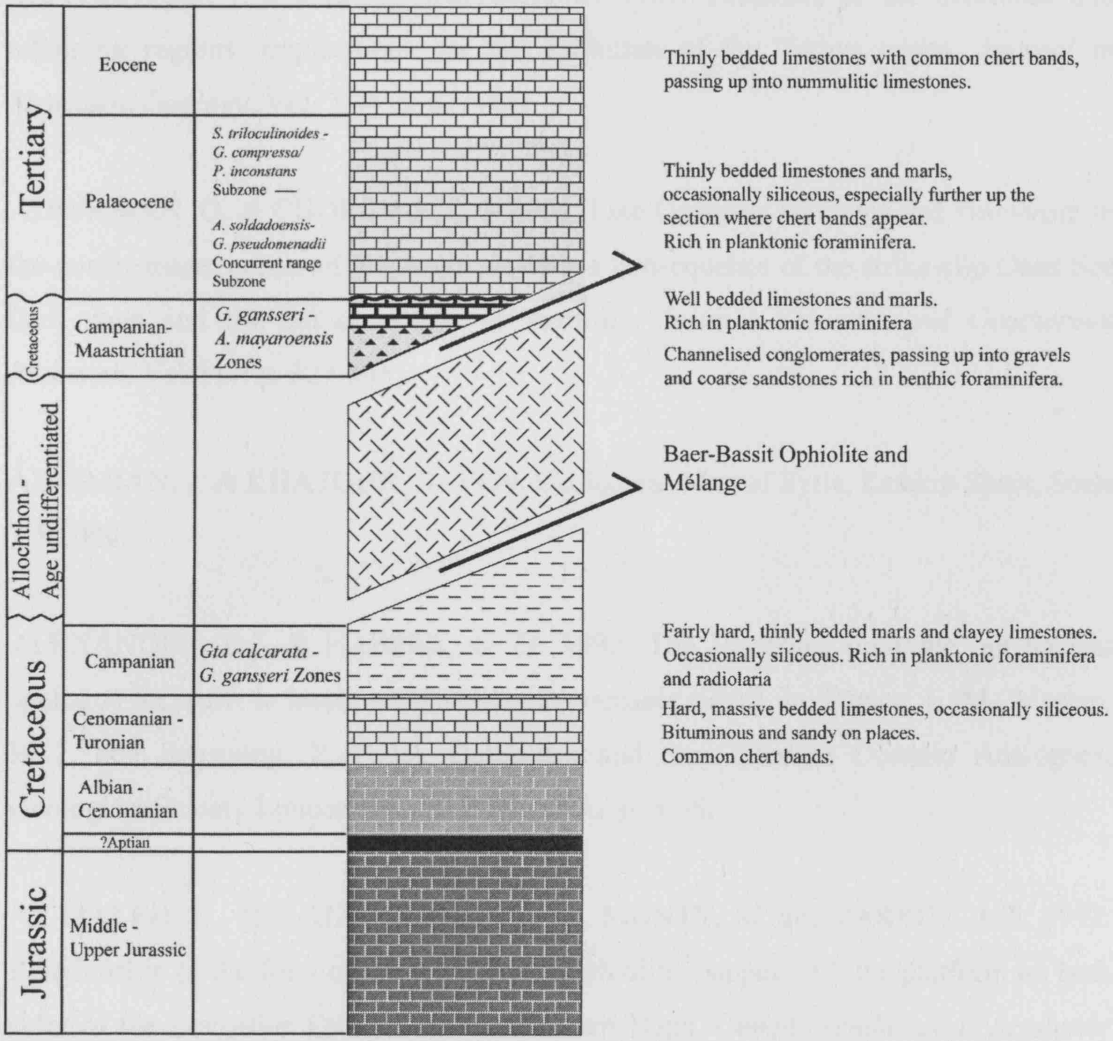

Figure 7.1. A simple summary stratigraphic column, highlighting the new age ranges of the studied interval.

REFERENCES

ABBATE, E., BORTOLOTTI, V. and PRINCIPI, G. 1983. Oceanic metamorphism and tectonics in Western "Tethys". *Ofioliti*, Supplement, 8, p. 5.

ABBATE, E., BORTOLOTTI, V., PASSERINI, P. and PRINCIPI, G. 1985. The rhythm of phanerozoic ophiolites. *Ofioliti*, Vol. 10, p. 109-138.

ADAMIA, S. A., CHKHOTUA, M., KEKELIA, M., LORD-KIPANIDZE, M., SHAVISHVILI, I. and ZACHARIADZE, G. 1981. Tectonics of the Caucasus and adjoining regions: implications for the evolution of the Tethys ocean. *Journal of Structural Geology*, Vol. 3(4): p. 437-447..

ADIYAMAN, Ö. & CHOROWICZ, J. 2002. Late Cenozoic tectonics and volcanism in the northwestern corner of the Arabian plate: a consequence of the strike-slip Dead Sea fault zone and the lateral escape of Anatolia. *Journal Volcanic and Geothermal Research*, Vol.117: p. 327-345.

ADJEMIAN, J. & KHATOUN, A. 1999. Geological Map of Syria, Latakia Sheet. Scale 1:50,000.

ALEXANDER, R.J. & HARPER, G. D. 1992. The Josephine ophiolite: an ancient analogue for slow- to intermediate-spreading oceanic ridges. In: Parson, L. M., Murton, B. J. and Browning, P. (Eds), Ophiolites and their Modern Oceanic Analogues, Geological Society London Special Publication, p. 3-38.

AL-MALEH, K., DELAUNE-MAYÈRE, M., MONTY, M. and PARROT, J.-F. 1992. Relationship of the front of northern Syrian ophiolitic nappes with the platform on both sides of the Levantine Fault; Baer-Bassit, Kurd Dagh. *Compte rendus de l' Academie Francais de Science, Paris*, Vol. 314, série II, p. 1195-1202.

AL-RIYAMI, K. 2000. Mesozoic-Tertiary sedimentary and tectonic evolution of the South-Tethyan continental margin and Late Cretaceous ophiolite in Baer-Bassit region (NW Syria). Unpublished PhD thesis, Edinburgh University, UK.

AL-RIYAMI, K., ROBERTSON, A. H. F., XENOPHONTOS, C., DANELIAN, T. and DIXON, J. E. 1998. Mesozoic tectonic and sedimentary evolution of the Arabian continental margin in Baer-Bassit (NW Syria). In: Malpas, J., Xenophontos, C. and Panayides, A. (Eds), *Proc. 3rd Internat. Conf. on the Geology of the Eastern Mediterranean, Nicosia, Cyprus, September 23-26, 1998*. Cyprus Geol. Surv. Dept., Nicosia, Cyprus. 61-81.

AL-RIYAMI, K. & ROBERTSON, A. H. F. 2002. Mesozoic sedimentary and magmatic evolution of the Arabian continental margin, northern Syria: evidence from the Baer-Bassit Melange. *Geology Magazine*, Vol. 139 (4). P. 395-420.

AL-RIYAMI, K., DANELIAN, T. and ROBERTSON, A. H. F. 2002. Radiolarian biochronology of Mesozoic deep-water successions in NW Syria and Cyprus: implications for south-Tethyan evolution. *Terra Nova*, vol. 14, p. 271-280.

AL-RIYAMI, K., ROBERTSON, A., DIXON, J. and XENOPHONTOS, C. 2002. Origin and emplacement of the Late Cretaceous Baer-Bassit ophiolite and its metamorphic sole in NW Syria. *Lithos*, Vol. 65, 225-260.

AMSTUTZ, G. C. 1980. The early history of the term ophiolites and its evolution until 1945. In: *Proc. Inter. Ophiolite Symposium*, Geological Survey Department, Cyprus, p. 149-152.

ANDREW, T. & ROBERTSON, A. H. F. 2002. The Beyşehir-Hoyran-Hadim Nappes: genesis and emplacement of Mesozoic marginal and oceanic units of the northern Neotethys in southern Turkey. *The Journal of the Geological Society*, Vol. 159, no. 5, p. 529-543.

ANONYMOUS. 1972. Penrose field conference on ophiolites. *Geotimes*, Vol. 17, p. 24-25.

AUBOUIN, J. 1964. *Geosynclines.* Amsterdam, Elsevier. 335pp.

BADAWY, A. & HORVÁTH, F. 1999. The Sinai subplate and tectonic evolution of the northern Red Sea region. *Geodynamics*, Vol. 27: p. 433-450.

BAUMGARTNER, P. O., O'DOGHERTY, L., GORICAN, S., URQUHART, E., PILLEVUIT, A. and DE WVER, P. (Eds) 1995. *Middle Jurassic to Lower Cretaceous Radiolaria of Tethys: Occurrences, Systematics, Biochronology, Memoires de Géologie (Lausanne),* no, 23, pp. 1172.

BECCALUVA, L., OHNENSTETTER, D. and OHNENSTETTER, M. 1979. Geochemical discrimination between ocean-floor and island-arc tholeiites-Application to some ophiolites. *Canadian Journal Earth Sciences*, Vol. 16, p. 1874-1882.

BECCALUVA, L., COLTORI, M., PREMTI, L., SACCANI, E., SIENA, F. and ZEDA, O. 1994. Mid-ocean ridge and supra-subduction zone ophiolites in Albania. *Ofioliti*, Vol. 19, p. 77-79.

BENSON, W. N. 1926. The tectonic conditions accompanying the intrusion of basic and ultrabasic igneous rocks, *National Academy Science U. S. A.*, Vol. 19: p. 1-90.

BERGGREN, W. A. and NORRIS, R. D. 1997. Biostratigraphy, phylogeny and sytematics of Paleocene trochospiral planktic foraminifera. *Micropaleontology*, vol. 43, suppl. 1, pp. 116.

BLOME, C. D. and IRWIN, W. P. 1985. Equivalent radiolarian ages from ophiolitic terranes of Cyprus and Oman. *Geology*, **13**, 401-404.

BOLLI, H. M. 1966. Zonation of Cretaceous to Pliocene marine sediments based on planktonic foraminifera. *Boletino Informativo Associacion Venezolana de Geologia, Mieraria y Petroleo*, Vol. 9, p. 3-32.

BOSTRÖM, K. 1973. The origin and fate of ferromanganoan active ridge sediments. *Stockholm Contributions Geology*, Vol. 27, p. 149-243.

BOSTROM, B. and PETERSEN, M. N. A. 1969. The origin of aluminium poor ferromanganoan sediments in areas of high heat flow on the East Pacific Rise. *Marine Geology*, 7, 427-447.

BOUDIER, F., NICOLAS, A. and BOUCHEZ, J. L. 1982. Kinematics of oceanic thrusting and subduction from basal sections of ophiolites. *Nature*, Vol. 296, p.825-828.

BOWEN, N. L. 1927. The origin of ultrabasic and related rocks, *American Journal Science*, Vol. 14, p. 89-108.

BOWEN, N. L. & SCHAIRER, J. F. 1935. The system MgO-FeO, SiO_2, *American Journal Science*, Vol. 29, p. 151-217.

BOWEN, N. L. & TUTTLE, O. F. 1949. . The system MgO-SiO_2-H_2O, *Geological Society of America Bulletins*, Vol. 60, p. 439-460.

BRAGIN, N. Y. & BRAGINA, L. G. 1991. Radiolarian biostratigraphy of Troodos Upper Cretaceous Sediments (Cyprus). *Abstracts Volume, 6th meeting of the International Association of Radiolarian Paleontologists, Firenze,* 17.

BRONGNIART, A. 1813. Essai d'une classification minéralogique des roches mélangées. *Journalle Des Mines*, Vol. 199, p. 5-48

BRONGNIART, A. 1821. Sur le gisement ou position relative des ophiolites, euphotides, jaspes, etc. dans quelques parties des Apennins. *Annales Des mines*, Vol. 6, p. 177-238.

BRONGNIART, A. 1827. *Classification et caractères minéralogiques des roches homogènes et hétérogènes*, F. G. Levrault, Paris, pp. 144.

BRUNN, J. H. 1940. Conditions de gisement des roches basiques en Macedoine accidentale. *C. R. Acad. Sci. Paris*, Vbol. 210, p. 735.

BRUNN, J. H. 1959. La dorsale médio-atlantique et les épanchements ophiolitiques, *C. R. Societé Géologique France.*, Vol. 8, p. 234-236.

BRUNN, J. H. 1960. Mise en place et différeciation pluto-volcanique du cortège ophiolitique, *Revue Geographie Physique Gèologie Dynamique*, Vol. 3, p. 115-132.

BRUNN, J. H. 1961. Les sutures ophiolitique: Contribution a l'études des relations entre phènoméne magmatique et orogénique, *Revue Geographie Physique Gèologique Dynamique*, Vol. 4, p. 89-96, 181-202.

CARON, M. 1985. Cretaceous planktonic foraminifera. In: Bolli, H. M., Saunders, J. B. and Perch-Nielson, K., Eds., *Plankton Stratigraphy*. Cambridge University Press, vol. 1: p. 17-86.

CASEY, J. F. & DEWEY, J. F. 1984. Initiation of subduction zones along transform and accreting plate boundaries, triple junction evolution, and forearc spreading centres-implications for ophiolite geology and obduction. In: Gass, I. G., Lippard, S. J., Shelton, A. W. (Eds), *Ofiolites and Oceanic Lithosphere.* Geological Society London Special Publication, Vol. 13, p. 269-290.

CHENEVOIX, M. 1953. Le substratum métamorphiques des roches vertes dans le Baër-Bassit (Syrie Septentrionale). *Notes et Mémoires Moyen Orient*, 7, 1-18.

CHURCH, W. R. 1972. Ophiolite: its definition, origin as oceanic crust, and mode of emplacement in orogenic belts, with special reference to the Appalachians, *Department Energy, Mines Research Canada Publication*, Vol. 42, p. 71-85.

COLEMAN, R. G. 1971. Plate tectonic emplacement of upper mantle peridotites along continental edges, *Journal Geophysical Research*, Vol. 76, p. 1212-1222.

COLEMAN, R. G. 1977. *Ophiolites-Ancient oceanic lithosphere? Minerals and Rocks*, Vol. 12, Springer-Verlag, New York, pp. 229.

CONSTANTINOU, G. & GOVETT, G. J. S. 1972. Genesis of sulphide deposits ochre and umber of Cyprus. *Transactions Institution Mineralogy and Metallurgy*, Vol. 81, p.34-46.

CORLISS, J. B., GRAF, J. L., SKINNER, B. J. and HUTCHINSON. 1972. Rare earth data for iron and manganese rich sediments associated with sulfide ore bodies of the Troodos Massif, Cyprus. *Geological Society America Abstracts Program*, Vol. 4, no. 7, p. 476.

DAVIES, H. L. 1971. Peridotite-gabbro-basalt complex in eastern Papua. *Burmese Mineralogical Resources Bulletin*, Vol. 128, pp. 48.

DELALOYE, M. and DESMET, A. 1979. Nouvelles donnees radiométrique sur les pillow-lavas du Troodos (Chypre). *Académie des sciences, Paris, Comptes Rendus Série D*, 288, p. 461-464.

DELALOYE, M. and WAGNER, J-J. 1984. Ophiolites and volcanic activity near the western edge of the Arabian plate. In: Dixon, J. E. & Robertson, A. H. F. (Eds), *The Geological Evolution of the Eastern Mediterranean.* Geological Society London Special Publication, **17**, 225-233.

DELALOYE, M., DE SOUZA, H., WAGNER, J, -J. & HEDLEY, I. 1980. Isotopic ages of ophiolites from the Eastern Mediterranean. *In*: PANAYIOTOU, A. (ed.). *Ophiolites, Proc. Int. Oph. Symp. Cyprus*, 292-295.

DELAUNE-MAYÈRE, M. 1978. Cherts Mésozoiques du basin Téthysien oriental: Mineralogie et géochimie des sediments siliceux du secteur de Tammima (NY Syrien). *Cahiers de l'ORSTROM., série Géologie*, Vol. 10, p. 191-200.

DELAUNE-MAYÈRE, M. 1983. Polarities géochimiques paléogeographie des series volcano-sedimentaires peltiques du NW Syrien au Cretacé basal. *Cahiers de l'ORSTROM, série Géologie*, Vol. 13, p. 19-30.

DELAUNE-MAYÈRE, M. and PARROT, J-F. 1976. Évolution du mésozoique de la marge continentale méridionale du basin téthysienne oriental d'après l'étude des series sédimentaires de la region ophiolitiques du nord-ouest Syrien. *Cahiers de l'ORSTROM., série Géologie*, Vol. 8, no. 2, p. 173-184.

DELAUNE-MAYÈRE, M., FONTAINE, J-M. and PERINCEK, D. 1983. La Bordure de la Plaque Arabo-Africaine Mesozoique en Syrie et an Turquie du Sud-Est: Une Comparison. *Cahiers de l'ORSTROM., série Géologie*, Vol. 13, no. 1, p. 31-41.

DELAUNE-MAYÈRE, M. and SAINT-MARC, P. 1979/1980. Données stratigraphiques nouvelles sur les sediments oceaniques Mésozoiques associées aux nappes ophiolitiques du Baer-Bassit (N. W. Syrien). *Cahiers de l'ORSTROM., série Géologie*, Vol. 11, p. 151-164.

DERCOURT, J., ZONENSHAIN, L. P., RICOU, L. –E., KAZMIN, V. G., LE PICHON, X., KNIPPER, A. L., GRANDJACQUET, C., SBORTSHIKOV, I. M., GEYSSANT, J., LEPVRIER, C., PECHERSKY, D. H., BOULIN, J., SIBUET, J. -C., SAVOTSIN, L. A., SOROKHITIN, O., WESTPHAL, M., BAZHENOV, M. L., LAUER, J. P. and BIJU-DUVAL, B. 1986. Geological evolution of the Tethys belt from the Atlantic to the Pamirs since the Lias. *Tectonophysics*, Vol. 123; p. 241-315.

DERCOURT, J., RICOU, L. –E., AND ADAMIA, S., CSASZAR, G., FUNK, H., LEFELD, J., RAKÚS, M., SANDULESCU, M., TOLLMAN, A., TCHOUMACHENKO, P. 1990. *Northern Margin of Tethys:* Paleogeographical Maps 1:10,000000. IGCP: Project198. Bratislava

DEWEY, H. L. 1976. Ophiolite obduction. *Tectonophysics.* Vol. 31, p. 93-120.

DEWEY, J. F. & BIRD, J. M. 1971.Origin and emplacement of the ophiolitic suite: Appalachian ophiolites in Newfoundland, *Journal Geophysical Research*, Vol. 76, p. 3179-3206.

DILEK, Y. & MOORES, E. M. 1990. Regional tectonics of the eastern Mediterranean ophiolites. In: Malpas, J., Moores, E. M., Panayiotou, A. and Xenophontos, C. (Eds) *Ophiolites, Oceanic Crustal Analogues.* Geological Survey Dept., Cyprus, Nicosia, p. 295-309.

DILEK, Y. & THY, P. 1998. Structure, petrology and seafloor spreading tectonics of the Kizildag Ophiolite, Turkey. In: Mills, R. A. & Harrison, K. (eds) *Modern Ocean Floor Processes and the Geological Record*, Geological Society London Special Publication, Vol. 148, p. 43-69.

DUBERTRET, L. 1933. La téctonique de la Syrie septentrionale à la fin du Cretacé et au debut du Tertiaire, *Notes et Memoires du Beyrouth, Paris.*

DUBERTRET, L. 1953. Géologie des roches vertes du NW de la Syrie et du Hatay (Turquie). *Notes et Memoires Moyen Orient*, Vol. 6, p. 13-179.

ELDERFIELD, H., GASS, I. G., HAMMOND, A. and BEAR, L. M. 1972. The origin of ferromanganese sediments associated with the Troodos Massif of Cyprus. *Sedimentology*, **19**, 1-19.

FLEET, A. J. & ROBERTSON, A. H. F. 1980. Ocean-ridge metalliferous and pelagic sediments of the Semail Nappe, Oman. *Journal Geological Society*, Vol. 137, p. 403-422.

FOREMAN, H. P. 1975. Radiolaria from the north Pacific, Deep Sea Drilling Project, Leg 32. *Initial Reports of the Deep Sea Drilling Project* 32, 579-676.

FOREMAN, H. P. 1977. Mesozoic Radiolaria from the Atlantic Basin and its Borderlands. In F. M. SWAIN (ed.). *Stratigraphic Micropalaeontology of Atlantic Basin and Borderlands*, 305-320.

FRIANCHI, S. 1902. Contribuzione allo studio delle roccie a glaucofane e del metamorfismo onde ebbero origine nelle regione liguro-alpine occidentale, *Boll. R. Comitato Geol. Italia.*, Vol. 33, p. 255-318.

FROELICH, P. N., BENDER, M. L. & HEATH, G. R. 1977. Phosphorous accumulation rates in metalliferous sediments on the East Pacific Rise. *Earth Planetary Science Letters*, Vol. 34, p. 351-359.

GANSSER, A. 1974. The ophiolitic mélange, a world-wide problem on Tethyan examples. *Eclogae Geologae Helvetica*, Vol. 67, p. 479-507.

GLENNIE, K. W., BOUEF, M. G. A., HUGHES CLARK, M. W., MOODY-STUART, M., PILAAR, W. F. H. and REINHARDT, B. M. 1974. The Geology of the Oman Mountains. *Konin. Neder. Geo. Mijnbouw. Genoot. Verdh.* Vol. 31(1): pp. 423.

GOULDING, H. C., MILLS, R. A. & NESBITT, R. W. 1998. Precipitation of hydrothermal sediments on the active TAG mound: implications for ochre formation. In: Mills, R. A. & Harrison, K. (eds) *Modern Ocean Floor Processes and the Geological Record*, Geological Society London Special Publication, Vol. 148, p. 201-216.

HALL, G. E. M., PELCHAT, J. C. & LOOP, J. 1988. Separation and recovery of various sulfur species in sedimentary rocks for stable isotope determination. *Chemical Geology*, Vol. 67, p. 36-45.

HASSANIPAK, A. A. & GHAZI, A. M. 2000. Petrology, geochemistry and tectonic setting of the Khoy ophiolite, northwest Iran: implications for Tethyan tectonics. *Journal Asian Earth Sciences*, Vol. 18, p. 109-121.

HEATH, G. R. & DYMOND, J. 1977. Genesis and transformation of metalliferous sediments from the East Pacific Rise, Bauer Deep and Central Basin. *Bulletin Geological Society America*, Vol. 88, p. 723-733.

HESS, H. H. 1938. A primary peridotite magma, *American Journal Science*, Vol. 35, p. 321-344.

HÖCK, V., KOLLER, F., ONUZI, K., KNERINGER, E. and MEISEL, T. 2001. From MORB to SSZ – the south Albanian ophiolites and their Dinaric-Hellenic framework. Fourth International Turkish Geology Symposium, Abstracts, p. 241.

IRWIN, W. P. & COLEMAN, D.L. 1972. Preliminary map showing global distribution of Alpine-type ultramafic rocks and blueschists, *United States Geological Survey Map1/40,000,000.*

JONES, G., ROBERTSON, A. H. F. and CANN, J. R. 1991. Genesis and emplacement of the supra-subduction zone Pindos ophiolite, northwestern Greece. In Peters, T. J., Nicholas, A. and Coleman, R. G. (Eds), *Ophiolite Genesis and Evolution of the Oceanic Lithosphere.* Kluwer Academic Publishing, Dordrecht, p.771-799.

JONES, G., DE WEVER, P. and ROBERTSON, A. H. F. 1992. Significance of radiolarian age data to the Mesozoic tectonic and sedimentary evolution of the northern Pindos Mountains, Greece. *Geology Magazine*, Vol. 129 (4), p. 385-400.

KANANIAN, A., JUTEAU, T., BELLON, H., DARVISHZADEH, A., SABZEHI, M., WHITECHURCH, H., RICOU, L-E. 2001. The ophiolite massif of Kahnuj (western Makran, southern Iran): new geological and geochronological data. *Earth Planetary Science Letters*, Vol. 332, p. 543-552.

KAZMIN, V.G. & KULAKOV, V. V. 1968. The Geological Map of Syria. Scale 1:50,000. (Sheet Al-Lathequiyeh). *Explanatory note.* Technoexport, Nedra, Moscow, pp. 124.

KAZMIN, V. G., SBORTSHIKOV, I. M., RICOU, L. –E., ZONENSHAIN, L. P., BOULIN, J. and KNIPPER, A. L. 1986. Volcanic belts as markers of the Mesozoic-Cenozoic active margin of Eurasia. *Tectonophysics*, 123; p. 123-152.

KNIPPER, A., RICOU, L. –E. and DERCOURT, J. 1986. Ophiolites as indicators of the geodynamic evolution of the Tethyan Ocean. *Tectonophysics*, Vol. 123: p.213-240.

KNIPPER, A. L., KOPAEVICH, L. F. and RUKIEH, M. 1990. Age and origin of ophicalcites from the Baer-Basit ophiolite massif, Syria. *Ofioliti*, **15**,

KOEPKE, J., SEIDEL, E. and KREUZER, H. 2002. Ophiolites on the southern Aegean Islands, Crete, Karpathos and Rhodes. *Lithos*, Vol. 65, p. 183-204.

KOLLER, F & HÖCK, V. 1990. Mesozoic Ophiolites in the Eastern Alps. In: Malpas, J., Moores. E. M., Panayiotou, A., Xenophontos, C. (Eds), *Ophiolites, Oceanic Crustal Analogues*, Geological Survey Department, Nicosia, Cyprus, p. 253-264.

KRASHENINNIKOV, V.A., 1994. Stratigraphy of the Maastrichtian and Cenozoic Deposits of the Coastal Part of North western Syria (Neoautochthon of the Bassit Ophiolite Massif). In Krasheninnikov, V. A. and Hall, J. K. (Eds) *Geological Structure of the Northeastern Mediterranean (Cruise 5 of the Research Vessel Akademik Nikolaj Strakhov).* Historical Productions-Hall Ltd. p. 265-276.

KRASHENINNIKOV, V. A., GOLOVIN, D. I. & MOURAVYOV, V. I. 1996. The Paleogene of Syria – Stratigraphy, Lithology, Geochronology. *Geol. Jahrbuch*, Vol. B86, pp. 136.

LAPIERRE, H. and PARROT, J-F. 1972. Identité géologique des regions de Paphos (Chypre) rt du Baër-Bassit (Syrie). *C. r. hebd. Séance. Acad. Sci., Paris*, **D, 274**, 1999-2002.

LIPPARD, S. J., SHELTON, A. W. & GASS, I. G. 1986. *The Ophiolite of Northern Oman.* Memoirs of the Geological Society of London, Vol. 11, pp. 178.

LIVERMORE, R. A. & SMITH, A. G. 1984. Some boundary conditions for the evolution of the Mediterranean region. In Stanley, D. J., & Wezel, F. –C. (Eds), *Geological Evolution of the Mediterranean Basin*: Berlin (Springer-Verlag), p.83-100.

LOTTI, B. 1886.Paragone fra la roccie ofiolitiche terziare italiane e la roccie basiche pare terziare della Scozia et dell'Irlande, *Boll. R. Comiato Geol. Italia.*, Vol. 76.

MACDONALD, K. C. 1982. Mid-ocean ridges: fine scale tectonic, volcanic and hydrothermal processes within the plate boundary zone. *Annual Revue Earth Planetary Science*, Vol. 10, p. 155-190.

MAXWELL, J. C. & AZZAROLI. A. 1962. Submarine extrusion of ultramafic magma, *Geological Society America Abstracts Annual Meeting*, Vol. 103A.

McCALL, G. J. H. (Ed.). 1983. Ophiolitic and related Mélanges, *Benchmark Papers in Geology*, Vol. 66, Hutchinson Ross Pub. Co. pp. 336.

MIYASHIRO, A. 1973. The Troodos complex was probably formed in an island arc, *Earth Planetary Science Letters*, Vol. 19, p. 218-224.

MIYASHIRO, A. 1975a. Origin of the Troodos and other ophiolites: A reply to Hynes, *Earth Planetary Science Letters*, Vol. 25, p. 217-222.

MIYASHIRO, A. 1975b. Origin of the Troodos and other ophiolites: A reply to Moores, *Earth Planetary Science Letters*, Vol. 25, p. 227-235.

MIYASHIRO, A. 1975c. Classification, characteristics, and origin of ophiolites, *Journal Geology*, Vol. 83, p. 249-281.

MONOD, O. & AKAY, E. 1984. Evidence for a Late Triassic-Early Jurassic orogenic event in the Taurides. In Dixon, J. E. & Robertson, A. H. F. (Eds), *The Geological Evolution of the Eastern Mediterranean.* Geological Society Special Publication London, 17: p. 113-122.

MIYASHIRO, A. 1975c. Classification, characteristics, and origin of ophiolites, *Journal Geology*, Vol. 83, p. 249-281.

MOORES, E. M. 1970.Ultramafics and orogeny, with models for the U. S. Cordillera and the Tethys, *Nature*, Vol. 228, p. 837-842.

MOORES, E. M. 1982. Origin and emplacement of ophiolites, *Revue Geophysics Space Physics*, Vol. 20, p. 735-760.

MOORES, E. M. & VINE, F. J. 1971. The Troodos massif, Cyprus, and other ophiolites as oceanic crust: Evaluation and implications, *Transactions Royal Society London, Ser. A*, Vol. 268, p. 443-466.

MORRIS, A., CREER, K. M. ROBERTSON, A. H. F. 1990. Palaeomagnetic evidence for clockwise rotations related to dextral shear along the Southern Troodos Transform Fault (Cyprus). *Earth and Planetary Science Letters*, Vol. 99: p. 250-262.

MORRIS, A., ANDERSON, M., AL-RIYAMI, K., ROBERTSON, A. H. F. and DIXON, J. E. 1999. First palaeomagnetic results from the Baer-Bassit ophiolite of N. Syria. *Journal of Conference Abstracts, 10th European Union of Geosciences, 4, p. 407.*

MORRIS, A., ANDERSON, M. W., AL-RIYAMI, K. and ROBERTSON, A. H. F. 2001. Net tectonic rotation analysis of extreme rotations in the Baër-Bassit ophiolite of N. Syria. *Fourth International Turkish Geological Symposium Abstracts* Çukurova University, Adana, Turkey. 235.

MORRIS, A. and ANDERSON, M. W. 2002. Palaeomagnetic results from the Baer-Bassit ophiolite of northern Syria and their implications for fold tests in sheeted dyke terrains. *Phys. Chem. Earth.* **27**, 1215-1222.

MOUTY, M. & SAINT-MARC, P. 1982. Le Crétacé Moyen du Massif Alaouite (NW Syrie). *Cahiers de Micropaléontologie*, 3, p. 55-68.

MUKASS, S. B. & LUDDEN, J. N. 1987. Uranium-Lead ages of plagiogranites from the Troodos ophiolite, Cyprus, and their tectonic significance. *Geology*, vol. 15, p. 825-828.

NEDERBRAGT, A. J. 1990. Biostratigraphy and paleoceanographic potential of the Cretaceous planktonic foraminifera Heterohelicidae. PhD Dissertation, Vrije Universiteit te Amsterdam, pp. 203, Centrale Huisdrukkerij Vrije Universiteit, Amsterdam.

NICOLAS, A. 1988. Structure of Ophiolites and Dynamics of Oceanic Lithosphere, *Petrology and structural geology*, Vol. 4, Kluwer Academic publishers, pp. 367.

NICOLAS, A. & BOUDIER, F. 1975. Kinematic interpretation of folds in Alpine-type peridotites. *Tectonophysics.* Vol. 25, p. 233-260.

NICOLAS, A. & LE PICHON, Z. 1980. Thrusting of young lithosphere in subduction zones with special reference to the structures in ophiolite peridotites. *Earth Planetary Science Letters*, Vol. 46, p. 397-406.

OLSSON, K. R., HEMLEBEN, C., BERGGREN, W. A. and HUBER, B. T. 1999. Atlas of Paleocene Planktonic Foraminifera. *Smithsonian Contributions to Paleobiology*, no. 85. pp. 252.

PANTAZIS, T. M. 1986. Ophiolites of Cyprus. Ofioliti, Vol. 11, p. 239-278.

PARLAK, O., BOZKURT, E. and DELALOYE, M. 1996a. The obduction direction of the Mersin ophiolite: Structural evidence from subophiolitic metamorphics in the Central Tauride belt, southern Turkey. *International Geology Revue*, Vol. 38, p. 778-786.

PARLAK, O., DELALOYE, M. and BİNGÖL, E. 1996b. Phase and cryptic variation through the ultramafic-mafic cumulates in the Mersin ophiolite (southern Turkey). *Ofioliti*, Vol. 21 (2), p. 81-92.

PARLAK, O., HÖCK, V. and DELALOYE, M. 2002. The supra-subduction zone Pozanti-Karsanti ophiolite, southern Turkey: evidence for high-pressure crystal fractionation of ultramafic cumulates. *Lithos*, Vol. 65, p. 205-224.

PARROT, J-F. 1974a. L'assemblage ophiolitique du Baër-Bassit (Nord-ouest de la Syrie): Etude pétrographique at géochimique du complexe filonien, des laves en cousins qui lui sont associées, et d'une partrie des formations effusives du volcanosédimentaire. *Cah. ORSTOM, sér. Géol.*, **6**, 2, 97-126.

PARROT, J-F. 1974b. Le secteur de Tamima^{h} (Tourkmannli): Étude d'une sequence volcano-sédimentaire de la region ophiolitique du Baër-Bassit (Nord-Ouest de la Syrie). *Cah. ORSTOM, sér. Géol.*, **6**, 2, 127-146.

PARROT, J-F. 1977. Assemblage ophiolitique de Baer-Bassit et termes éffusives du volcano-sedimentaire. *Trav. Doc. ORSTROM*, 72. pp.333.

PARROT, J-F. 1980. The Baër-Bassit (Northwestern Syria) ophiolitic area. *Ofioliti.* **2**, 279-295.

PARROT, J. F. & DELAUNE-MAYERE, M. 1974. Les terres d'ombre du Bassit (nord-ouest syrien). Comparison avec les termes similaires du Troodos (Cypre). *Cahiers Orstrom Série Géologie*, Vol. 6, 127-159.

PARROT, J-F. and VATIN-PERIGNON, N. 1974. Répartition de quelques elements en trace dans les différentes roches effusives de la region ophiolitique du Nord-ouest Syrien. *Cah. ORSTOM, sér. Géol.*, **6**, 2, 185-226.

PEARCE, J. A. & CANN, J. 1973. Tectonic setting of basic volcanic rocks using trace element analysis. *Earth Planetary Science Letters*, Vol. 19, p. 290-300.

PEARCE, J. A., LIPPARD, S. J. and ROBERTS, S. 1984. Characteristics and tectonic significance of supra-subduction zone ophiolites. In: Kokelaar, B. P. and Howells, M. F. (Eds), *Marginal Basin Geology.* Geological Society London Specia; Publication, Vol. 16, p. 77-89.

PESSAGNO, E. A. 1976. Radiolarian zonation and stratigraphy of the Upper Cretaceous portion of the Great Valley Sequence, California Coast Ranges, *Micropaleontology, Special Publication*, 2, p. 1-95.

PESSAGNO, E. A. 1977. Lower Cretaceous radiolarian biostratigraphy of the California Coast Ranges. *Cushman Foundation, Special Publication*, 15, p. 1-87.

PISKIN, O. 1986. Carte Géologique du Hatay et du NW-Syrien. *Ofioliti*, Vol. 11.

PIŞKIN, O., DELALOYE, M., SELÇUK and WAGNER, J. –J. 1986. Guide to Hatay geology (SE Turkey). *Ofioliti*, Vol. 11, p. 87-104.

PREMOLI-SILVA, I. & SLITER, W. V. 1999. Cretaceous paleoceanography: Evidence from planktonic foraminiferal evolution. *Geological Society of America, special paper*, 332, p. 301-328.

PRICHARD, H. M. & MALIOTIS, G. 1998. Gold mineralization associated with low-temperature, off-axis, fluid activity in the Troodos ophiolite, Cyprus. *Journal Geological Society London*, Vol. 155:2, p. 223-231.

RAVIZZA, G., BLUSZTAJN, J. & PRICHARD, H. M. 2001. Re-Os systematics and platinum group element distribution in metalliferous sediments from the Troodos ophiolite. *Earth Planetary Science Letters*, Vol. 188, p. 369-381.

PRICHARD, H. M. and MALIOTIS, G. 1998. Gold mineralization associated with low-temperature, off-axis, fluid activity in the Troodos ophiolite, Cyprus. *Jour. Geol. Soc. London*, **155**, 2, 223-231.

RICHARDS, H. G. & BOYLE, J. F. 1986. Origins, alteration and mineralization of interlava metalliferous sedimnets of the Troodos Ophiolite, Cyprus. In: Gallagher, M. J. (ed)., *Metallurgy of basic and ultrabasic rocks*. Institute Mining Metallurgy London, p. 22-31.

RICOU, L. –E. 1971. Le croissant ophiolitique peri-arabe, une ceinture de nappes mises en place au Cretacé supérieur: *Revue Géographie Physique Géologie Dynam.*, Vol. 13, p. 327-349.

RICOU, L. E., MARCOUX, J. and WHITECHURCH, H. 1984. The Mesozoic organization of the Taurides: one or several ocean basins? In Dixon, J. E. & Robertson, A. H. F. (Eds), *The Geological Evolution of the Eastern Mediterranean.* Geological Society Special Publication, London, 17: p. 349-359.

ROBASZYNSKI, F. & CARON, M. 1995. Foraminifères planctoniques du Crétacé: commentaire de la zonation Eurpoe-Méditérranée. *Boll. Soc. Géol. France*, Vol. 166, p. 681-692.

ROBASZYNSKI, F., CARON, M., GONZALEZ DONOSO, J. M. and WONDERS, A. A. H., & European Working Group on Planktonic Foraminifera. 1984. Atlas of Late Cretaceous globotruncanids. *Revue de Micropaléontologie*, vol. 26, p. 145-305, pls. 1-54.

ROBERTS, S. 1992. Influence of the partial melting regime on the formation of ophiolitic chromite. In: Parson, L. M., Murton, B. J. and Browning, P. (Eds), *Ophiolites and their Modern Oceanic Analogues*, Geological Society London Special Publication, Vol. 60, p. 203-218

ROBERTSON, A. H. F. 1975. Cyprus umbers: basalt sedimentation relationships on a Mesozoic ocean ridge. *Journal Geological Society London*, Vol. 131, p. 511-531.

ROBERTSON, A. H. F. 1986. Geochemistry and tectonic implications of metalliferous and volcaniclastic sedimentary rocks associated with late ophiolitic extrusives in the Hatay area, southern Turkey. *Ofioliti*, Vol. 11, p. 121-140.

ROBERTSON, A. H. F. 1986b. The Hatay Ophiolite (Southern Turkey) in its Eastern Mediterranean Tectonic Context: A report on some aspects of the field excursion. *Ofioliti*, Vol. 11, p. 105-119.

ROBERTSON, A. H. F. 1990. Tectonic evolution of Cyprus. In Malpas, J., Moores, E. M., Panayiotou, A. and Xenophontos, C. (Eds), *Ophiolites Oceanic Crustal Analogues.* Proceedings Symposium. "Troodos 1987". Geological Durvey Department, Cyprus. p.235-252.

ROBERTSON, A. H. F. 1998. Mesozoic-Tertiary tectonic evolution of the easternmost Mediterranean area: Integration of marine and land evidence. in: Robertson, A. H. F., Emeis, K.-C., Richter, C. and Camerlenghi, A. (Eds), 1998. *Proceedings of the Ocean Drilling Program, Scientific Results*, Vol. 160; p. 723-783.

ROBERTSON, A. H. F. 2002. Overview of the genesis and emplacement of Mesozoic ophiolites in the Eastern Mediterranean Tethyan Region. *Lithos*, Vol. 65, p. 1-67.

ROBERTSON, A. H. F. & HUDSON, J. D. 1973. Cyprus umbers: chemical precipitates on a Tethyan ocean ridge, *Earth Planetary Science Letters*, Vol. 18, p. 93-101.

ROBERTSON, A. H. F. & HUDSON, J. D. 1974. Pelagic sediments in the Cretaceous and Tertiary history of the Troodos Massif, Cyprus. *Special Publication International Association Sedimentologists*, Vol. 1, p. 403-436.

ROBERTSON, A. H. F. & WOODCOCK, N. H. 1983. Zabyat Formation: sedimentation onto an emplacing ophiolite. *Sedimentology*, Vol. 30, p. 105-116.

ROBERTSON, A. H. F. & XENOPHONTOS, C. 1983. Development of concepts concerning the Troodos ophiolite and adjacent units in Cyprus. In Prichard, H. M., Alabaster, T., Harris, N. B. and Neary, C. R. (Eds), *Magmatic Processes and Plate Tectonics.* Geological Society Special Publication, London, 70: p. 85-120.

ROBERTSON, A. H. F. & DIXON, J. E. 1984. Introduction. In Dixon, J. E. & Robertson, A. H. F. (Eds), *The Geological Evolution of the Eastern Mediterranean.* Geological Society Special Publication, London, 17: p. 1-74.

ROBERTSON, A. H. F. WOODCOCK, N. H. 1984. The SW segment of the Antalya Complex, Turkey, as a Mesozoic-Tertiary Tethyan continental margin. In Dixon, J. E. & Robertson, A. H. F. (Eds), *The Geological Evolution of the Eastern Mediterranean.* Geological Society Special Publication, London, 17: p. 251-272

ROBERTSON, A. H. F. & SHALLO, M. 2000. Mesozoic-Tertiary tectonic evolution of Albanian in its regional Eastern Mediterranean context. *Tectonophysics*. Vol. 316, p. 197-214.

ROBERTSON, A. H. F., SEARLE, M. P. and RIES, A.C. (Eds). *The Geology and Tectonics of the Oman Region*, Geological Society special Publication, 49, pp. 845.

ROCCI, G., OHNENSTATTER, D. and OHNENSTATTER, M. 1975. The duality of Tethyan ophiolites. *Petrology*, Vol. 1, p. 172-174.

RONA, P. A. 1980. TAG hydrothermal field: mid-Atlantic Ridge crest at latitude at 26°N. *Journal Geological Society London*, Vol. 137, p. 385-402.

ROSENBAUM, G., LISTER, G. S. and DUBOZ, C. 2002. Relative Motions of Africa, Iberia and Europe during Alpine Orogeny. *Tectonophysics*, Vol. 359: p. 117-129.

SANFILIPPO, A. and RIEDEL, W. R. 1985. Cretaceous Radiolaria. In: Bolli, H. M., Saunders, J. B. and Perch-Nielson, K., Eds., *Plankton Stratigraphy*. Cambridge University Press, 1: 573-630.

SAVOTSIN, L. A., SIBUET, J. -C., ZONENSHAIN, L. P., LE PICHON, X. and ROULET, M. –J. 1986. Kinematic evolution of the Tethys belt from the Atlantic Ocean to the Pamirs since the Trias. *Tectonophysics*, Vol. 123; p. 1-35.

SAVU, H. 1980. Ophiolitic rocks and other initial magmatites in the Carpathians. *Ofioliti*, Vol. 1, p. 97-103.

ŞENGÖR, A. M. C., YILMAZ, Y. and KETIN, I. 1980. Remnants of a pre-Late Jurassic ocean in northern Turkey: fragments of a Permian-Triassic Paleo-Tethys? *Geological Society America Bulletins*, Vol. 91, p. 599-609.

SENGÖR, A. M. C. & YILMAZ, I. 1981. Tethyan evolution of Turkey: a plate tectonic approach. *Tectonophysics*. Vol. 75, p. 81-241.

ŞENGÖR, A. M. C., YILMAZ, Y. and SÜNGÜRLÜ, O. 1984. Tectonics of the Mediterranean Cimmerides: nature and evolution of the western termination of Palaeo-Tethys. In Dixon, J. E. & Robertson, A. H. F. (Eds), *The Geological Evolution of the Eastern Mediterranean.* Geological Society Special Publication, London, 17: p. 77-112.

SHALLO, M., KODRA, A. and GJATA, K. 1990. Geotectonics of the Albanian ophiolites. In: Malpas, J., Moores. E. M., Panayiotou, A., Xenophontos, C. (Eds), *Ophiolites, Oceanic Crustal Analogues*, Geological Survey Department, Nicosia, Cyprus, p. 265-270.

SHERIDAN, R. E. 1987. Pulsation tectonics as the control of continental breakup. *Tectonophysics*, Vol. 143, p. 59-73.

SMITH, A. G. 1993. Tectonic significance of the Hellenic-Dinaric ophiolites. In: Pritchard, H. M., Alabaster, T., Harris, N. B. W. and Neary, C. R. (Eds), *Magmatic Processes and plate Tectonics.* Geological Society London Special Publications.

SPRAY, J. G., BÉBIEN, J., REX, D. C. & RODDICK, J. C. 1984. Age constraints on the igneous and metamorphic evolution of the Hellenic-Dinaric ophiolites. In Dixon, J. E. & Robertson, A. H. F. (Eds), *The Geological Evolution of the Eastern Mediterranean.* Geological Society London Special Publication, 17: p. 619-628.

STAMPFLI, G. M. & BOREL, G. D. 2002. A plate tectonic model for the Paleozoic and Mesozoic constrained by dynamic plate boundaries and restored synthetic oceanic isochrons. *Earth and Planetary Science Letters*, Vol. 196: p. 17-33.

STEININGER, F. F. & RÖGEL, F. 1984. Paleogeography and palinspatic reconstruction of the Neogene of the Mediterranean and Paratethys. In Dixon, J. E. & Robertson, A. H. F. (Eds), *The Geological Evolution of the Eastern Mediterranean.* Geological Society Special Publication, London, 17: p. 659-668.

STEINMANN, G. 1905. Geologische Beobachtungen in den Alpen, II; Die schardtsche Überfaltungs, Theorie und die geologischen Bedeutung der Tiefseeabsätze und der ophiolitische massengesteine, *Ber. Naturforsch. Ges. Frieburgi Br.*, Vol. 16, p. 44-65.

STEINMANN, G. 1927. Die ophiolitischen Zonen in der mediterranean Kettingebirgen, *International Geology Congress 14th*, Vol. 2, p. 638-667.

SWARBRICK, R. E. & NAYLOR, M. A. 1980. The Kathikas Melange, southwest Cyprus: late Cretaceous submarine debris flows. *Sedimentology*, Vol. 27, p. 63-78.

TANKUT, A. 1984. Basic and ultrabasic rocks from the Ankara Melange. In: Dixon, J. E. & Robertson, A. H. F. (Eds), *The Geological Evolution of the Eastern Mediterranean.* Geological Society London Special Publication, 17: p. 449-454.

TANKUT, A. & GORDON, M. P. 1990. Geochemistry of a mafic-ultramafic body in the Ankara melange, Anatolia, Turkey: Evidence for a fragment of oceanic lithosphere. In: Malpas, J., Moores, E. M., Panayiotou, A. and Xenophontos, C. (Eds) *Ophiolites, Oceanic Crustal Analogues.* Geological Survey Dept., Cyprus, Nicosia, p. 339-349.

THUIZAT, R., WHITECHURCH, H., MONTIGNY, R. and JUTEAU, T. 1981. K-Ar dating of some intra-ophiolite metamorphic soles from the East Mediterranean: new evidence for oceanic thrusting before obduction. *Earth Planetary Science Letters*, Vol. 52, p. 302-310.

TIPPIT, P. R. & PESSAGNO, E. A. 1981. The stratigraphy of sediments in the volcanic unit of the Semail ophiolite. *Journal Geophysical Research*, Vol. 86, p. 2756-2762.

URQUHART, E. and BANNER, F. T. 1991. Biostratigraphy of the supra-ophiolite sediments of the Troodos Massif, Cyprus: the Cretaceous Perapedhi, Kannaviou, Moni and Kathikas formations. *Geology Magazine*, Vol. 131, p. 499-581. Supra-ophiolite bistratigraphy, Cyprus.

USTAÖMER, T. & ROBERTSON, A. H. F. 1997. Tectonic–sedimentary evolution of the north Tethyan margin in the Central Pontides of northern Turkey. In: Robinson, A. G. (Ed), *regional and Petroleum Geology of the Black Sea and the Surrounding Region.* AAPG Memoirs, Vol. 68, p. 255-290.

VIDAL, N., ALVAREZ-MARRON, J. and KLAESCHEN, D. 2000. Internal configuration of the Levantine Basin from seismic reflection data (eastern Mediterranean). *Earth and Planetary Science Letters*, Vol. 180: p. 77-89.

VUAGNAT, M. 1963. Remarques sur la trilogie serpentinite-gabbro-diabases dans le bassin de la Méditerranée occidentale, *Geol. Rundsch.*, Vol. 53, p. 336-358.

VOGT, P. R. 1924. Role of Fe in the origin of ultramafic magma, *Skr. Nor. Vidensk. Acad. Kl. I. Mat. Naturvidensk. Kl.*, Vol. 15, p. 97

WALLEY, C. D. 1998. Some outstanding issues in the geology of Lebanon and their importance in the tectonic evolution of the Levantine region. *Tectonophysics*, Vol. 298: p. 37-62.

WHITECHURCH, H. 1977. Les roches métamorphiques infraperidotitiques du Baer-Bassit (NW Syrien), temoins de l'écaillage intraocéanique téthysien. Étude pétrologique et structurale, Thesis (unpublished), Nancy University, France, 194 pp.

WHITECHURCH, H. and PARROT, J-F. 1974. Les écailles métamorphiques infrapéridotitiques du Baér-Bassit (Nord-ouest de la Syrie). *Cah. ORSTOM, sér. Géol.*, **6**, 2, 173-184.

WHITECHURCH, H., JUTEAU, T. and MONTIGNY, R. 1984. Role of the Eastern Mediterranean ophiolites (Turkey, Syria, Cyprus) in the history of the Neo-Tethys. In: Dixon, J. E. & Robertson, A. H. F. (Eds), *The Geological Evolution of the Eastern Mediterranean.* Geological Society London Special Publication, 17: p. 301-318.

YILMAZ, Y., TÜYSÜZ, O., YIĞITBAŞ, E. GENÇ, S. C. and SENGÖA. M. C. 1997. Geology and tectonic evolution of the Pontides. In: Robinson, A. G. (Ed), *regional and Petroleum Geology of the Black Sea and the Surrounding Region.* AAPG Memoirs, Vol. 68, p. 183-226.

APPENDICES

APPENDIX 1.1 PROCESSING METHODS

Foraminifera

Where samples were soft enough standard washing techniques over a 63μm sieve were employed.

If samples were too hard for washing, or if larger benthic foraminifera were present, then thin-sections were made.

Nannofossils

Simple smear slides were made of all samples with a carbonate content.

Radiolaria

Radiolaria were extracted from carbonaceous samples by dissolution of the carbonate using concentrated HCL, and then washing over a 45μm sieve.

Radiolaria were extracted from the umbers using standard washing techniques over a 45μm sieve. The coarse fraction was then further processed using the method illustrated below, adapted from Pessagno and Newport, 1971.

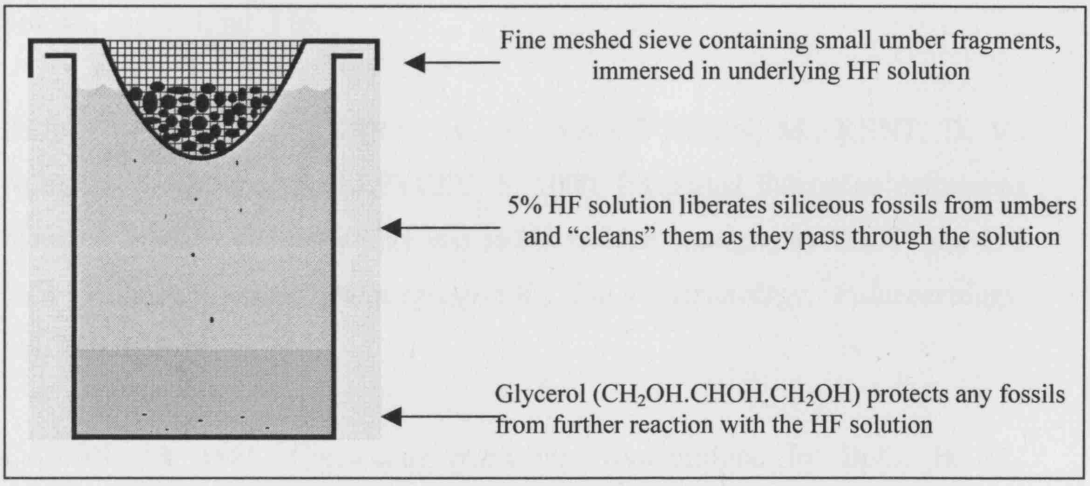

Sketch of the apparatus used to liberate siliceous microfossils from the umbers.

Palynology

Standard palynomorphs were sought standard palynological processing techniques were employed (see Travers 1988).

APPENDIX 1.2 TAXONOMIC LITERATURE

Below is a list of key taxonomic literature used for the identification of the microfossils discussed in the project, as well as regional biostratigraphic literature which have not been cited in the main body of the text.

ABDEL-KIREEM, M.R. and ABDOU, H. F. 1984. Upper Cretaceous - Lower Tertiary Planktonic Foraminifera from South Galala Plateau, Eastern Desert, Egypt. *Revista Española de Micropaleontologia.* vol. 11, no. 2, p. 175-222.

ALMOGI-LABIN, A., REISS, Z., and CARON, M., 1986. Globotruncanidae from Israel. *Eclogae Geologicae Helvetiae*, vol. 79: p.849-895.

BARR, F. T., 1972. Cretaceous biostratigraphy and planktonic foraminifera of Libya. *Micropaleontology*, vol. 18, no. 1: p. 1-46.

BERGGREN, W. A. and NORRIS, R. D. 1997. Biostratigraphy, phylogeny and sytematics of Paleocene trochospiral planktic foraminifera. *Micropaleontology*, vol. 43, suppl. 1, pp. 116.

BERGGREN, W. A., AUBRY, M. –P., VAN FOSSEN, M., KENT, D. V., NORRIS, R. D. and QUILLÉVÉRÉ, F. 2000. Integrated Paleocene calcareous plankton magnetobiochronology and stable isotope stratigraphy DSDP Site 384 (NW Atlantic Ocean). *Palaeogeography, Palaeoclimatology, Palaeoecology*, vol. 159, p. 1-51.

CARON, M. 1985. Cretaceous planktonic foraminifera. In: Bolli, H. M., Saunders, J. B. and Perch-Nielson, K., Eds., *Plankton Stratigraphy*. Cambridge University Press, vol. 1: p. 17-86.

CHUNGKHAM, P. and CARON, M., 1996. Comparative study of the Late Maastrichtian (*A. Mayaroensis* Zone) foraminiferal assemblage from two distant parts of the Tethys Ocean: Semsales, Wildflysch Zone, Switzerland and Ukhrul, Mélange Zone, India. *Revue de Paléobiologie. Muséum d' Histoire Naturelle de Geneve, Suisse*, vol. 15, no. 2: p. 449-517.

CHUNGKHAM, P. and JAFAR, S. A., 1998. Late Cretaceous (Santonian-Maastrichtian) integrated Coccolith-Globotruncanid biostratigraphy of pelagic limestones from the accretionary prism of Manipur, north-eastern India. *Micropaleontology*, vol. 44, no. 1: p. 69-83.

DE WEVER, P., DUMITRICA, P., CAULET, J. P., NIGRINI, C. and CARIDROIT, M. 2001. *Radiolarians in the Sedimentary Record*, Gordon and Breach Scientific Publishers, pp. 533.

ELLIS, B. F., MESSINA, A. R., CHARMATZ, R. and RONAI, L. E. 1969. *Catalogue of Index Smaller Foraminifera*, Special Publication The American Museum of Natural History, New York. Vols. I, II, III.

EMPSON-MORIN, K. M. 1981. Campanian Radiolaria from DSDP Site 313, Mid-Pacific Mountains. *Micropaleontology*, vol. 27, no. 3: p.249-292.

EMPSON-MORIN, K. M. 1984. Depth and latitude distribution of Radiolaria in Campanian (Late Cretaceous) tropical and subtropical oceans. *Micropaleontology*, vol.30, no. 1: p. 87-119.

FOREMAN, H. P. 1968. Upper Maestrichtian Radiolaria of California. *Special Papers in Palaeotology*, no. 3, pp. 82.

GEORGESCU, M-D. 1996. Santonian-Maastrichtian planktonic foraminiferas (Globigerinelloididae, Hedbergellidae, Globotruncanidae and Rugoglobigerinidae) in the Romanian Black Sea offshore. *Micropaleontology*, vol. 42, p. 305-333.

HUBER, B. T. and BOERSMA, A. 1994. Cretaceous Origination of *Zeauvigerina* and its Relationship to Paleocene Biserial Planktonic Foraminifera. *Journal of Foraminiferal Research*, vol. 24, no. 4, p. 268-287.

JENKINS, D. G. 1985. Southern mid-latitude Paleocene to Holocene planktic foraminifera. In: Bolli, H. M., Saunders, J. B. and Perch-Nielson, K., Eds., *Plankton Stratigraphy*. Cambridge University Press, 263-282.

JENKINS, D. G. and MURRAY, J. W. (Eds). 1989. *Stratigraphical Atlas of Fossil Foraminifera*, second edition, Ellis Horwood Publishers Limited, pp. 593.

KASSAB, I. I. M. 1975. *Globotruncana falsocalcarata* Kerdany and Abdelsalam from northern Iraq. *Micropaleontology*, vol. 21, no. 3, p. 346-351.

KASSAB, I. I. M., 1976. Some Upper Cretaceous planktonic foraminiferal genera from northern Iraq. *Micropaleontology*. vol. 22, p. 215-238.

KELLER, G., ADATTE, T., STINNESBECK, W., LUCIANI, V., KAROUI-YAAKOUB, N. and ZAGHBIB-TURKI, D. 2002. Paleoecology of the Cretaceous-Tertiary mass extinction in planktonic foraminifera. *Palaeogeography, Palaeoclimatology, Palaeoecology*, vol. 178, p. 257-297.

KUCERA, M. and MALMGREN, B. A. 1996. Latitudinal variation in the planktic foraminifer *Contusotruncana contusa* in the terminal Cretaceous ocean. *Marine Micropaleontology*, vol. 28, p. 31-52.

KUCERA, M. and MALMGREN, B. A. 1998. Differences between evolution of mean form and evolution of new morphotypes: an example from Late Cretaceous planktonic foraminifera. *Paleobiology*, vol. 24, no. 1, p. 49-63.

KRASHENINNIKOV, V. A. and HOSKINS, R. H. 1973. Late Cretaceous, Paleogene and Neogene Planktonic Foraminifera. *Initial Results of the Deep Sea Drilling Project*, vol. 20, p. 105-187.

LOEBLICH, A. R. and TAPPAN, H. 1987. *Foraminiferal Genera and their Classification.* New York: Van Nostrand Reinhold Company. Vol I and II. pp. 1182.

LONGORIA, J. F. and VONFELDT, A. E., 1991. Taxonomy, phylogenetics and biochronology of single-keeled globotruncanids (Genus *Globotruncanita* Reiss). *Micropaleontology*, vol. 37, no 3: 197-243.

MALMGREN, B. A., 1991. Biogeographic patterns in terminal Cretaceous planktonic foraminifera from Tethyan and warm Transitional waters. *Marine Micropaleontology*, vol. 18. p. 73-99.

MANCINI, E. A., MARKHAM PUCKETT, T. and TEW, B. H. 1996. Integrated biostratigraphic framework for Upper Cretaceous strata of the eastern Gulf Coastal Plain, USA. *Cretaceous Research*, vol. 17, p. 645-669.

MASTERS, B. A., 1993. Re-evaluation of the species and subspecies of the genus *Plummerita* Brönnimann and a new species of *Rugoglobigerina* Brönnimann (Foraminiferida). *Journal of Foraminiferal Research*, vol. 23, no. 4, p. 267-274.

NAKKADY, S. E., 1950. A New foraminiferal fauna from the Esna shales and Upper Cretaceous chalk of Egypt. *Journal of Paleontology*, vol. 24, p. 675-692.

NEDERBRAGT, A. J. 1990. Biostratigraphy and paleoceanographic potential of the Cretaceous planktonic foraminifera Heterohelicidae. PhD Dissertation, Vrije Universiteit te Amsterdam, pp. 203, Centrale Huisdrukkerij Vrije Universiteit, Amsterdam.

NEDERBRAGT, A. J. 1991. Late Cretaceous biostratigraphy and the development of Heterohelicidae (planktic foraminifera). *Micropaleontology*, vol. 37, no. 4, p. 329-372.

NEDERBRAGT, A. J. 1998. Quantative biogeography of late Maastrichtian planktonic foraminifera. *Micropaleontology*, vol. 44, no 4, p. 385-412.

OLSSON, K. R., HEMLEBEN, C., BERGGREN, W. A. and HUBER, B. T. 1999. Atlas of Paleocene Planktonic Foraminifera. *Smithsonian Contributions to Paleobiology*, no. 85. pp. 252.

PESSAGNO, E. A. Jr, 1967. Upper Cretaceous Planktonic Foraminifera from the western Gulf Coast Plain. *Palaeontographica Americana*, vol. 5, no. 37, p. 245-445.

PESSAGNO, E. A. 1976. Radiolarian zonation and stratigraphy of the Upper Cretaceous portion of the Great Valley Sequence, California Coast Ranges, *Micropaleontology, Special Publication*, 2, p. 1-95.

PESSAGNO, E. A. 1977. Lower Cretaceous radiolarian biostratigraphy of the California Coast Ranges. *Cushman Foundation, Special Publication*, 15, p. 1-87.

PETRIZZO, M. R. 2000. Upper Turonian-lower Campanian planktonic foraminifera from southern mid-high latitudes (Exmouth Plateau, NW Australia): biostratigraphy and taxonomic notes. *Cretaceous Research*, vol. 21, p. 479-505.

PREMOLI SILVER, I. and SLITER, W. V., 1985. Cretaceous planktonic foraminiferal biostratigraphy and evolutionary trends from the Botacione section, Gubbio, Italy. *Paleontographica Italia*, vol. 82, p. 1-89.

PREMOLI-SILVA, I. & SLITER, W. V. 1999. Cretaceous paleoceanography: Evidence from planktonic foraminiferal evolution. *Geological Society of America, special paper*, 332, p. 301-328.

PREMOLI SILVA, I., SPEZZAFERRI, S. and D'ANGELANTONIO, A. 1998. Cretaceous Foraminiferal Bio-isotope Stratigraphy of Hole 967E and Paleogene Planktonic Foraminiferal Biostratigraphy of Hole 966F, Eastern Mediterranean. *Proceedings of the Ocean Drilling Program,* vol. 160, p377-394.

QUILTY, P. G. 1992. Upper Cretaceous Planktonic Foraminifers and Biostratigraphy, Leg 120, Southern Kerguelen Plateau. *Proceedings of the Ocean Drilling Program, Scientific Results*, vol. 120, p. 371-392.

RIEDEL, W. R. and SANFILIPPO, A. 1974. Radiolaria from the southern Indian Ocean, DSDP Leg 26. *Initial Results of the Deep Sea Drilling Project*, vol. 26, p. 771-813.

ROBASZYNSKI, F., CARON, M., GONZALEZ DONOSO, J. M. and WONDERS, A. A. H., & European Working Group on Planktonic Foraminifera. 1984. Atlas of Late Cretaceous globotruncanids. *Revue de Micropaléontologie*, vol. 26, p. 145-305, pls. 1-54.

ROBASZYNSKI, F. and CARON, M. 1995. Foraminifères planctoniques du Crétacé: commentaire de la zonation Europe-Méditerranée. *Bolletin Societié Geologique de France*, Vol. 1666, no. 6, p. 681-692.

SANFILIPPO, A. and RIEDEL, W. R. 1985. Cretaceous Radiolaria. In: Bolli, H. M., Saunders, J. B. and Perch-Nielson, K., Eds., *Plankton Stratigraphy*. Cambridge University Press, 1: 573-630.

SCOTT STAERKER, T. 1998. *Data Report:* Biostratigraphy of Eocene and Upper Cretaceous chalks from the Eratosthenes seamount Region in the Eastern Mediterranean Sea. *Proceedings of the Ocean Drilling Program,* vol. 160, p.395-401.

SLITER, W. V. 1989. Biostratigraphic zonation for the Cretaceous planktonic foraminifers examined in thin section. *Journal of Foraminiferal Research*, vol. 19, no. 1, p. 1-19.

SNYDER, S. W. and WATERS, V. J. 1985. Cenozoic Planktonic Foraminiferal Biostratigraphy of the Goban Spur Region, Deep Sea Drilling Project Leg 80[1]. *Initial Results of the Deep Sea Drilling Project*, vol. 80, p. 439-472.

TMALLA, A. F. A. 1996. Latest Maastrichtian and Palaeocene Planktonic Foraminiferal Biostratigraphy of Well A1a-NC29A, Northern Sirt Basin, Libya. P. 195-232.

TOURMARKINE, M. and LUTERBACHER, H., 1985. Paleocene and Eocene planktic foraminifera. In: Bolli, H. M., Saunders, J. B. and Perch-Nielson, K., Eds., *Plankton Stratigraphy*. Cambridge University Press, 1: 87-154.

VAN EIJDEN, A. J. M. and SMIT, J. 1991. Eastern Indian Ocean Cretaceous and Paleogene Quantative Biostratigraphy. *Proceedings of the Ocean Drilling Program, Scientific results*, vol. 121, p. 77-123.

WIDMARK, J. D. V. and SPEIJER, R. P. 1997. Benthic foraminiferal ecomarker species of the terminal Cretaceous (late Maastrichtian) deep-sea Tethys. *Marine Micropaleontology*, vol. 31, p. 135-156.

WONDERS, A. A. H., 1980. Middle and Upper Cretaceous planktonic foraminifera of the Western Mediterranean area. *Utrecht Micropaleontological Bulletins*, 24, 158pp, pls. 1-10.

WONDERS, A. A. H., 1992. Cretaceous planktonic foraminiferal biostratigraphy, Leg 122, Exmouth Plateau, Australia. *Proceedings of the Ocean Drilling Program, Scientific Results*, vol. 122, p. 587-599.

APPENDIX 1.3 SAMPLE LOCALITIES AND PROCESSING SUMMARY

Processing methods are as follows: W = Washing for foraminifera/general microfossils
R = Processing for radiolaria
P = Processing for palynoology
T-S = Thin section
Nannofossils slides were made for all samples.

Sample No.	Locality	Grid Reference	Lithology	Colour	Processing Method
11120.1	Latakia	35'29'49.2N/35'46'40.9E	calcarenite	yellow-brown	W
11120.2	Latakia	35'29'49.2N/35'46'40.9E	cemented marl	yellow-brown	W
11121.1	Latakia	35'29'49.2N/35'46'40.9E	cemented marl	pale grey	W
11121.2	Latakia	35'29'49.2N/35'46'40.9E	fine calcarenite	pale grey	W
11122	Kessab	35'55'44.5N/35'59'40.6	limestone	dark grey	T-S
11123	Kessab	35'55'44.5N/35'59'40.6	limestone	pale grey	T-S
11124	Kessab	35'55'44.5N/35'59'40.6	limestone	pale grey	W / R
11125	Kessab	35'55'27.5N/35'58'54.9/E	marl	grey-green	W / R
11126	Kessab	35'55'27.5N/35'58'54.9/E	marl	reddy-brown	W / R
11127	Kessab	35'55'27.5N/35'58'54.9/E	marl	grey-green	W / R
11128	Shaik Hassan	35'52'.078N/35'54'.318E	limestone	beige	T-S
11129	Shaik Hassan	35'52'.078N/35'54'.318E	limestone	beige	T-S
11130	Shaik Hassan	35'52'.078N/35'54'.318E	calcarenite	pale brown	T-S
11131	Shaik Hassan	35'52'.078N/35'54'.318E	limestone	pink	T-S
11132	Al-Wadi	35'49'.966N/35'55'.937E	limestone	dark grey	T-S
11133	Quiraanive	35'49,.318N/35'58.323E	limestone	beige	T-S
11134	Quiraanive	35'49,.318N/35'58.323E	limestone	beige	T-S
11135.1	Raas Al Bassit		conglomerate	brown	W
11135.2	Raas Al Bassit		conglomerate	brown	W
11136	Ain el Kebir	35'48'.156N/35'51.655E	marl	green	W
11137	Ain el Kebir	35'48'.156N/35'51.655E	calcarenite	beige	T-S
11138	Ain el Kebir	35'48'.156N/35'51.655E	chalk	pale yellow	W
11139	Ain el Kebir	35'48'.156N/35'51.655E	calcarenite	brown	T-S
11140	Ain el Kebir	35'48'.156N/35'51.655E	calcarenite	yellow	W
11141	Ain el Kebir	35'48'.156N/35'51.655E	chalk	white	W
11142	Al Ghas'saniyeh	35'48.703N/35'54.562E	conglomerate	brown	
11143	Al Ghas'saniyeh	35'48.703N/35'54.562E	conglomerate	brown	T-S
11144	El Kebir	35'49.851N/36'00.941E	conglomerate	pale beige	T-S
11145	Damate	35'43.183N/35'51.168E	chalk	beige	W
11146	Damate	35'43.183N/35'51.168E	marl	pale grey	W
11147	Damate	35'43.183N/35'51.168E	chalk	grey-green	W
11148	Damate	35'43.247N/35'51.776E	marl	grey-green	W
11149.1	Damate	35'43.247N/35'51.776E	chalk	beige	W
11149.2	Damate	35'43.247N/35'51.776E	marl	grey-green	W
11150.1	Damate	35'43.431N/35'51.739E	chalk	grey	W
11150.2	Damate	35'43.431N/35'51.739E	marl	dark grey	W
11151	Damate	35'43.716N/35'51.689E	chalk	pale yellow	W
11152	Damate	35'43.941N/35'51.545E	chert	brown	T-S
11153	Damate	35'43.941N/35'51.545E	shale	white	W
11154	Damate	35'43.941N/35'51.545E	chalk	white	W
11155	Damate	35'40.893N/35'47.270E	limestone	beige	T-S

11156	Damate	35'40.893N/35'47.270E	limestone	beige	
11157	Damate	35'40.893N/35'47.270E	chalk	beige	W
11158	Latakia depression	35'29.369N/36'09.084E	chalk	grey-beige	W
11159.1	Latakia depression	35'29.369N/36'09.084E	chalk	white	W
11159.2	Latakia depression	35'29.369N/36'09.084E	marl	green	W
11160	Latakia depression	35'28.939N/36'03.403E	chalk	pale grey	W
11161	Latakia depression	35'28.939N/36'03.403E	chalk	pale grey	W
11162	Latakia depression	35'28.939N/36'03.403E	chalk	beige	W
11163	Latakia depression	35'29.429N/36'03.328E	chalk	beige	W
11164	Latakia depression	35'29.804N/35'57.915E	mudstone	grey-brown	W
11165	Latakia depression	35'30.341N/36'00.451E	chalk	white	W
11166.1	Latakia depression	35'35.717N/35'53.887E	chalk	white	W
11166.2	Latakia depression	35'35.717N/35'53.887E	chalk	white	W
11167	Latakia depression	35'35.717N/35'53.887E	chalk	grey	W
11168	Latakia depression	35'36.829N/35'57.106E	marl	grey	W
11169	Latakia depression	35'47.400N/36'00.791E	chalk	beige	W
11170	Latakia depression	35'46.841N/36'02.717E	chalk	yellow	W
11171	Latakia depression	35'46.604N/36'02.894E	marl	grey	W
11172	Latakia depression	35'44.004N/36'04.141E	marl	beige-grey	W
11173	Latakia depression	35'43.966N/36'05.767E	chalk	white	
11174	Latakia depression	35'43.966N/36'05.767E	marl	grey	W
11175	Latakia depression	35'44.513N/36'06.015E	chalk	white	W
11176	Latakia depression	35'44.166N/36'06.819E	marl	pale brown	W
11177	Latakia depression	35'44.166N/36'06.819E	marl	pale grey	W
11178	Latakia depression	35'54.544N/36'12.707E	marl	pale brown	W
11179	Latakia depression	36'50.295N/36'13.683E	chalk	white	W
11180	Latakia depression	36'50.295N/36'13.683E	limestone	yellow	W
AP 1		35'40N/36'04E	Bituminous limestone	black/white	W
REB 1	Ein el Beida	35'38'11N/35'55'50E	Sandy limestone	beige	W
AGS 1	Al Ghas'saniyeh	35'48'48N/35'54'28E	Calcarenite	brown	T-S
AGS 2	Al Ghas'saniyeh	1	Calcarenite	pale brown	T-S
AGS 3	Al Ghas'saniyeh	1	Calcarenite	brown	T-S
AGS 4	Al Ghas'saniyeh	1	Calcarenite	yellow-grey	W
AGS 5	Al Ghas'saniyeh	35'48'44N/35'54'29E	Calcirudite	brown	T-S
ZUGH 1	Zerhine	35'43'55N/35'53'11E	marl	beige	W
ZUGH 2	Zerhine	35'43'55N/35'53'11E	marl	pale beige	W
ZUGH 3	Zerhine	35'43'55N/35'53'11E	sandy marl	pink-brown	W
ZUGH 4	Zerhine	35'44'02N/35'52'56E	hard limestone	grey-green	T-S
ZUGH 5	Zerhine	35'44'11N/25'53'15E	chalk	grey	W
ZUGH 6	Zerhine	35'43'48N/35'53'16E	soft marl	white-pale beige	W
ZUGH 7	Zerhine	35'43'48N/35'53'16E	hard marly limestone	pale grey-green	W
ZUGH 8	Zerhine	35'43'48N/35'53'16E	soft marl	pale grey	W
ZUGH 9	Zerhine	35'43'48'N/35'53'16E	soft marl	pale grey	W
ZUGH 10	Zerhine	35'43'48'N/35'53'16E	soft chalky marl	beige-pale grey	W
KANT 1	Kandil Jouk	35'44'24N/35'52'56E	chalky marl	beige-pale grey	W
BALL 1	Ballourane	35'45'55N/35'53'50E	hard marly limestone	grey-green	T-S
BALL 2	Ballourane	35'45'54N/35'53'45E	soft calcarenite	reddy brown	W
BALL 3	Ballourane	35'45'54N/35'53'45E	soft marly chalk	beige	W
BALL 4	Ballourane	35'45'54N/35'53'45E	sandy marl-calcarenite	beige	W
BALL 5	Ballourane	35'45'54N/35'53'45E	soft calcarenite	brown	W

BALL 6	Ballourane	35'45'54N/35'53'45E	calcarenite	pink-brown	T-S
BALL 7	Ballourane	35'45'54N/35'53'45E	marl	grey-green	W
BALL 8	Ballourane	35'45'54N/35'53'45E	marl	grey-green	W
CR2M 1	Kasbba	35'45'11N/36'10'51E	hard chalk	pale yellow-beige	W
CR2M 2	Kasbba	35'45'00N/36'09'38E	marl	pale blue/green - grey	W
CR2M 3	Kasbba	35'44'58N/36'10'32E	marly chalk	beige	W
CR2M 4	Kasbba	35'44'58N/36'10'32E	marl	grey-green	W
CR2M 5	Kasbba	35'45'03N/36'10'32E	marly chalk	beige	W
CR2M 6	Kasbba	35'45'12N/36'10'01E	soft chalky marl	yellow-beige	W
CR2M 7	Kasbba	35'44'59N/36'09'58E	hard chalky marl	grey-green	W
CR2M 8	Kasbba	35'44'49N/36'09'49E	chalk	pale beige-grey	W
CR2M 9	Kasbba	35'44'49N/36'09'49E	marly chalk	beige	W
OLIG 1		36'54'40.9N/36'21.057E	crumbly chalk	white	W
OLIG 2		36'54'40.9N/36'21.057E	crumbly chalk	white	W
NEW 1		35'42'02N/35'52'28E	hard marl	grey	W
NEW 2		35'42'12N/35'52'58E	marly chalk	beige	W
QUIR 1	Quiraanive	35'45'35N/35'53'33E	soft chalk	white	W
QUIR 2	Quiraanive	35'45'46N/35'53'12E	fine sandstone	grey-brown	W
QUIR 3	Quiraanive	35'45'46N/35'53'12E	hard marl	grey-green	T-S
QUIR 4	Quiraanive	35'45'58N/35'53'25E	soft marl	grey-green	W
QUIR 5	Quiraanive	35'45'58N/35'53'25E	mudstones and cherts	reddy brown	W
QUIR 6	Quiraanive	35'46'00N/35'53'28E	soft marl	grey-green	W
QUIR 7	Quiraanive	35'46'00N/35'53'28E	marl	grey-green	W
QUIR 8	Quiraanive	35'46'00N/35'53'28E	soft marl	grey-green	W
QUIR 9	Quiraanive	35'46'15N/35'53'38E	soft marl	pale yellow-green	W
QUIR 10	Quiraanive	35'46'15N/35'53'38E	marl	grey-brown	W
MARK 1	Markhous	35'39'59N/35'55'00E	hard chalk	white-pale grey	W
MARK 2	Markhous	35'39'59N/35'55'00E	conglomerate	blue-grey	T-S
MARK 3	Markhous	35'39'59N/35'55'00E	hard chalk	white	W
MARK 4	Markhous	35'39'54N/35'54'49E	hard marly chalk	grey-green	W
MARK 5	Markhous	35'39'50N/35'54'44E	hard chalk	white	W
MARK 6	Markhous	35'39'44N/35'54'27E	soft chalk	white	W
MARK 7	Markhous	35'39'52N/35'54'48E	soft chalk	white	W
MARK 8	Markhous	35'40'07N/35'54'48E	hard marly chalk	pale grey	W
DAMA 1	Damate	35'43'24N35'50'52E	marl	pale blue-grey	W
DAMA 2	Damate	35'43'15N/35'50'55E	marl	blue-grey	W
DAMA 3	Damate	35'43'15N/35'50'55E	calcarenite	beige	T-S
DAMA 4	Damate	35'43'00N/35'51'02E	soft marl	pale grey	W
DAMA 5	Damate	35'43'00N/35'51'02E	soft marl	medium grey	W
DAMA 6	Damate	35'43'00N/35'51'02E	hard marl	medium grey	W
DAMA 7	Damate	35'43'00N/35'51'02E	hard marl	medium grey	W
DAMA 8	Damate	35'43'00N/35'51'02E	soft marl	medium grey	W
DAMA A	Damate	35'43'13N/35'51'46E	marly chalk	grey-green	W
DAMA B	Damate	35'43'15N/35'51'44E	soft marl	grey-green	W
DAMA C	Damate	35'43'16N/35'51'31E	marl	grey-green	W
DAMA D	Damate	35'43'14N/35'51'15E	hard marl	medium grey	W
DAMA E	Damate	35'43'14N/35'51'15E	marl	medium grey	W
DAMA F	Damate	35'43'14N/35'51'15E	soft marl	brown	W
DAMA G	Damate	35'43'14N/35'51'15E	hard marl	brown	W

DAMA H	Damate	35'43'14N/35'51'15E	hard marl	grey-green	W
DAMA I	Damate	35'43'14N/35'51'15E	hard marl	grey-green	W
BEIT 1	Beit Nasser	35'41'18N/35'54'03E	soft marl	pale beige-grey	W
BEIT 2	Beit Nasser	35'41'11N/35'54'18E	soft marl	medium beige	W
BEIT 3	Beit Nasser	35'41'11N/35'54'18E	soft marl	medium grey-green	W
BEIT 4	Beit Nasser	35'41'28N/35'54'30E	soft marl	beige	W
UMM 1	Umit'tiur	35'45'48N/35'51'13E	marl	grey	W
UMM 2	Umit'tiur	35'45'48N/35'51'27E	hard, rubbly chalk	white	W
UMM 3	Umit'tiur	35'45'55N/35'51'31E	calcarenite	brown	W
UMM 4	Umit'tiur	35'45'30N/35'51'03E	hard sandy limestone	yellow	T-S
KESS 1	Kessab	35'55'26N/35'58'53E	hard limestone	yellow	T-S
KESS 2	Kessab	35'55'26N/35'58'53E	hard sandy limestone	yellow	T-S
KESS 3	Kessab	35'55'26N/35'58'53E	soft calcareous sandstone	orange	W
KESS 4	Kessab	35'55'26N/35'58'53E	marly limestone	pale yellow-grey	T-S / R
KESS 5	Kessab	35'55'26N/35'58'53E	marly limestone	medium grey	T-S / R
KESS 6	Kessab	35'55'26N/35'58'53E	marly limestone	grey-orange	T-S / R
KESS 7	Kessab	35'55'26N/35'58'53E	marl	grey-green	W / R
KESS 8	Kessab	35'55'26N/35'58'53E	marl	grey-green	W / R
KESS 9	Kessab	35'55'26N/35'58'53E	marl	pale grey-green	W / R
KESS 10	Kessab	35'55'26N/35'58'53E	marl	blue-grey	W / R
KESS 11	Kessab	35'55'26N/35'58'53E	soft marl	blue-grey	W / R
BADR 1	Badroussiyeh	35'53'59N/35'53'19E	marl	grey-green	W
BADR 2	Badroussiyeh	35'53'59N/35'53'19E	hard marl	green	T-S
BADR 3	Badroussiyeh	35'53'59N/35'53'19E	hard marly limestone	grey-green	T-S
BADR 4	Badroussiyeh	35'53'59N/35'53'19E	hard marly limestone	grey-green	T-S
BADR 5	Badroussiyeh	35'53'59N/35'53'19E	marl	grey-green	T-S
DPH 1	Qafar Fawkani	35'43'28.1N/35'51'44.5E	marl	beige	W
DPH 2	Qafar Fawkani	l	marl	beige	W
DPH 3	Qafar Fawkani	l	marl	beige	W
DPH 4	Qafar Fawkani	l	marl	beige	W
DPH 5	Qafar Fawkani	l	marl	beige	W
DPH 6	Qafar Fawkani	l	marl	beige	W
DPH 7	Qafar Fawkani	l	marl	beige	W
DPH 8	Qafar Fawkani	l	marl	beige	W
DPH 9	Qafar Fawkani	l	marl	beige	W
DPH 10	Qafar Fawkani	35'43'32.0N/35'51'44.9E	marl	beige	W
DPH 11	Qafar Fawkani	l	marl	medium grey	W
DPH 12	Qafar Fawkani	l	marl	grey	W
DPH 13	Qafar Fawkani	l	marl	beige	W
DPH 14	Qafar Fawkani	l	marl	blue-grey	W
DPH 15	Qafar Fawkani	l	marl	pale blue	W
DPH 16	Qafar Fawkani	l	marl	pale grey	W
DPH 17	Qafar Fawkani	l	marl	pale grey	W
DPH 18	Qafar Fawkani	l	marl	dark grey	W

DPH 19	Qafar Fawkani	1	marl	brown	W
DPH 20	Qafar Fawkani	35'43'36.6N/35'51'40.6E	marl	brown	W
DPH 21	Qafar Fawkani	1	marl	pale grey	W
DPH 22	Qafar Fawkani	1	marl	dark grey	W
DPH 23	Qafar Fawkani	1	marl	beige	W
DPH 24	Qafar Fawkani	1	marl	beige	W
DPH 25	Qafar Fawkani	1	marl	beige	W
DPH 26	Qafar Fawkani	1	marl	beige	W
DPH 27	Qafar Fawkani	1	marl	beige	W
DPH 28	Qafar Fawkani	1	marl	beige	W
DPH 29	Qafar Fawkani	1	marl	beige	W
DPH 30	Qafar Fawkani	35'43'46.5N/35'51'38.6E	marl	beige	W
DPH 31	Qafar Fawkani	1	marl	beige	W
DPH 32	Qafar Fawkani	1	marl	beige	W
DPH 33	Qafar Fawkani	1	marl	beige	W
DPH 34	Qafar Fawkani	1	marl	beige	W
DPH 35	Qafar Fawkani	1	marl	beige	W
DPH 36	Qafar Fawkani	1	marl	beige	W
DPH 37	Qafar Fawkani	1	marl	beige	W
DPH 38	Qafar Fawkani	1	marl	beige	W
DPH 39	Qafar Fawkani	1	marl	beige	W
DPH 40	Qafar Fawkani	35'43'59.2N/35'51'35.3E	paper shales	white	W
MAZZ 1	Mazzra	38'48'53N/35'57'18E	umber	dark brown	W / R / P
MAZZ 2	Mazzra	38'48'24N/35'57'23E	clay and mudstone	purple/green	W / R
MAZZ 3	Mazzra	38'48'53N/35'57'18E	umber	black/white	W / R / P
MAZZ 4	Mazzra	38'48'53N/35'57'18E	umber	terracotta	W / R / P
ALBAL 1	Al Baluta	35'49'45N/35'52'61E	calcareous cement	grey-green	W / R / P
AOU 1	Beit Aouane	35'45'09N/35'58'27E	calcareous cement	white-pink	W / R
AOU 2	Beit Aouane	35'45'09N/35'58'27E	calcareous cement	white-pink	W / R
EK 1	Kessab	35'55'72N/35'59'77E	limestone	beige	R
EK 2	Kessab	35'55'72N/35'59'77E	limestone	beige	R
EK 3	Kessab	35'55'72N/35'59'77E	limestone	medium grey	R
FELL 1	Fellah	35'48'97N/35'53'55E	calcareous cement	pink-brown	W
GHAS 1	Al Ghas'saniyeh	35'48.703N/35'54.562E	calcarenite	brown	W
DEF 1	Deflah	35'49'54N/35'51'88E	umber	purple-brown	W / R / P
DEF 2	Deflah	35'49'54N/35'51'88E	umber	purple-brown	W / R / P
DEF 3	Deflah	35'49'54N/35'51'88E	umber	purple-brown	W / R / P
DEF 4	Deflah	35'49'54N/35'51'88E	umber	purple-brown	W / R / P

APPENDIX 1.4 SAMPLE CONTENTS

KANT 1	ZUGH 10	ZUGH 9	ZUGH 8	ZUGH 7	ZUGH 6	ZUGH 4	ZUGH 3	ZUGH 2	ZUGH 1	AGS 4	11163	11162	11161	11160	11158	11150.2	11149.2	11148	11147	11146	11127	11126	11125	11122	
			X																						*Abathomphalus mayaroensis*
								X				X										X	X		*Arcgaeoglobigerina blowi*
								X							X								X		*Archaeoglobigerina cretacea*
																									Clavihedbergella sp.
		X	X		X							X		X	X										*Contusotruncana contusa*
X						X		X	X	X		X			X						X	X	X		*Contusotruncana fornicata*
																									Contusotruncana patelliformis
																									Contusotruncana plicata
																									Contusotruncana walfischensis
																									Farusella washitensis
	X	X	X		X	X						X					X		X	X		X			*Gansserina gansseri*
																									Gansserina wiedenmayeri
																									Globigerinelloides blowi
											X		X									X	X		*Globigerinelloides prairehillensis*
	X						X					X			X							X			*Globigerinelloides subcarinatus*
								X														X			*Globigerinelloides sp.*
																							X		*Globigerinelloides ultramicrus*
																					X				*Globigerinelloides volutus*
X	X	X					X			X	X	X	X	X	X		X		X		X	X	X		*Globotruncana aegyptica*
X	X	X	X		X		X	X	X	X	X	X	X	X	X		X	X			X	X	X		*Globotruncana arca*
													X		X						X				*Globotruncana bulloides*
X	X	X	X		X							X	X	X	X						X	X	X		*Globotruncana falsostuarti*
																					X				*Globotruncana lapparenti*
															X							X			*Globotruncana linneiana*
																						X			*Globotruncana rosetta*
																					X				*Globotruncana rugosa*
X		X	X	X					X												X	X	X		*Globotruncana sp*
										X					X										*Globotruncana ventricosa*
X											X	X													*Globotruncanella citae*
X																	X								*Globotruncanella havanensis*
								X			X	X		X			X								*Globotruncanella petaloidea*
																							X		*Globotruncanella sp.*
																					X		X		*Globotruncanita angulata*
																									Globotruncanita calcarata
		X	X														X		X				X		*Globotruncanita conica*
													X	X											*Globotruncanita elevata*
X	X	X	X		X		X	X		X	X	X	X	X	X										*Globotruncanita stuarti*
X	X	X	X		X	X	X		X	X	X	X	X	X	X		X								*Globotruncanita stuartiformis*
												X	X												*Globotruncanita subspinosa*
X	X		X	X					X		X			X								X			*Globotruncanita sp.*
X											X			X	X								X		*Hedbergella holmdelensis*

KANT 1	ZUGH 10	ZUGH 9	ZUGH 8	ZUGH 7	ZUGH 6	ZUGH 4	ZUGH 3	ZUGH 2	ZUGH 1	AGS 4	11163	11162	11161	11160	11158	11150.2	11149.2	11148	11147	11146	11127	11126	11125	11122	
																									Hedbergella monmouthensis
																						X		X	*Hedbergella sp.*
X	X	X	X	X	X		X				X	X	X	X	X		X		X	X	X	X	X		*Heterohelix globulosa*
																									Heterohelix labellosa
												X			X						X	X	X		*Heterohelix navarroensis*
																									Heterohelx planata
																						X			*Heterohelix punctulata*
		X	X				X	X			X		X	X											*Heterohelix striata*
			X	X	X		X		X		X												X		*Heterohelix sp.*
																					X	X			*Laeviheterohelix sp.*
								X			X														*Planoglobulina acervulinoides*
										X															*Planoglobulina sp.*
						X																			*Planohedbergella sp.*
																									Plummerita hantkenoides
	X	X			X							X		X	X		X		X	X	X	X	X		*Psudoguembelina costulata*
			X									X		X	X		X								*Pseudoguembelina excolata*
																									Psedoguembelina hariaensis
																									Pseudoguembelina kempensis
											X				X										*Pseudoguembelina palpebra*
																				X		X			*Pseudoguembelina sp.*
X	X	X	X	X	X			X		X	X			X	X				X		X		X		*Pseudotextularia elegans*
	X	X			X																				*Pseudotextularia intermedia*
															X										*Pseudotextularia nutalli*
					X																				*Racemiguembelina fructicosa*
																									Racemiguembelina powelli
																									Rotalipora montsalvensis
																									Rotalipora sp.
X	X			X	X		X					X	X		X		X								*Rugoglobigerina hexacamerata*
		X													X				X						*Rugoglobigerina macrocephala*
																									Rugoglobigerina reichali
X	X	X	X	X			X	X		X	X		X	X	X	X	X		X		X	X	X		*Rugoglobigerina rugosa*
																									Rugoglobigerina scotti
X			X	X		X		X	X						X							X			*Rugoglobigerina sp.*
X		X	X		X		X				X	X	X												*Rugotruncana subcircumnodifer*
					X																				*Rugotruncana subpennyi*
					X			X		X												X	X		*Rugotruncana sp.*
																									Schackoina cenomana
								X																	*Schackoina multispinata*
																									Schackoina sp.

QUIR 8	QUIR 7	QUIR 6	QUIR 4	QUIR 3	QUIR 2	NEW 2	CR2M 9	CR2M 8	CR2M 7	CR2M 6	CR2M 5	CR2M 4	CR2M 3	CR2M 2	CR2M 1	BALL 8	BALL 7	BALL 6	BALL 5	BALL 3	BALL 2	BALL 1	
			X			X	X	X															*Abathomphalus mayaroensis*
																							Archaeoglobigerina blowi
																							Archaeoglobigerina cretacea
																							Clavihedbergella sp.
						X	X	X	X	X		X	X										*Contusotruncana contusa*
					X		X	X	X		X	X				X	X		X		X	X	*Contusotruncana fornicata*
																							Contusotruncana patelliformis
																							Contusotruncana plicata
								X															*Contusotruncana walfischensis*
																							Fansella washitensis
X		X	X				X													X			*Gansserina gansseri*
			X																				*Gansserina wiedenmayeri*
																							Globigerinelloides blowi
									X	X			X										*Globigerinelloides prairiehillensis*
		X	X							X	X	X	X										*Globigerinelloides subcarinatus*
							X									X							*Globigerineloides sp.*
												X											*Globigerinelloides ultramicrus*
																							Globigerinelloides volutus
X			X			X	X	X	X		X	X		X	X								*Globotruncana aegyptica*
			X			X	X	X	X	X	X	X	X	X	X	X	X		X	X		X	*Globotruncana arca*
				X						X		X											*Globotruncana bulloides*
		X						X	X		X		X	X	X		X						*Globotruncana falsostuarti*
																							Globotruncana lapparenti
									X													X	*Globotruncana linneiana*
					X																		*Globotruncana rosetta*
																							Globotruncana rugosa
			X						X						X	X	X			X			*Globotruncana sp*
																			X				*Globotruncana ventricosa*
													X										*Globotruncanella citae*
						X		X															*Globotruncanella havanensis*
		X	X			X		X	X	X	X	X	X										*Globotruncanella petaloidea*
																	X						*Globotruncanella sp.*
							X																*Globotruncanita angulata*
																							Globotruncanita calcarata
						X		X			X			X	X								*Globotruncanita conica*
																							Globotruncanita elevata
X		X	X			X	X	X	X	X	X	X	X	X		X	X						*Globotruncanita stuarti*
	X	X	X	X		X	X	X	X	X	X	X	X	X	X	X	X			X		X	*Globotruncanita stuartiformis*
																							Globotruncanita subspinosa
																	X			X			*Globotruncanita sp.*
			X			X	X			X		X	X										*Hedbergella holmdalensis*

QUIR 8	QUIR 7	QUIR 6	QUIR 4	QUIR 3	QUIR 2	NEW 2	CR2M 9	CR2M 8	CR2M 7	CR2M 6	CR2M 5	CR2M 4	CR2M 3	CR2M 2	CR2M 1	BALL 8	BALL 7	BALL 6	BALL 5	BALL 3	BALL 2	BALL 1	
																							Hedbergella monmouthensis
				X														X				X	*Hedbergella sp.*
X		X	X	X	X	X	X	X	X	X	X	X	X	X	X	X					X		*Heterohelix globulosa*
																							Heterohelix labellosa
		X										X											*Heterohelix navarroensis*
																							Heterohelix planata
																							Heterohelix punctulata
						X	X				X	X											*Heterohelix striata*
X				X			X							X									*Heterohelix sp.*
																							Laeviheterohelix sp.
																							Planoglobulina acervulinoides
																							Planoglobulina sp.
																							Planohedbergella sp.
																							Plummerita hantkenoides
							X				X	X	X										*Psudoguembelina costulata*
							X		X		X		X										*Pseudoguembelina excolata*
																							Psedoguembelina hariaensis
																							Pseudoguembelina kempensis
																							Pseudoguembelina palpebra
																							Pseudoguembelina sp.
X		X	X			X	X	X	X	X	X	X	X	X	X	X				X			*Pseudotextularia elegans*
						X		X			X												*Pseudotextularia intermedia*
						X																	*Pseudotextularia nuttalli*
X		X				X	X																*Racemiguembelina fructicosa*
																							Racemiguembelina powelli
																							Rotalipora montsalvensis
																							Rotalipora sp.
		X	X				X	X			X	X		X						X			*Rugoglobigerina hexacamerata*
														X									*Rugoglobigerina macrocephala*
																							Rugoglobigerina reicheli
	X	X	X			X	X	X		X	X	X	X	X	X	X	X		X	X			*Rugoglobigerina rugosa*
												X		X	X								*Rugoglobigerina scotti*
				X			X									X	X	X		X		X	*Rugoglobigerina sp.*
						X	X	X	X											X			*Rugotruncana subcircumnodifer*
						X	X		X						X								*Rugotruncana subpennyi*
																				X			*Rugotruncana sp.*
																							Schackoina cenomana
																							Schackoina multispinata
																							Schackoina sp.

BEIT 4	BEIT 3	BEIT 2	BEIT 1	DAMA I	DAMA H	DAMA G	DAMA F	DAMA E	DAMA D	DAMA C	DAMA B	DAMA A	DAMA 7	DAMA 6	DAMA 5	DAMA 4	MARK 8	MARK 4	MARK 3	MARK 1	
						X					X				X						*Abathomphalus mayaroensis*
																					Archaeoglobigerina blowi
																		X			*Archaeoglobigerina cretacea*
																					Clavihedbergella sp.
X	X		X			X		X		X								X	X		*Contusotruncana contusa*
X	X	X				X	X											X			*Contusotruncana fornicata*
																					Contusotruncana patelliformis
	X																				*Contusotruncana plicata*
																		X			*Contusotruncana walfischensis*
																					Favusella washitensis
X			X			X				X									X	X	*Gansserina gansseri*
X																			X		*Gansserina wiedenmayeri*
																					Globigerinelloides blowi
											X								X		*Globigerinelloides prairiehillensis*
	X	X									X						X		X		*Globigerinelloides subcarinatus*
																	X				*Globigerineloides sp.*
																					Globigerinelloides ultramicrus
																					Globigerinelloides volutus
X	X	X	X				X				X					X	X	X	X	X	*Globotruncana aegyptica*
X	X	X	X	X		X	X	X	X	X	X	X	X	X	X			X	X	X	*Globotruncana arca*
																					Globotruncana bulloides
						X					X								X	X	*Globotruncana falsostuarti*
																					Globotruncana lapparenti
																					Globotruncana linneiana
																					Globotruncana rosetta
																					Globotruncana rugosa
							X										X				*Globotruncana sp*
																					Globotruncana ventricosa
X																					*Globotruncanella citae*
X	X		X							X	X								X	X	*Globotruncanella havanensis*
X	X		X								X		X				X	X	X	X	*Globotruncanella petaloidea*
																				X	*Globotruncanella sp.*
																					Globotruncanita angulata
																					Globotruncanita calcarata
X	X		X		X	X		X										X		X	*Globotruncanita conica*
																					Globotruncanita elevata
X	X	X	X	X		X	X	X			X				X		X	X		X	*Globotruncanita stuarti*
X	X	X	X			X	X	X	X	X	X	X	X	X	X	X	X	X		X	*Globotruncanita stuartiformis*
																					Globotruncanita subspinosa
							X	X				X						X			*Globotruncanita sp.*
X	X	X															X	X	X		*Hedbergella holmdelensis*

BEIT 4	BEIT 3	BEIT 2	BEIT 1	DAMA I	DAMA H	DAMA G	DAMA F	DAMA E	DAMA D	DAMA C	DAMA B	DAMA A	DAMA 7	DAMA 6	DAMA 5	DAMA 4	MARK 8	MARK 4	MARK 3	MARK 1	
																					Hedbergella monmouthensis
																					Hedbergella sp.
X	X	X	X		X	X	X	X	X		X	X	X		X		X	X	X	X	*Heterohelix globulosa*
																					Heterohelix labellosa
X	X		X														X	X			*Heterohelix navarroensis*
																					Heterohelx planata
																					Heterohelix punctulata
X				X	X		X	X			X		X	X	X	X	X			X	*Heterohelix striata*
X			X			X	X	X	X	X		X		X			X			X	*Heterohelix sp.*
																					Laeviheterohelix sp.
																	X				*Planoglobulina acervulinoides*
																					Planoglobulina sp.
																					Planohedbergella sp.
																					Plummerita hantkenoides
X				X			X	X			X			X	X					X	*Psudoguembelina costulata*
																		X			*Pseudoguembelina excolata*
																					Psedoguembelina hariaensis
																					Pseudoguembelina kempensis
																					Pseudoguembelina palpebra
																					Pseudoguembelina sp.
X	X	X	X	X		X	X	X		X	X	X	X	X	X		X	X	X	X	*Pseudotextularia elegans*
		X	XX					X													*Pseudotextularia intermedia*
						X					X		X								*Pseudotextularia nutalli*
			X					X								X			X	X	*Racemiguembelina fructicosa*
																				X	*Racemiguembelina powelli*
																					Rotalipora montsalvensis
																					Rotalipora sp.
X			X	X		X		X									X	X		X	*Rugoglobigerina hexacamerata*
	X							X									X	X			*Rugoglobigerina macrocephala*
					X												X				*Rugoglobigerina reicheli*
X	X	X	X	X		X	X	X	X			X			X	X	X	X	X	X	*Rugoglobigerina rugosa*
X																	X		X		*Rugoglobigerina scotti*
																	X				*Rugoglobigerina sp.*
	X		X				X				X								X	X	*Rugotruncana subcircumnodifer*
X	X		X								X	X								X	*Rugotruncana subpennyi*
																					Rugotruncana sp.
																					Schackoina cenomana
																					Schackoina multispinata
																					Schackoina sp.

DPH 21	DPH 20	DPH 19	DPH 18	DPH 17	DPH 11	DPH 10	KESS 11	KESS 10	KESS 9	KESS 8	KESS 7	KESS 6	KESS 5	KESS 4	KESS 2	KESS 1	UMMI	
																		Abathomphalus mayaroensis
								X			X							*Archaeoglobigerina blowi*
							X	X										*Archaeoglobigerina cretacea*
																		Clavihedbergella sp.
																		Contusotrucana contusa
							X	X	X	X	X	X	X					*Contusotruncana fornicata*
								X										*Contusotruncana patelliformis*
								X										*Contusotruncana plicata*
																		Contusotruncana walfischensis
															X	X		*Farusella washitensis*
																	X	*Gansserina gansseri*
																		Gansserina wiedenmayeri
																		Globigerinelloides blowi
							X	X		X	X	X	X	X				*Globigerinelloides prairehillensis*
							X											*Globigerinelloides subcarinatus*
					X		X			X								*Globigerinelloides sp.*
												X						*Globigerinelloides ultramicrus*
								X										*Globigerinelloides volutus*
				X		X	X	X	X	X	X						X	*Globotruncana aegyptica*
X		X					X	X		X	X		X	X			X	*Globotruncana arca*
							X	X	X	X	X		X					*Globotruncana bulloides*
							X	X		X	X	X						*Globotruncana falsostuarti*
													X					*Globotruncana lapparenti*
							X	X	X		X	X		X				*Globotruncana linneiana*
							X											*Globotruncana rosetta*
																		Globotruncana rugosa
	X						X	X	X	X	X	X	X					*Globotruncana sp*
								X	X		X	X	X					*Globotruncana ventricosa*
																		Globotruncanella citae
											X							*Globotruncanella havanensis*
							X	X										*Globotruncanella petaloidea*
							X				X							*Globotruncanella sp.*
											X							*Globotruncanita angulata*
																		Globotruncanita calcarata
								X				X	X					*Globotruncanita conica*
																		Globotruncanita elevata
					X			X	X	X	X	X	X				X	*Globotruncanita stuarti*
	X						X	X	X	X	X	X		X				*Globotruncanita stuartiformis*
																		Globotruncanita subspinosa
									X	X	X			X				*Globotruncanita sp.*
																		Hedbergella holmdelensis

DPH 21	DPH 20	DPH 19	DPH 18	DPH 17	DPH 11	DPH 10	KESS 11	KESS 10	KESS 9	KESS 8	KESS 7	KESS 6	KESS 5	KESS 4	KESS 2	KESS 1	UMM1	
																		Hedbergella monmouthensis
										X			X	X	X	X		*Hedbergella sp.*
							X	X	X	X	X						X	*Heterohelix globulosa*
																		Heterohelix labellosa
							X	X		X								*Heterohelix navarroensis*
																		Heterohelx planata
								X										*Heterohelix punctulata*
										X								*Heterohelix striata*
	X					X					X	X		X				*Heterohelix sp.*
							X											*Laeviheterohelix sp.*
																		Planoglobulina acervulinoides
																		Planoglobulina sp.
													X					*Planohedbergella sp.*
																		Plummerita hantkenoides
		X		X	X		X	X	X	X	X							*Psudoguembelina costulata*
																		Pseudoguembelina excolata
																		Psedoguembelina hariaensis
										X								*Pseudoguembelina kempensis*
																		Pseudoguembelina palpebra
X		X	X			X		X	X	X								*Pseudoguembelina sp.*
							X		X	X	X	X						*Pseudotextularia elegans*
																		Pseudotextularia intermedia
																		Pseudotextularia nutalli
																		Racemiguembelina fructicosa
																		Racemiguembelina powelli
																		Rotalipora montsalvensis
															X			*Rotalipora sp.*
																		Rugoglobigerina hexacamerata
							X	X						X				*Rugoglobigerina macrocephala*
																		Rugoglobigerina reicheli
		X		X	X		X	X			X	X	X	X				*Rugoglobigerina rugosa*
																		Rugoglobigerina scotti
							X					X	X	X				*Rugoglobigerina sp.*
																		Rugotruncana subcircumnodifer
																		Rugotruncana subpennyi
							X											*Rugotruncana sp.*
															X	X		*Schackoina cenomana*
																X		*Schackoina multispinata*
													X					*Schackoina sp.*

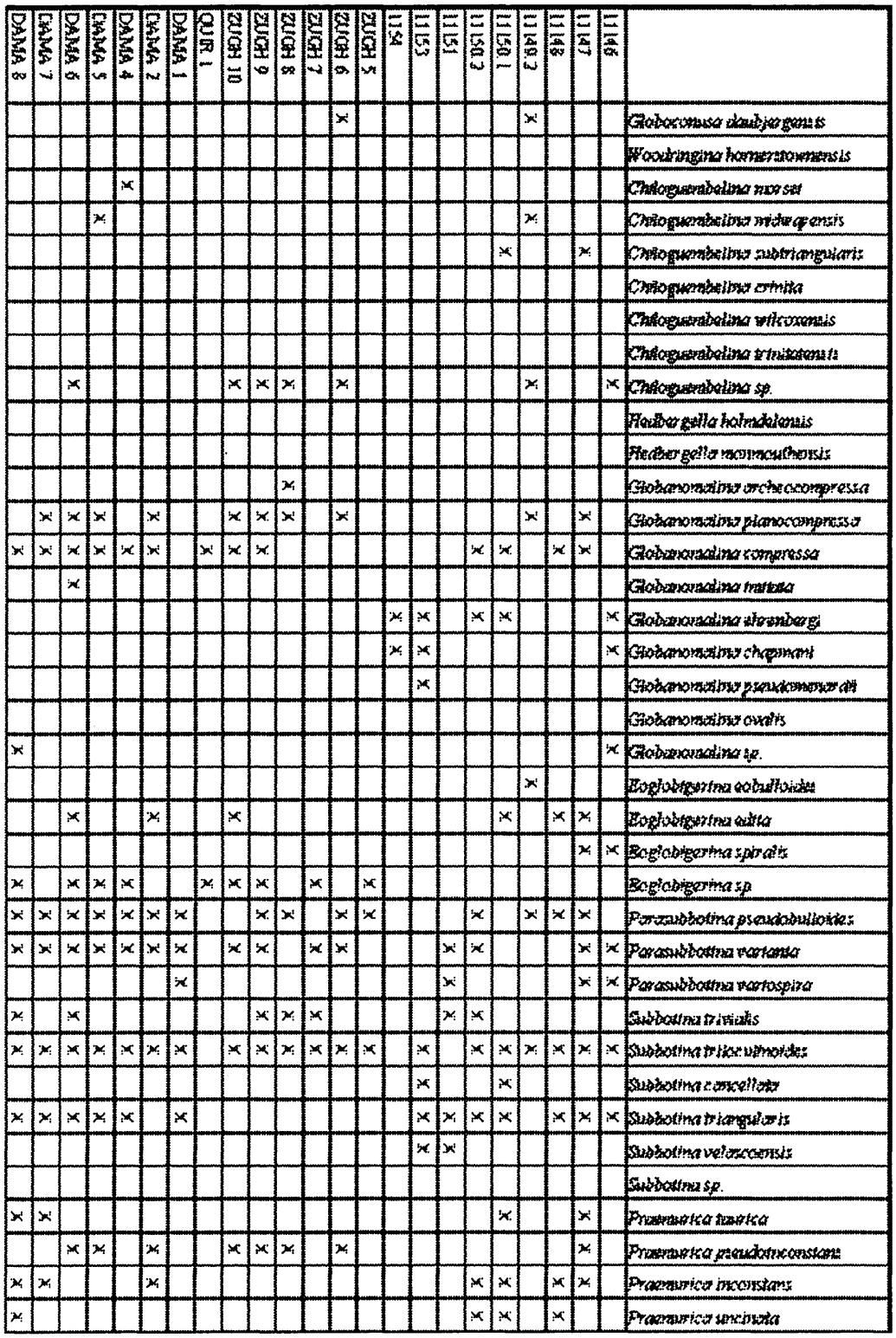

	1146	1147	1148	1149.2	1150.1	1150.2	1151	1153	1154	ZUGH 5	ZUGH 6	ZUGH 7	ZUGH 8	ZUGH 9	ZUGH 10	QUR 1	DAMA 1	DAMA 2	DAMA 3	DAMA 4	DAMA 5	DAMA 6	DAMA 7	DAMA 8
Globoconusa daubjergensis				x																				
Woodringina hornerstownensis																								
Chiloguembelina morsei																				x				
Chiloguembelina midwayensis				x															x					
Chiloguembelina subtriangularis		x			x																			
Chiloguembelina crinita																								
Chiloguembelina wilcoxensis																								
Chiloguembelina trinitatensis																								
Chiloguembelina sp.	x			x							x		x	x	x						x	x		
Hedbergella holmdalensis																								
Hedbergella monmouthensis																								
Globanomalina archaecompressa													x											
Globanomalina planocompressa		x		x							x		x	x	x			x			x	x		
Globanomalina compressa		x	x		x	x								x	x	x		x		x	x	x	x	x
Globanomalina ineaqua																						x		
Globanomalina luterbacheri	x				x			x	x															
Globanomalina chapmani	x							x	x															
Globanomalina pseudomenardii								x																
Globanomalina ovalis																								
Globanomalina sp.	x																							x
Eoglobigerina eobulloides				x																				
Eoglobigerina edita			x		x										x			x						
Eoglobigerina spiralis	x	x																						
Eoglobigerina sp.		x	x							x		x		x	x	x				x	x			x
Parasubbotina pseudobulloides		x	x	x		x				x	x		x	x			x	x		x	x	x	x	x
Parasubbotina varianta	x	x				x	x			x	x	x		x	x		x	x		x	x	x	x	x
Parasubbotina variospira	x	x					x										x							
Subbotina trivialis						x	x					x	x	x								x		x
Subbotina triloculinoides	x	x	x	x	x	x		x		x	x	x	x	x	x		x	x		x	x	x	x	x
Subbotina cancellata								x																
Subbotina triangularis	x	x	x		x	x	x	x									x			x	x	x	x	x
Subbotina velascoensis							x	x																
Subbotina sp.																								
Praemurica taurica		x			x																		x	x
Praemurica pseudoinconstans		x	x								x		x	x	x			x			x			
Praemurica inconstans		x	x		x	x												x					x	x
Praemurica uncinata			x		x	x																		x

DAMA 8	DAMA 7	DAMA 6	DAMA 5	DAMA 4	DAMA 2	DAMA 1	QUIR 1	ZUGH 10	ZUGH 9	ZUGH 8	ZUGH 7	ZUGH 6	ZUGH 5	1134	11153	11151	11150.2	11150.1	11149.2	11148	11147	11146	
																							Igorina pusilla
																							Igorina albeari
																							Igorina tadjikistanensis
																							Igorina sp.
																							Acarinina strabocella
															x								*Acarinina nitida*
															x								*Acarinina subsphaerica*
															x								*Acarinina mckannai*
														x									*Acarinina coalingensis*
														x		x							*Acarinina soldadoensis*
																x							*Acarinina sp.*
						x											x						*Morozovella praeangulata*
						x									x								*Morozovella angulata*
						x									x							x	*Morozovella conicotruncata*
																							Morozovella apanthesma
														x	x								*Morozovella velascoensis*
																							Morozovella passionensis
																							Morozovella occlusa
														x		x							*Morozovella acuta*
														x		x							*Morozovella aequa*
														x		x							*Morozovella subbotinae*
														x									*Morozovella gracilis*
																							Morozovella sp.
																							Zeauvigerina sp.

	DAMA A	DAMA C	DAMA D	DAMA E	DAMA F	DAMA G	DAMA H	DAMA I	UMA 4	DPH 1	DPH 2	DPH 3	DPH 4	DPH 5	DPH 6	DPH 7	DPH 8	DPH 9	DPH 10	DPH 11	DPH 12	DPH 13	DPH 14	DPH 15
Globoconusa daubjergensis										X														
Woodringina hornerstownensis														X				X	X	X	X		X	X
Chiloguembelina racoti												X	X	X										
Chiloguembelina midwayensis											X					X		X	X	X	X		X	X
Chiloguembelina subtriangularis											X	X	X	X	X	X	X	X	X		X	X		
Chiloguembelina crinita																								
Chiloguembelina velascoensis																								
Chiloguembelina trinitatensis																								
Chiloguembelina sp.					X																			
Hedbergella holmdelensis																								
Hedbergella monmouthensis																								
Globanomalina archaecompressa																								
Globanomalina planocompressa	X	X	X		X	X	X	X		X	X													
Globuconadina compressa					X					X	X	X				X	X	X	X	X	X	X		
Globuconadina trattsa																								
Globuconadina shamberge														X	X	X	X	X	X	X	X	X	X	
Globanomalina chapmani																			X	X	X	X	X	X
Globanomalina pseudomenardii																							X	X
Globanomalina ovalis																								
Globuconadina sp.																								
Eoglobigerina eobulloides				X										X										
Eoglobigerina edita	X	X	X				X			X	X								X					
Eoglobigerina spiralis													X		X		X							
Eoglobigerina sp.	X		X	X		X	X	X																
Parasubbotina pseudobulloides	X	X	X	X	X	X	X	X		X	X	X	X	X	X	X	X	X	X	X	X	X		X
Parasubbotina variantia											X	X	X		X	X	X	X	X				X	
Parasubbotina variospira																							X	
Subbotina trivialis	X	X	X							X	X	X	X											
Subbotina triloculinoides	X	X	X	X		X	X			X	X	X	X	X	X	X	X	X	X	X	X	X	X	X
Subbotina cancellata																			X	X	X			
Subbotina triangularis	X	X	X											X	X	X	X	X	X	X		X	X	X
Subbotina velascoensis																								X
Subbotina sp.					X	X	X	X																
Praemurica taurica										X														
Praemurica pseudoinconstans	X			X						X	X	X	X								X			
Praemurica inconstans	X									X	X	X	X	X	X	X	X	X	X	X		X	X	
Praemurica uncinata											X	X	X	X	X	X	X	X	X	X	X	X	X	X

	DAMA A	DAMA C	DAMA D	DAMA E	DAMA F	DAMA G	DAMA H	DAMA I	UMM 4	DPH 1	DPH 2	DPH 3	DPH 4	DPH 5	DPH 6	DPH 7	DPH 8	DPH 9	DPH 10	DPH 11	DPH 12	DPH 13	DPH 14	DPH 15
Igorina pusilla																							X	X
Igorina albeari																								
Igorina tadjikistanensis																								
Igorina sp.																								
Acarinina strabocella																		X	X	X	X		X	
Acarinina nitida																								
Acarinina subsphaerica																								
Acarinina mckannai																								
Acarinina coalingensis																								
Acarinina soldadoensis																								
Acarinina sp.																								
Morozovella praeangulata													X	X	X	X	X	X	X	X	X	X	X	
Morozovella angulata															X	X	X	X	X	X	X	X	X	X
Morozovella conicotruncata																							X	
Morozovella aparthesma																			X	X				
Morozovella velascoensis									X															
Morozovella passionensis																								
Morozovella occlusa																								
Morozovella acuta																								
Morozovella aequa																								
Morozovella subbotinae																								
Morozovella gracilis																								
Morozovella sp.																								
Zeauvigerina sp.																								

	DEPH 16	DEPH 17	DEPH 18	DEPH 19	DEPH 20	DEPH 21	DEPH 22	DEPH 23	DEPH 24	DEPH 25	DEPH 26	DEPH 27	DEPH 28	DEPH 29	DEPH 30	DEPH 31	DEPH 32	DEPH 33	DEPH 34	DEPH 35	DEPH 36	DEPH 37	DEPH 38	DEPH 39	DEPH 40
Globocassidulina davisbergensis																									
Woodringina hornerstownensis		X	X		X																				
Chiloguembelina morsei						X	X																		
Chiloguembelina midwayensis	X		X					X																	
Chiloguembelina subtriangularis		X			X	X	X																		
Chiloguembelina crivita										X		X	X	X	X	X						X	X		X
Chiloguembelina wilcoxensis																									
Chiloguembelina trinitatensis																								X	X
Chiloguembelina sp.																									
Hedbergella holmdelensis																									
Hedbergella monmouthensis																									
Globanomalina archaecompressa																									
Globanomalina planocompressa																									
Globanomalina compressa		X				X																			
Globanomalina imitata																									
Globanomalina ehrenbergi		X	X	X	X	X	X																		
Globanomalina chapmani	X	X	X	X	X			X		X	X	X	X	X	X	X	X	X	X	X	X	X	X	X	X
Globanomalina pseudomenardii	X													X	X	X	X				X		X	X	X
Globanomalina ovalis																				X		X	X	X	X
Globanomalina sp.																									
Eoglobigerina eobulloides																									
Eoglobigerina edita																									
Eoglobigerina spiralis				X																					
Eoglobigerina sp.																									
Parasubbotina pseudobulloides	X	X	X		X	X	X			X															
Parasubbotina variospira	X	X			X	X				X	X			X	X		X								
Parasubbotina variocamera				X		X		X																	
Subbotina triloculinoides																									
Subbotina trivialis	X	X		X	X	X	X																		
Subbotina triloculinoides			X	X	X	X	X			X		X						X	X						
Subbotina conceiliata					X		X			X		X						X	X						
Subbotina triangularis	X	X	X	X	X	X	X	X	X	X	X	X	X	X	X	X	X	X	X	X	X	X	X	X	X
Subbotina velascoensis										X	X	X	X	X											
Subbotina sp.																									
Praemurica taurica																									
Praemurica pseudoinconstans																									
Praemurica inconstans		X	X	X	X																				
Praemurica uncinata	X	X	X	X	X	X																			

DPH 40	DPH 39	DPH 38	DPH 37	DPH 36	DPH 35	DPH 34	DPH 33	DPH 32	DPH 31	DPH 30	DPH 29	DPH 28	DPH 27	DPH 26	DPH 25	DPH 24	DPH 23	DPH 22	DPH 21	DPH 20	DPH 19	DPH 18	DPH 17	DPH 16	
														X	X	X	X	X			X	X	X	X	*Igorina pusilla*
X	X	X	X	X	X	X	X	X	X		X	X	X	X	X	X	X	X							*Igorina albeari*
	X	X	X	X	X	X	X	X	X		X	X	X	X			X								*Igorina tadjikistanensis*
															X	X									*Igorina sp.*
								X					X		X				X						*Acarinina strabocella*
X	X	X	X		X	X	X		X																*Acarinina nitida*
																									Acarinina subsphaerica
X	X	X	X	X																					*Acarinina mckannai*
X																									*Acarinina coalingensis*
X	X																								*Acarinina soldadoensis*
																									Acarinina sp.
																				X	X	X	X		*Morozovella praeangulata*
									X	X	X	X	X	X	X	X	X	X	X	X	X	X	X	X	*Morozovella anguiata*
										X	X			X	X		X	X							*Morozovella conicotruncata*
X		X	X	X	X	X	X	X	X	X	X	X	X	X	X	X		X	X	X			X	X	*Morozovella apanthesma*
X	X	X	X		X			X	X					X											*Morozovella velascoensis*
																									Morozovella passionensis
X	X			X	X	X	X	X			X	X	X												*Morozovella occlusa*
X		X		X	X	X	X	X	X	X															*Morozovella acuta*
			X	X																					*Morozovella aequa*
																									Morozovella subbotinae
																									Morozovella gracilis
																									Morozovella sp.
		X	X	X		X					X	X													*Zeauvigerina sp.*

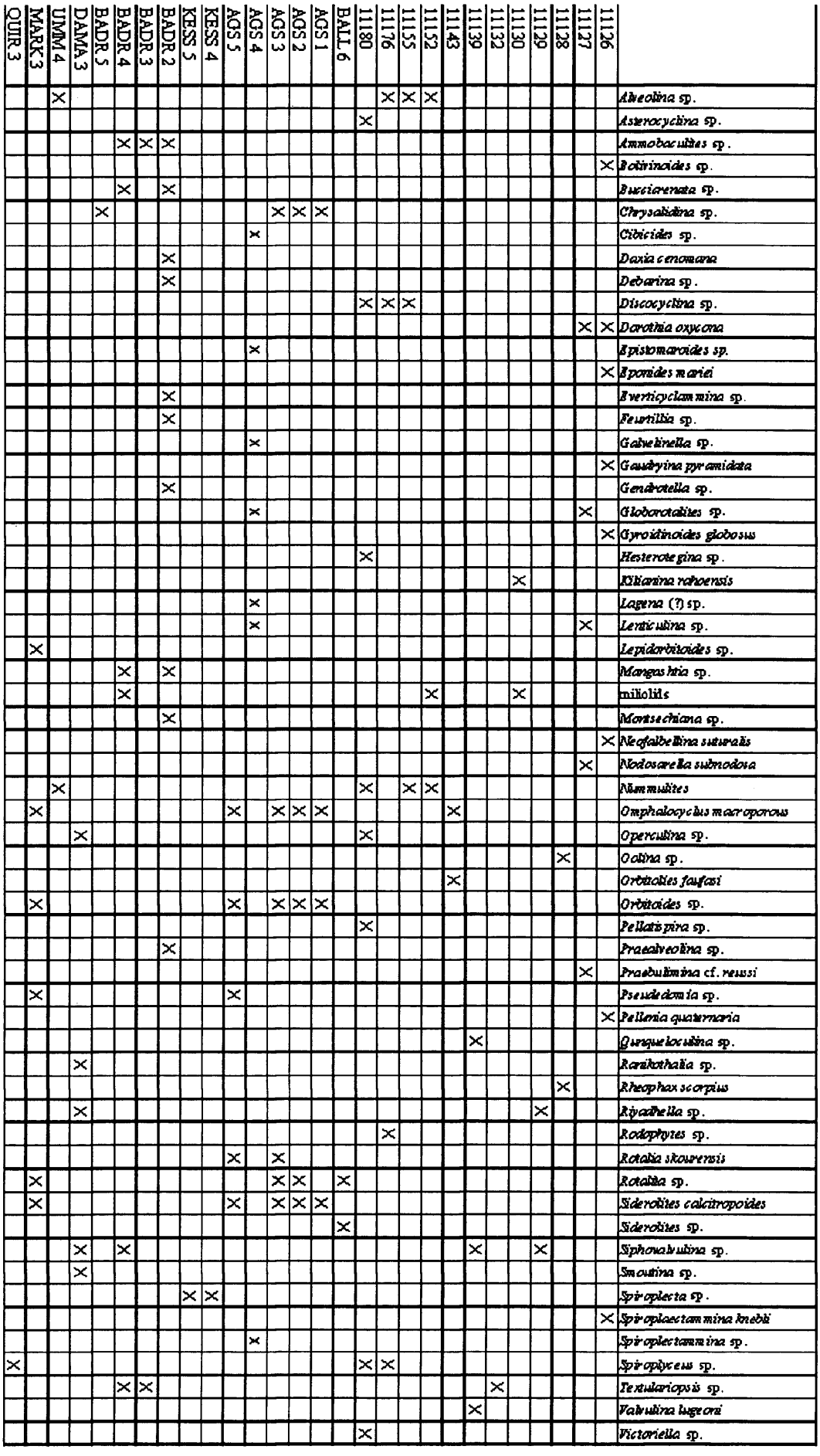
QUIR 3
MARK 3
UMM 4
DAMA 3
BADR 5
BADR 4
BADR 3
BADR 2
KESS 5
KESS 4
AGS 5
AGS 4
AGS 3
AGS 2
AGS 1
BALL 6
11180
11176
11155
11152
11143
11139
11132
11130
11129
11128
11127
11126
Alveolina sp.
Asterocyclina sp.
Ammobaculites sp.
Botrincides sp.
Bucciarenata sp.
Chrysalidina sp.
Cibicides sp.
Daxia cenomana
Debarina sp.
Discocyclina sp.
Dorothia oxycona
Epistomaroides sp.
Eponides mariei
Everticyclammina sp.
Feurtillia sp.
Gaheltinella sp.
Gaudryina pyramidata
Gendrotella sp.
Globorotalites sp.
Gyroidinoides globosus
Hesterotegina sp.
Kilianina rahoensis
Lagena (?) sp.
Lenticulina sp.
Lepidorbitoides sp.
Mangashtia sp.
miliolids
Montsechiana sp.
Neoalveolina suturalis
Nodosarella submodosa
Nummulites
Omphalocyclus macroporous
Operculina sp.
Ootina sp.
Orbitolites faufasi
Orbitoides sp.
Pellatispira sp.
Praealveolina sp.
Praebulimina cf. reussi
Pseudedomia sp.
Pellenia quaternaria
Quinqueloculina sp.
Ranikothalia sp.
Rhephax scorpius
Rivadhella sp.
Rodophytes sp.
Rotalia skourensis
Rotalia sp.
Siderolites calcitropoides
Siderolites sp.
Siphonaltulina sp.
Smoutina sp.
Spiroplecta sp.
Spiroplaectammina knebli
Spiroplectammina sp.
Spiropyrcus sp.
Textulariopsis sp.
Valvulina lugeoni
Victoriella sp.

KESS 11	KESS 10	KESS 9	KESS 8	KESS 7	KESS 6	KESS 5	KESS 4	EK3	EK2	EK1	11127	11126	11125	11124	
														X	*Acanthocircus* sp.
								X							*Acientyle* sp.
	X	X	X		X		X		X	X	X			X	*Alievium gallowayi*
				X	X			X							*Alievium* sp.
	X	X	X	X	X	X	X	X	X	X	X		X	X	*Amphipyndax pseudoconulus*
											X		X		*Amphipyndax* cf.*pseudoconulus*
	X	X	X	X	X	X	X	X	X	X	X		X	X	*Amphipyndax stocki*
															Amphipyndax cf. *stocki*
	X	X	X	X	X	X	X	X	X	X	X		X	X	*Amphipyndax tylotus*
X									X	X		X		X	*Amphipyndax* sp.
	X	X	X	X	X	X	X	X	X	X	X		X	X	*Archaeodictyomitra lamellicostata*
		X	X	X	X		X				X		X		*Archaeodictyomitra* sp.
					X			X						X	*Archaeospongoprunum andersoni*
				X											*Archaeospongoprunum* cf. *andersoni*
						X									*Archaeospongoprunum* cf. *bipartium*
			X		X	X	X							X	*Archaeospongoprunum hueyi*
				X		X									*Archaeospongoprunum* cf. *hueyi*
							X								*Archaeospongoprunum* cf. *triplum*
		X	X	X	X	X	X			X				X	*Archaeospongoprunum* sp.
	X	X	X	X	X	X							X	X	*Archicapsa* sp.
									X						*Bisphaerocephalina amazon*
					X										*Bisphaerocephalina* (?) *amazon*
			X	X	X	X	X	X					X		*Cavidiscus* sp.
							X								*Cromyomma* (?) sp.
								X							*Crucella* cf. *espartoensis*
					X	X	X	X	X	X				X	*Crucella* sp.
		X	X	X											*Cryptamphorella conara*
	X										X				*Cryptamphorella* sp.
				X	X										*Dicanthocapsa* sp.
										X					*Dictyomitra andersoni*
				X											*Dictyomitra* cf. *denticostata*
				X											*Dictyomitra formosa*
	X						X								*Dictyomitra* cf. *formosa*
									X	X					*Dictyomitra koslovae*
			X								X				*Dictyomitra* cf. *koslovae*
X	X	X	X	X	X	X	X	X	X	X	X	X	X	X	*Dictyomitra multicostata*
					X										*Dictyomitra* cf. *multicostata*
X	X	X	X	X	X	X	X	X	X	X	X		X	X	*Dictyomitra rhadina*
X	X	X	X	X	X	X				X			X	X	*Dictyomitra* sp.

KESS 11	KESS 10	KESS 9	KESS 8	KESS 7	KESS 6	KESS 5	KESS 4	EK3	EK2	EK1	11127	11126	11125	11124	
					X					X					*Eastonerius acuminatus*
					X										*Eostichomitra warzigita*
	X	X	X	X	X	X	X	X	X	X	X		X		*Forenanina schona*
		X			X		X								*Forenanina* cf. *schona*
	X	X	X	X	X	X	X	X	X	X	X	X	X	X	*Holocryptocanium barbui*
					X										*Holocryptocanium* sp.
				X											*Kuppelela* (?) sp.
							X								*Lithocampe* (?) sp.
			X												*Mylocerion* sp.
					X								X	X	*Novixitus* sp.
		X													*Orbiculiforma* cf. *monticelloensis*
					X		X	X	X	X			X		*Orbiculiforma* sp.
		X	X												*Orbiculiforma sacramentoensis*
									X						*Orbiculiforma* cf. *sacramentoensis*
							X								*Parazonella* (?) sp.
	X						X	X	X		X		X		*Patellula ewessceei*
			X		X				X	X	X				*Patellula verteroensis*
		X			X		X								*Patellula* sp.
			X												*Patellula* (?) sp.
														X	*Patulibrachium lawsoni - dickinsoni* transitional form
								X	X						*Patulibrachium marshensis*
						X	X								*Patulibrachium* cf. *marshensis*
						X									*Patulibrachium* cf. *petroluemensis*
										X					*Patulibrachium teslaensis*
				X	X	X	X	X		X				X	*Patulibrachium* sp.
			X												*Patulibrachium* (?) sp.
							X				X			X	*Phaseliforma carinata*
			X												*Phaseliforma* cf. *laxa*
					X	X		X			X		X		*Phaseliforma* sp.
X		X	X	X	X										*Phaseliforma* (?) sp.
X		X	X	X	X	X	X	X	X	X				X	*Praeconocarryomma universa*
							X					X			*Praeconocarryomma* sp.
X					X		X								*Praeconocarryomma* (?) sp.
									X						*Praecrucella kubischa*
														X	*Praestylosphaera* sp.
				X			X								*Praestylosphaera* (?) sp.
				X											*Protoxiphotractus kirbyi*
			X												*Protoxiphotractus perplexus*
						X									*Protoxiphotractus* sp.

KES8 11	KES8 10	KES8 9	KES8 8	KES8 7	KES8 6	KES8 5	KES8 4	EK3	EK2	EK1	11127	11126	11125	11124	
	x	x	x		x										*Protumma* sp.
	x	x	x	x	x	x	x	x	x	x	x		x	x	*Pseudocaulophacus floresensis*
	x			x		x	x	x	x	x	x			x	*Pseudocaulophacus lenticulatus*
		x													*Pseudocaulophacus* cf. *lenticulatus*
										x					*Pseudocaulophacus parguerensis*
										x					*Pseudocaulophacus riedeli*
					x	x									*Pseudocaulophacus* (?) cf. *riedeli*
					x			x	x						*Pseudocaulophacus setosettigus*
x						x					x				*Pseudocaulophacus* sp.
						x	x			x				x	*Rhopalosyringium klausum*
	x	x	x	x	x	x	x	x	x	x	x		x	x	*Rhopalosyringium magnificum*
							x		x				x		*Rhopalosyringium* sp.
	x	x	x	x											*Rhopalosyringium* (?) sp.
								x							*Saturnalis* sp.
						x		x		x				x	*Sciadocapsa* sp.
								x						x	*Spongosaturnalis* sp.
							x							x	*Spongosaturninus* cf. *hueyi*
															Spongosaturninus sp.
														x	*Stichomitra asymbatos*
			x		x		x		x	x			x		*Stichomitra communis*
				x		x									*Stichomitra* cf. *communis*
		x													*Stichomitra* cf. *magna*
					x										*Stichomitra* cf. *toasaensis*
	x	x			x		x	x	x	x				x	*Stichomitra* sp.
x	x			x	x	x									*Stichomitra* (?) sp.
			x	x	x					x					*Theocampe apicata*
	x					x									*Theocampe* (?) sp.
		x	x		x		x						x		*Theocapsomma cavus*
															Xitus asymbatos
								x	x	x	x			x	*Xitus spicularis*
								x	x		x		x		*Xitus* sp.
		x	x	x	x	x	x								Indeterminate spongodiscids
x				x				x	x	x		x	x	x	Indeterminate spumellarians
x	x	x	x	x	x		x			x	x	x	x		Indeterminate nassellarians